DEVELOPMENT OF COIR FIBRE CEMENT AND CASHEW NUT SHELL LIQUID BONDED COMPOSITE BOARDS

By

David Adewuyi OKE

(Matric. No.: 120249)

B.Eng. Akure, M.Sc. Ibadan

A Thesis in the Department of CIVIL ENGINEERING

Submitted to the Faculty of Technology

in Partial fulfilment of the requirements for the Degree of

DOCTOR OF PHILOSOPHY

of the

UNIVERSITY OF IBADAN

JUNE, 2023

CERTIFICATION

This is to certify that, this work was carried out by Mr. David Adewuyi, Oke of Civil Engineering Department, University of Ibadan.

…………………………………………………..
Supervisor
B.I.O. Dahunsi,
B.Sc (Ife), M.Sc., PhD (Ibadan), MNSE, FNIEE, MNICE Reg. Engr. (COREN)
Professor, Department of Civil Engineering, University of Ibadan, Nigeria

DEDICATION

This thesis is dedicated to Almighty God the giver of lives and to the homeless.

ACKNOWLEDGEMENTS

encouragement. And for my loving children, Bayo, Busayo and Damola for their prayers, affection and always welcoming me back home with wonderful hugs and kisses.

ABSTRACT

There are enormous Agricultural Residues (AR) such as Coir Dust (CD), Coir Fibre (CF), and cashew nut shells, which are sources of environmental pollution in Nigeria. However, these residues can be deployed in Cement Composite (CC) production as alternative building material. Ce0ment composites are however susceptible to unwarranted dimensional instability which can be curtailed by the incorporation of polymeric substances such as Cashew Nut Shell Liquid (CNSL). Literature on properties of CCs produced from AR with the incorporation of CNSL is sparse. Therefore, this study was designed to investigate the properties of CCs made from CD, CF and CNSL.

Cashew nuts were collected from a local site at Ogbomoso, milled to about 3.35 mm sizes. The CNSL was chemically extracted from the milled particles using IS methods, while coconut husk were reduced to obtain CF and CD using IS and ASTM methods. Cement composites were produced at four levels of CF (5.0, 7.5, 10.0 and 15.0%), four levels of CD (5.0, 7.5, 10.0 and 15.0%) and four levels of CNSL (2.5, 5.0 7.5, 10.0%) based on cement weight at 2:1 cement: water ratio following the preliminary tests. A CC board machine was developed and tested for the production of CC boards using Schaum's Machine Design methods. The physical and sorption properties such as density, Water Absorption (WA), Thickness Swelling (TS) were determined using ASTM standards. The mechanical properties such as, Compressive Strength (CS), Modulus of Rupture (MOR), Modulus of Elasticity (MOE), and Impact Strength (IS) were evaluated using ASTM standards. Data were analysed using ANOVA at $\alpha_{0.05}$.

A 5.5 kW electrically operated CC board machine developed has an amplitude of 2 mm; frequency of 350 rpm; CC size of $520 \times 290 \times 8mm$ and capacity of 360 CCs per hour. The densities, WA and TS of CF composites without CNSL ranged from 1350.00 to 1690.00 kg/m^3, 33.1 to 69.5% and 1.1 to 3.2%, respectively. Their respective CS, MOR, MOE and IS in Nmm^{-2} were 5.72–11.43, 4.37–5.34, 813.24–1428.85, and 1.19–4.35. The densities, WA and TS of CD composite without CNSL ranged 1030.00–1480.00 kg/m^3, 27.5– 69.1% and 1.9–5.1%, respectively. Their respective CS, MOR, MOE and IS in Nmm^{-2} were 0.9–11.16, 1.6–3.79, 330.64–1916.31 and 0.86 – 2.18. However, composites with CNSL had densities, WA and TS that ranged from 1310.00 to 1510.00 kg/m^3, 7.1 to 17.8% and 0.9 to 2.7%, respectively. Their respective CS, MOR, MOE and IS in Nmm^{-2} were 2.18–7.25, 1.71–2.36, 306.01 - 1054.09 and 1.09 to 2.57. The incorporation of CNSL significantly affected the physical, sorption and mechanical properties of the manufactured CCs and can be utilised in both indoor and outdoor applications. There was significant differences in the properties of CC produced from CF, CD and those treated with CNSL.

Cashew nut shell liquid enhanced the properties and performance of cement bonded composites made from coconut coir fibre and dust for indoor and outdoor applications.

Keywords: Cement composites, Coconut coir waste, Cashew nut shell liquid, Sorption and Mechanical properties

Word count: 496

TABLE OF CONTENTS

LIST OF TABLES

LIST OF FIGURES

LIST OF PLATES

LIST OF ABBREVATIONS

Symbols	Description	Unit
R_l	Internal Radius	mm
M_b	Mass of board	Kg
F_c	Fibre content	kg
C_c	Cement content	Kg
F_{ac}	Actual quantity of fibre	Kg
V_b	Volume of board	m^3
L_b	Length of board	mm
V_T	Total Volume of constituents mixed	m^3
d	Diameter of the circular steel bar	mm
H_m	Height of the mixing chamber	m
V_m	Volumetric capacity of the chamber	m^3
W_q	Quantity of water	Kg
V_w	Volume of water required to mix the other constituent	N/mm
M	Maximum bending moment	N/mm
Z	Sectional modules	mm^3
σ_b	Permissible bending stress	Nmm^{-2}
V_r	Total Volume of bars	m^3
M_r	Mass of steel bars	kg
P_{steel}	Density of steel bars	kg/m^3
P	Power capacity of belt drive	W
D	Diameter of pulley driven (conveyor belt)	mm
α_1	Angle of wrap of smaller pulley (driven)	degree
α_2	Angle of wrap of larger pulley (driven)	degree
$(hp)_d$	Design horsepower of the chain drive	hp
N_L	Number of teeth on driven sprocket	Ns
n_L	Rotational speed of driven sprocket	rpm
V	The linear chain velocity	ft/min/ m/s
C	Selected centre distance	Inches
σ_{ys}	The yield strength on the material	N/mm^2
Z_x	The plastic sectional modules	mm^3

$V_{applied}$	The maximum shear force imposed on the beam	N
d	The beam depth	mm
t_w	The thickness of the web	mm
g	Acceleration due to gravity	gm^{-2}
W_r	Weight of mixing bars	N
n_p	Shaft speed	rpm
M_t	Maximum torsional moment	Nm
P	Power transmitted to the shaft	kw
N	Number of revolution	rev/mm
θ	Angle of twist	degree
G	Torsional modulus of elasticity	Nm^{-2}
$N_{R.G}$	Reduction gear revolution	rpm
$N_{E \cdot m}$	Electric motor revolution	rpm
N_1	Revolution of reduction gear box	rpm
N_2	Revolution of the shaft moving the conveyor belt	rpm
D_1	Diameter of output pulley on the reduction gear	mm
D_2	Diameter of the pulley attached to the shaft	mm
R	Radius of the larger pulley	mm
r	Radius of the smaller pulley	mm
C	Centre distance between the pulleys	mm
N	Rotational speed of driven pulley	rps
V	Belt speed	m/s
T_1	Belt tension in tight side	N
T_2	Tension on the stack side of the belt	N
s	Maximum allowable stress	N/m^2
ω	Uniform distributed load on the shaft	N/mm

CHAPTER ONE
INTRODUCTION

1.1   Background to the study

The use of agricultural and forest residues for industrial purposes is an environment-safe and friendly method of waste disposal. The construction industry is turning its research and development efforts to investigate cellulose from agriculture wastes and the use of forest residues for the creation of building materials. The enormous potential of agriculture and forest leftovers can provide a solution to the issues of insufficient material supply, high prices for conventional timbers, and an excessive reliance on imported building materials. The large volume of farm and forest plantation waste would then serve as a reliable source of alternate building materials that are cheap for the majority of the people of the nation.

Coir fibre is obtained from the husk and outer layer of the fruit of coconut tree. This outer layer is called the coconut husk. The husk (exocarp) of the coconut consists of a smooth waterproof outer skin (epicarp) and fibrous zone (mesocarp). The mesocarp comprises of strands of fibro vascular bundles of coir embedded in a non-fibrous paranchymatous "corky" connective tissue usually referred to as pith; which ultimately becomes coir dust (Woodroof, 1970).

Chemically, coir fibre is made up of a highly lignified type of cellulose (cellulose-lignin complex), which accounts for its colour, abrasiveness, and relative brittleness when compared to fibre made entirely of cellulose. Pectin and hemicelluloses, on the other hand, make up the majority of the ground tissues of the husk (Gordon, 2002). As a spongy binding substance, pectin and hemicelluloses hold the big fibre cells together to form the husk. Coir is graded according to the length, colour, toughness, and general cleaniness of its fibres in relation to the amount of pith it contains (Pillai, Sudhakaran and Vasudev, 2001).

White coir and brown coir are the two main types of coir fibre that make up the entire material.

The reasons for the variations are the uses, physical characteristics, extraction techniques, and husk conditions. The white fibre known as coir that is collected from immature, green coconuts is typically considered to be finer than the brown fibre that is derived from mature, brown coconuts that are typically older than 12 months and have lost their green colour. Both forms of fibre are widely utilised, and each has a specific type of application that is distinct from the other (Belas, 2007).

1.2   Research problem

With the population of Nigeria growing at a high rate, the country is faced the challenge of improving the living standards of her people without destroying the environment. The country's rapidly expanding population has increased the demand for affordable housing materials, which has resulted in a high rate of slum development and the destruction of national forests, woodlands, and wild grass, as well as a decrease in rainfall and a rise in desertification.

Particleboard is made from sawdust and trimmings from trees that were cut down for timber and plywood production. The effects of planting and cutting down these trees must be taken into account, while solving the environmental issue. Information gathered from industry on the production capacity in the United States and Canada uses some virgin wood, with an average of 34% of the production capacity. Lumber harvesting for timber promotes deforestation (Green Report, 2001).

The environmental impact of the production of wood-based products has become a global problem. Wood fibres are not considered environmentally responsible materials, as they are not annually renewable. Also, the resin binder; urea formaldehyde is derived from petrochemicals, a non-renewable resource. Moreover, the use of the resin has become a health hazard as urea formaldehyde is known to be a human carcinogen according to the Environmental Protection Agency (EPA), harmful when consumed or breathed in.

Formaldehyde exposure, even at low levels, raises the chance of developing lung and nose cancer. The coconut pulp contains around one-third coir fibres, with the

remaining component called pith or dust taking a long time to decompose. The study therefore look into the possibility of employing the coir dust waste and cashew nut shell liquid, which can be easily extracted from cashew to produce a housing material that is environmentally friendly.

The issues of deforestation can be addressed by, appropriate technologies affordable to the rural population are required through the development of plant-fibre reinforced composites using an appropriate solution that is environmentally friendly. Nigeria boasts of abundant variety of plant fibre materials such as cotton, banana, palm leaf, maize stalk, bamboo and coir, whose fibres could be used to reinforce polymeric and ceramic materials to produce useful building composite materials. In addition, Nigeria is rich in naturally occurring matrix materials available from natural trees such as cashew tree.

1.3   Aim and objectives

The aim of this research is to determine the suitability of particleboards produced from agricultural wastes of coir dust/fibre and Cashew Nut Shell Liquid (CNSL) for building construction.

The specific objectives were to:

i.   develop light weight composite boards from coir fibre, coir dust, CNSL, cement and water

ii.   develop and evaluate the performance of particleboard production machine

iii.   evaluate the physical and mechanical properties of the boards produced

1.4   Justification

The use of timber in the production of wood-based particleboards is becoming economically unbearable. Also the amount of cement needed in block making and corrugated roofing sheet manufacturing is becoming alarming. Lumber quality is deteriorating, prices are erratic, and some experts believe future supplies may be constrained (Smith, Vissage, Darr and Sheffield 2002).

While the need for particleboard is rising, there is concern that supply cannot keep up with demand and that prices may rise as a result (Green Report, 2002). Also, the use

of the resin, urea formaldehyde has become a health hazard as urea formaldehyde is known to be a human carcinogen (EPA, 2002).

These have prompted research into the possible use of coir fibre, coir dust, cashew nut shell liquid and cement in the manufacture of particleboards. This is because both coir fibre and cashew nut shell liquid are renewable resources, cheap and readily available, but yet underutilised. The purpose of this study was to evaluate the acceptability of coir dust waste, coir fibre, and liquid from cashew nut shells for making particleboards that might be used in home construction.

1.5   Scope of study

The investigation was limited to the use of coconut coir fibre (*Cocosnucifera*), coir dust, Cashew Nut Shell Liquid (CNSL) and cement in the production of particleboards.

1.6   Significance of the study

The significance of the study is to provide an environment-safe method of waste disposal, reduce deforestation, provide an alternative solution to the issues of insufficient building materials and also reduce the excessive importation of building materials. The use of agricultural waste and materials such as coir fibre and coir dust due to its availability in large quantities from farms and forest plantations can be beneficial in the production of composite boards for the construction industry with the inclusion of CNSL which can significantly improve all the physical properties and also results in a more dimensionally stable composite. Moreover, the addition of CNSL will reduce the health hazard that may be resulted from the usage of conventional materials like formaldehyde.

CHAPTER TWO

LITERATURE REVIEW

2.1 Agricultural wastes

Agricultural residues are the materials produced as a by-product after agricultural crops have been used for their intended or primary functions. They consist of straws made from grains including wheat, rice, barley, and oats, seed grass made from flax and rye, broken sugarcane stalks known as bagasse, sorghum, and corn stalks, and cotton linters made from short fibre that stick to cotton seed after cotton ginning (www.rethinkpaper.org).

In the absence of proper utilization, agricultural residues are produced annually in enormous amounts as waste products, creating disposal issues. Due to the significant amounts of cellulose, hemicelluloses, and lignin they contain, these lignocellulosic crop residues can be recycled to create a number of useful products. For the manufacture of single-cell proteins used in animal feed, fuel, paper, particleboard, and structural and non-structural panels, they may provide good starting materials as listed in the building materials from agricultural wastes presented in Table 2.1 (FAO, 1994).

Table 2.1: Building materials from agricultural wastes

Item	Source	Application in Building Materials
Risk Husk	Rice mills	As a fuel source for the production of building products such bricks, rice husk cement, fibrous building panels, and cement that is acid proof.
Banana leaves/ stalk	Banana plants	Fire resistance fibre board is used to make building boards.
Cotton Stalk	Cotton plantation	Paper, autoclaved cement composite, fibre boards, panels, door shutters, and wall plastering.
Groundnut Shell	Groundnut oil mills	for manufacturing chipboards, roofing sheets, particle boards, and building panels.
Jute Fibre	Jute Industry	for manufacturing roofing sheets, door shutters, and chipboards.
Rice/Wheat Straw	Agricultural Farm	Making of roofing units and wall panels and/or boards.
Saw Mill Waste	Sawmills/wood	Production of cement-bonded wood chip, particle, insulation, and briquettes boards.
Sisal Fibres	Sisal plantation	Used in the production of roofing sheets, roofing tiles, paper and pulp, and composite boards with rice husk cement roofing sheets.
Coconut Husk	Coir fibre industry	In the manufacture of building boards and roofing sheets, as a lightweight aggregate, coir fibre-reinforced composite, cement board, geotextile, and rubberised.

Source: ICFRE, 1995

2.2 Lignocellulosic composites

Currently, any wood substance that has been adhesively glued together is referred to as composite. The wood composites range from fibreboards to laminated beam and components. Composites are utilised in a variety of structural and non-structural product lines, including furniture and support structures in various types of buildings as well as panels for interior and external use (Maloney, 1993).

Based on particle size, lignocellulosic composites can be divided into three primary categories: materials made of veneer, particles, and fibres. These categories and the subgroups within them are essential since the properties of the board are diminished as component sizes decrease. Lignocellulosic fibre is used to make fibre boards, whether they are derived from wood or agricultural products (English, John and Andrej 1994).

2.2.1 Veneer–based materials

Many glued wood items are made from veneer, comprising decorative panels, structural panels for covering applications, and structural timber elements like beams and trusses (www.lhc.org.uk).

2.2.2 Plywood

A glued wood panel known as plywood is constructed of several thin veneer layers (0.5 to 5 mm), with the adjacent layers' grains typically running perpendicular to one another. Depending on the needs of the final application, the layers' quantity, thickness, and quality vary. The primary benefits of plywood over solid wood are:

      (i)   Almost equal numbers of attributes are spread out across the panel's length and width.

      (ii)   Higher splitting resistance.

      (iii)   Manufacturing capacity for very huge sheets.

Due to its ability to cover huge areas with a small amount of material, plywood improves the use of wood. The plywood's qualities are depending on the kind of wood, the veneer quality, the sequence in which the layers are arranged, and the adhesives that are employed (English *et al*., 1994)

2.2.3 Laminated veneer lumber

Laminated veneer lumber is made by parallel laminating veneers into boards that have thicknesses comparable to solid-sawn lumber (19.0–63.5mm) (LVL). The industry for laminated veneer timber currently employs veneers that are 2.5–3.2mm thick and hot-pressed with phenol formaldehyde glue into lengths of at least 2.4–18.0m. Joints, knots, and other imperfections are spaced apart when assembling the individual veneers for LVL production to prevent severe defects that would weaken the material significantly.

Rising prices and a lack of high-grade solid sawn lumber were driving factors behind some of the initial applications of LVL for scaffold planks and parallel-chord trusses. The use of LVL in light trusses and I-sections is made possible by the nearly non-existent strength-reduction flaws. In I-sections, the web is frequently composed of a structural panel product, such as plywood or hardboard, and is glued into a groove that has been machined in the LVL flanges. At the moment, light frame construction uses these I-section beams as joint and rafters (English *et al*, 1994).

2.3 Particle-based materials

Oriented strand board (OSB), chipboard, particleboard, wafer board, cement board, and many other subcategories are all included in the category of particle-based panel material. In contrast to solid wood, these manufactured wood products can be altered to satisfy the property requirements of certain purposes or a specific range of end uses (English *et al*, 1994).

2.3.1 Wafer board and Oriented strand board

The two main types of exterior panel products are wafer board and oriented strand board (OSB). The dimensions of the particles are 25–75 mm long, 10–30 mm broad, and 0.5-2 mm thick. The particles of wafer board are not purposefully orientated, and exterior-type glue is used to bind the board together. In general, the bending properties of OSB in the aligned direction outperform those of a randomly oriented wafer board when exterior-type resin is applied to wood strand alignment. As with any particle panel product, the manufacturing procedures significantly affect the properties (English *et al,* 1994).

2.4 Particleboards

Particleboards are particle panel products that are often formed from lignocellulosic particles like rice husks or small wood particles from mill leftovers such as sawdust, shavings, or flakes. Particleboards are challenging to classify due to the infinitely changing manufacturing processes employed to create the goods (English *et al*, 1994).

2.4.1 Cement board

Commercially, Portland cement is used as the binding agent for cement boards, a particular kind of lignocellulosic particle panel. Because they are lengthy (up to 250mm) and stringy, the wood particles that are generally employed are known as excelsior of wood wool. Cement is mixed with medium- to low-density wood species to create excelsior, which is then molded into mats and compressed to a density of 480 to 640 kg/m^3 (English *et al,* 1994).

Cement board is also made from non-wood lignocellulosic resources such bagasse, rattan, and fibre from coconut husks. Cement board is frequently used for roof decking because of its fire resistance and sound absorption capabilities. Other cement-bonded particle products include construction blocks and panels formed of flakes that can be used for exterior panelling, load-bearing walls, partitions, and doors (English *et al*., 1994).

2.4.2 Fibre-based panel materials

All of these panel components are made from lignocellulosic resources like bagasse or reconstituted wood. The wood is first broken down into fibres or bundles of fibre, and then it is put back together using special molds to create panels with quite big diameters. Based on the production methods, characteristics, and intended applications, different kinds of fibre-based panel materials have been developed (English *et al,* 1994).

2.4.3 Insulation board

This is the general term for a uniform panel made of wet-formed, disturbed lignocellulosic fibres (usually wood or bagasse). The panels are heated and pressed into a range of specific gravities between 0.16 and 0.50 (English *et al*, 1994)

2.4.4   Medium density fibreboard (MDF)

When lignocellulosic fibres are heated, typically in combination with a synthetic resin or another suitable binder, medium density fibreboard (MDF) is produced. MDF has a specific gravity range of 0.60 to 0.80. In MDF's homogenous structure, there are no discernible grains or knots visible at the edge, end, or face, nor are there any internal gaps, pits, or variations; it has a uniform texture and quality throughout (English *et al,* 1994).

MDF can be machined more easily than natural wood and is just as easy to laminate, paint, route, sand, and screw as natural wood products. It can be utilised in various applications, such as the production of doors, mouldings, external trim, and pallet decking, as a perfect substitute for solid wood since it possesses mechanical and physical qualities that are approaching those associated with solid woods (English *et al.,* 1994).

2.4.5   Hardboard

According to the American Hardboard Association, the term "hardboard" refers to a panel made mostly from interfelted lignocellulosic fibres that have been compressed under pressure and heat to a specific gravity of 0.50-1.45. Hardboards are classified according to their density, surface quality, thickness, and minimum physical characteristics. Both a wet and a dry technique are used to produce them (English *et al,* 1994).

Hardboards did not undergo any refinement to make discrete fibres or fibre bundles from the wood chips and particles. Hardboards are used for a variety of purposes, although they may generally be classified into the following groups: building, furniture and furnishing, cabinets, stone fixture work, appliances, automobiles, and rolling stock. Typical hardboard items include prefinished panelling, siding for houses, floor underlayment, and concrete forms (English *et al.*, 1994).

2.5   Bio-composite based on agricultural wastes

The potential use of agricultural waste in the production of particle- or fibre-based boards has been the subject of extensive research. There has also been research into the

use of natural resins as an alternative to formaldehyde resins (Odozi, Onu and Nweke 1986).

By combining naturally occurring tannins from red-onion peel extract and mangrove, an effort was made to lessen the cost-influencing effects of adhesives. The boards with the highest dry and wet strengths and the least amount of water absorption after five hours of soaking were manufactured from a blend of bagasse, mangrove bark, wood shavings, and corncob (4.4 percent). The strength levels could result from both the use of a high resin dosage and a high tannin content that can polymerize (Odozi et al. 1986).

Particleboards Coffee husks, a combination of coffee husks and cottonseeds, and a combination of coffee husks and pulverized nutshells were used to create 1.27cm thick sheets. As a binder, urea formaldehyde resin in various concentrations was utilized. The board strength and water resistance improved as a result of the material pressure, exceeding the British regulatory minimum strength for boards with a density of 1.1g/cm3 and a15% resin content. Boards had less strength when made from coffee husks combined with other debris than when made from coffee husks alone (Tropical Products Institute, 1963).

The treated cotton stalk particles were heat-pressed onto mats to develop particleboard. Cotton stalk particles were treated with aqueous solutions of ammonium chloride and urea formaldehyde condensate to manufacture particleboard. The 5 per cent ammonium chloride and urea formaldehyde solution is sprayed onto cotton stalk particles to produce 8 percent urea formaldehyde resin, which is subsequently dried at 60 degrees Celsius to 27 percent moisture content. In order to create a particleboard with a density of 0.71g/cm3, a moisture content of 8.1%, a tensile strength of 2.9MPa, a modulus of rupture of 6.6MPa, and a water absorption rate of 38% after two hours of soaking, the board was cold pressed to form a mat (Pandey, Mehta and Tamhankar 1979).

Crushed peanuts were coated with urea formaldehyde resin and catalyst to create a solid, self-supporting building and facing panel, which was then heated and pressure-cured into a panel. The produced panels can be used for ceiling and wall panelling

because they are devoid of layer and places for internal rupture (Anonymous, 1975). Pressurized Bauer treated corncobs and corn stalks, including husk and leaves, hammer-milled kenaf stalks, sunflower seed hull sand commercial oak flakes, created from a pall-man, were all employed in the production of dry-process, medium-density interior type experimental boards (Chow, 1975).

Bagasse fibreboards made of paraffin wax and pH-OH modified urea formaldehyde copolymer have good bending strength and improved water absorption resistance. At 170 degrees Celsius, bagasse fibre was moulded with a compressive strength of 2.5 to 7.8 MPa to produce a 4.29-mm-thick sample with a bending strength of 58.5 MPa and water absorption of 11.3 percent. The bagasse fibre contained 5.24 percent pH-OH modified urea formaldehyde copolymer and 2.5 to 7.8 percent paraffin wax (Shukla and Prasad, 1985).

Coir-ply boards were created using oriented jute as the face veneer and waste rubber wood and coir inside. Compared to teak wood, which has a lignin content of 39%, coir fibre has roughly 46%. As a result, it is more resistant to rotting than teak wood in both wet and dry circumstances and has higher tensile strength. This composite is mainly produced commercially in India by Natural Fibretech Ltd., Bangalore (Pravin and Viveka, 2015)

The rice husk board has become a versatile alternative to wood in many applications. The board has a clear advantage over wood and plywood because of the following benefits:

    i.   Termite resistance

    ii.   Resistance to decay

    iii.   Increase fire resistance

    iv.   Excellent mechanical qualities like internal bond strength, elasticity, dimensional stability, ability to hold screws and nails, resistance to abrasion, and surface hardness.

    v.   Increased water resistance

    vi.   Good durability.

    (Source: www.nrdc.org)

2.6   Palm product categories

It is helpful to think of the individual products as falling into three separate categories: primary, secondary or by-products, and salvage products when examining and evaluating palms for the variety of items they may and do provide (Butty, 1989)

2.6.1   Primary products

These are the main commercial, or occasionally food-related, products that come from palms. Typically, primary product processing takes place some distance from the actual harvesting. For instance, when palm stem starch or vegetable oil made from palm fruit is retrieved from the wild and offered for sale as a live ornamental plant, the entire plant may serve as the main product. (Butty, 1989)

2.6.2   Secondary and by-products

By-products are valuable objects produced directly from the primary product during processing. Secondary products are ones that need to go through one more processing step to become the final product that is wanted. The press cake left over after extracting seed oil and the coir fibre from the coconut mesocarp are two examples of by-products that can be given to cattle (Butty, 1989)

 However, some by-products have little to no economic value and, if they can't be used as fuel or fertilizer, even pose disposal issues. Arrack serves as an example of a secondary product since palm wine, the major product, must first be produced before arrack can be distilled (Butty, 1989)

2.6.3   Salvage products

This nomenclature describes those palm goods that are produced secondarily after the principal product is harvested. Products in this category are normally thrown away at the area of the harvest and are not moved as part of primary processing. Taking a palm heart from a wild tree; any leftover stem wood or leaves used as such are salvage palm products (Butty, 1989).

Salvage palm goods can also come from other activities, including cutting down palms for land-use purposes, replacing senescent palms, or repairing or replacing palms that have been damaged or destroyed by a tropical cyclone or other natural disaster. Living

decorative palms removed from a clearing site to prevent them from being destroyed would be regarded as salvage products in such a case (Cabrera, Hodgson, Armas, Santiago, Lorenzo, Prendes and Plata 1990)

2.7   Coir availability and potential

In tropical countries' coastal regions, coconut trees abound. The nutritive nut protective husk is widely available as a cheap by product of coconut production, which is also known to produce coarse coir fibre and pith, annual productions of coconuts in tropical Africa (in 1000 tons) as presented in Table 2.2. Timber has significant commercial potential. Around 300 million tons of wood are consumed globally each year (Martin, Edwin, Martien and Jan 2005)

More than 2 million tons of fibre are produced each year from the world's estimated 40 million tons of coconuts (or 25.000 million coconuts), yet only a small portion is used. According to estimates, approximately 400.000 tons of coir fibres are produced globally each year. Since approximately 15 to 20% of the available coir fibres are now used, there is no need to increase the volume of the annual output (Martin et al., 2005)

Table 2.2: Annual productions of coconuts in tropical Africa (in 1000 tons)

Country	1961-70	1971-80	1981-90	1995	1999
Benin	30	20	20	20	20
Cameroon	3	3	4	4	4
Cape Verde	10	10	10	5	5
Cote d'Ivoire	26	101	315	190	221
Equatorial Guinea	6	7		8	8
Ghana	237	240	267	245	310
Guinea	18	18	18	18	18
Guinea-Bissau	24	26	25	42	44
Kenya	69	73	42	50	72
Liberia	6	7	7	7	7
Madagascar	16	36	79	82	84
Mozambique	379	432	415	438	450
Nigeria	87	90	102	149	152
Sao Tome and Principe	46	37	35	26	29
Senegal	5	4	5	5	5
Sierra Leone	2	3	3	3	3
Somalia	3	8	14	9	7
Tanzania, United Rep.	275	291	332	370	340
Togo	22	14	14	14	14
World	27,768	33,472	38,693	48,451	48,569
Africa	1,370	1,502	1,780	1,762	1,874

Source: FAO, 1994.

2.7.1 Coir structure

Coir fibres lie between the husk and the coconut outer shell. The individual fibre cells are composed of cellulose and have thick, hollow walls that are narrow and hollow. They are light in colour while young, but as they age, they turn hard and yellow as a layer of lignin is deposited on their walls. Coir is available in two varieties. From completely ripened coconuts, brown coir is collected. It has a good resistance to abrasion and is thick and sturdy. It frequently appears in sacking, matting, and brushes (Bismarck, Mohanty, Aranberri, Czapla, Misra and Hinrichsen 2001).

The mature brown coir fibres have more lignin and less cellulose than fibres like flax and cotton, making them stronger but less flexible (Bismarck et al., 2001). They are composed of tiny threads that are 10 to 20 micrometres in diameter and 1 millimetre long each. Before they are fully ripe, coconuts are plucked for their white coir fibres. They are also weaker. Typically, they are spun to create yarn for mats or rope. One of the few natural fibres that is resistant to harm from salt water is the coir fibre, which is comparatively water-proof. White coir is made using both freshwater and seawater.

2.7.2 Coir fibre structure

The dimensions and configuration of the numerous unit cells, which also affect the fibre characteristics, determine the coir fibre structure. According to certain theories, the type of species, location, and plant maturity all affect how big different individual cells' fibres are. The length-to-diameter (l/d) ratio of the fibre influences its flexibility and ability to rupture and it also affects the products that can be created from it (Fowler, Hughes and Elias 2006).

A central hollow chamber known as the lumen is present in the transverse parts of the unit cell of a fibre. Its size and shape are determined by two elements: the cell thickness wall and the origin of the fibres. Because it reduces the bulk density of the fibre, the hollow hole acts as an acoustic and thermal insulator (Fowler et al., 2006).

2.7.3 Influence of fibre property on mechanical strength

A fibre structure and properties are determined by the quantity of cellulose and non-cellulose components present, which affect crystallisation and moisture regain. The internal structure of composition of fibre affects characteristics like tensile strength,

density, and Young modulus. Higher lignin content, a lower length-to-diameter ratio, and a higher microfibrillar angle result in fibres with lower mechanical strength and Young's modulus but better and greater extensibility (Fowler *et al.*, 2006).

Contrarily, fibres with higher cellulose content, greater levels of polymerisation, and lower microfibrillar angles offer better mechanical characteristics. Composition, structure, and defect density all affect all fibre mechanical properties, including Young modulus, stress, and strain. When intracellular or intercellular modes of stress result in tensile failure, the fibres with high cellulose crack cause intracellular fracture without the removal of microfibrils, while the fibres with low cellulose crack cause intercellular fracture without the removal of microfibrils. The capacity of a fibre to elongate is influenced by its orientation, high degree of crystallisation, and angle of inclination of the microfibrils to the fibre axis (Fowler *et al.*, 2006).

2.7.4   Coir processing

The coconut is a fruit that grows on palm trees that flower monthly and takes a year to maturity. Every stage of fruit maturity can be found on a normal palm tree. 50–100 coconuts can be produced annually by a mature tree. Both while still on the tree and after they have ripened and fallen to the ground, coconuts can be collected. A human climber can cut down about 25 trees per day, while a pole-mounted knife can cut down up to 250 trees each day. Although trained monkeys can also collect coconuts, this approach is less effective than others (George, 1982).

Green coconuts have supple white fibres and are picked after growing for around six to twelve months. Harvesting fully developed coconuts produces brown fibre, and the nutrient-rich layer surrounding the seed is ready for processing into copra. The fruit is driven down onto a spike to split it, and the fibrous layer is then manually extracted from the hard shell (De-husking). A skilled husker is capable of physically separating 2,000 coconuts every day. There are now machines that can smash the entire fruit to release the free fibres. These devices have a capacity of up to 2,000 coconuts per hour (George, 1982).

2.7.5   Brown fibres

The fibres in the fibrous husks softened and swelled as a result of being soaked in pits or nets of slowly moving water. The long bristle fibres are separated from the shorter mattress fibres under the nut skin using a process called wet milling. The mattress fibres were sifted to eliminate dirt and other trash, and then dried outside before being bundled into bales. Some mattress fibres are permitted to absorb more moisture so that they can maintain their flexibility for the manufacture of twisted fibres. The coir fibre is flexible enough to twist without snapping, and it keeps its curl as if it were permanently waved (Nagaraja and Basavaiah, 2010).

Making a rope out of the fibre hank and twisting it either by hand or by machine is how you twist. The longer bristle fibre is dried after being cleaned in clean water and is then wrapped into bundles or husks. After that, it can be cleaned with a steel comb to straighten the fibres and remove any shorter fibre fragments. Remove any shorter fibre fragments from the coir bristle. Additionally, coir bristle can be bleached and dyed to produce hanks in a variety of colours (Nagaraja and Basavaiah, 2010).

2.7.6   White fibres

For up to ten months, the immature husks are suspended in a river or pit filled with water. Microorganisms loosen the fibre-encircling plant tissues at this time, a process known as retting. The long fibres are then separated out of the husk segments by hand, dried, and cleaned. Clean fibre can be spun into yarn either by a simple one-handed method or on a spinning wheel (Nagaraja and Basavaiah, 2010).

2.8 Coir dust

2.8.1 Composition of coir dust

With a carbon-nitrogen ratio of about 112:1, coir dust has high levels of cellulose (26.7%) and lignin (30–31%). The cellulose in cell walls is surrounded by lignin, a complex amorphous polymer of phenyl propane that is relatively resistant to hydrolysis. Coir dust takes decades to degrade because of the high lignin content that was left in it. (Das, Radhakrishnan, Sumy, Abesh, Geena, Divya, Sinjula and Satheeshkumar 2016)

2.8.2 Structure of coir dust

A structural function similar to that of epoxy resin and glass fibre in a fibre glass boat is provided by the interaction of lignin and cellulose in plants. While the matrix, consisting of lignin or epoxy resin, offers stiffness and rigidity, the fibrous components cellulose or glass fibres serve as the main load-bearing elements. Since grasses (lignin concentration below 20%) cannot bend under their own weight, trees (lignin content between 20% and 30% of dry weight) can grow much taller before they can. The fact that there are numerous potential bending patterns between individual units adds to the intricacy of lignin (Das *et al*, 2016).

In addition to its position as a structural component, lignin has a number of additional crucial biological functions in plants. Compared to cellulose and hemicellulose, it is significantly less hydrophilic, which inhibits these polysaccharides from absorbing water in plant cell walls and promotes effective water transport in vascular tissue. Lignin-based barriers also successfully repel insect and fungal attack. (Das *et al*, 2016).

2.8.3 Properties of coir dust

Coir dust is a resistant agricultural residue with high levels of lignin and cellulose that resists microbial breakdown in the environment. The presence of lignin is what makes coir dust so resistant. 8–12% of it is soluble tannin, similar to phenolics. The high water holding capacity of coir dust is eight times its weight. It contains lipids, ash, fixed carbon, and low sulphur (Radhakrishnan, Anita, Abesh, and Geena, 2018).

The amount of nutrients in coir dust varies according to location, decomposition rate, and storage method.

Major characteristics of coir dust include:

    i.   High water capacity, equivalent to 6–8 times its weight.

    ii.   Excellent retention of moisture even after drying

    iii.   Slow decomposition because of a high lignocellulosic boundary

    iv.   High porosity; nutrients are stored and released over a long length of time.

    v.   Better physical resilience to tolerate compression

    vi.   Outstanding aeration and oxygenation enhance root penetration.

vii. Acceptable cation exchange capacity(CEC) , electrical conductivity (EC), and pH

viii. Organic, renewable resource that is completely biodegradable.

ix. Has naturally occurring substances that are good for plant growth.

(Source: Das et al, 2016).

2.9   Cashew

The botanical name of cashew is *Anacardium occidentale* L. Coastal regions in Asia and Africa are where cashew trees thrive**.** The sketch of a cashew fruit is presented in Figure 2.1. Brazil, India, and Mozambique are the largest world producers of cashew nuts and cashew nut shell liquid (Nayak, and Paled, 2018).
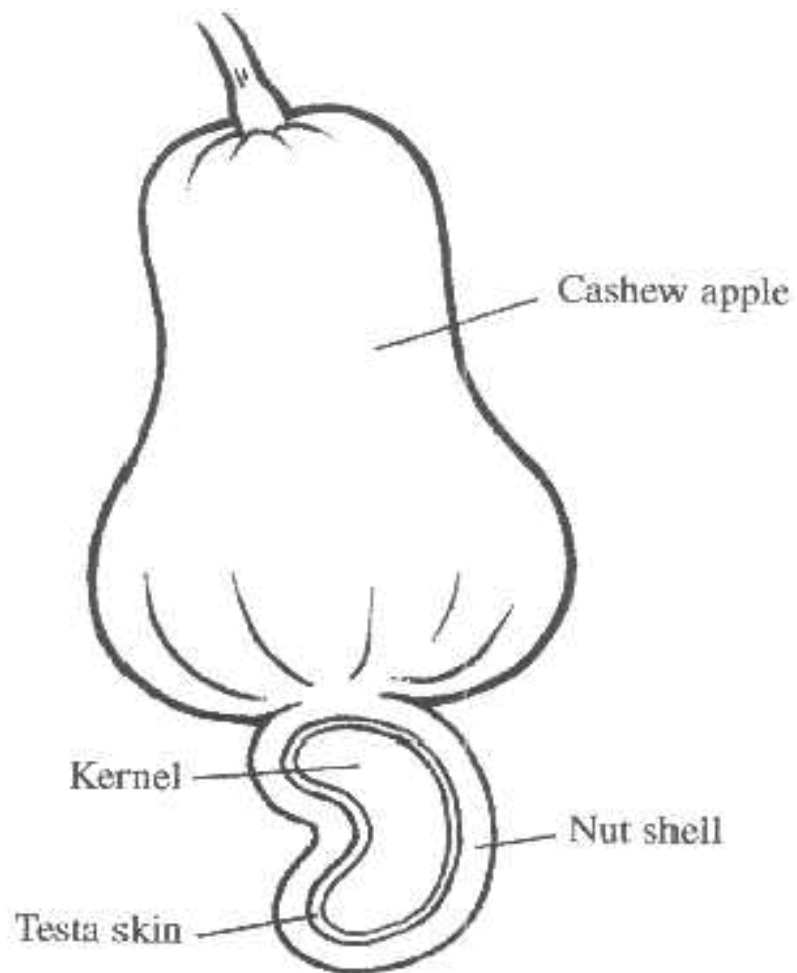
Figure 2.1: Cross section of a cashew fruit

2.9.1 Composition of cashew nut shell

The nut includes the following:

    *Kernel 20 to 25%

    * 20–25% of the kernel is liquid.

    *Testa 2% others are the shell of the cash

2.9.2 Uses of cashew

Since 400 years ago, cashew trees have been grown for food and medicine. Cashews have fulfilled dietary, medical, and military demands. They have more recently been utilised in the production of resins, adhesives, and natural pesticides. The cashew tree became expensive during World War II as the source of valuable oil extracted from the shell (FAO, 2001).

The cashew kernel is a high source of calcium, phosphorus, and iron, as well as a rich source of fat (46 per cent) and protein (18 per cent). It contains a lot of polyunsaturated fatty acids, especially linoleic acid, an important fatty acid. The sour apple contains calcium, iron, and vitamin C. There are medicinal uses for the bark, leaves, gum, and shell. The leaves and bark are frequently used to treat toothaches and sore gums, and the leaf or bark extract cooked in water is employed as a mouthwash. Ringworm is treated topically with a paste made from crushed bark and water; however, because of the potential for irritation, neither skin of children nor delicate skin should be exposed to it (George, 1982).

A purgative has been made from the root. The leaves' fibres can be used as a vitamin supplement, to reinforce fishing lines and nets, as a traditional remedy for intestinal colic and calcium deficiencies, and more. Boats and ferries are made of water-resistant wood, and resin is used for a variety of industrial purposes as well as expectorants, cough remedies, and insect repellent (George, 1982).

2.9.3 Uses of cashew nut

The shell, the kernel, and the adhering testa are the three components that make up a cashew nut kernel (Figure 2.1). The kernel is the edible part of cashew nuts, which can be consumed in three different ways:

    i.   Consumed directly.

22

ii. By a salted and roasted nut.

iii. Finely chopped kernels, for instance, are used in the manufacture of sweets, ice creams, cakes, and chocolates, both at home and in factories, as well as a paste for spreading on bread.

At least 60% of cashew kernels are believed to be consumed as salted nuts, although the relative importance of these uses changes from year to year and country to country. Separately packaged cashew nuts are a successful product, primarily used as an aperitif with cocktail cocktails. The snack food industry includes salted cashews. They primarily compete with other nuts, but chips, salted popcorn, and other savoury treats can also affect the nut market. Cashew nuts cost a lot more than peanuts or other snacks; hence, consumers' strong taste preferences must be the driving factor in sales. Generally speaking, cashew nuts are a luxury good, and this perception may contribute to some of their attractiveness (Ikhuoria and Aigbodion, 2006).

2.9.4   Uses of cashew apple

The nut is just one of the goods consumed by locals in nations that produce cashews. An edible food high in vitamin C is the cashew "apple" or fake fruit. You can consume it fresh off the tree, dry it, or can it as a preserve. Alternatively, it can be squeezed to produce fresh juice, which can then be fermented to produce cashew wine, a popular drink in West Africa. It is employed in some regions of India to distil "feni," a type of cashew liquor. Some locals in South America prefer eating apples to nut kernels as a delicacy. Apples are used to produce jams, soft drinks, and alcoholic beverages in Brazil. (Menon, Aigbodion, Pilla, Mathew and Bhagawan 2002)

The cashew tree produces a fake fruit called an "apple of cashew," from which the nut protrudes. The cashew apple has smooth, shiny skin and is between three and five inches long. As it ages, its green skin changes to a vivid red, orange, or yellow. Its structure is pulpy and luscious, and its flavour is nice yet strongly astringent (Menon, 2002).

2.9.5 Using cashew apples in recipes

The goal should be to have the fruit arrive in the best condition possible when collecting and transporting it for processing. Only mature, undamaged cashew apples should be chosen for use in recipes after being sorted in order to prevent contamination. Prior to usage, these should be rinsed in clean water. (ASTM 1991)

2.9.6 Cashew wine

Many nations in Asia and Latin America produce cashew wine. It is a bright yellow alcoholic beverage with a 6–12% alcohol level.

2.9.7 Processing

When cashew apples are crushed in the juice press, they are sliced into slices to promote a quick rate of juice extraction. To get rid of any wild yeast, the fruit juice is heated to 85 °C and sanitised in stainless steel pans. The juice is filtered and treated with sodium or potassium metabisulfite to either kill or stop the growth of unwanted microorganisms such as acetic acid bacteria, wild yeasts, and moulds (Menon *et al*, 2002).

It is necessary to include wine yeast (Saccharomyces cerevisiae var. varellipsoideus). The juice is thoroughly agitated after the yeast has been introduced, and then it is allowed to ferment for about two weeks. Fining ingredients, such as gelatin, pectin, or casein, are combined with the wine to clarify it and separate it from the sediment. Filter aids like earth fuller are used during the filtering process. Wine that has been purified is then put into wooden vats (Menon *et al*, 2002).

At 50–60 °C, the wine is pasteurized. Due to the fact that alcohol vaporises at a temperature between 75 and 78 °C, the temperature should be kept under70 °C. The wine is then allowed to mature while being kept in wooden vats. Ageing should be allowed for a minimum of six months. Before bottling, the wine should, if necessary, undergo another clarification. Numerous processes, including oxidation, take place while wine is aged and then matured in bottles. Together with the tannin and acids that are already present, the creation of traces of esters and aldehydes improves the flavour of wine, fragrance, and preservation abilities (Wimalsiri, Sinnatamby, Samaranayake,

and Samarasinghe 1971). Glass bottles with corks are used to package the product, which needs to be kept out of direct sunlight.

2.9.8 Dried cashew fruits

Due to their high concentration of astringent chemicals, cashews are rarely eaten in their raw state. The fruit can be transformed into a valuable dried good if these are removed and it is sweetened. So, before drying, the fruit needs to go through a lot of processing. (ASTM, 1991)

The following steps are taken in the preparation of fruits:

i. Fruits are gathered from trees using specialised hooked sticks (note that fruits harvested at this stage of maturity contain nuts that are immature). To get rid of the astringent ingredients, the fruit is washed and cooked in salted water (a 2% solution) for five minutes.

ii. To extract the juice, a tiny hand press is used to press the fruit after poking the skin with a fork. The juice that has been collected is set aside for future use.

iii. The fruit is boiled for three hours in a mixture of cashew juice and unrefined sugar (2 kg of raw sugar in 10 litres of juice). Other sweeteners, such as 1.2 litres of cane juice in 1 litre of cashew juice, 0.5 kg of white sugar in 1.8 litres of cashew juice, and 250 ml (1 cup) of honey in 2 litres of cashew juice.

iv. The fruit is set out on screens and put in a dryer after being boiled and sugared. Drying takes three days or so in a basic solar dryer.

v. Airtight, moisture-resistant packaging is used to package the fruit.
   Source: Brown, 1992.

2.9.9 Specification of cashew nut shell

The shell is around 0.3 cm thick, with a thin, hard inner skin and a soft, feathery outer skin. The honeycomb structure with the phenolic substance known as CNSL is sandwiched between these skins. The kernel is contained inside the shell and is covered by a thin layer of skin called the testa (Nayak, and Paled, 2018).

2.9.10 Chemical composition of CNSL

Low water solubility and low vapour pressure characterise the liquid known as CNSL. It is made from phenols that are naturally present in cashew nut shells. By weight, the

shell makes up around 50% of the raw nut, followed by the kernel at 25% and the natural CNSL, a viscous reddish brown liquid, at 25% (Maria and Gouvan, 1999). Approximately 30–35% of the CNSL, or about 67% of the nut, is found in the shell, as presented in Table 2.3.

Traditionally, the process of separating the cashew kernel from the nut yields cashew nutshell juice as a byproduct (US-EPA, 2009). The extracted oil contains alkyl-substituted phenolic compounds, and as a result of their structural makeup, these molecules exhibit antioxidant capabilities (Maria, Franscisco and Selma 2009). The CNSL can be extracted in hot oil using the technical CNSL method, in liquid form (solvents), mechanically from the shells, or by vacuum distillation.

Anacardic acid, cardanol, cardol, and 2-methyl-cardol are all present in varying amounts, depending on the extraction procedure, but generally speaking, the composition of natural CNSL is a mixture of these substances (Maria, Selma, Jose and Glaucione 2007; Maria, 2008). Anacardic acid, which makes up around 70% of the solvent-extracted CNSL (Figure 2.2), cardanol, which makes up 18% of it, and the remaining phenols and less polar compounds make up the rest of the liquid. With varying degrees of unsaturation in the akyl side chain, anacardic acid, cardanol, and cardol are mixtures of components as presented in Figures 2.2, 2.3, and 2.4.

Anacardic acid is decarboxylated to produce cardanol during the heating process in heat-extracted CNSL (technical CNSL). Heat-extracted CNSL typically contains 52% cardanol, 10% cardol, and 30% polymeric material, with the remaining ingredients being miscellaneous compounds. To get rid of the polymeric material, the technical CNSL is frequently further processed by distillation under decreased pressure. About 78% of distilled technical CNSL is made up of cardanol; 8% of it is cardanol; 2% of it is polymeric material; less than 1% of it is 2-methyl cardanol; 2.3% of it is heptadecyl homologue triene; 3.8% of it is heptadecyl homologue diene; and the rest is various homologous phenols (Nayak, and Paled, 2018).

Table 2.3: Physical–chemical properties of cashew nut shell liquid

Property	Value
CASRN	8007-24-7
Molecular Weight	298-320
Physical State	Liquid
Melting Point	Liquid at room temperature
Boiling Point	Polymerizes and decomposes prior to boiling[3]
Vapor Pressure (measured)	3.8×10^{-7} mm Hg at 25°C
Water Solubility (measured)	0.305 mg/L at 20°C
Dissociation Constant (pKa)	~10.06 (estimated)[2]
Henry's Law Constant	2.6×10^{-10}–9.7×10^{-5} atm-m3/mole (estimated)
Log Kow	>6.2 (measured)

Source: Cardolite Corporation, 2006; [2]SPARC. 2008. [3]BP 225°C @ 10 mmHg US Patent 2,098,824
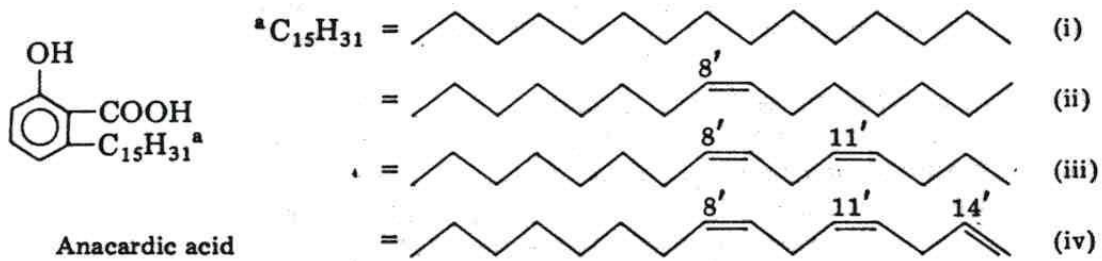
Figure 2.2: Structure of Anacardic acid
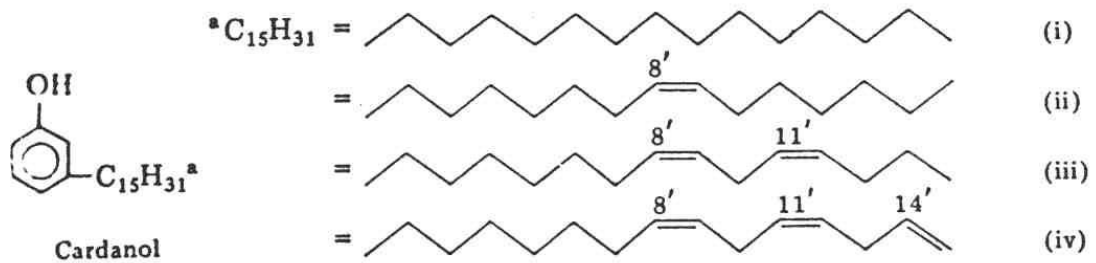
Figure 2.3: Structure of Cardanol
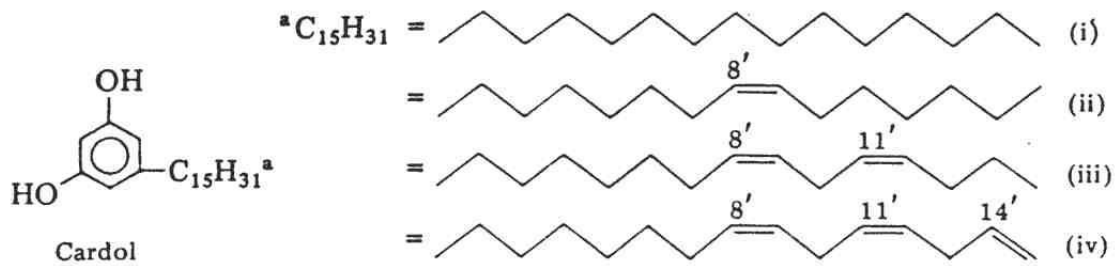
Figure 2.4: Structures of Cardol
(Sources: **US-EPA, 2009)**

2.9.11 Uses of cashew nut shell liquid (CNSL)

A significant and useful industrial raw material is cashew nut shell liquid (CNSL). In particular, more than 200 patents cover its use as a source of phenolic resins and friction powder for the automotive sector (brake linings and clutch disks). Cashew resins serve as fillers and maybe as binders in compounds used to line drum brakes. Resin of cashew function in disc pads is limited to acting as filler for friction dust. The benefit of using cashew resins over synthetic phenolic resins is that they are more affordable and result in softer materials, hence a quieter braking action (Tola, and Mazengia, 2019).

In addition to being employed as insecticides and fungicides, Furthermore, CNSL is utilised in moulds, acid-resistance paints, foundry resins, varnishes, enamels, and black lacquers for vase decoration. CNSL has been used to treat leprosy, elephantiasis, psoriasis, ringworm, warts, and corns in tropical medicine (Tola, and Mazengia, 2019).

Similar to cashew nuts, CNSL has a robust international market, and its imports, which account for the sale of the raw liquid, have reached about ₦5.4 billion ($10 million) annually. However, exporting manufactured goods would bring in far more foreign exchange for the exporting nation (Xing, 2016).

The cashew nut shells can be used to make agglomerates or burned after the CNSL has been extracted to provide heat for the decorticating process. It can be used, along with the testa, to make dyestuff or to make fishing lines and hammocks more durable (Xing, 2016).

2.9.12 New applications of CNSL

Liquid crystalline polyester that is new and less expensive and that can replace polymer films and fibres in specialised applications has been created using cashew nut shell liquid. Since they have the potential to be used as high-performance materials, liquid crystalline (LC) polymers have received a lot of attention (Xing, 2016).

2.9.13 Paints and enamels

CNSL is used to create dark-coloured paints and enamels due to its dark colour. The Regional Research Laboratory in Hyderabad, the Central Institute of Fisheries

Technology in Cochin, Bombay University, and the Research, Design, and Standards Organisation in Lucknow have all developed several anti-corrosive paint formulas for ship bottoms. The qualities of paints and varnishes made from CNSL are better than those of traditional oils or synthetic resins. Sulphur has been added to CNSL in order to create varnishes that are resistant to water and gasoline (Sharma, Gaur, Sirohi, Larroche, Kim, and Pandey, 2020).

The lacquers made from CSNL could be used as decorative, protective, or insulating coverings for furniture, buildings, and cars. The films are strong and flexible, have great gloss, and have superfine adhesive properties. Regarding resistance to oils, grease, moisture, and chemicals, the dried films outperform those of regular oil paints Ordinary oil varnishes are more expensive than cashew lacquers (Kyei, Eke, Darko, and Akaranta, 2022).

2.9.14 Electrical insulating varnishes

Electrical insulating varnishes are produced by treating CNSL with formaldehyde and then combining the resulting material in the correct proportions with pure phenolic resin varnish or alkyd resin. Films made from these materials can be used as surfaces for lab tables, bobbin enamels, and insulating varnishes with high electrical resistance (Voirin, Caillol, Sadavarte, Tawade, Boutevin, and Wadgaonkar, 2014). Additionally, they are resistant to chemicals and water.

2.9.15 Polymers

The formaldehyde reaction of cashew polymers produces a rubbery gel that can be used as a cement hardening agent that is resistant to the reactions of acids and alkalis. Cementing floors that have been subjected to chemical attack is possible with it (Li, Wu, Chen, and Jiang, 2018).

By enhancing CNSL by heating it at 160 °C in the presence of specific accelerators, it is possible to produce stove enamels that are resistant to alkali and acid solutions, mineral and fatty oils, and a variety of organic solvents. Insecticidal coating formulations can be created by treating CNSL or chlorinated CNSL with formaldehyde gums and resins, drying or semi-drying oils, and DDT and gamagexane (Li, *et al.,* 2018).

In addition to polymeric goods, CNSL serves as the primary raw material for other crucial chemicals and chemical intermediates used in industry. Cardanol's chlorinated by-products and its hydrogenated form have been discovered to have pesticidal effects. The cardanol numerous constituents can be appropriately changed to produce emulsifiers, surface-active agents, dyestuffs, antioxidants, plasticizers, stabilisers, accelerators, curatives, reclamation agents, and ion-exchange resins (Voirin, 2014).

2.9.16 Laminating resin

CNSL and cardanol derivatives are widely used in the laminating industry to reduce brittleness and increase laminate flexibility. This sort of resin is created by combining phenol, CNSL, and formaldehyde. Additionally, the resins have better age hardening and substrate bonding. The synthesis of cardanol and the creation of laminating resins require the use of 900–1000 metric tonnes of CNSL in the lamination sector (Anonymous, 2010a).

2.9.17 Rubber products

It has been discovered that adding CNSL to rubber formulations enhances the performance of rubber goods. It facilitates processing and improves the characteristics vulcanisate. The natural rubber vulcanisates' insolubility in petroleum solvents is improved by CNSL. It facilitates the addition of chemicals to rubber and raises the material moisture resistance of material. Cu, Ba, and Zn oxydes harden CNSL and produce products with a hard texture (Voirin, 2014).

2.9.18 Phenoplasts

Cardanol and its derivatives can also be used to create phenoplasts, which have advantages over traditional phenol-based systems in terms of process-ability, hydrocarbon solubility, and acid and alkali tolerance. It has been discovered that CNSL molding powders, shellac, and fillers including wood flour, sawdust, and asbestos produce items with great finishes, good flexural and tensile strengths, and enough water resistance (Li, Wu, Chen, and Jiang, 2018).
.

The combination of CNSL, formalin, natural rubber, synthetic rubber, and other common chemicals is used to make stiff or flexible covering materials in the form of tiles or sheets. Composite panels appropriate for partitions, claddings, and flush doors

33

have been created using resins based on CNSL, lightweight sandwich-type polymers (Lubi, and Thachil, 2000).

There have also been foam polymers created using CNSL and its derivatives. It has been discovered that adding CNSL to rubber formulations enhances the performance of rubber goods. It facilitates processing and improves the characteristics of vulcanisate. Natural rubber vulcanisates are more insoluble in petroleum-based solvents when treated with CNSL. The assimilation of moisture is aided by it. Hardened CNSL and hard products are produced by the oxidation of Cu, Ba, and Zn (Lubi, and Thachil, 2000).

In addition, CNSL is used to make oil-cloth finishes, floor tile laminate resins, rubefaciants, and vessicants for the treatment of skin disorders and in tropical medicine. At CNSL, various polymeric products made from unsaturated phenols can be polymerized to provide chemical intermediates that can be used in industry (Voirin, 2014).

2.9.19 Modified CNSL

By appropriately modifying the various cardanol constituents, emulsifiers, surface-active agents, dyestuffs, antioxidants, plasticizers, stabilisers, accelerators, curatives, reclamation agents, and ion-exchange resins can be produced. Stove enamels are produced by heating CNSL modified with certain accelerators between 160 and 3000 °C. These enamels are resistant to mineral and fatty oils, alkali and acid solutions, and various organic solvents (Lubi, and Thachil, 2000). When CNSL or chlorinated CNSL is treated with formaldehyde, gums and resins, drying or semi-drying oils, and DDT and gammexane, coating formulations with insecticidal capabilities can be created (Lubi, and Thachi 2000).

The extracts from peanut shell tannin, aldehydes, and cashew nut shell liquid were copolymerized into resins. To create oleoresinous wood varnishes, the resins were combined with bitumen (Akaranta and Aluko, 1994).   .

2.9.20 CNSL as a fuel for carbonisation

Cashew nut shell liquid contains characteristics similar to those of fuel that merit further research. A 40 per cent oil output maximum had been reached (15–16% up to 150 °C plus 24% from pyrolysis). The largest proportion of oil could be produced with the best results at 500^0 C for pyrolysis. But in the temperature range between 400^0 C and 500^0 C, the liquid-to-oil ratios were unaffected by the maximum temperature of pyrolysis. As a result of the oil from CNSL is very high calorific value, which is comparable to that of petroleum fuels. It is a promising bio-oil that has the potential to be used as fuel (Das and Ganesh, 2003).

When CNSL was heated to 175^0C, it produced dark brown oil, which was then extracted. The CNSL was then pyrolysed under vacuum. In order to obtain a flammable oil fraction and an incombustible watery fraction, the pyrolysis vapours were condensed. Liquid column chromatography was one of the techniques used to perform in-depth chemical compositional analysis of both the oil and aqueous fractions (Das and Ganesh, 2003).

The CNSL oils were discovered to be a naturally occurring, renewable supply of unsaturated phenols with long linear chains and a clear absence of anacardic acid. In comparison to other bio oils, CNSL oils have been found to be relatively stable. The oils promised to be a possible fuel because they were totally miscible in diesel and would not corrode copper or stainless steel (Das, Sreelatha and Ganesh 2004).

2.9.21 Adhesives

Adhesives suitable for plywood are made by oxidising CNSL with potassium permanganate or manganese dioxide at 100 °C, reacting with paraformaldehyde, and compounding with $CuCl_2$. Effective plywood adhesives are also produced by CNSL when it is combined with furfural, aniline, and xylol (Voirin, 2014).

2.9.22 Foundry core oil and other chemicals

The use of CNSL as foundry core oil demonstrates its adaptability. After baking, CNSL resins are known to give sand cores good scratch hardness. Furthermore, it provides exceptional green strength, surface polish, and resistance to moisture and weathering to moulded items. In this regard, it specifically replaces linseed oil. In

comparison to traditional core binders, modified CNSL resin was found to improve the collapsibility of core, bench life, and anti-damp behaviour (Anonymous, 2010a).

2.9.23 Medicinal applications

The king of dry fruits, the cashew, is not only the greatest garnish for a sumptuous dessert but also an aphrodisiac with a long list of medicinal benefits. According to research data released by the Cashew Export Promotion Council of India, in Kochi, cashews, of which India is the top grower in world, have immense latent and therapeutic potential. Cashews, which contain 21% protein and an equal amount of polyunsaturated fatty acids, significantly lower blood cholesterol levels, reducing the risk of heart attacks (Brufau, Boatella, and Rafecas, 2006).

Cashews have extremely low levels of soluble sugar and saturated fat, which may help someone lose weight. Additionally, the calcium, phosphorus, and iron-rich cashew kernels helps guard against anemia and disorders of the nervous system. In actuality, the plant proteins found in cashew kernels are comparable to those found in milk, eggs, and meat. Additionally, it has a high concentration of essential acids in the appropriate amounts, which are typically relatively rare in nuts (Voirin, 2014).

An average cashew kernel has 47% fat, of which 82% are unsaturated fatty acids. The level of blood cholesterol is reduced by this unsaturated fatty acid. A, D, and E vitamins are the most prevalent vitamins in cashews. These vitamins boost immunity while assisting with fat absorption. Consuming cashew kernels can also help preserve the nervous system because they are a great source of nutrients like calcium, phosphorus, and iron (Menon *et al*., 2002).

According to the Indian Cashew Journal, an official magazine of the Cashew Export Promotion Council, the cashew kernel has a very low carbohydrate content as little as 1% of soluble sugar which implies that one is able to enjoy a sweet taste without worrying about eating too many calories. Diabetes management is one of the key benefits of cashew. Adding that these vitamins have a moderating effect on the B group vitamins and help with the digestion of lactose and thiamine, roasting cashews also produces the recently discovered vitamin PP (Menon *et al*., 2002).

All reproductive issues are resolved by the vitamin E in cashews, which also stops the growth of oxidative rancidity in fats. The experts of council claim that the kernel of cashew has high linoleic acid content makes it the perfect digestive assimilative stimulus because linoleic acid has a structure that is ideal for the synthesis of prostaglandins, a wonder compound found in many body organs and having a significant impact on a variety of bodily functions. These qualities are improved by roasting and toasting the kernels (Menon *et al*., 2002).

As a carrier for linaments and other external uses, cashew kernel oil is also regarded as an effective mechanical and chemical antidote for irritating toxins. The kernel is a suitable diet for people with persistent and frequent vomiting and is also sometimes used as a substitute for almond paste (Menon *et al*., 2002).

One of the most well-known Indian medical systems, Ayurveda, recommends Indian cashew nut as a good stimulant, rejuvenator, appetiser, superb hair tonic, aphrodisiac, and restorative, in addition to listing quite a few other uncommon healing benefits of the nut. Leprosy patients were given cashew fruit as an anaesthetic, and it was also used to treat warts, corns, and ulcers (Aigbodion and Okiemen, 1995).

While the oil extracted from the shell is beneficial for foot cracks, the juice from the nut can be used as an iodine alternative. The cashew apple has very excellent antiscorbutic characteristics, and both the fruit and the wine prepared from it do, since it contains 261.5 mg of vitamin C per 100 grammes and 10.44 percent fermentable sugar. A diuretic having positive effects on kidney health and advanced cholera cases, the liquor is also prized for its other properties (Aigbodion and Okiemen, 1995).

In addition to its commercial significance as an alcoholic beverage, cashew feni, which is quite common in Goa, is reported to have considerable therapeutic value. For ages, Goans have used it as a remedy for illnesses including diarrhoea, cholera, and even worm sickness in infants (Aigbodion and Okiemen, 1995).

2.10 Cement material

There are several different kinds of cement binders, but Portland cement is the most widely used. Compounds of calcium are widely used in the production of the binding

agents. These are powdered substances, which form a plastic mass and mixed with water set into a strong solid. They include cement, gypsum and lime (Simatupang, 1979).

Chemically, cement is mainly a silicate and aluminates of calcium i.e. contain Si and A1 elements which are liable to form hetero chain polymers (based on Si-O-Si and A1-O-A1 bonds) as presented in Table 2.4. Various types of cement are distinguishable according to silicate cement (Portland) and aluminates (aluminous) cement (Simatupang, 1979).

Silicate cement are synthesized by calcining a finely ground mixture of limestone and clays rich in SiO_2 at 1400^0C to 1600^0C until the Si-O-Si bonds are partially broken to form silicates simple in structure with the librations of carbon dioxide (CO_2).When this ground clinker is mixed with water, a partly mass is obtained that gradually sets (Simatupang, 1979).

The hardening of cement is due to complicated processes of the hydration and poly condensation of the constituent of the clinker, resulting in the formation of high molecular calcium silicates (Portland cement). The use of Portland cement of lower calcium content (di-calcium) over higher tri-calcium silicate content for cement bonded panel is advantageous in that the compression strength exhibited by this type of cement following a 24 hour curing period is high. This confirmed the fact that the type of cement used affects the strength properties of the board (Simatupang, 1979). Chemical composition of ordinary Portland cement is shown below (ECO-CARE, 2005).

Table 2.4: Typical Ordinary Portland Cement's chemical content

Ingredient	Percentage (%)
Lime (CaO)	62
Silica (SiO_2)	22
Alumina (Al_2O_3)	5
Calcium sulphate ($CaSO_4$)	4
Iron oxide (Fe_2O_3)	3
Magnesia (MgO)	2
Sulphate (S)	1
Alkali	1
Total	**100**

Source: ECO--CARE (2005)

2.10.1 Inorganic-bonded lignocelluloses composites

These are composite materials with a mineral or mineral mixture acting as the binding agent. The three most common inorganic binder methods are Portland cement, gypsum, and magnesium oxide. Because gypsum and magnesium oxide (magnesite cement) are both moisture-sensitive, interior applications are where composite products created with them are most often used (English, 1994).

Products made of Portland cement are more durable and can be used both inside and outside (English, 1994). lignocellulosic fibres and cement are combined to create cement board. The product has good insulating qualities, is lightweight, and is simple to saw and nail (English, 1994). Additionally, it has a high resistance to decay, insect, and vermin attacks. There are several different types of buildings that use cement-bonded lignocellulosic composites. In the Philippines, cement board is made primarily by hand and used in pricey modular housing (English, 1994)..

Cement board is a versatile material that is mechanised and utilised in pricey modular housing. The versatility of cement board production makes it the perfect choice for wood recycling. Good-quality cement boards can be made on a modest scale, utilizing primarily unskilled labour, with only a minimal initial expenditure and the most basic tool (English, 1994).

2.10.2. Hydration of regular Portland cement

Tricalcium silicate (commonly known as "alite"), dicalcium silicate (sometimes known as "belite"), tricalcium aluminate (C_3A), and calcium ferro-aluminate are the four primary ingredients of standard Portland cement (C_4AF). Taylor, 1997 provides a summary of the primary hydration reaction of the cement constituent parts, whereas Table 2.5 lists the many forms of Portland cement that are standard in ASTM C-150 (Taylor, 1997).

The aluminates, in particular C_3A, swiftly react with the water and harden, producing a lot of heat during hydration. Gypsum ($3CSH_2$), which slows this process, is a tiny component of Portland cements. Gypsum is added to concrete to help it hydrate more slowly and to enable the aluminates to react more quickly. This extends the window of opportunity for placing fresh concrete before it sets. The aluminates form mainly

calcium aluminates (C_4AH_{13}) and calciumferrit-hydrates (C_4FH_{13}) and in connection with gypsum, ettringite ($C_6AS_3H_{32}$) and monosulphate (C_4ASH_{18}). At a later stage of the hydration process, ettringite can change into monosulfate. Portlandite (CH) and calcium silicate hydrates are the two major silicates that make up a cemented cement matrix (C-S-H). Portlandite, which differs from the other hydration products in that it forms huge chemically active crystals, is thought to be the reason why concrete lacks good durability, creep resistance, and strength (Gregor, 2003).

In addition, Portlandite ensures that the pore solution is very alkaline, which prevents corrosion of the reinforcing steel (Gregor, 2003). Table 2.5 gives typical composition of Portland cement types in the US which was follow by Portland cement hydration reaction (Mindess, Young, and Darwin, 2003).

Table 2.5: Percentage composition of different types of Portland cement in the US

Cement Type	C_3S	C_2S	C_3A	C_4AF	CSH_2
I	55	18	10	8	6
II	55	19	6	11	5
III	55	17	10	8	6
IV	42	32	4	15	4
V	55	22	4	12	4

Source: Mindess et al, 2003.

Portland cement hydration reactions as stated by Taylor, (1997) were:

1. $C_3A + 3CSH_2 + 26H \longrightarrow C_6AS_3H_{32}$ (ettringite)

2. $C_3A + CSH_2 + 16H \longrightarrow C_4ASH_{18}$ (monosulphate)

3. $C_6AS_3H_{32}$ (ettringite) $+ 2C_3A \longrightarrow C_4ASH_{18}$ (monosulphate)

4. $C_4AF + 4CH + 22H \longrightarrow C_4AH_{13} + C_4FH_{13}$

5. $2C_3S + 6H \longrightarrow C_3S_2H_3$ (C-S-H) $+ 3CH$ (Portlandite)

6. $2C_2S + 4H \longrightarrow C_3S_2H_3$ (C-S-H) $+ CH$ (Portlandite)

2.10.3. Optimising concrete mixes

Specific hydration parameters and the qualities of the hardened concrete matrix can be changed by modifying the basic mixture proportions and adding additives. Making a dense matrix and reducing pore volume are frequently stated goals. Simple geometry can be used to optimise the particle size distributions of cements, sand, and coarse aggregates to obtain optimal compactness even before water is added to start the hydration process (Millrath, 2002).

To fill in the remaining spaces between particles, a wide range of fillers are also readily accessible. Active fillers, which have pozzolanic qualities and actively participate in cement hydration, are distinguished from inert fillers by their use in place of cement, such as crushed limestone or quartz (Millrath, 2002).

Theoretically, total hydration of cement can be attained with a water-to-cement (w/c) ratio of just 0.21 percent. Higher water/cement ratios are necessary to ensure acceptable workability, which can be assessed by slump or flow tests. Here, hydration reactions do not completely use the available water. Once the cement matrix has hardened, any remaining water may eventually evaporate, causing the concrete to shrink and develop pores. Super plasticizers, also known as high-range water reducers, can be utilised to create a denser concrete matrix while still ensuring adequate workability at lower w/c ratios (Rixom and Mailvaganam, 1999).

Even if the constituent particle size distributions are optimised and the water content is reduced, the hydrated cement paste is still intrinsically heterogeneous because of the many phases, especially C-S-H and CH. Theoretically, Portlandite can be produced from cement in amounts of up to 28% by weight after complete hydration. (Asselanis and Mehta, 2001)

Pozzolans can be used to partially substitute cement and reduce or even completely change hazardous Portlandite into more durable C-S-H phases by actively assisting in the cement hydration. Fly ash, a byproduct of industry, silica fume, and metakaolin, a type of thermally activated kaolinite, are a few examples of pozzolanic (clay) materials that are commonly used. Fly ash is especially useful in the manufacturing of mass concrete, such as dams and enormous foundations, since it promotes workability, slows cement hydration, and significantly reduces the heat of hydration (Mehta and Monteiro, 1993).

Since the particles are so small (0.1 m), silica fume serves as filler. The large surface area causes it to be very reactive, but it also significantly reduces workability. Super plasticizers are frequently used with it to produce high early strengths (Soukatchoff, 2000). It has been found that small-sized hydration products can develop into fibre bundles when used with reinforcement, which can lead to mechanical degradation of the fibres.

2.11. Water (Solvent)

Water is the universal solvent used for cement-bonded board production. Water acts as solvent for the chemical additives and as well helps in forming the cement-lignocelluloses mixture into homogenous mixture. Water also takes the material to fibre saturation point and the inhibited cement to hydration temperature (Fan, Ndikontar, Zhou and Ngamveng, 2012).

In calculating the amount of water requirement for board production, the moisture content of the particles (lignocelluloses materials) must be taken into consideration. For the hydration process, cement needs a quantity of water equal to 23% of its own weight for the process to be completed (Oyagade, 1990). Oyegade (1988) reported that an amount of water equivalent to 65% mass of cement was found necessary for

cement-bonded particle board production with good qualities in terms of dimensional properties at the ratio lignocelluloses material: cement of 1:1.55 to 1:3.10 were employed.

2.12. Composite durability

Natural fibres are becoming more common in cement-based materials because of advantages like widespread resource availability, high fibre tensile strength, high fibre modulus of elasticity, and relatively low cost, as well as the well-developed technology to extract the fibres and others depending on their application (Banthia, Yan and Mindess 1996).

Building materials made of fibre cement provide a number of advantages over traditional building materials. When compared to masonry, fibre-cement products enable faster, less expensive, and lighter construction; Fibre-cement products may provide better toughness, ductility, and flexural capacity in comparison to cement-based materials without fibres, as well as better crack resistance and nail ability. Additionally, fibre-cement materials have better fire resistance, moisture resistance, decay resistance, and dimensional stability (Banthia, Yan and Mindess 1996).

Their primary disadvantage is that they could decay quickly in the alkaline Portland cement environment (Banthia, Yan and Mindess 1996). According to the American Society for Testing and Materials (ASTM 1994), "durability" refers to capacity an object to continue functioning for at least a predetermined period of time. Durability is defined as the loss (or retention) of mechanical or physical qualities when subjected to ageing or natural processes. However, it is acknowledged that accelerated ageing tests are typically insufficient for predicting the long-term performance of composite materials. Accelerated ageing tests expose samples to extreme wet-dry cycles in order to determine durability faster than natural exposure.

The use of additional cementing material has received the majority of attention in efforts to increase durability. By reducing the pH of the pore solution, reacting with calcium hydroxide to produce CSH, and fine-tuning the pore structure, artificial pozzolans have been shown to delay or minimize composite degradation. It is believed

that doing so will prevent fibres from becoming embrittled when exposed to a cement matrix, reducing their mineralization (Banthia *et al.,* 1996).

2.13. Findings from the literature review

Government and other agencies of various developing countries are becoming more interested in low-cost housing for the masses in recent years. This gave rise to advent of cement-bonded board, which is gradually gaining acceptance as a semi-structural panel product for the building and construction industries (Aigbomian, 2013).

Cement boards are a flexible building material for roofs, ceilings, floors, partitions, and cladding due to their inherent great qualities, particularly their strong resistance to moisture, fire, termites, fungi, and other types of degrading agents (Ajayi, 2002). The high interest in the production of cement- bonded board in Nigeria has been associated with their relatively low cost, since they are produced from wood and agricultural residues (Badejo, 1987).

The low in tensile strength and constrained ductility, make concrete a brittle substance by nature. Its performance is impacted by widespread cracking in fresh concrete, which is frequently caused by secondary factors like temperature and shrinkage (Ortiz, Khedmatgozar Dolati, Malla, Nanni, and Mehrabi, 2023). In contrast to plain concrete, the introduction of discontinuous, discrete, uniformly dispersed fibres in the matrix of concrete or mortar may alter the tensile and flexural strength, ductility, toughness, and impact and fatigue resistance of the composite (FRC) manifold (Wilson and Philip, 2015).

Also, CNSL has also been found useful in paints and enamels as anti-corrosive paint formulations and as electrical insulating varnishes. CNSL as a rubbery gel can be used as a hardening agent for cement that is resistant to the reactions of acids and alkalis (Philqsqphy, 2007). Despite all these, there is still need for more research work on the application of CNSL in building construction.

CHAPTER THREE

MATERIALS AND METHODS

3.1   Material collection and preparation

The materials used in the production of composite boards are coir fibre, coir dust, CNSL, cement and potable water.

3.1.1   Coir fibre

3.1.1.1 Pre-treatment of the coir fibre with cold water extraction

The coir fibre waste used in the study was obtained by harvesting fully matured coconuts and nuts were separated manually from the husks (Plate 3.1). Cold water extraction techniques were employed to remove extractives from the husks. The coir samples were soaked in cold water at room temperature (25 ± 2^{0}C) in a plastic drum for 48 hours while being stirred occasionally to perform cold water extraction. The extracts were drained off and the coir fibres washed with cold water for about 10 minutes, sun-dried until a moisture content range of 7–10% was achieved as shown in Plate 3.2. The samples were stored in labelled polythene bags.

Plate 3.1: Coconut husk

Plate 3.2: Coir fibre

3.1.2 Coir dust

3.1.2.1 Coconut coir dust

The coir dust waste used in the study was obtained by harvesting fully grown coconuts when the nutrient-rich layer surrounding the seed was prepared to be processed into copra and dried coconut; the fibrous covering of the fruits was then detached from the hard shell, a process known as de-husking.

When a coconut is harvested, its entire body is split into its husk and kernel, with the latter being used to make culinary goods or oil. In the process of removing coir fibre from the husk, typically one-third of it is collected as coir dust. The coir dust is a by-product of coir fibre. Coconut coir dust (also known as cocopeat, coir waste on fibre dust) can be characterised as low-density, brown, spongy particles that are shed with the fibre from the husk.

3.1.2.2   Extraction of coir dust

In the extraction of coir fibre from the coconut husk and in the production of finished materials from the extracted fibre, a large amount of coir dust is produced. Spongy particle of low weight which falls out when the fibre is shredded from the husk is known as coir dust.

3.1.3. Cashew nut shell liquid

Cashew nut shell liquid (CNSL), a viscous, dark liquid that is incredibly caustic, is found inside the cashew nut shell. Between the nut's delicate outer layer and its hard inner shell lies a thin honeycomb structure that houses it. In the manufacturing of the particleboard, CNSL will take the place of urea formaldehyde as the binder.

The extraction of cashew nut shell liquid typically involves one of three techniques: solvent extraction, solvent roasting, or mechanical extraction. Solvent extraction is the major technique employed. Roasting the nuts over an open flame is how CNSL is traditionally extracted. The liquid, which is a valuable source of natural phenol, is wasted as a result of this process, which eliminates the CNSL via charring or degradation.

3.1.3.1 Pre-treatment of cashew nuts

Before extraction, certain simple physical procedures were performed on the samples (cashew nuts) to guarantee a high level of product purity and quality. These procedures include size reduction, drying, washing, and shelling. To remove any potential pollutants and debris, the nuts were thoroughly washed with water before the juicy portion was removed.

The nuts were then dried, which made it easy to remove the shells. The nuts were dried out for 10 days by being stretched out in the sun to achieve this. Wearing hand gloves and using a tool shaped like a plier, the nuts were then shelled to remove the shells. The dried shells were then properly crushed into small pieces using a crusher and pestle to improve the surface area of contact between the shell and solvent and facilitate the easy removal of the CNSL.

3.1.3.2 Extraction of CNSL

The extraction of CNSL was carried out at the Dispensing Laboratory of Faculty of Pharmacy, University of Ibadan. The cashew nuts (Plate 3.3) collected were washed using potable water to get rid of dirty foreign materials on their surfaces before they were stored at room temperature between 23-25^{0}C. The leathery cashew nut shell is depicted on Plate 3.4. The shells housing the nuts were manually removed using a table knife to remove the seeds inside them. A hand-driven milling machine was used for shelling before soaking the seeds and milled shells in ether for 48 hours to extract the CNSL.

The extracted oil was poured inside a plastic sieve and a conical cloth was used to sieve out before allowing the oil to settle down. Another round of ether was applied to the oil, with the resulting clearer oil rinsed using conical cloth and sieve again. The oil was then open to the air for about four days while a stirrer was used consistently to mix oil on regular basis.

Plate 3.3: Unprocessed cashew nuts

Plate 3.4: Cashew nuts shell stored in a container

3.1.4 Cement and water

Commercially bagged general purpose Type 1 Portland (Ordinary Portland) cement sold in the standard bag of 50kg was used. The cement was procured from local markets in Ibadan, Oyo State and meets the specifications of the British Standards for Ordinary Portland cement BS 12 (1996). The cement bags were air-tight and used up as quickly as possible to minimize loss of strength. Water used for the experiment was potable water.

3.2   Materials and sample preparation

3.2.1   Materials and sample preparation of coir fibre composite board

The material used for this work, were water, coconut fibre, and ordinary Portland cement. The coconut fibre ratio was varied according to the mass of cement. Coconut fibre was weighed according to the percentage ratio of cement weight (3kg). Electronic balance was used for batching fibre (Plate 3.5), cement and water.

Samples were produced with four levels of coconut fibre of 5.0, 7.5, 10.0 and 15.0 % contents. The value of cement and water ratio were kept constant at 2:1. A mechanical mixer was used to combine all the basic components until slurry was created. To improve workability and prevent coconut fibre aggregation, the composites were thoroughly mixed. Then, in accordance with the mould size, the homogenous slurry was put into the mould.

Depending on the type of test performed on the composite sample. The sample was kept in the mould for 24 hours before it was de-moulded and cured for 3, 7, 14, 21 and 28 days of curing. The production process of coir fibre composite board in Figure 3.1 was followed and the four levels (5%, 7.5%, 10% and 15%) of composite boards produced were shown in Plates 3.6, 3.7, 3.8 and 3.9 respectively.
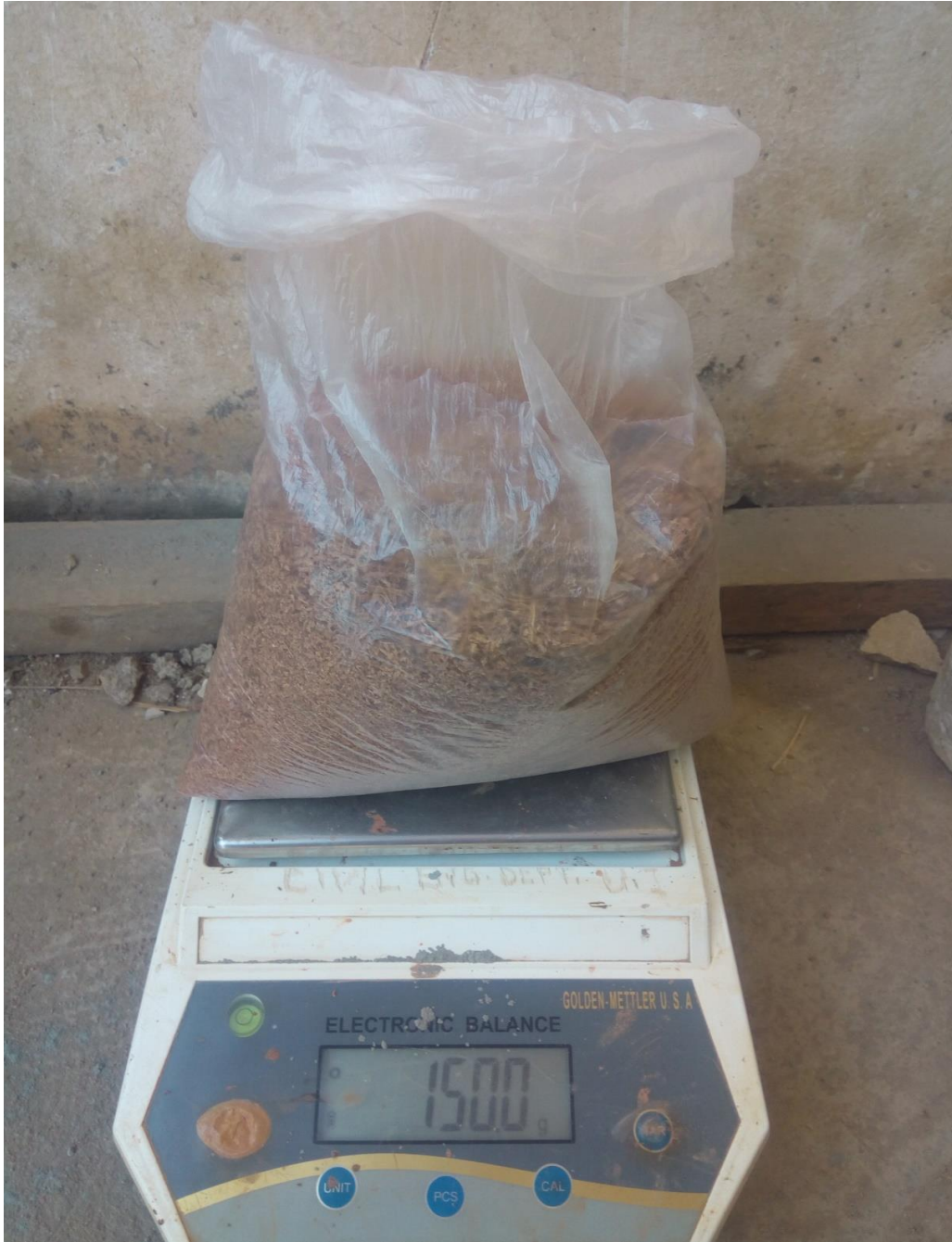
Plate 3.5: Batching of coir fibre
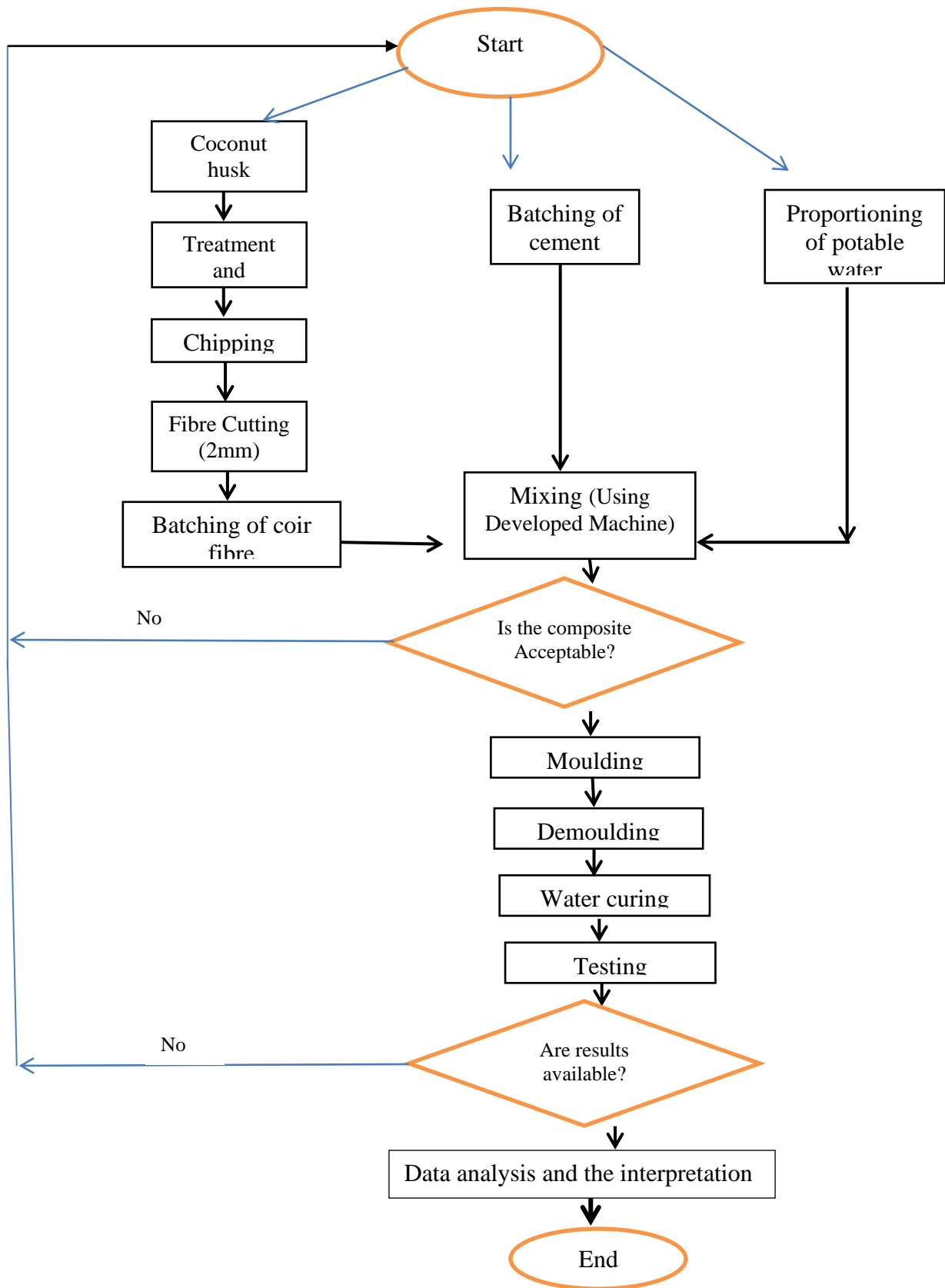
Fig. 3.1 Production process of coir fibre composite board
Source: Adapted from Lucidchart.com
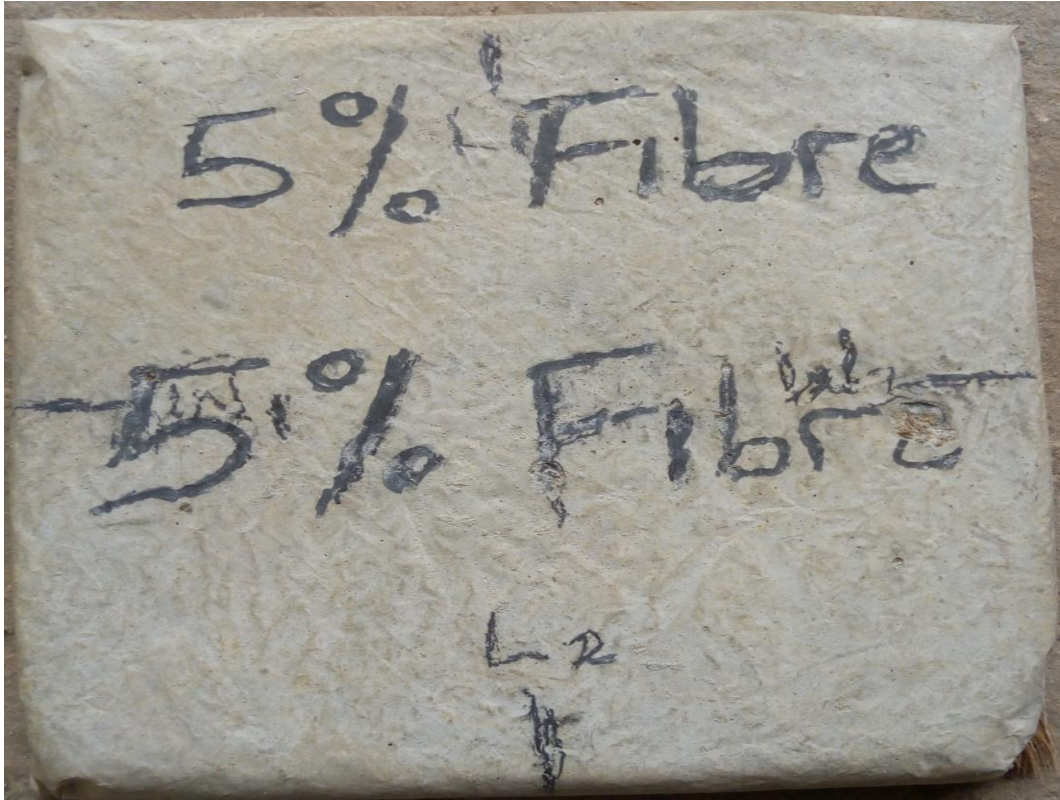
Plate 3.6: 5% coir fibre composite board
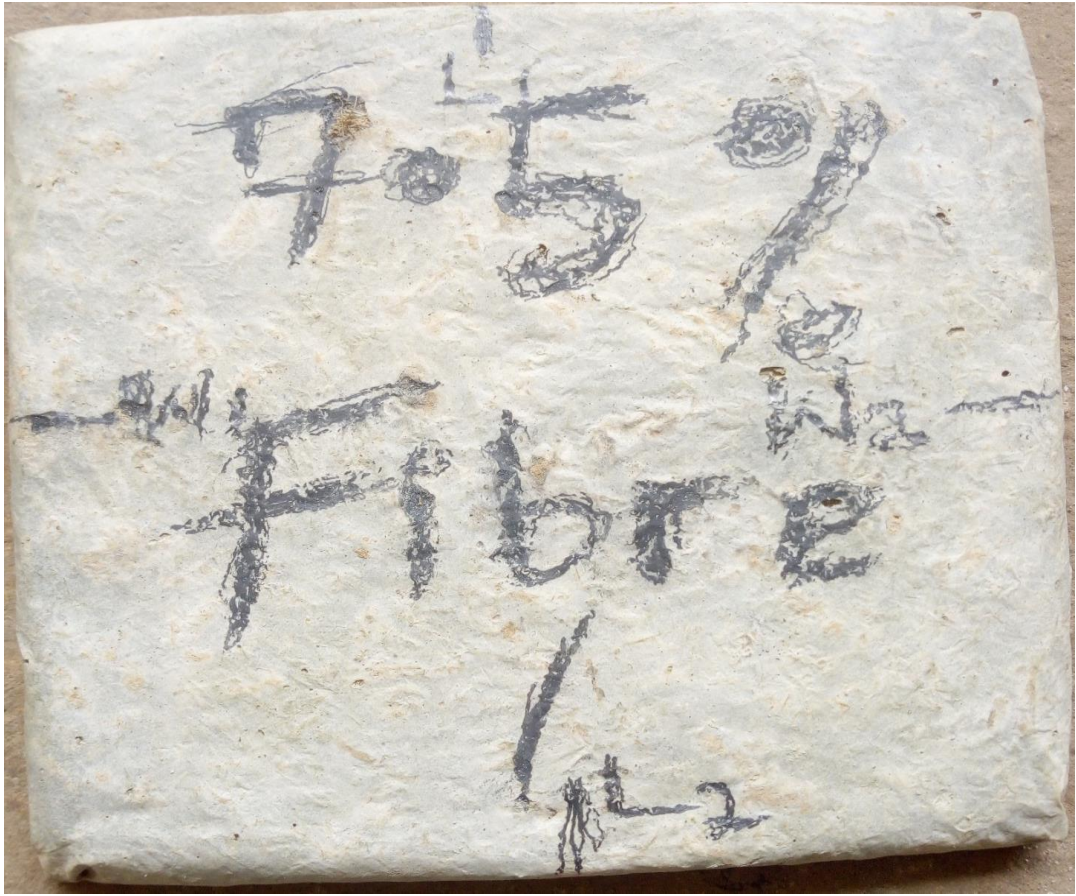
Plate 3.7: 7.5% fibre composite board
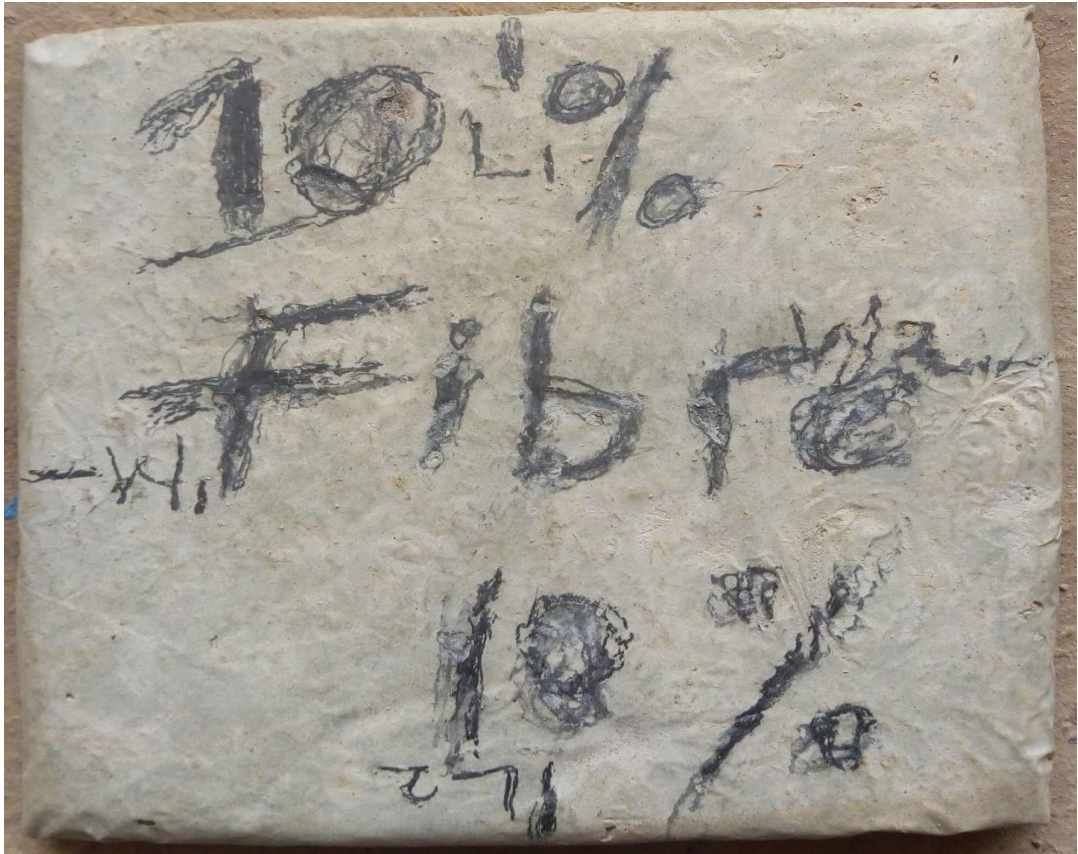
Plate 3.8: 10% fibre composite board
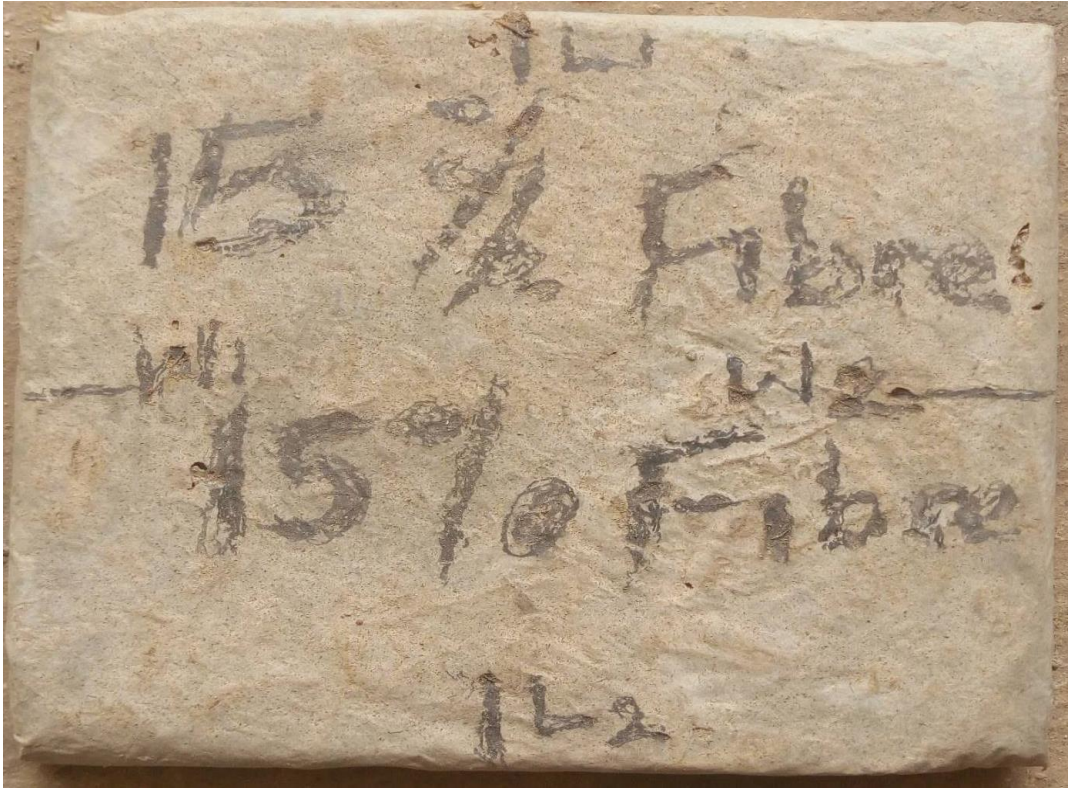
Plate 3.9: 15% fibre composite board

3.2.2 Materials and sample preparation of coir dust composite board

The purpose of particle mix design is to ensure the most optimum proportions of the constituent materials to fulfil the requirements. The cement used was Ordinary Portland cement, water and coconut coir dusts were used in this work.

Samples were produced with coir dust contents of 5.0, 7.5, 10.0, and 15.0%. The values of cement and water ratio were kept constant at 2:1. The coconut coir dust was weighed according to the percentage ratio of cement weight. Electronic balance was used for batching of coir dust (Plate 3.10), cement and water.

A mechanical mixer was used to mix all the basic materials until slurry was formed. Then, in accordance with the mould size, the homogenous slurry that had been formed was put into the mould. The size of the mould varies based on the kind of testing done on the composite samples. After the samples had been in the mould for 24 hours, they were taken out and allowed to cure for 3, 7, 14, 21, and 28 days. Production process in Figure 3.2 of coir dust composite board was followed and the four levels (5%, 7.5%, 10% and 15%) of composite boards produced were shown in Plate 3.11, 3.12, 3.13 and 3.14 respectively.
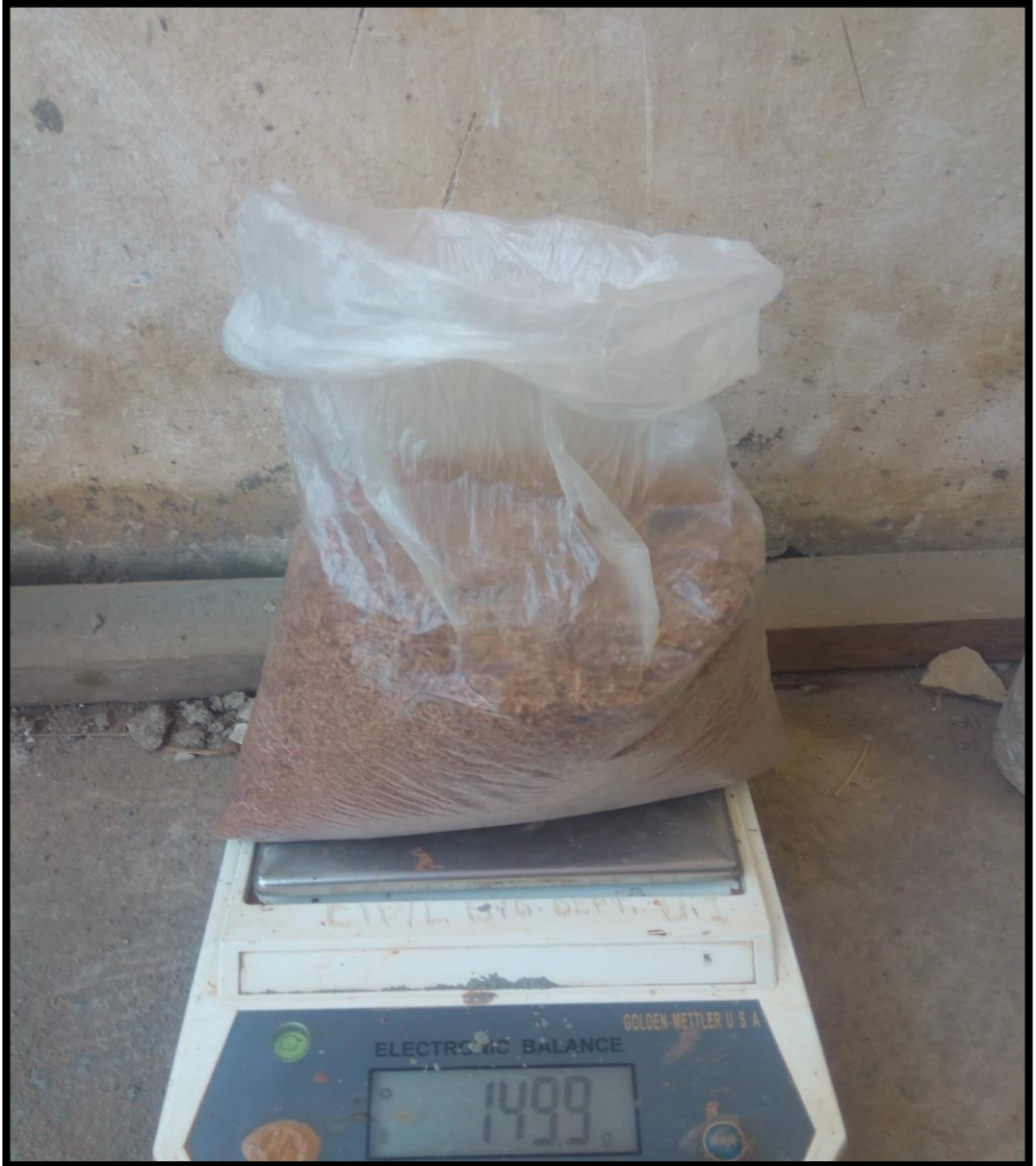
Plate 3.10: Batching of coir dust
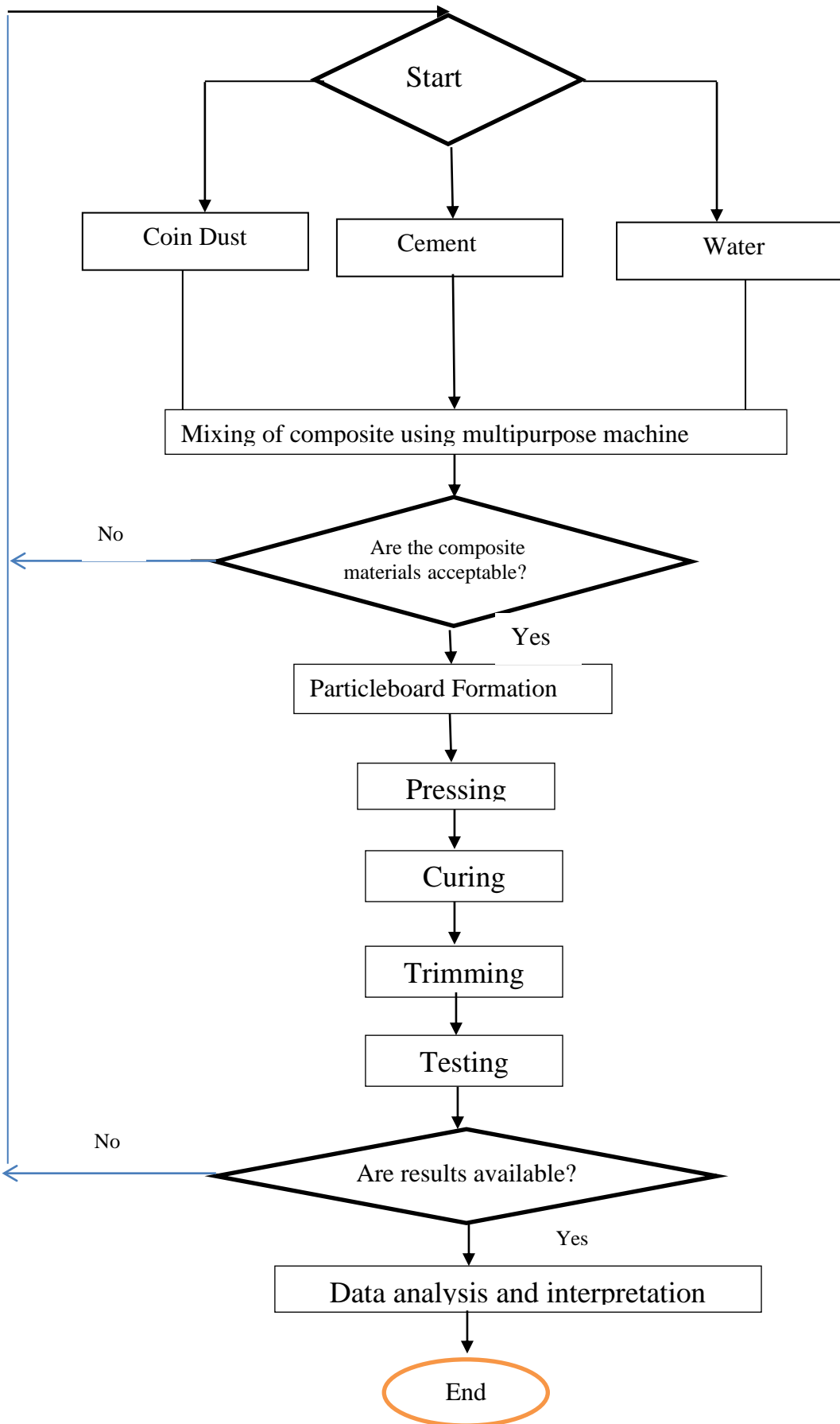
Fig 3.2 Production process of coir dust composite board
Source: Adapted from Lucidchart.com
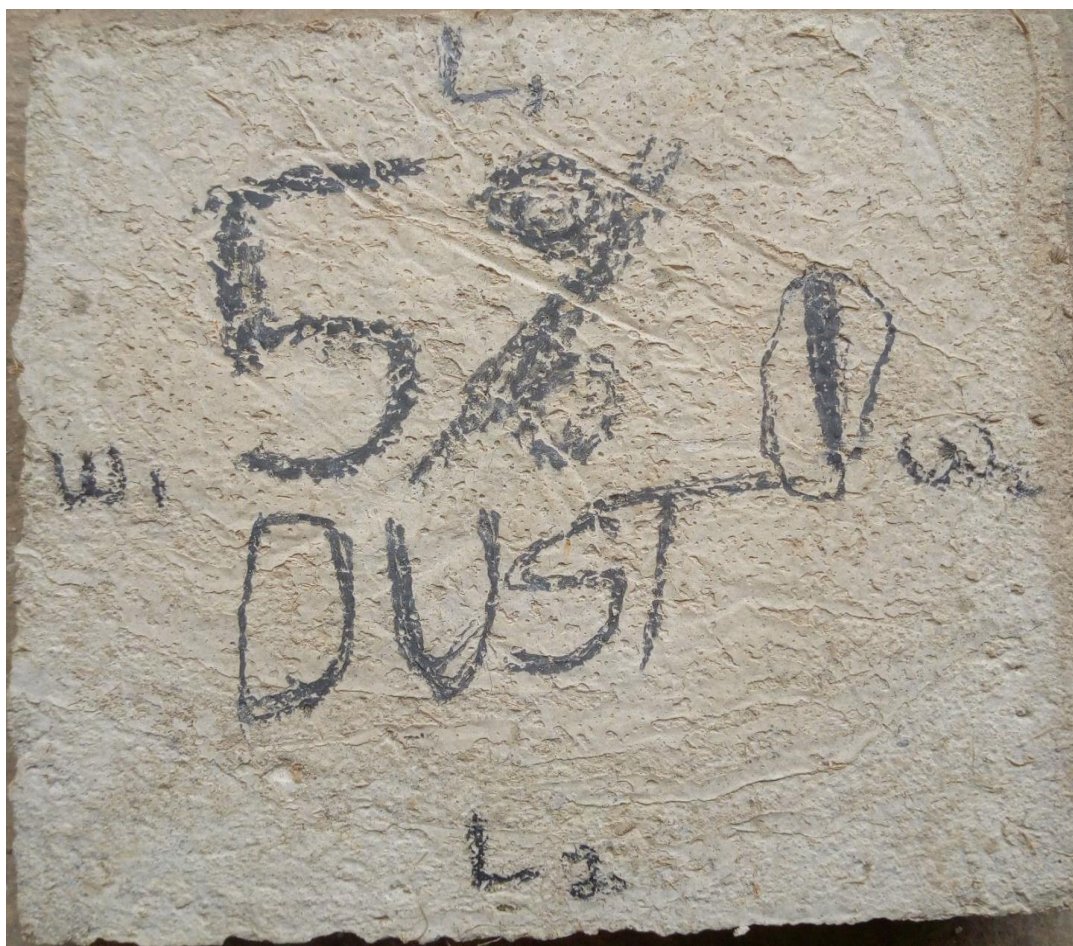
Plate 3.11: 5% coir dust composite board
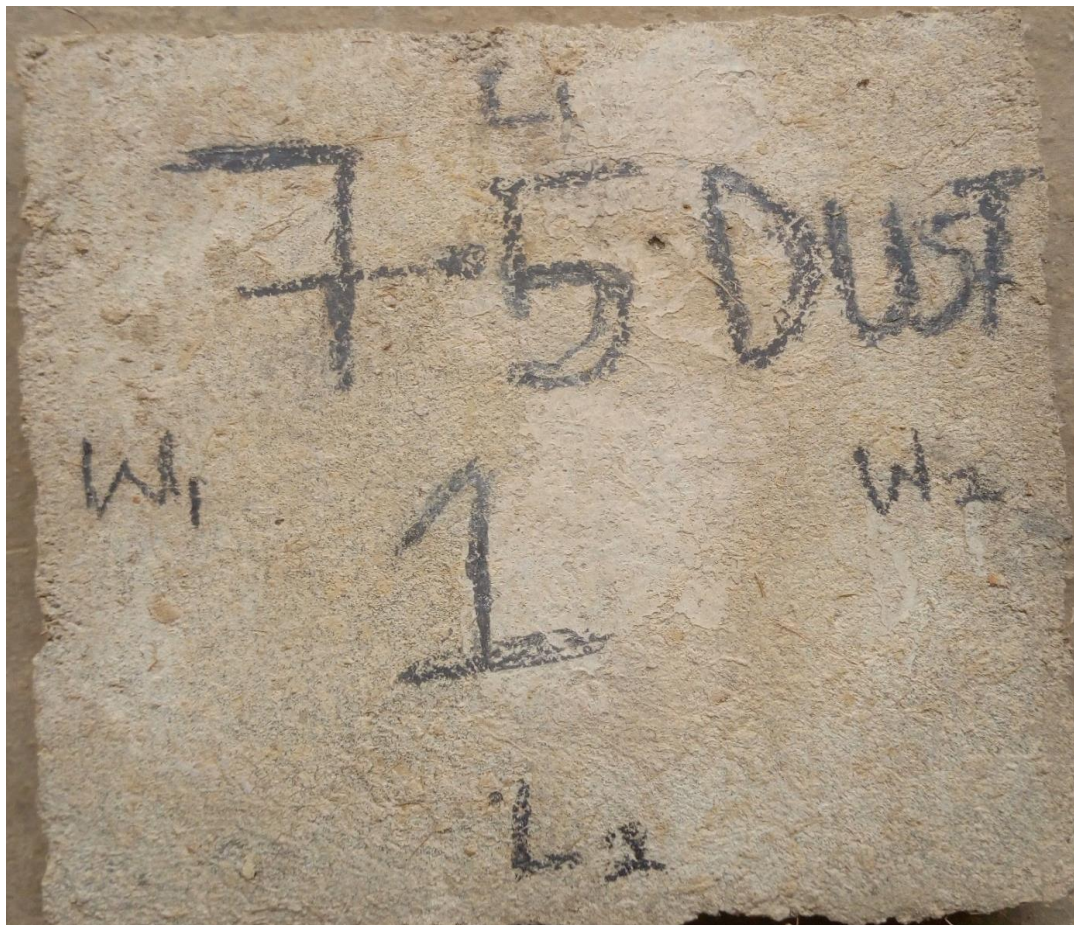
Plate 3.12: 7.5 % coir dust composite board
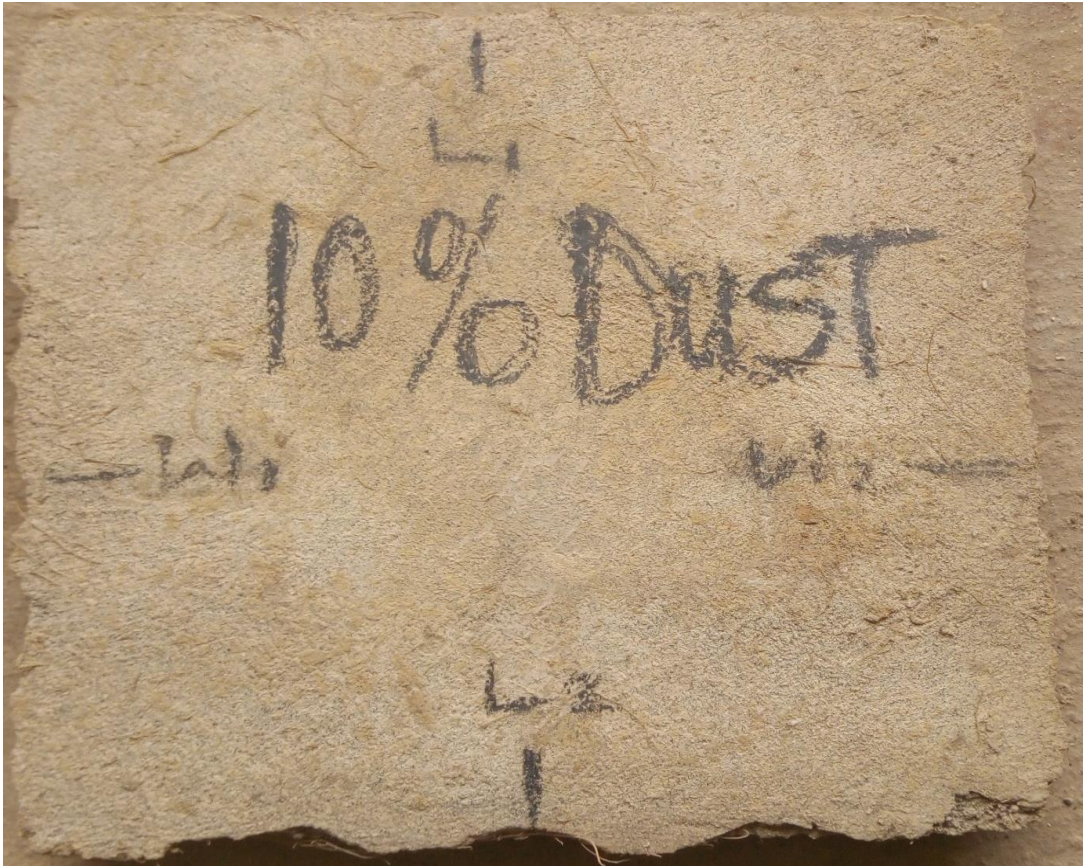
Plate 3.13: 10% coir dust composite board
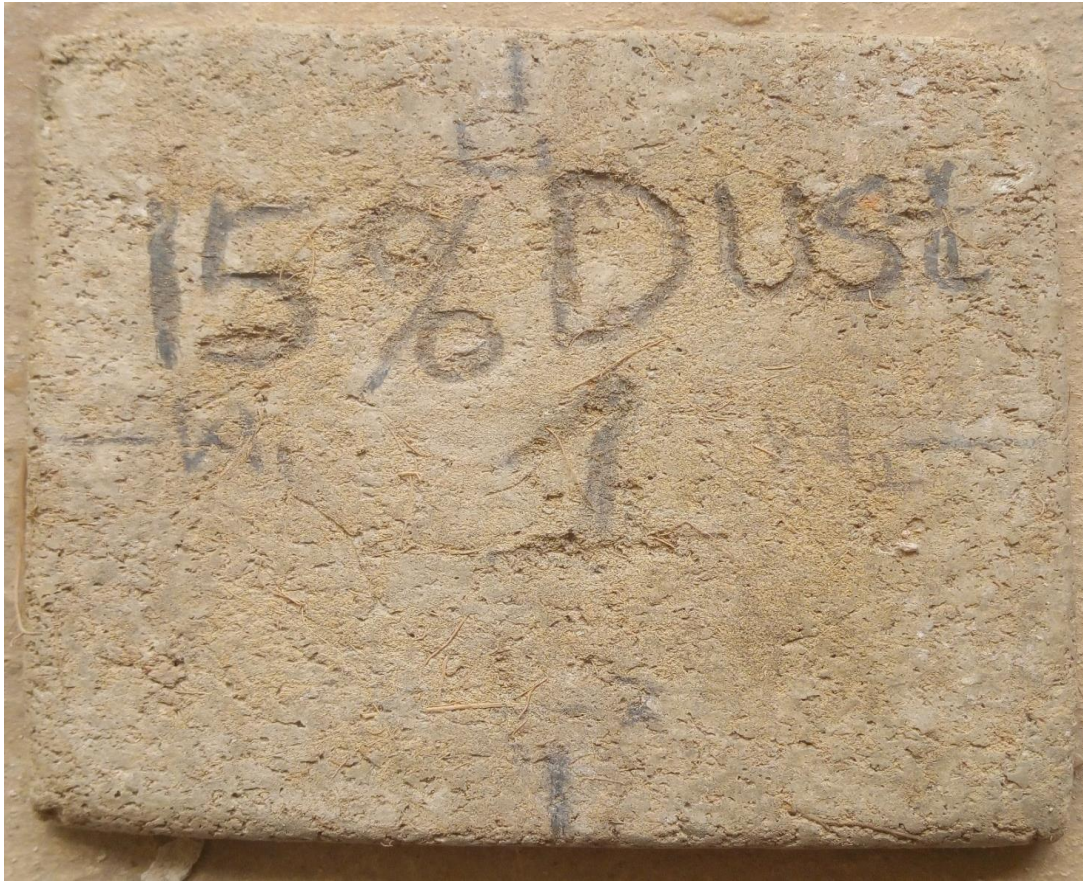
Plate 3.14: 15% coir dust composite board

3.2.3 Materials and sample preparation of CNSL composite board

The purpose of particles mix design is to ensure the most optimum proportions of the constituent materials to fulfil the requirements. The cement used was ordinary Portland cement, coir dust. CNSL and water were used in this work. Four levels of CNSL, 2.5, 5.0, 7.5, and 10.0% contents, were used to produce the samples. The values of cement,

water and coir dust ratio were kept constant at 2:1:0.1. The CNSL ratio was varied in the mixed. CNSL was weighed and according to the percentage ratio of cement weight. Electronic balance was used for batching CNSL (Plate 3.15), dust, cement and water.

In a mechanical mixer, each raw material was added until a slurry mixture was produced. The composites were mixed thoroughly to provide better workability of composites. Then, in accordance with the mould size, the homogenous slurry that had been formed was put into the mould. The size of the mould varies based on the kind of testing done on the composite samples.

The samples were left in the mould for 24 hours, after which they were removed and allowed to cure for 3, 7, 14, 21, and 28 days. The production process of CNSL/coir dust composite board in Figure 3.3 was followed and the levels (2.5%, 5%, 7.5% and 10%) of composite boards produced were shown in Plate 3.16, 3.17, 3.18 and 3.19 respectively.

Plate 3.15: Batching of CNSL
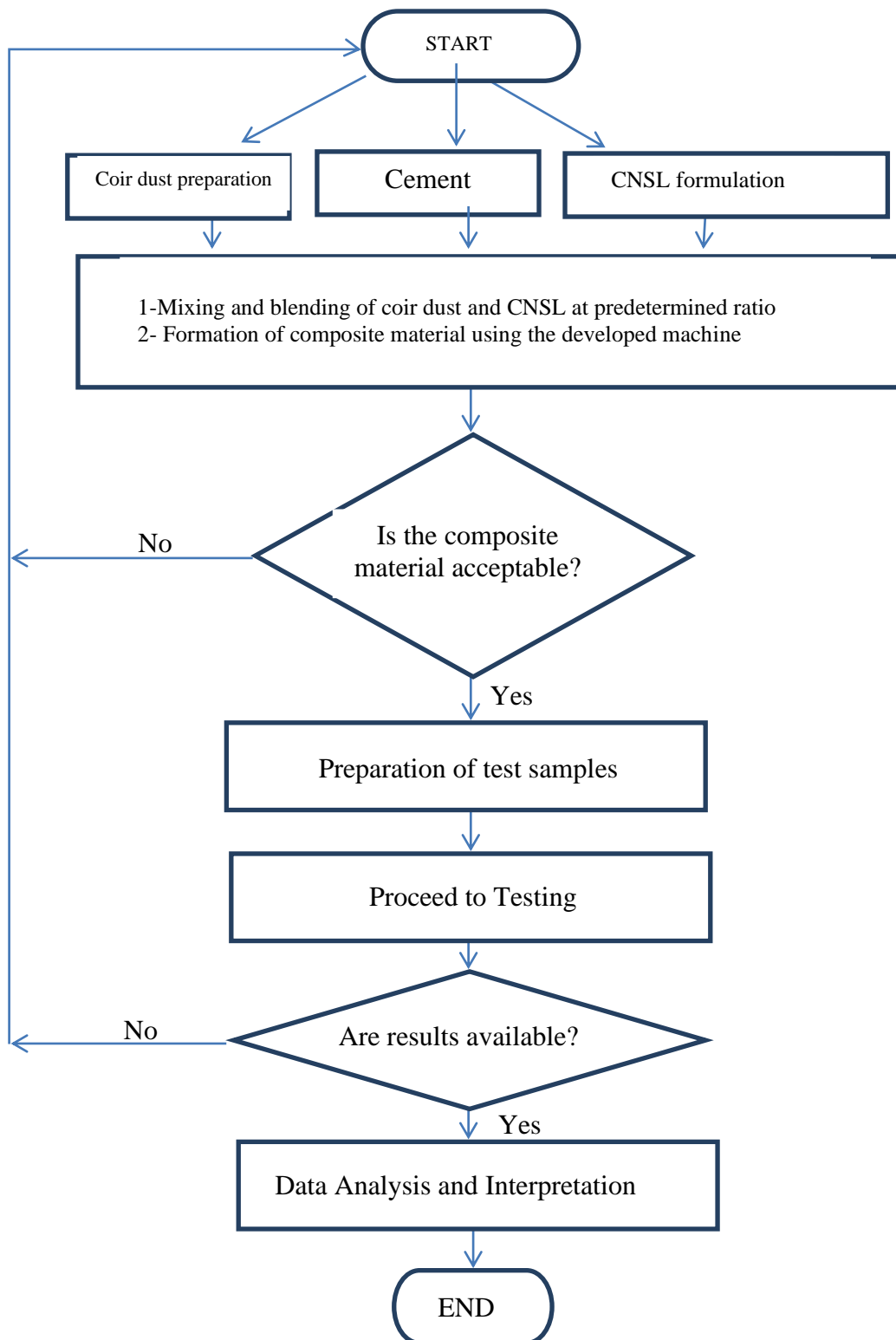
Figure 3.3: Flowchart of the processes involve in the production of composite boards from coir dust and CNSL
Source: Adapted from Lucidchart.com
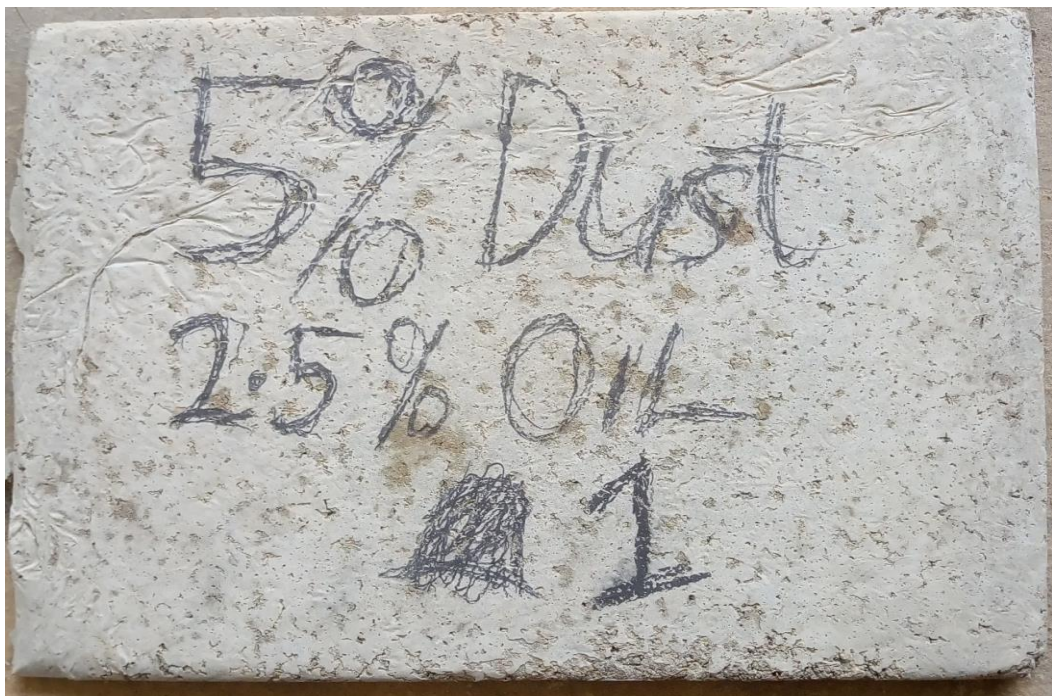
Plate 3.16: 2.5% CNSL composite board
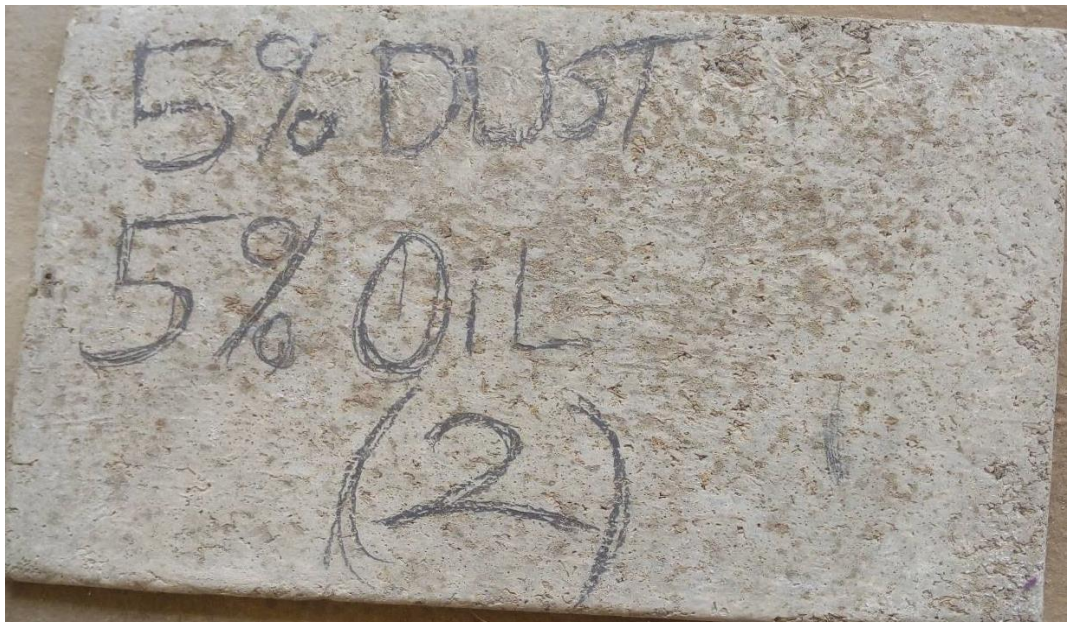
Plate 3.17: 5% CNSL composite board
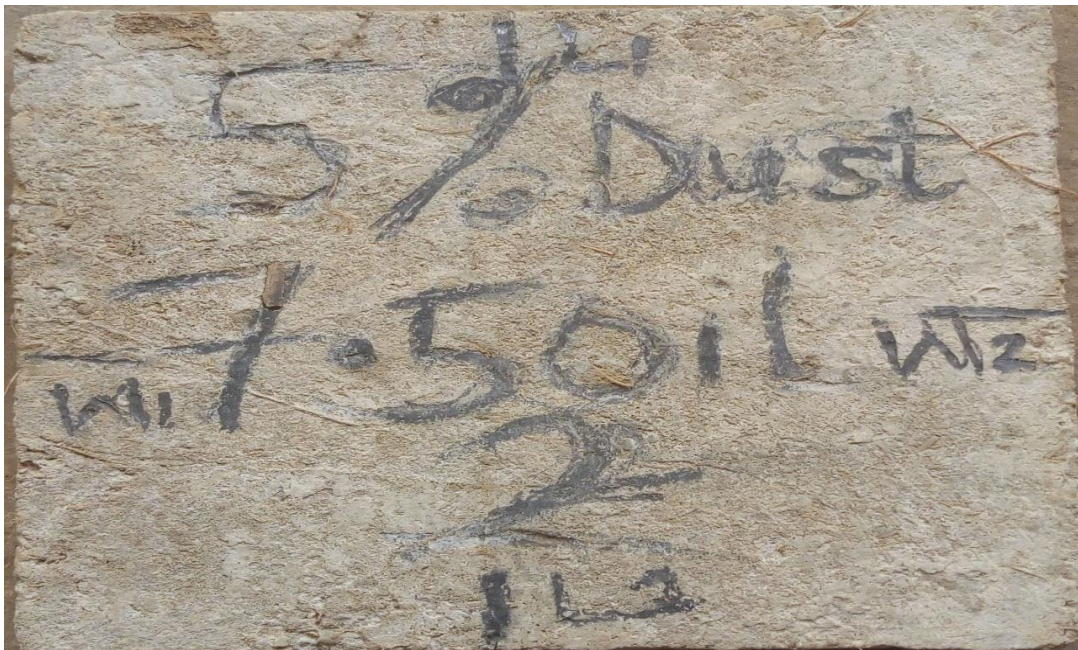
Plate 3.18: 7.5% CNSL composite board
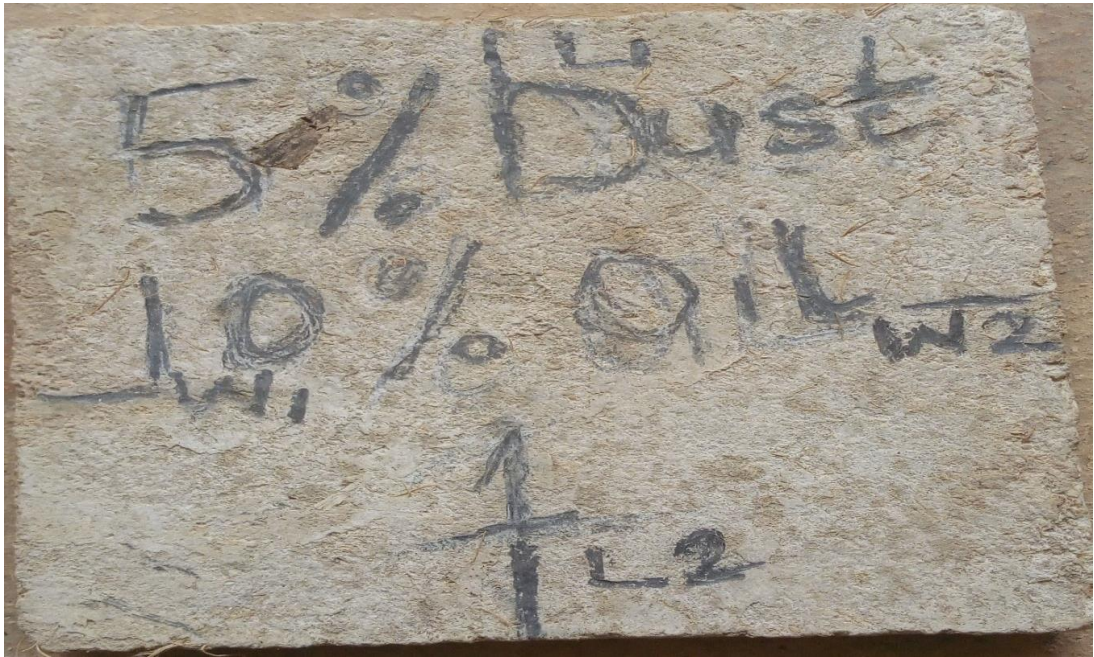
Plate 3.19: 10% CNSL composite board

3.3 Development process of equipment

3.3.1 Preamble

The major equipment/machine required for composite board production was made up of three different units: the mixing, forming and heat treatment units. These units were designed and fabricated prior to board production. This section gives details about the design and construction of the equipment. The mixer aids in the blending of the constituents to ensure uniform distribution of coir fibres in cement matrix at the desired workability, consistency and mobility.

Workability of concrete mainly refers to how easily concrete mix can be handled. Consistency, flexibility, and compatibility are the three primary qualities needed. Wetness or fluidity is measured by consistency. Mobility is the ease with which a mixture can flow into the formwork and fill it entirely, whereas compatibility is the ease with which the specified mixture can be thoroughly compressed with all trapped air being eliminated. The forming unit functions primarily to attain desired board dimension and vibrate the slurry in order to compact it and facilitate full initial strength. The heat treatment section is required only for coir-CNSL bonded composites as heat is not required for cement hydration.

3.3.2 Design and construction objectives

The machine/equipment is required to achieve the following objectives:

i. Production of homogenous mix of coir fibres in cement matrix to enhance the strength properties and the quality of the final products,

ii. vibration of the mortar to remove air voids which tends to reduce the strength of the final product,

iii. compaction of the mortar mix to develop full initial strength, and

iv. production of uniform, non-porous and consistent products.

The expected properties of the final coir-cement products are presented in Table 3.1.

Table 3.1: General design parameters related to the boards

Parameters	Values
Density	1350- 1690kg/m^3
Dimension of boards	520 x 290 x 8mm
Number of boards per batch	30
Wood-cement ratio	Variable (0.1:2,0.15:2; 0.2:2, & 0.3:2}
Moisture content of lignocellulosic fibre	12%

3.3.3 Quantity of each constituent required for producing 30 boards / batch

Quantity of constituents required to make 30 boards per batch as summarised in terms of total mass of 30 boards, cement content, fibre content, and quantity of water is presented in Table 3.2.

(a) Total mass of 30 boards

Using the relationship between the density of a substance, volume and its mass, the amount of materials required to produce 30 boards is calculated thus:

$$M_b = \text{density of the boards x volume (of 30 boards)}.$$

$$\text{Volume of boards} = 30(0.52 \text{ x } 0.29 \text{ x } 0.008) = 0,0362m^3$$

$$\therefore M_b = 1690 \text{ x } 0.0362 = 61.18kg \qquad \text{……………………………… 3.1}$$

(b) Cement content

Based on a fibre/cement ratio of 0.1:2, the cement proportion is calculated from:

$$\text{Cement Content, } C_c = \text{Cement proportion x } M_b$$

$$= \frac{2}{2.1} \times 61.18kg = 58.27kg \qquad \text{………………………………. 3.2}$$

(c) Fibre content

The fibre content required to produce 30 Nos. of 520mm × 290mm × 8mm dimension board is calculated using:

$$F_c = M_b - C_c \qquad \text{……………………………3.3}$$

$$61.18 - 58.27 = 2.91kg$$

Since the moisture content of fibre at the time of use is 12%, the actual quantity of fibre required is calculated thus:

$$F_{ac} = (1 + MC) \qquad \text{……… …………………………….. 3.4}$$

$$2.91 (1 + 0.12) = 3.26kg$$

(d) Quantity of water

The optimum amount of water required to produce the board is assume to be 50% of cement content.

$$\text{Therefore,} \qquad W_q = 0.5 \text{ x } C_c \qquad \text{…. ……………………… 3.5}$$

$$0.5 \text{ x } 58.27 = 29.14kg$$

Thus, the volume of water required to mix the other constituents, $V_w = 0.02914m^3$.

Table 3.2: Summary of quantity of constituents required to make 30 boards per batch

Constituents	Quantity (kg)	Weight (N)
Coir Fibre (at 12% m.c.)	3.26	31.97
Cement	58.27	571.45
Water	29.14	285.78
Total	**90.67**	**889.20**

Therefore, the total weight of the constituents required to make 30 boards is approximately equal to 889.20 or 0.89 kN

3.3.4 Design method

The stresses and forces imposed on each component part were first determined. These included the self-weight of each part and weight of the constituents (i.e. coir fibre, cement and water). Therefore, to determine the least permissible geometry of each component part, these stresses were analysed and appropriate design assumptions and equations were done in accordance to Schaum machine design method.

3.3.4.1 General design considerations

Components of the machine are constantly in contact with cement paste (alkaline substance) which tends to cause serious corrosion damage. In order to avoid this, make sure to choose materials that are unaffected when in contact with cement paste. Priority was given to locally available materials to reduce the cost of production as much as possible and make the entire fabrication process economical.

The least permissible geometry of each component was adhered to so as to prevent frequent repair that can lead to unavoidable failure of the machine. Other factors that influenced the specifications include strength, appearance, size, rigidity, weight and durability

3.3.4.2 Mixing and blending of the constituents

The proper dispersion of the fibres and the workability of the mortar are essential for the successful manufacture of fibre-reinforced composites. The mixer helps to reduce labour input and time required to achieve homogenous mix which is the basis of producing products of consistent properties. The mixing unit is made up of the following components:

i. Mixing chamber
ii. Pulley system
iii. Mixing shaft and rods
iv. Portable electric motor.

3.3.4.3 Design of mixing chamber

Design Assumptions

1. The mixer was made to be perfectly cylindrical to ease the mixing of the constituents of the mortal thoroughly.

2. The capacity of the mixer was assumed to be 25% higher (i.e. factor of safety of 1.25) than the volume of mortal/materials required to produce 30 boards of dimension 520 x 290 x 8mm for a single batch production. This is important to give clearance to the coiled mixing bars to rotate freely without any obstruction inside the mixing chamber.

Total volume of boards (Vol_b) is given as:

$$Vol_b = \text{length x breath x thickness x No. boards}$$

$$520 \text{ x } 290 \text{ x } 8 \text{ x } 30 \quad \dots\dots\dots\dots\dots\dots\dots 3.6$$

$$= 3.6192 \text{x} 10^7 \text{mm}^3 = 0.0362 \text{m}^3$$

Total volume of constituents (V_T) mixed is given as:

$$V_T = \text{Volume of boards } (V_b) + \text{volume of water } (V_w) \quad \dots\dots\dots\dots 3.7$$

$$\text{Where, } Vol_b = 0.0362 \text{m}^3$$

$$\text{And } V_w = 0.02914 \text{m}^3$$

$$\therefore V_T = 0.0362 + 0.0914 = 0.0653 \text{m}^3$$

From the second assumption, with a factor of safety of 1.25, the volumetric capacity (V_m) of the mixing chamber is given as:

$$V_m = V_T \text{ x } 1.25 \quad \dots. \dots\dots\dots\dots\dots\dots\dots 3.8$$

$$\text{Where } V_T \text{ is the total volume of constituents mixed.}$$

$$\therefore V_m = 0.0653 \text{ x } 1.25 = 0.0816 \text{m}^3$$

A slot was made on the mixing chamber from which thoroughly mixed constituents move out, the height of the chamber (H_m) is assumed to be 20% more than the length of the board produced.

Therefore, the height of the mixing chamber (H_m) is given as:

$$H_m = \text{length of board } (l_b) \text{ x } 1.20 \quad \dots\dots\dots\dots\dots\dots\dots 3.9$$

$$\text{Where } l_b = 520 \text{mm}$$

$$\therefore H_m = 520 \text{ x } 1.20 = 624 \text{mm} = 0.624 \text{m}$$

The internal radius (Ri) is calculated using the relationship between the volume of a cylinder and its height.

$$\text{Thus, } V_m = \pi Ri^2 H \quad \dots\dots\dots\dots\dots\dots\dots\dots 3.10$$

$$\text{Where, } V_m = \text{volumetric capacity of the chamber} = 0.0816 \text{m}^3$$

$$\text{H}_\text{m} = \text{height of mixing chamber } 0.624\text{m}$$

$$\pi = 3.142$$

$$\therefore \text{R}_\text{i} = \sqrt{\frac{V_m}{\pi H_m}} = \sqrt{\frac{0.0816}{3.142 \times 0.624}} \qquad \text{……………………………… 3.11}$$

$$= 0.204\text{m} = 204\text{mm}$$

Therefore, the internal radius of mixing chamber is approximately 204mm.

Since the mixer is constantly in contact with material paste (mortal) during mixing, it implies that the critical stress developed within the chamber is tangential or circumferential. A 4mm thick mild steel plate was considered adequate and thus selected for the fabrication of the chamber. Therefore, the outer and the inner diameters of the mixing chamber are 416mm and 408mm respectively.

3.3.4.4 Design of mixing bars

The bars are steel rods of 4mm gauge which were systematically coiled and wound round the mixer shaft in a serpentine manner in order to allow for easy and uniform mixing of the materials in the chamber. Three bars perform this function as they revolve round the shaft from end to the other covering 650mm length of the height of the chamber, while leaving a small clearance (about 20mm) off the chamber's wall to give room for the rotation of the shaft not to be disturbed by the internal wall of the chamber, loading system of the beam as uniform distributed loading as presented in Figure 3.4.

For the purpose of the design, it is assumed that 10% of the total weight of the maximum constituents that can be mixed in the chamber acts on the bars attached to the shaft.

$$\text{i.e 10\% x total weight of maximum constituents ……………..3.12}$$

$$= \frac{10}{100} \times 1200\text{N} = 120\text{N}$$

For the 650mm length of shaft, the uniformly distributed load (u.d.l.) on the shaft due to the attached mixing bars is given as:

$$\text{u. d. l, } \omega = \frac{120\text{N}}{650\text{mm}} = 0.185\text{N/mm} \qquad \text{………………………..3.13}$$

$$\omega = 0.185\text{Nmm}^{-1}$$

$\omega = 0.185 Nmm^{-1}$

650mm

d
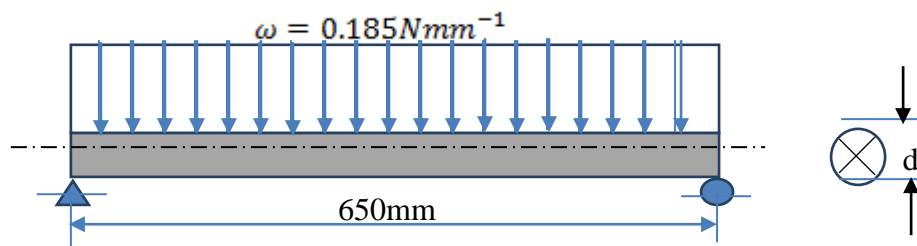
Figure 3.4: Loading system of the beam (I)

To determine the diameter of the steel bars to be used for the fabrication work, the maximum bending moment of the bars is calculated thus:

$$M = \frac{\omega L^2}{8} \qquad \text{.....................................3.14}$$

$$M = \frac{0.185 \times 650^2}{8} = 9770 \text{Nmm}$$

The resisting moment, M is given as:

$$M = Z \times \sigma_b \qquad \text{...........................3.15}$$

Where Z = sectional modulus in mm^3

9 = permissible bending stress in Nmm^{-2}

For a circular cross section,

$$Z = \frac{\pi d^3}{32} \qquad \text{...............................3.16}$$

Where d = diameter of the circular steel bars in mm

For mild steel material, $\sigma_b = 124.1$MPa

$$\text{Therefore, } M = \frac{\pi d^3}{32} \times \sigma_b \qquad \text{...............} \quad 3.17$$

$$\text{From which, } d = \sqrt[3]{\frac{M \times 32}{\pi \times \sigma_b}} = \sqrt[3]{\frac{9770 \times 32}{3.142 \times 124.1}} \qquad \text{...........................3.18}$$

$$d = 9.29 \text{mm} \cong 9 \text{mm}$$

Based on availability of materials in the market, a steel bar of 8mm diameter was used for the fabrication.

3.3.4.5 Total weight of the mixing bars

Since the steel bars wound round the mixing shaft are attached in a serpentine (thread-like) manner, it is assumed that the three of them covers the 650mm length of the shaft. Therefore, the total volume of the bars is given as:

Total volume of bars = 3 x volume of a bar

$$= 3 \times \frac{\pi d^2 h}{4} \qquad \text{....................................... 3.19}$$

Where d = diameter of the bar = 8mm

And h = length of the mixing shaft covered = 650mm

$$\text{Therefore, total volume of bars, } V_r = \frac{3 \times 3.142 \times 8^2 \times 650}{4} \qquad \text{.............. 3.20}$$

$$V_r = 98.02 \times 10^3 \text{mm}^3 = 9.802 \times 10^{-5} \text{m}^3$$

Mass of steel bars, M_r = density of steel bars x V_r 3.21

For steel material, density $\rho_{steel} = 7850 \text{kg/m}^3$

$$M_r = \rho_{steel} \times V_r = 7850 \times 9.802 \times 10^{-5} \qquad \ldots\ldots\ldots\ldots\ldots\ldots 3.22$$

$$M_r = 0.769\text{kg}$$

Therefore, weight of the mixing bars, $W_r = M_r \times g$ $\qquad \ldots\ldots\ldots\ldots\ldots... 3.23$

Where g = acceleration due to gravity = 10gm^{-2}

$$\therefore W_r = 0.768 \times 10 = 7.69\text{N}$$

3.3.4.6 Design of mixing shaft

The mixing shaft on which the steel rods/bars are wound is subjected to both bending and twisting moments, with the total weight acting on it being the sum of the weights of the constituents and the mixing steel bars totaling 1207.69N (approximately 1208N). A shaft length of 700mm was selected, 16mm longer than the 684mm length of the mixing chamber to give room for the bearings to be attached at each end of the shaft. For the purpose of the design, it is assumed that the total load of 1208N is distributed uniformly on the shaft, loading system of the beam as presented in Figure 3.5.

Thus, the uniformly distributed load (u.d.l) on the shaft is given as:

$$\text{u.d.l on the shaft, } \omega = \frac{\text{total load(N)}}{\text{shaft length(mm)}} \qquad \ldots\ldots\ldots\ldots\ldots\ldots\ldots\ldots\ldots 3.24$$

$$\omega = 1208/650 = 1.86\text{Nmm}^{-1}$$

$\omega = 1.86 Nmm^{-1}$

Pulley

700mm

d
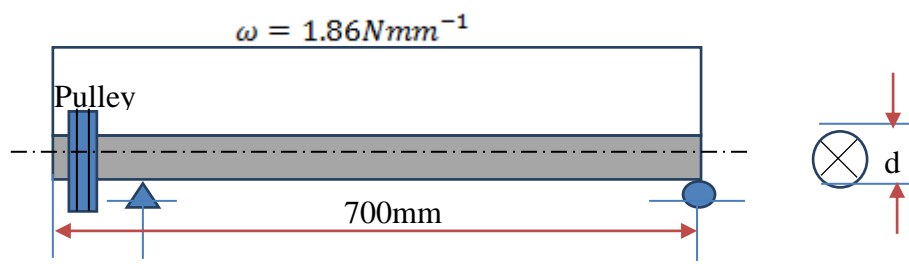
Figure 3.5: Loading system of the beam (II)

The shaft has two bearings at its ends with a pulley of weight 1000N overhanging at the left end, from which a 7.5hp (5.5kW) at 1440 r.p.m electric motor is attached to rotate the shaft. The pulley is keyed to the shaft and the belt drive is vertical. For the purpose of the design, a factor of safety of 1.5 is used to take care of the vertical downward pull of the pulley necessitated by the effect of the belt on the pulley, loading and bending moment diagram of the beam as presented in Figure 3.6.

Therefore, the total concentrated load due to the effect of the pulley is given as a

Total concentrated load = pulley weight x factor of safety ……………….3.25

$$= 1000 \times 1.5 = 1500N = 1.5kN$$

u.d.l

Pulley Bearing   Bearing

Pulley

T_1 W T_2

50mm ——— 650mm

$T_1 + W + T_2 =$

1500N

$\omega = 1.86 Nmm^{-1}$

LOADING
DIAGRAM

50mm   650mm

2219.38N   488.62N

60.57Nm

BENDING
MOMENT
DIAGRAM
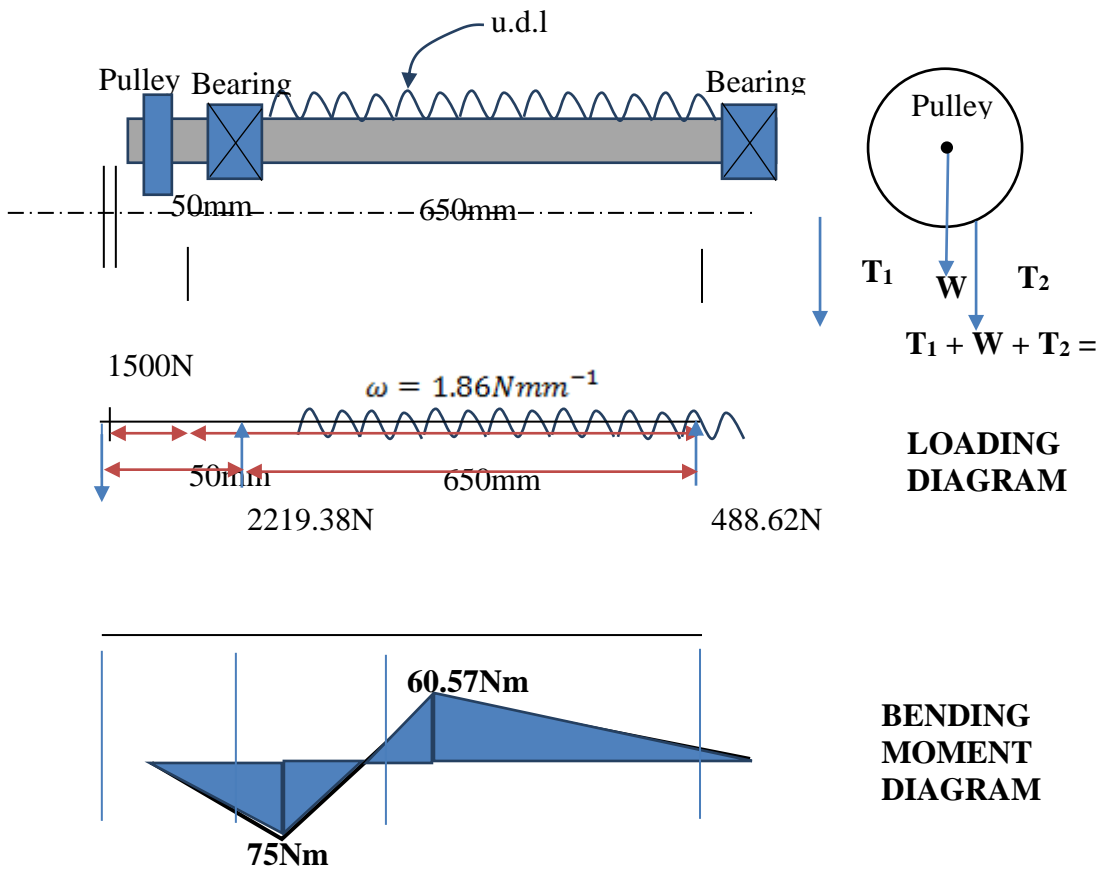
75Nm

Figure 3.6: Loading and bending moment diagram of the beam

From the bending moment diagram, the maximum bending moment acting on the shaft is given as:

Maximum bending moment, M_b (max.) = 75Nm

Maximum torsional (twisting) moment, M_t (max.) is given as:

$$M_t(\text{max.}) = \frac{9550 \times P}{N} \qquad \dots\dots\dots\dots\dots\dots\dots\dots\dots 3.26$$

Where P = power transmitted to the shaft in kW

N = number of revolution in rev/min

$$\therefore M_t(\text{max.}) = \frac{9550 \times 5.5}{1440} = 36.48\text{Nm}$$

Allowable shear stress for commercial steel shafting with keyways,

S_s (allowable) = 40MNm^{-2}

For a rotating shaft with gradually applied load, combined shock and fatigue factor applied to bending moment, K_b = 1.5 and combined shock and fatigue factor applied to torsional moment, K_t = 1.0

Using ASME code equation, for a solid shaft having little or no axial loading,

$$d^3 = \frac{16}{\pi S_s} \sqrt{(K_b M_b)^2 + (K_t M_t)^2} \qquad \dots\dots \dots\dots\dots\dots\dots\dots.3.27$$

Where, d = diameter of the shaft in metres

$$\text{Thus,} \quad d^3 = \frac{16}{3.142 \times 40 \times 10^6} \sqrt{(1.5 \times 75)^2 + (1.0 \times 36.48)^2}$$

$$d = 0.02469\text{m}$$

$$\therefore d \cong 24.7\text{mm}$$

Therefore, a standard size of shaft having a diameter of 25mm was selected and used for the fabrication.

The design work was exclusively carried out using Schaum's Outline of Theory and Problems of Machine Design (S.I. Metric Edition) by Hall, Holowenko and Laughlin (2002). All other information and formulae used from other sources are clearly indicated at the point of usage.

For torsional rigidity, the expected angle of twist in the shaft designed is given as:

$$\text{Angle of twist, } \theta = \frac{584 M_t L}{G \times d^4} \qquad \dots\dots\dots\dots\dots\dots\dots\dots 3.28$$

Where, G = torsional modulus of elasticity in Nm^{-2}

For commercial steel shaft, G = 80GNm^2

$$\therefore \theta = \frac{584 \times 36.48 \times 0.7}{80 \times 10^9 \times 0.025^4} = 0.477$$

$$\theta = 0.48^0 \text{ twist per metre length of shaft}$$

Thus, the expected angle of twist between the bearings is 0.48^0, which is within the permissible limits of 0.3 – 3.0 degree/m quoted for machine tool shafts and general line shafting.

3.3.4.7 Selection of pulleys and belt drives

The 5.5kW electric motor revolves at 1440 rpm which is far greater than the desired revolutions needed to rotate both the mixing shaft and move the conveyor belt on the U-channel beam. Based on design experience and availability of materials in spare part markets, a reduction gear box of 1:13 was selected and installed, before a system of interconnected pulleys and belts were used to achieve the required result, pulley-belt connection diagram as shown in Figure 3.7.

Thus, from the reduction gear box with output shaft diameter of 30mm, the output revolution is given as:

$$N_{R.G.} = 1/3 \times N_{E.M.} \qquad \text{…………………………………….3.29}$$

Where, $N_{R.G.}$ = reduction gear revolution in rpm

$N_{E.M.}$ = electric motor revolution in rpm

$\therefore N_{R.G.} = 1/13 \times 1440 = 110.77$

$N_{R.G.} \cong 110 \text{ rpm}$

Note that the value of the revolution of reduction gear was rounded down due to the likely frictional loss during transmission. From preliminary engineering estimates, it is believed that shafts running at approximately 40 rpm should provide satisfactory mixing of the constituents in the chamber and the slow gradual movement of the conveyor belt on the U-channel beam as desired. In view of this, with a single groove 60mm diameter pulley attached to the output shaft from the reduction gear box, the required pulley diameters to drive the shaft moving the conveyor belt and equally rotate the mixing shaft are designed as follows:

Reduction gear
box pulley
ø 60mm

Conveyor belt
pulley ø = ?
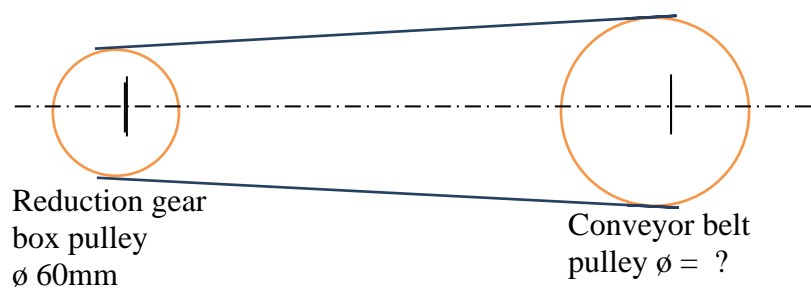
Figure 3.7: Pulley-belt connection diagram

To estimate the diameter of the pulley that moves the conveyor belt, the following relation was used:

$$N_1D_1 = N_2D_2$$ …………………3.30

Where, N_1 = revolution of reduction gear box in rpm

N_2 = revolution of the shaft moving the conveyor belt in rpm

D_1 = diameter of output pulley on the reduction gear in m

D_2 = diameter of the pulley attached to the shaft in mm

From the design parameters available,

$$N_1 = 110 \text{ rpm}, N_2 = 40 \text{ rpm}, D_1 = 60\text{mm}$$

Therefore, using the equation, $D_2 = \dfrac{N_1 D_1}{N_2}$ ……………………….3.31

$$\therefore D_2 = \frac{110 \times 60}{40} = 165$$

$$D_2 = 165\text{mm}$$

Based on availability, a pulley of 150mm was utilized for the fabrication work. Similarly, a pulley of the same diameter was used for the rotation of the shaft in the mixing chamber since both are so designed to rotate at approximately 40 rpm.

Two A-type, V-Belts were selected and positioned tightly around the grooves of the pulleys at the required centre distances, are pulley-belt connection arrangement as presented in Figure 3.8. The parameters of the belt based on arrangement on the pulleys are given. For the belt transmitting power from the reduction gear to the pulley rotating the shaft that moves the conveyor belt on the U-channel beam.

Driver

Driven

Reduction
gear pulley

Conveyor belt
pulley

Figure 3.8: Pulley-belt connection arrangement
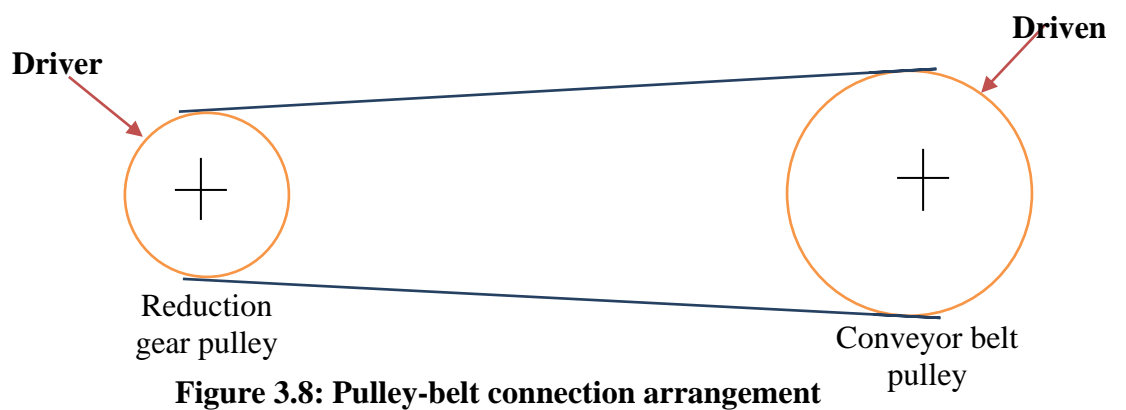
Diameter of pulley driver (reduction gear box), d = 60mm

Diameter of pulley driven (Conveyor belt), D = 150mm

Number of revolution of pulley driver = 110 rpm

Number of revolution of pulley driven = 40 rpm

V – Belt material of construction = leather material

Type of V- Belt = angle type A (A40 12.5 x 1075La)

Belt thickness = 8mm

Belt width = 12.5mm

Centre distance between the pulleys, C = 400mm

Coefficient of friction of leather on iron cast pulley = 0.35

Allowable stress for the leather belt = 2MPa

Factor of safety chosen = 1.5

Belt density = 970kg/m^3

From these parameters, the power capacity of the belt is estimated thus:

Angle of wrap of smaller pulley (driver)

$$\alpha_1 = 180^0 - 2\sin^{-1}(R - r) / C \qquad \dots\dots\dots\dots\dots\dots\dots\dots\dots\dots\dots\dots\dots 3.32$$

$\alpha_1 = 180^0 - 2\sin^{-1}(75 - 30) / 400$

$= 167.1^0$

Angle of wrap of larger pulley (driven)

$$\alpha_2 = 180^0 + 2\sin^{-1}(R - r) / C \dots\dots\dots\dots\dots\dots\dots\dots 3.33$$

$\alpha_2 = 180^0 + 2\sin^{-1}(75-30)/400$

$= 192.9^0$

Where, α = angle of wrap

R = radius of the larger pulley (driven) = D/2

r = radius of the smaller pulley (driver) = d/2

C = centre distance between the pulleys

The pulley that governs the design is the one that has a smaller value of $e^{f\alpha}$, where **f** is the coefficient of friction between the belt and the pulley. Here, the smaller pulley (driver) governed the design since $e^{f\alpha2} < e^{f\alpha2}$. This implies that the smaller pulley is transmitting its maximum power with te belt on the point of slip while the larger pulley is not developing its maximum capacity.

Mass of the pulley belt is given as:

$$m = bt\rho \qquad \dots\dots\dots\dots\dots\dots\dots\dots\dots\dots\dots\dots\dots\dots\dots 3.34$$

Where, m = mass of 1m of belt in kg/m

b = width of belt in m

t = thickness of belt in m

ρ = density of belt in kg/m^3

From the design parameters,

b = 12.5 x 10^{-3} m; t = 8 x 10^{-3}; p = 970kg/m^3

$\therefore$ m = 12.5 x 10^{-3} x 8 x 10^{-3} x 970

m = 0.097kg/m

The speed of belt is given as:

$$v = \pi DN \qquad \dots\dots\dots\dots\dots\dots\dots\dots\dots\dots\dots\dots\dots\dots\dots 3.35$$

Where, v = belt speed in m/s

D = diameter of the smaller pulley (driver) in m

N = rotational speed of driver pulley in rps (revolution per second)

From the belt driver parameters,

D = 60mm = 0.06 m

$$N = 40 \text{ rpm} = \frac{40}{60}\text{rps} = 0.667 \text{ rps}$$

$\therefore$ v = 3.142 x 0.06 x 0.667

v = 0.126 m/s

Tension in the tight side of the belt is given as:

$$T_1 = \frac{bts}{K} \qquad \dots\dots\dots\dots\dots\dots\dots\dots\dots\dots\dots\dots 3.36$$

Where, T_1 = belt tension in tight side (N)

s = maximum allowable stress (N/m^2)

K = factor of safety

From the belt drive parameters,

$$s = 2MPa = 2 \times \frac{10^6 \text{N}}{\text{m}^2} \quad \text{and } K = 1.5$$

$$T_1 = \frac{bts}{K} = \frac{12.5 \times 10^{-3} \times 8 \times 10^{-3} \times 2 \times 10^6}{1.5} \qquad \dots\dots\dots\dots\dots\dots\dots\dots\dots\dots\dots\dots\dots\dots\dots\dots\dots 3.37$$

T_1 = 133.33N

Tension, T_2, in the slack side of the belt is given as:

$$\frac{T_1 - mv^2}{T_2 - mv^2} = e^{f\alpha_1} \qquad \dots\dots\dots\dots\dots\dots\dots\dots\dots\dots\dots\dots\dots 3.38$$

$$\frac{133.33 - 0.097 (0.126)^2}{T_2 - 0.097 (0.126)^2} = e^{0.35 \left(167.1 \times \frac{\pi}{180}\right)}$$

$$\frac{133.33-0.00154}{T_2-0.00154} = 2.775$$

$$\therefore T_2 = \frac{133.33-0.00154}{2.775} + 0.00154 \quad \dots\dots\dots\dots\dots\dots 3.39$$

$T_2 = 48.05N$

Therefore, the power transmitted by the belt drive is given as:

$$P = (T_1 - T_2)v \qquad \dots\dots\dots\dots\dots\dots\dots\dots\dots\dots.. 3.40$$

Where, P = power capacity of belt drive (W)

T_1 = tension in the tight side of the belt (N)

T_2 = tension on the slack side of the belt (N)

v = belt speed (m/s)

P = (133.33 – 48.05) x 0.126

= 10.75W

Therefore, the power transmitted by the belt drive is approximately 10.75W.

For the belt connected between the pulley rotating the shaft controlling the movement of the conveyor belt and the pulley rotating the shaft in the mixing chamber, no power is transmitted because the pulley diameters are essentially the same i.e. only motion is transmitted between the two pulleys.

3.3.4.8 Design of chain drive

The rotation of the conveyor belt-driven shaft is transmitted to the sprocket at the other end of the shaft, which in turn transmits motion to the roller through a chain drive. Sprockets are arranged at the ends of each roller with alternating system of chains in which the combined effects of their rotation move the conveyor belt and its mortal content from one end to another.

Design horsepower of the chain drive is given as:

$$(hp)_d = \frac{K_a(hp)_{nom}}{K_{st}} \qquad \dots\dots \dots\dots\dots\dots\dots\dots.3.41$$

Where, $(hp)_d$ = design horsepower of the chain drive

$(hp)_{nom}$ = horsepower of the chain drive

K_a = application factor

K_{st} = multiple – strand factor

For a single-strand chain under moderate shock loading, K_a = 1.25 and K_{st} = 1.0

$$\therefore (hp)_d = \frac{1.25 \times (10.75)}{1.0} = 13.44W$$

Converting to horsepower,

$$(hp)_d = 13.44/750 = 0.0179 \text{ hp}$$

$$\cong 0.02 \text{hp}$$

For 0.02 design horsepower, single strand and drive (pinion) sprocket speed of 40 rpm, a chain number of #25 was selected (as indicated in Fig. 17.14 in Collins et al. (2010)). For a #25 chain, the pitch, P = 0.25 inches = 6.35 mm.

The recommended centre distance between sprockets is 30 – 50 chain pitches, i.e. 190.5 – 317.5mm. Thus, a centre distance of 200mm was chosen within the recommended limits.

For a low speed application, it is expected that the driver (small sprocket) should have at least 12 teeth. Based on availability, a sprocket of 21 teeth was selected for the driver.

The number of teeth on the driven sprocket is calculated from:

$$N_L = \frac{N_s n_s}{n_L} \qquad \qquad \text{...3.42}$$

Where, N_L = number of teeth on driven sprocket

Ns = number of teeth on driver sprocket

n_L = rotational speed of driven sprocket (rpm)

n_s = rotational speed of driver sprocket (rpm)

Since the chain drive is needed to transfer motion from the shaft to the rollers, the rotational speeds of the driver and driven sprockets are the same, i.e. $n_s = n_L = 40$ rpm

$$\therefore N_L = \frac{N_s n_s}{n_L} = N_s \qquad \qquad \text{...3.43}$$

$N_L = N_S = 21$ teeth

The linear chain velocity is given as:

$$V = \frac{PNn}{12} \text{ ft/min} \qquad \qquad \text{.............................3.44}$$

Where, P 0.25; N = 21; and n = 40 rpm

$$V = \frac{0.25 \times 21 \times 40}{12} = 17.5 \text{ ft/min}$$

$$V = \frac{17.5 \times 0.3048}{60} \text{ m/s}$$

= 0.0889 m/s

The chain length, L, in pitches is given as:

$$L = 2\left[\left(\frac{N_L + N_s}{2}\right) + 2C + \frac{(N_L - N_s)^2}{4\pi^2 C}\right] \quad\quad …………………3.45$$

Where, C = Selected centre distance in inches

i.e C = 200 mm = 7.874 inches

$$\therefore L = 2\left[\left(\frac{21+21}{2}\right) + 2(7.874) + \frac{(21-21)^2}{4 \times 3.142^2 \times 7.874}\right]$$

$L =$ 2[21 + 2(7.874) + 0]

$L =$ 73.50 Pitches

For there not be a half-links chain, it is expected that he chain length be even number of pitches, therefore a chain length of 74 pitches was used.

i.e. chain length = 74 pitches = 74 x P   ………………………..3.46

= 74 x 6.35 mm = 469.9 mm

= 470 mm

In summary, a single-strand standard number #25 was used, with chain length of 470mm (74 pitches), centre distance of 200mm and pitch of 6.35mm. The dimension and nominal ultimate tensile strength of the chain as given in Table 17.6 (Collins *et al.*, 2010) are:

ANSI Chain Number = #

Pitch = 6.35mm

Roller diameter = 3.30mm

Roller width = 3.187mm

Pin diameter = 2.31mm

Link-Plate thickness = 0.76mm

Nominal ultimate tensile strength = 4.7kN

Average specific weight = 3.30N/m

Similar sprocket-chain arrangement was used for other rollers, alternating the chains at each end of the roller, with a total of six (6) rollers and chains systematically positioned to move the conveyor belt at the desired speed.

3.3.4.9 Design of the beam (U-Channel) for frame

The design of a beam must satisfy three criteria: bending strength, shear strength and deflection. The total load acting on the beam is the sum of the weights of the following elements:

  i.   Rollers and shafts;
  ii. Ball bearings;

iii. Sprockets and chains;

iv. Compacting roller and

v. Anchors for the compacting roller

(i) Bending strength criterion

The cumulative of these weights gives a total of 1101.36N. A factor of safety of 1.5 was considered; hence, a load of 1700N was designed for. It is assumed that the cumulative effects of these loads act uniformly on the beam of length L =2000mm, giving a uniformly distributed load of 850N/m,

$$R_1 = R_2 = wL/2 \qquad \dots\dots\dots\dots\dots\dots\dots\dots\dots\dots\dots 3.47$$

$$= \frac{850 \times 2}{2} = 850N$$

The maximum bending moment is considered to occur at the mid-span, and is given by Equation (27):

$$M_{max} = \frac{w^2}{8} \qquad \dots\dots\dots\dots\dots\dots\dots\dots\dots\dots 3.48$$

$$= \frac{850 \times 2^2}{8}$$

$$= 425 \text{ Nm}$$

The Sectional Modulus required (plastic section modulus) to support this moment is determined from the following relations:

The maximum bending moment (strength) of a steel beam is

$$M_{max} = 0.6\sigma_{ys}Z_x \qquad \dots\dots\dots\dots\dots\dots\dots\dots\dots\dots\dots 3.49$$

Where, σ_{ys}= the yield strength of the material

(for mild steel, $\sigma_{ys} = 50\text{kips/in}^2 = 344.75\text{N/mm}^2$)

Z_x = the plastic sectional modulus (mm^3)

$$\therefore 425 \times 1000 = 0.6 \times 344.75 \times Z_x \qquad \dots\dots\dots\dots\dots\dots\dots\dots 3.50$$

$$Z_x = 2054.628\text{mm}^3 = 2.054 \text{ cm}^3$$

This is an order of degree lower than the sectional modulus of MC100 channel used. For an MC100 channel, the sectional modulus is given as 33.5cm^3. Therefore, the beam can support the imposed load without exceeding its bending strength.

(ii) Shear strength criterion

The beam material is safe in shear if the condition in the following relation is sustained.

$$V_{applied} \leq 0.4\sigma_{ys}dt_w \qquad \ldots\ldots\ldots\ldots\ldots\ldots\ldots\ldots 3.51$$

Where,

$V_{applied}$ = the maximum shear force imposed on the beam (N),

σ_{ys} = the yield strength of the material (for mild steel, σ_{ys} = 344.75N/mm^2),

d = the beam depth (mm), and

t_w = the thickness of the web (mm).

The maximum shear force is 850N. From Appendix III, for an MC100, d=100mm, and t_w = 5.0

∴ an MC100 beam can support a shear load of

$$V_{applied} = 0.4 \text{ x } 344.75 \text{ x } 100 \text{ x } 5 = 68950N.$$

Since the actual shear load of 850N is less than 68950N, the beam will not fail in shear.

(iii) Deflection criterion

It is assumed that the maximum deflection of the beam does not exceed 20mm to avoid excessive deflection, i.e. Δ_{max} = 20mm. The maximum deflection for a simply-supported beam with a uniformly distributed load is given by:

$$\Delta_{max} = \frac{5wL^4}{384EI} \qquad \ldots\ldots\ldots\ldots\ldots\ldots\ldots\ldots \text{ 3.52}$$

Where E is the MOE of mild steel (200GN/m^2= 200kN/m) and I is the required Moment of Inertia to resist deflection

$$\therefore \quad 20 = \frac{5 \times 0.850 \times 2000^4}{384 \times 200 \times 10^3 \times I}$$

$$I = \frac{68000 \times 10^{-9}}{0.02 \times 384 \times 200} = 44.27 \times 10^{-9}m^4$$

$$= 0.04427 \text{ x } 10^6 mm^4$$

Therefore the moment of inertia required to resist the deflection of the beam is approximately 4.4 x 10^{4}mm^4

3.3.4.10   Design of the heating system

The heating system consist of a microcontroller, embedded in many control, monitoring, and processing systems, passive components (resistors, capacitors, diode,

indicators, and transformers), finned tubular heating elements, thermocouple, control box and a thermostat, Sketch of the equipment were presented in Figures 3.9, 3.10, 3.11, and 3.12 respectively.

The system is able to generate sufficient heat required to ensure adequate bonding of the coir-CNSL particleboard. A finned tubular heater is preferred as it is cheap, durable and produces consistent heat energy. It is positioned at the middle of the heating chamber to ensure uniform distribution of heat as the board is conveyed through it to the receiving end. The use of a thermocouple is necessary so as to indicate the heating temperature while the thermostat ensures distribution of heat at a constant temperature to guarantee sufficient bonding strength. The control box houses the switches in digital scale that control the heater, time and the metre connected to the thermocouple.
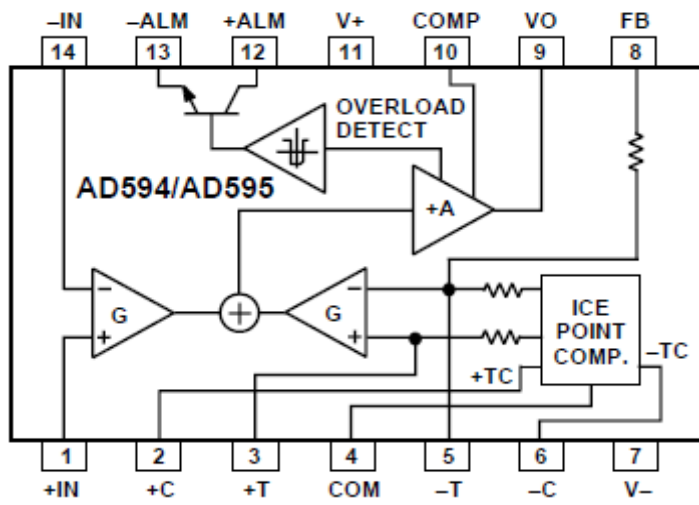
Figure 3.9: Block diagram for the heating device
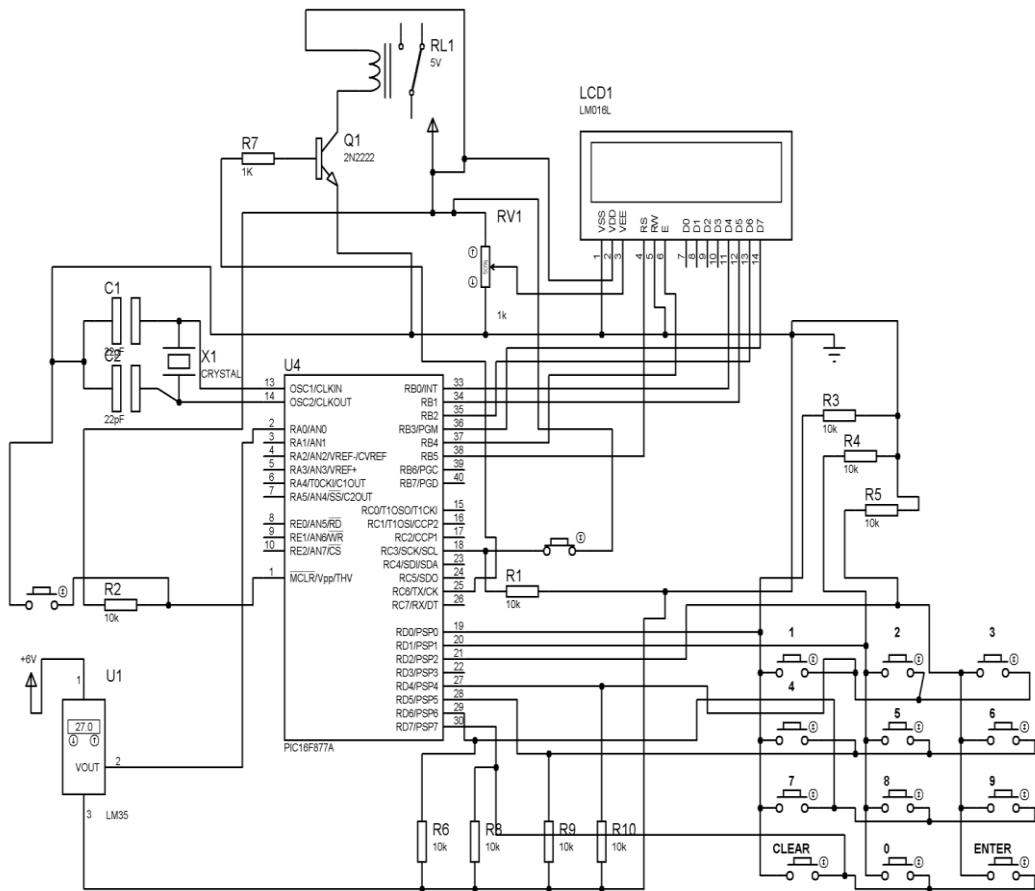
Figure 3.10: Circuit diagram of the control panel for the heating element section
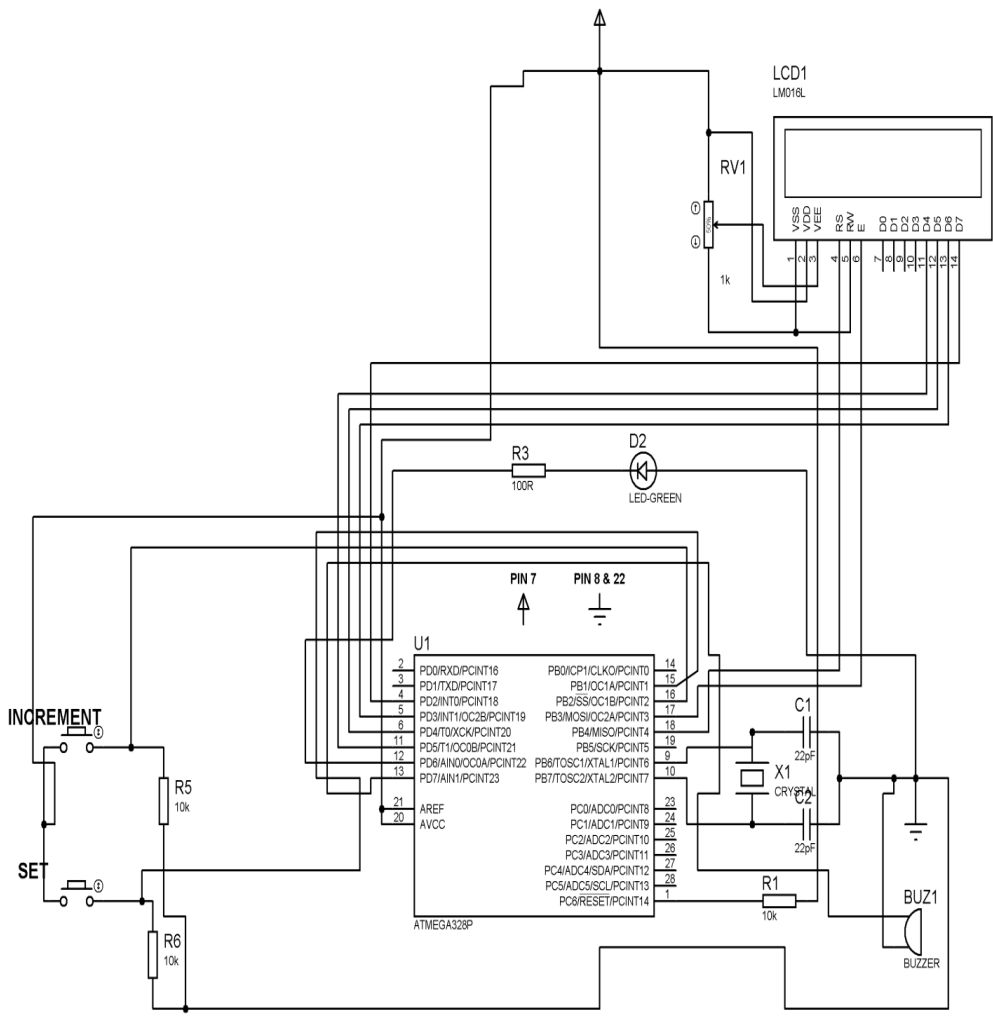
Figure 3.11: Circuit diagram of the control panel for the timer section
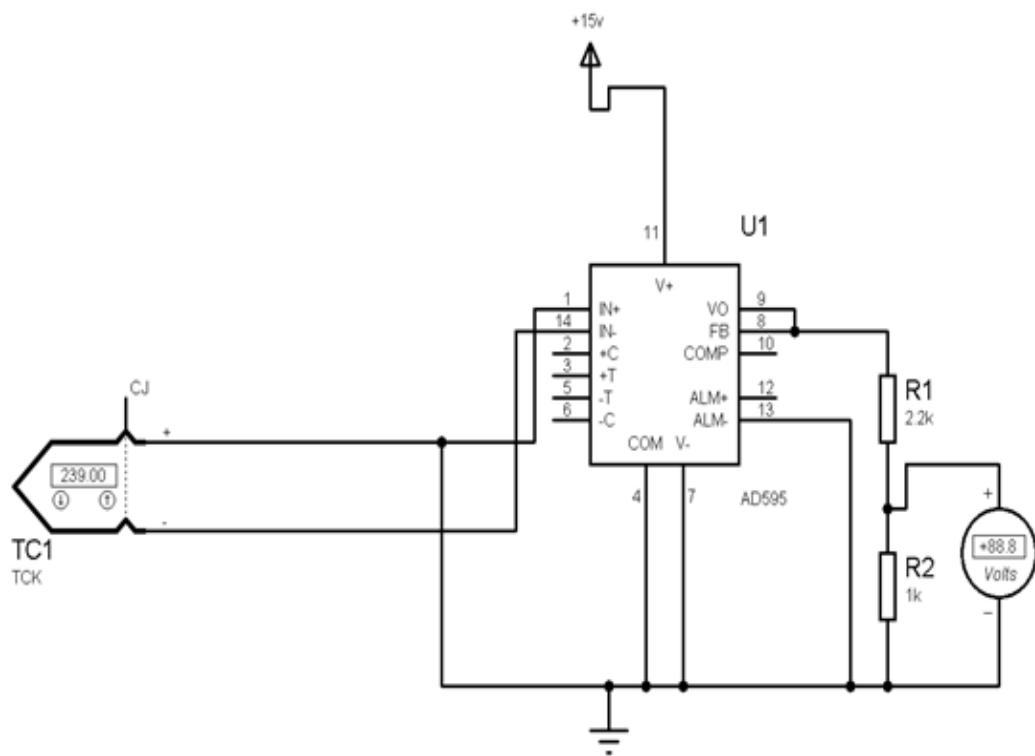
Figure 3.12: Circuit diagram of the thermocouple section.

3.3.4.11 Specifications of the components:

      Microcontroller*:*

Various factors are considered in the choice of microcontroller to use for a particular purpose. These include:

1. The total number of analogue and digital inputs in the system in question has certain requirements, which influence how many inputs and outputs (I/O) the selected microcontroller must have and how much of an internal analogue-to-digital converter module is required.
2. The size of program memory storage required
3. The clock frequency magnitude determines how quickly the microcontroller completes tasks.
4. The number of interrupts and timer circuits required.
5. An internal ADC stage

In a project of this kind where the number of computation that would be input is largely dependent on the amount of memory available, a microcontroller with a large memory sufficient input/output ports and analogue/digital channels such as the ATMEGA328P is quite acceptable for use.

      Heater*:*
- o A finned tubular heater with the following ratings: 1000watts, 250volts, 4A.

      Thermocouple*:*
- o K-type thermocouple with bare tip and glass braided insulation,
- o Length of wire: 1.5m
- o Wire diameter: 24gauge, 0.5mm
- o Insulation, fibre-glass braided
- o Outer dimension: 2.3 x 1.3mm
- o Maximum temperature 500°C

      Thermostat*:*
- o Digital type with variable gauge,

      Range of measurement: 1-250°C

3.4 Evaluation of properties of particleboards

3.4.1 Physical and mechanical properties determined

Water absorption, Thickness Swelling and Density were carried out to determine the dimensional stability properties of the composite boards produced while, Flexural Strength Tests, Compressive Strength Tests, Modulus of Elasticity, Modulus of Rupture and Impact Strength were carried out to determine the degree of the structural suitability.

3.4.1.1 Water absorption test procedure

The determination of water absorption was performed according to ASTM D-1037; 99 Three test samples of sizes 100mm x 100mm x 8mm (BS.5669: Part 1) were prepared and conditioned to constant weight. Oven dry the specimens until constant weight were attained (Plate 3.20). The samples weight were measured and recorded, the weight of particles board were measured using weighing balance.

The test sample was immersed in potable water that was kept at a temperature between 20 and 22 °C for 24 hours. The samples were removed from the water after 24 hours, and the surfaces were dried with a fresh, dry cloth. The samples were reweighed to the nearest 0.1g. The water absorption of each sample was calculated by the weight difference

Water Absorption was calculated by

$$WA = \frac{m_2 - m_1}{m_1} \times 100 \qquad \dots\dots\dots\dots\dots\dots\dots\dots\dots 3.53$$

m_1 = Initial mass (after the oven drying)

m_2 = Wetted mass (after submerged for 24hours)

Plate 3.20: Dry oven of composite boards during water absorption test

3.4.1.2 Thickness swelling test procedure

The determination of 2 hours and 24 hours of the Thickness Swelling (TS) test were performed according to ASTM D-1037;99. Three test sample sizes 100mm x 100mm x 8mm (BS. 5669; Part 1) were prepared and conditioned to constant weight. Oven-dry method was used to measure the moisture contents of samples. The thickness swelling of the boards was measured using electronic veneer calliper. The thickness measured along the samples edge at four different points to an accuracy of 0.3% and the average value for each sample is computed.

The samples tested were submerged in potable water maintained at a temperature of 20-20^{0}C (Plate 3.21). After the first 2 hours of immersion samples were drained for some minutes to remove excess water from the surface of the samples, the weight and thickness of each sample was then measured and recorded. The samples were further submerged under for additional period of 22 hours after which the successively weight and thickness were determined (Plate 3.22).

<div align="center">

Thickness Swelling (%)

T_i = Initial thickness

T_f = Final thickness

Thickness swelling (%)

</div>

$$\frac{T_f - T_i}{T_i} \times 100\% \qquad\qquad \ldots\ldots \ 3.54$$

Plate 3.21: Samples immersed in water during water absorption and thickness swelling test

Plate 3.22: Measurement of thickness swelling

3.4.1.3 Determination of density

The density of particleboard samples were determined by measuring the mass and volume. The relationship is expressed as:

$$\text{Density} = \frac{\text{mass of the test sample (g)}}{\text{volume of the test sample (cm}^3)} \qquad \text{.... 3.55}$$

3.4.1.4 Flexural strength test procedure

Test samples from developed composites were taken and tested for their flexural strength properties according to ASTM D -1037; 99 by using Universal Testing Machine (Plate 3.23). Cubic samples dimensions were 100 x 100 x 100 mm. The sample was carefully placed on the supported beams (a simple beam supported the sample at two point and loaded at its midpoint) and load at midpoint of the sample.

In accordance with the specification of BS 188: (1993), the flexural strength of the sample was determined using central point loading. Then, the bending load is carried out until the failure of the sample took place. Thereafter, the flexural bend strength of the sample is calculated by the load deflection curve which was calculated through the data obtained from the experiment.

The flexural strength was calculated using the following equation:

$$\text{Flexural} = \frac{PL^3}{4bd^3\Delta} \qquad \text{..........................} \qquad 3.56$$

Where, P – Maximum load in (N), L – Length of sample in (mm), b – Width of sample measured (mm), d – Thickness of sample measured (mm), Δ - Displacement in (mm)

3.4.1.5 Compressive strength test procedure

The compressive test was carried out in accordance to ASTM D-1037; 99. The samples sizes of 100mm x 100mm x 100mm were prepared and the testing was done by using Universal Testing Machine.

The sample were carefully place between the compression plate at its centre position in such a way that moving heads centre is placed vertically above the centre of the sample (central point loading in accordance with the requirement of BS 1881: part 118 1983). Moreover by giving direction to the advancing head, the load is applied to the sample until it break down (samples were crushed to evaluate the compressive strength test sample as prescribed by BS 1881: part 119, 1983).

For any material, the formula for compressive strength is provided as a load applied at the point of failure to the cross-sectional area of the force that delivered the load.

$$\text{Compressive strength} = \frac{P}{bd} \quad \dots\dots 3.57$$

Where, P – Maximum load in (N),

b – Width of sample measured (mm),

d – Thickness of sample measured (mm)

3.4.1.6 Modulus of rupture test procedure

The modules of rupture test was carried out in accordance to ASTM D – 1037 99. The samples of sizes 195 x 50 x 10 mm were prepared and the texting was done by using Universal Testing Machine (Plate 3.24). Samples shell were placed flatwise on the approximately uniform rate motion of the movable crosshead not less than ½mm (12 mm/min) nor until definite failure occurs and then note the maximum load to accuracy of testing machine.

Preceding the testing, the width, length and thickness of the samples were measured in order to calculate the Modulus of Rupture. Four numbers of samples were tested face-up and face-down. The testing machine speed used shall be recorded and the deflection at the centre of the sample shall be measured by measuring the deflection of the neutral axis.

The following equation was used to determine the MOR:

$$MOR = \frac{3PL}{2bd^2} \quad \dots\dots\dots\dots\dots 3.58$$

Where, b -Width of sample measured in (mm)

d – Thickness of sample measured in (mm)

L – Length of span in (mm)

P – Maximum load in (N)

R – Modulus of rupture (Mpa)

Plate 3.23: Universal Testing Machine for determining MOE and MOR

3.4.1.7 Modulus of elasticity test procedure

The determination of modulus of elasticity (MOE) test were performed according to ASTM D – 1037 99. The samples of sizes 195mm x50 x10mm were prepared and were carried out using Universal Testing Machine (Plate 3.24). Samples were placed flatwise on the parallel support. Load was applied continuously at mid span at an approximately uniform rate of motion of the movable crosshead not less than ½ min (12mm/min) until definite failure occurs, and the maximum load to accuracy of the testing machine was noted.

Proceeding to testing, the width, length and thickness of the samples were measured in order to calculate the MOE. Four numbers of samples were tested face-up and face-down. The testing machine speed used was recorded and the deflections at the centre of the sample were measured by measuring the deflection of the neutral axis.
The Modulus of Elasticity was calculated in accordance with the following equation:

$$MOE = \frac{PL^3}{4bd^3\Delta} \quad \dots \dots \dots \dots \dots \quad 3.59$$

Where, b – Width of sample measured in (mm)

d – Thickness of sample measured in (mm)

l – Length of span in (mm)

P – Maximum load in (N)

Δ -- Displacement in (mm)

E – Modulus of Elasticity (Mpa)

3.4.1.8 Impact strength test procedure

The composite board samples were tested for impact resistance in accordance to ASTM D1037.The test was carried out at Forestry Research Institute of Nigeria, Ibadan. Each test sample was cut into 300 x 300 x 6 mm and supported in rebated square frame without fastenings, while the experimental programme overview is presented in Table 3.3. A block having a wooden hemispherical end with a radius of 25mm was arranged to fall freely on the centre of the test sample, with the block being guided on its fall. The mass of the block is 3kg.
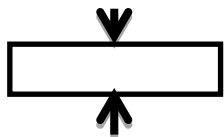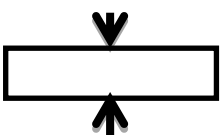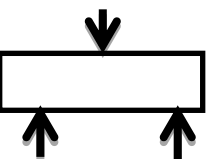
The block was allowed to fall from a height of 20mm measured from the upper surface of the test sample and then from successive heights measured in increment of 20mm

until failure of the sample occurred. The height of fall at which the failure of the sample occurred was recorded for each test sample, and is defined as the height producing the tension failure along the bottom surface of the sample. For each sample tested, the impact load strength is given as:

Impact strength = height of drop (at failure) x weight of falling part ,……………. 3.60

Where, height of fall is measured in metre (m) and weight of falling part is measured in Newton (N)

Table 3.3: Overview of the complete experimental programme

Test	Method	Dimension of specimen	Aim of Test
Water absorption	Submersion in water	100 × 100 × 8 mm	i. Exterior Use ii .Dimensional Stability.
Thickness swelling	Submersion in water	100 × 100 × 8 mm	i. Exterior Use ii. Dimensional Stability.
Compression		100 mm cubes	i. Quality control ii. Compressive strength.
Flexural strength		100 mm cubes	i. Flexural modulus ii. Flexural strength
MOR		195 × 50 × 10 mm	i. Multiple cracking evaluations. ii. Load cracking opening relations.
MOE		195 × 50 × 10 mm	i. Stiffness test ii. Load deflection diagram
Impact strength			i.Impact resistance ii.Toughness iii.Fracture resistance
Density	$\dfrac{mass}{volume}$	100 × 100 × 8 mm	

CHAPTER FOUR

RESULTS AND DISCUSSION

4.1   Machine development

The developed machine was capable of controlling the critical processes of feeding, mixing, pressing, compacting and heating involved in composite board production. It was made up of three units: the mixing chamber, the conveyor unit and the heating system.

The mixing unit was made up of the following components: mixing chamber, pulley system, mixing shaft and rods and electric motor. The mixer rotor bars was powered by a shaft 650 mm long at an average speed of 40 rpm and mixing chamber capacity was 0.0816 m^3. The mixer reduces the time needed to achieve a homogenous mix by more than 50%, compared to manual mixing and the machine can produce 30 No. 520 x 290 x 8 mm boards in a single batch.

The conveyor is 1980 mm long and stand at a height of 740 mm above the ground. It composed of 550 x 1200 mm U-channel, hollow pipes, legs and braces and roller hollow pipe interconnected with chain drives and a freely rotating press roll which was powered by a 7.5 hp (5.5 kw), the 3D view and exploded view are shown in Figure 4.1 and 4.2, respectively. The electric motor revolves at 1440rpm which is far greater than the desired revolution needed to rotate both the mixing shaft and equally moving conveyor belt on the U-channel beam and a reduction gear box of 1:13 was selected and installed.

The heating system consist of microcontroller, heater rating: 1000 watts, 250 volts, 4 A, thermocouple k-type thermocouple with bare tip and glass braided insulation with maximum temperature of 500^0C, thermostat digital type with variable gauge with range of measurement: $1-250^0C$ which required to generate sufficient heat required.
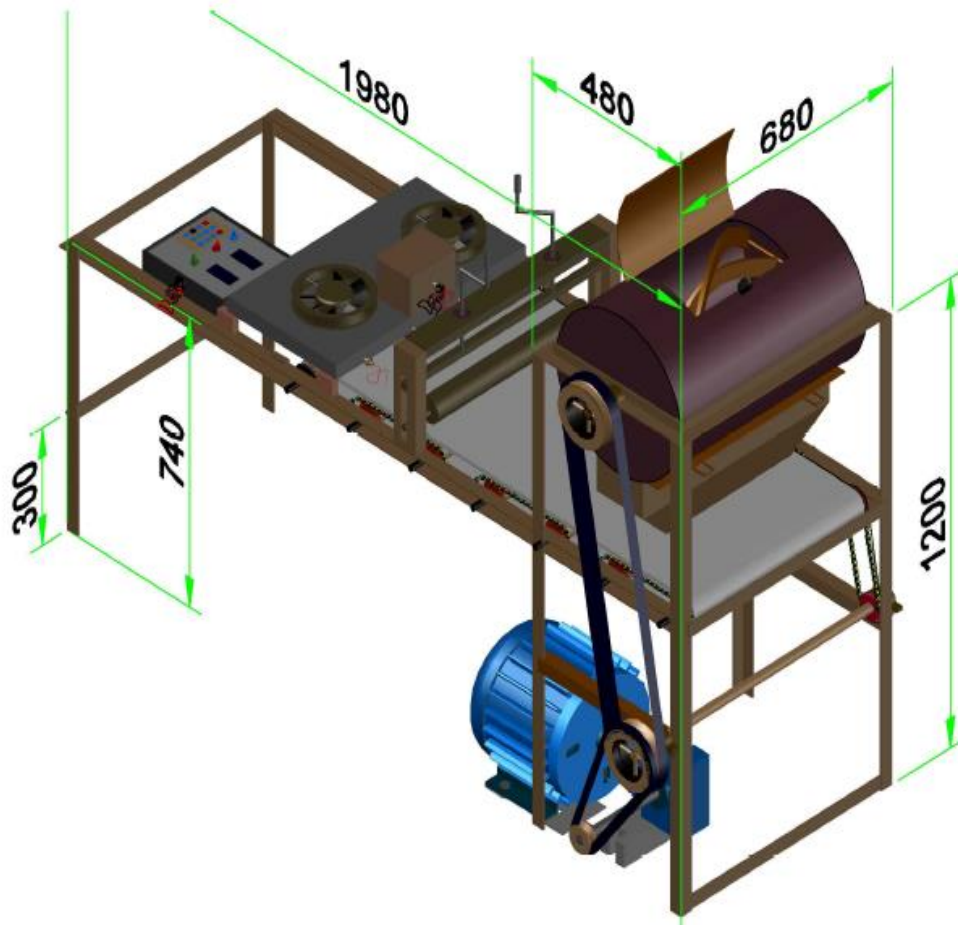
Figure 4.1: Isometric 3-D of the fabricated processing equipment
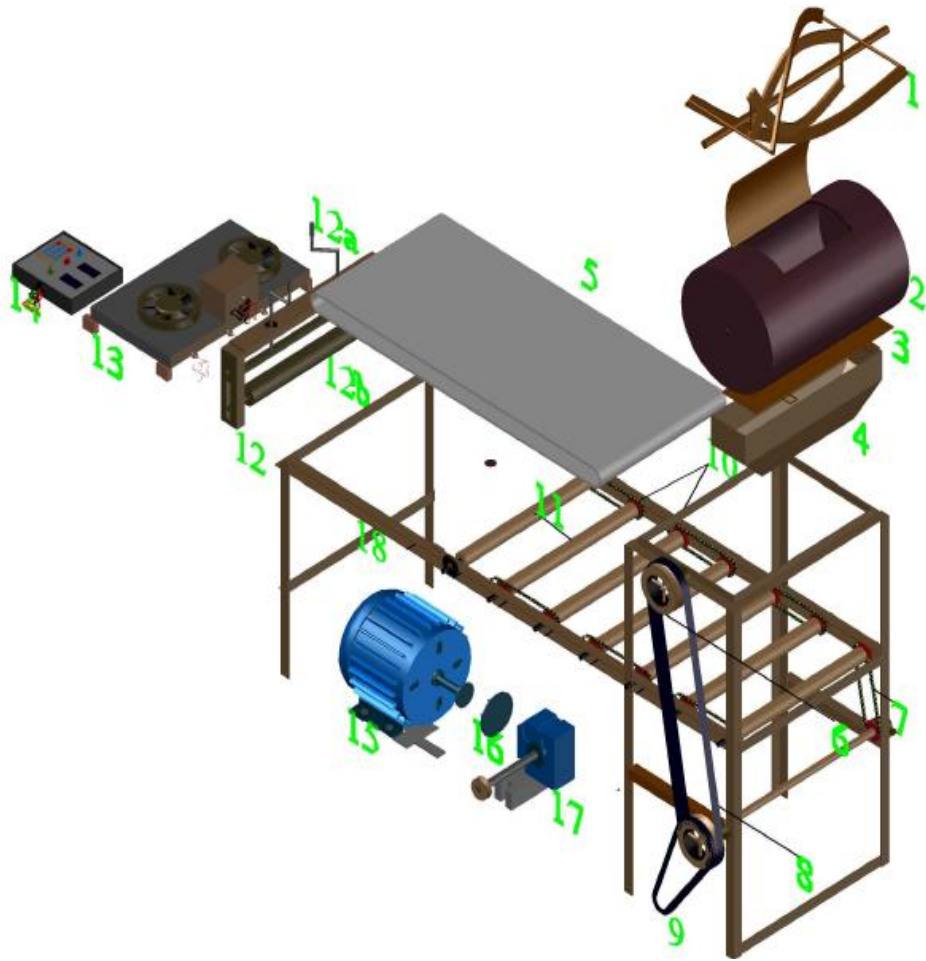
Figure 4.2: Exploded view of the fabricated processing equipment with part label

PART LABEL	
Label No.	Part Name
1	Mixer Rotor Bars
2	Mixing Chamber
3	Mixing Chamber Outlet Cover
4	Mixing Chamber Outlet
5	Conveyor Bed Belt
6	Transmission Belt Pulley
7	Transmission Chain
8	Transmission Belt
9	Power Transmission Belt
10	Roller Chains
11	Conveyor Bed Roller
12	a)Roller Press Handle b)Press Roller
13	Heating Device
14	Heating Device Control Box
15	Electric Motor
16	Coupling
17	Reduction Gear Box
18	Conveyor Bed Frame

4.1.1 Findings from machine developed

1. Mechanical mixer used to ensure workability of the mortar and to achieve homogenous mix of the composites.

2. The mixing bars (3bars) used were steel rods of 4mm gauge which were systematically coiled and wound round the mixer shaft in a serpentine manner in order to allow for easy and uniform mixing of the materials in the chamber.

3. Two A-type, V- belt were selected and which were positioned tightly around the grooves of the pulleys at the required centre distance.

4. The 5.5 kW electric motor used, revolves at 1440 rpm which is far greater than the desired revolutions to rotate both the mixing shaft and the conveyor belt on the U-channel beam.

5. The heating system is to generate sufficient heat required to ensure adequate bounding of the coir fibre, coir dust and coir dust/CNSL particleboard produced.

6. Thermocouple is necessary so as to indicate the heating temperature while the thermostat ensures distribution of heat at a constant temperature to guarantee sufficient bonding strength.

4.2   Results and discussion on composite board materials

4.2.1 Results and discussion on coir fibre

4.2.1.1 Effect of coir fibre quantity on water absorption

The effect of coconut fibres quantity in water absorption as presented in Table 4.1, shows that water absorption increased as the coir fibre quantity increases in the composite as presented in Figure 4.3. It was observed that the water absorption at 5% of coir fibre quantity in the composite increases slightly from 5% of fibre into the 15% of coir fibre quantity.

Among the all composites, 5% of fibre composite absorbs lowest moisture content with 33.14% while 15% fibre composite showed highest water absorption with 69.46% as shown in Table 4.1. Generally, the composite void content has a significant impact on the rate of water absorption. The higher the coir fibre quantity, the higher is the water absorption. The water absorption obtained here correspond to the previous works, by Akash, Gopta and Kuman (2016) in his study about Mechanical of Sisal/ coir fibre reinforced hybrid composites fabricated by cold pressing method that

TABLE 4.1: Summary of the result carried out using coir fibre quantity

Sample (Fibre)	5%	7.5%	10%	15%
Water Absorption (%)	33.14	43.08	52.79	69.46
Thickness Swelling 2 HRS **(%)**	0.67	1.11	1.44	1.61
24 HRS	1.12	1.89	2.54	3.23
Density (g/mm^3)	0.00169	0.00158	0.00143	0.00135
Flexural Strength (mpa)	6.09	6.86	7.61	5.35
Compressive Strength (mpa)	11.43	8.70	8.44	5.72
MOE (mpa)	1078.49	1306.25	1428.85	813.24
MOR (mpa)	4.37	5.11	5.34	4.62
Impact Strength (N/mm^2)	1.19	1.43	4.35	3.81
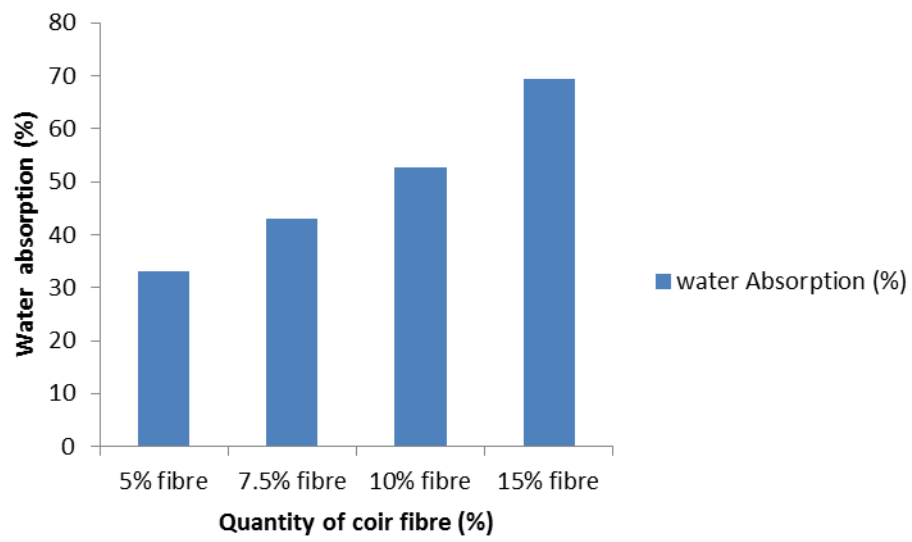
Figure 4.3: Influence of quantity of coir fibre on water absorption

water absorption increased as the coconut fibre increases (Rao, Gupta and Kumar 2016).

This occurrence may be due to the fact that coir fibres contain more polar hydroxide groups, which results in a high absorption level of natural fibre based polymer composite (Das and Biswas, 2016). In addition to the hydroxyl groups present in cellulose and hemicellose of natural fibres, which make it simple for water to enter composites, there are numerous other elements that can influence how well the composites absorb water, including porosity, void content, lumen size, and fibre-matrix adhesion.

The higher water absorption rates in coconut reinforced composites could be due to the highest porosity and hollowness of the coconut fibres (Siakeng, Jawaid, Ariffin and Sapuan 2018). Additionally, it has been noted that the water absorption process starts out sharply before levelling off for a while as it gets closer to equilibrium.

A one-way between subjects ANOVA was conducted and the results presented according to Table 4.1.1 to examine the effect of fibre quantity on Water Absorption. The different fibre quantity sizes considered are: 5% fibre, 7.5% fibre, 10% fibre and 15% fibre. It was observed from the results that there exist significant effect of fibre quantity on Water Absorption $p<.05$ level for at least two of the dust quantity sizes under consideration [$F_{(3,20)} = 7985$, $p <.001$.

From the mean plot computed from Figure 4.4 when examining the effect of fibre quantity on water absorption, it can be observed that 5% fibre quantity computed the lowest mean while 15% fibre computed the highest mean. The mean plot of density portrays a positive trend across the 4 categories of fibre quantity samples under consideration. This shows that as the percentage of fibre quantity increases, the water absorption increases.

Figure 4.5 shows the relationship between the water absorption and coir fibre which is express by Polynomial expression model

$$W.A = 1.6825q^2 + 3.454q + 28.362 \qquad \text{……….…… 4.1}$$

Table 4.1.1: Statistical result of water absorption test for coir fibre

Parameters	df	Sum sq	Mean sq	F-value	Pr (>F)
Sample	3	7.753	2.5843	6.27	0.00356
Residuals	20	8.243	0.4122		
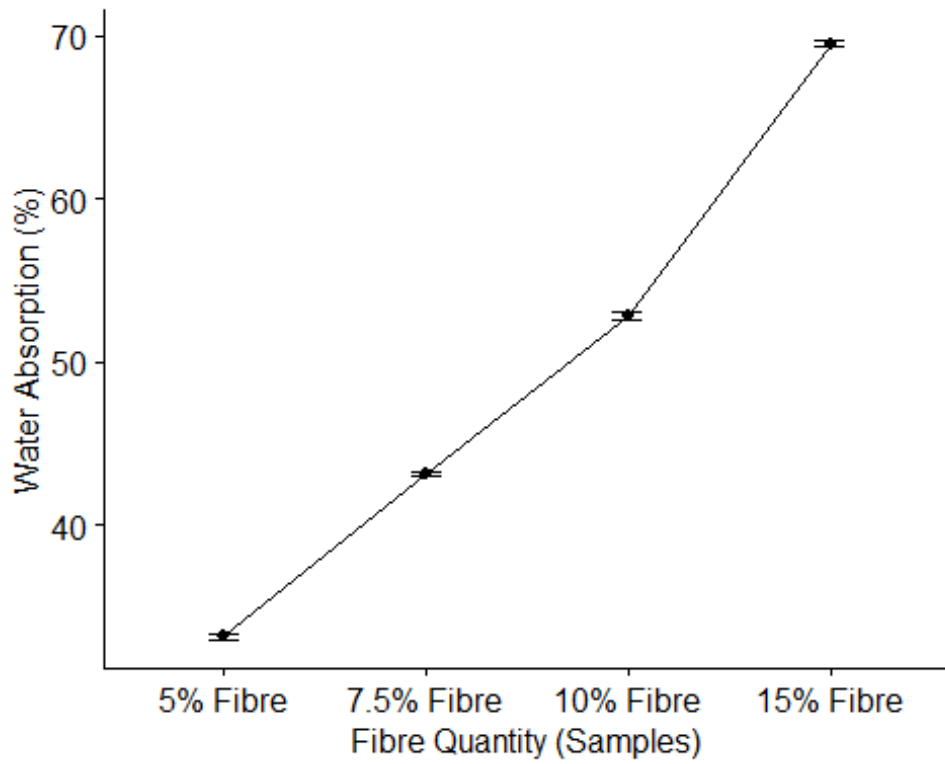
Figure 4.4: Generated quantity of coir fibre on water absorption
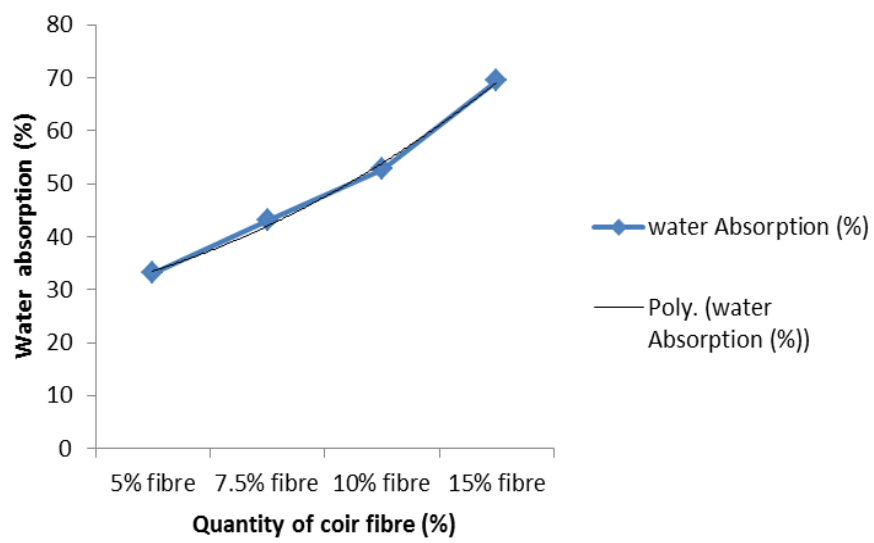
Figure 4.5: Relationship between water absorption (%) and quantity of coir fibre

$$W.A = 1.6825q^2 + 3.454q + 28.362$$
$$R^2 = 0.9964$$

This implies that as water absorption increases significantly, the quantity of fibre also increases.

4.2.1.2 Effect of coir fibre quantity on thickness swelling

Table 4.1 shows the results of thickness swelling of the coconut fibre composites after 2hours and 24hours of submersion in water. The effect of coir fibre quantity in thickness swelling indicated that the thickness swelling increased as the volume of coconut fibre quantity increase in the composites.

Thickness swellings started increasing from 5% of coconut fibre quantity and then continue to increase to the 15% of coconut fibre quantity. As shown in Figure 4.6, the lowest values of thickness swelling in 2hours and 24hours were 0.67% and 1.12% respectively, and the values are given by the composite with 5% of coconut fibre quantity and the composites that contains 15% of coconut fibre quantity has highest value of thickness swelling.

The thickness swelling results obtained in this work are similar to the previous works of Matoke, Owido and Nyaanga (2012) in his study about effect of production methods and material ratio on physical properties of the composites that thickness swelling values of bamboo fibre increased with increase in fibre quantity.

This is because the high cellulose content in the fibres causes more water to seep into the interface through the micro cracks that the swelling of the fibres caused, which led to the failure of the composite. Capillarity and transport via micro-cracks also become active as the composite fractures become active. The capillarity mechanism involves a process of diffusion through the bulk matrix and a flow of water molecules at the fibre-matrix interface (Matoke et al, 2012).

A one-way between subjects ANOVA was conducted and the results presented according to Table 4.1.2 to examine the effect of fibre quantity on thickness swelling. The different fibre quantity sizes considered are: 5% fibre, 7.5% fibre, 10% fibre and 15% fibre. The findings show that coir fibre composite has a significant influence of fibre quantity on thickness swelling $p < .05$ level for at least two of the fibre quantity sizes under consideration [$F(3,20) = 6.27$, $p < .01$.

Table 4.1.2: Statistical result of thickness swelling tests for coir fibre

Parameters	df	Sum sq	Mean sq	F-value	Pr (>F)
Sample	3	2154.7	718.2	7985	3..06e – 14
Residuals	8	0.7	0.1		
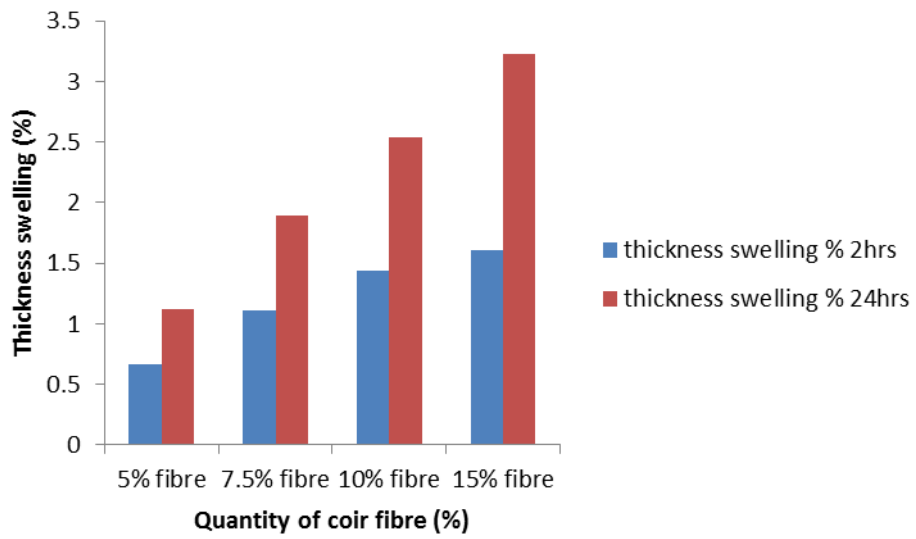
Figure 4.6: Influence of quantity of coir fibre on thickness swelling

From the mean plot computed from Figure 4.7 when examining the effect of fibre quantity on thickness swelling, it can be observed that 5% fibre quantity computed the lowest mean while 15% fibre computed the highest mean. The mean plot of density portrays a positive trend across the 4 categories of fibre quantity samples under consideration. This is an indication that the thickness swelling increases as the percentage of fibre quantity increases.

Figure 4.8 show the relationship between Thickness swelling and coir fibre which is express by Polynomial expression model for 2hrs and 24hrs is given respectively

$$T.S_2 = -0.0675q^2 + 0.6525q + 0.0825 \quad\quad\quad \ldots\ldots\ldots\ldots\ldots\ldots 4.2$$

$$T.S_{24} = -0.02q^2 + 0.798q + 0.35 \quad\quad\quad \ldots\ldots\ldots\ldots\ldots\ldots 4.3$$

This implies that as thickness swelling increases slightly, the quantity of coir fibre also increases.
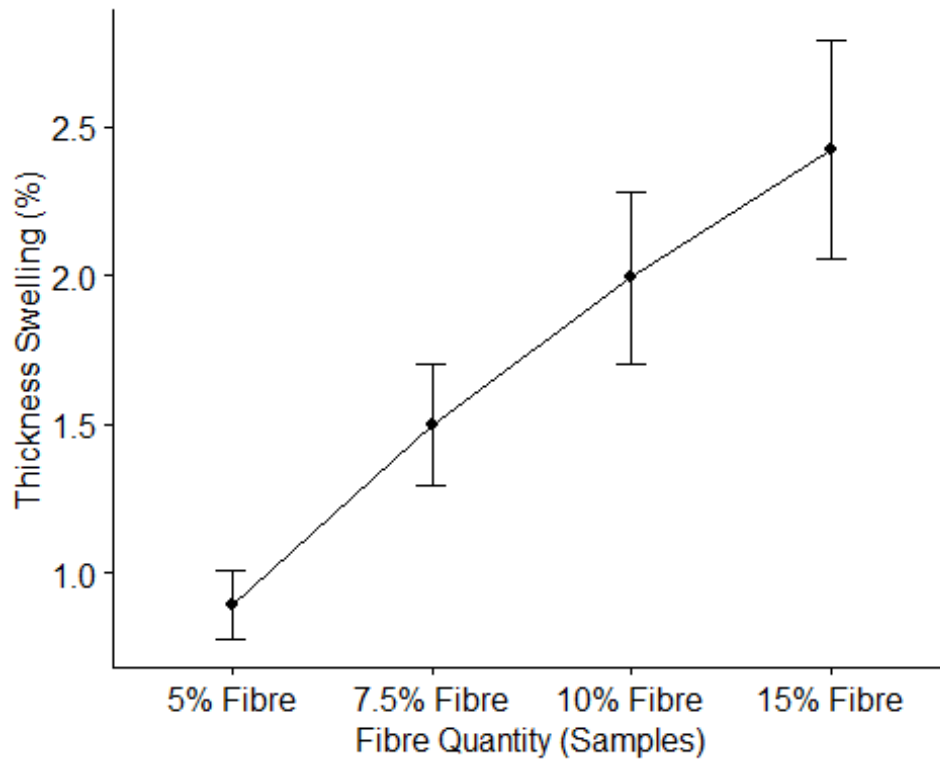
Figure 4.7: Generated quantity of coir fibre on thickness swelling
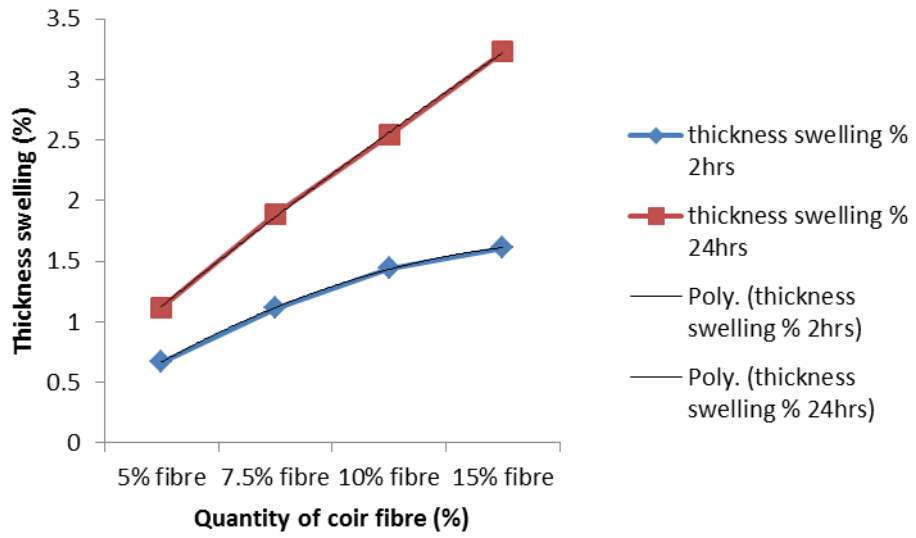
Figure 4.8: Relationships between thickness swelling (%) and quantity of coir fibre

$$T.S_2 = -0.0675q^2 + 0.6525q + 0.0825 \qquad .$$
$$R^2 = 0.9998$$
$$T.S_{24} = -0.02q^2 + 0.798q + 0.35$$
$$R^2 = 0.9995$$

4.2.1.3 Effect of coir fibre quantity on density

The result from Table 4.1 showed that the density of coconut fibre quantity decreased as the coconut fibre quantity increase in composite. Generally, when the density is lower, it will cause the strength to be lower Figure 4.9. Increase in volume percentage of coconut fibre lower the density of composite.

The lowest value of density ($0.00135g/mm^3$) is given by the composite with 15% of coconut fibre while the highest value of density which is $0.00169g/mm^3$ obtained from composite contains 5% of coconut fibre quantity. The density results obtained in this work correspond to the previous works (Abdullah, Baharin, Noor and Hussin 2011) in his study about composite cement reinforced coconut fibre.

Physical and mechanical properties and fracture behaviour that density values of coconut fibre composites decreased with increasing of coconut fibre quantity. Similarly the previous works of Aggarwal, (1995) according to his work on bagasse-reinforced cement composites, the density values of the composites decreased as the bagasse concentration increased. Density is one of the most important factors in determining the properties of composite materials. It mainly depends on the relative proportion of reinforcement and matrix.

Figure 4.10 shows the relationship between Density and coir fibre which is express by Polynomial expression model

$D = 8E\text{-}06q^2 – 0.0002q + 0.0018$ …………………………………………. 4.4

This implies that as Density decreases slightly, the quantity of fibre increases.
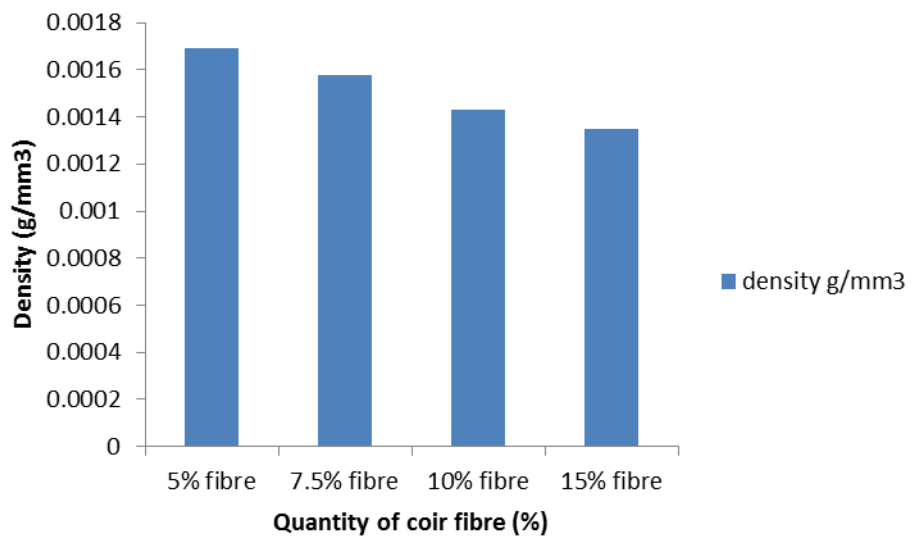
Figure 4.9: Influence of quantity of coir fibre on density
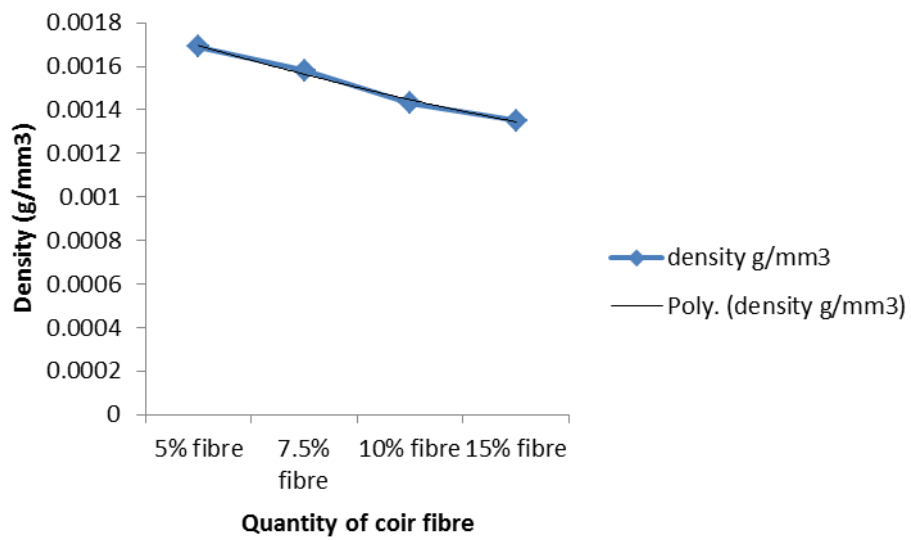
Figure 4.10: Relationship between density (g/mm^3) and quantity of coir fibre (%)
$$D = 8E\text{-}06q^2 - 0.0002q + 0.0018$$
$$R^2 = 0.9913$$

4.2.1.4 Effect of coir fibre quantity on flexural strength

The effect of coconut fibre quantity in the flexural strength of composite as presented in Table 4.1 shows that the variations in the flexural strength value at 5% of coconut fibre quantity gradually increased to the 10% of coconut fibre quantity and there is sharply decrease in flexural strength when the coconut fibre content is at 15%. The flexural strength of 10% coconut fibre quantity composite is found to be maximum (7.61mpa) and decrease with further increase of coconut fibre as shown in Figure 4.10. It was found that the coconut fibre composites show maximum mechanical properties between 5%-10% of the fibre reinforcements. The lowest value of flexural strength (5.35mpa) is given by the composite with 15% of coconut fibre Figure 4.11.

The flexural strength results obtained in this work are similar to the previous works, Ravikantha, Abishek and Dhyanchandra (2015) in his study about development and characterization of low cost polymer composites from coconut coir that flexural strength of coconut fibre increased from 5%-10% of coir fibre quantity and then decrease with further increase of coconut fibre. According to Das and Biswas (2016), the reasons for the lower flexural properties at higher fibre content are probably due to the weak fibre-to-fibre interaction, void, and poor dispersion of fibre in the matrix.

A one-way between subjects ANOVA was conducted and the results presented according to Table 4.1.3 to examine the effect of fibre quantity on Flexural Strength. The different fibre quantity sizes considered are: 5% fibre, 7.5% fibre, 10% fibre and 15% fibre. The findings show that coir fibre composite has a significant influence of fibre quantity on Flexural Strength p<.05 level for at least two of the fibre quantity sizes under consideration [F(3, 8) =*227.00*, p <.001.

From the mean plot computed from Figure 4.12 when examining the effect of fibre quantity on Flexural Strength, it can be observed that 10% fibre quantity computed the highest mean while 15% fibre computed the lowest mean. The mean plot of density portrays an inverted v-shaped plot across the 4 categories of fibre quantity samples under consideration.
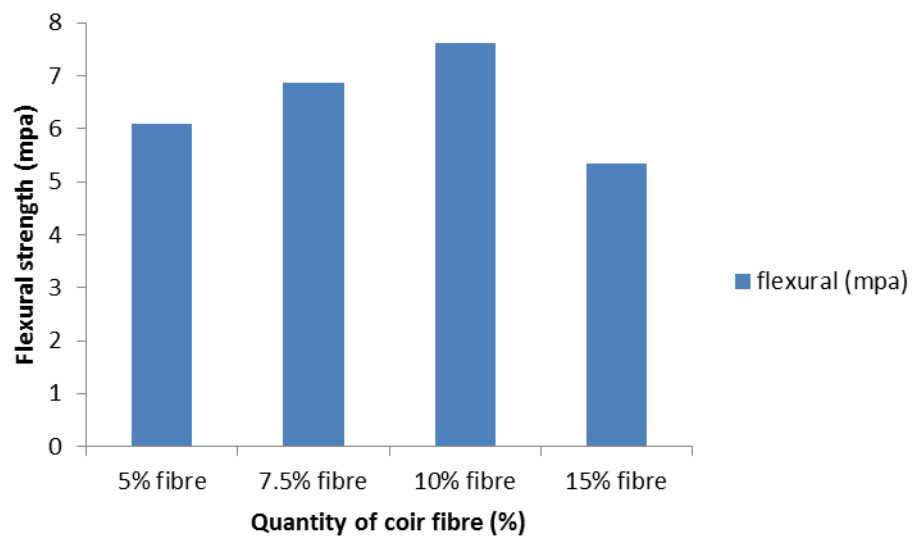
Figure 4.11: Influence of quantity of coir fibre on flexural strength

Table 4.1.3: Statistical result of flexural strength test for coir fibre

Parameters	df	Sum sq	Mean sq	F-value	Pr (>F)
Sample	3	8.6497	2.8831	227	4.45e-08
Residuals	8	0.102	0.0127		
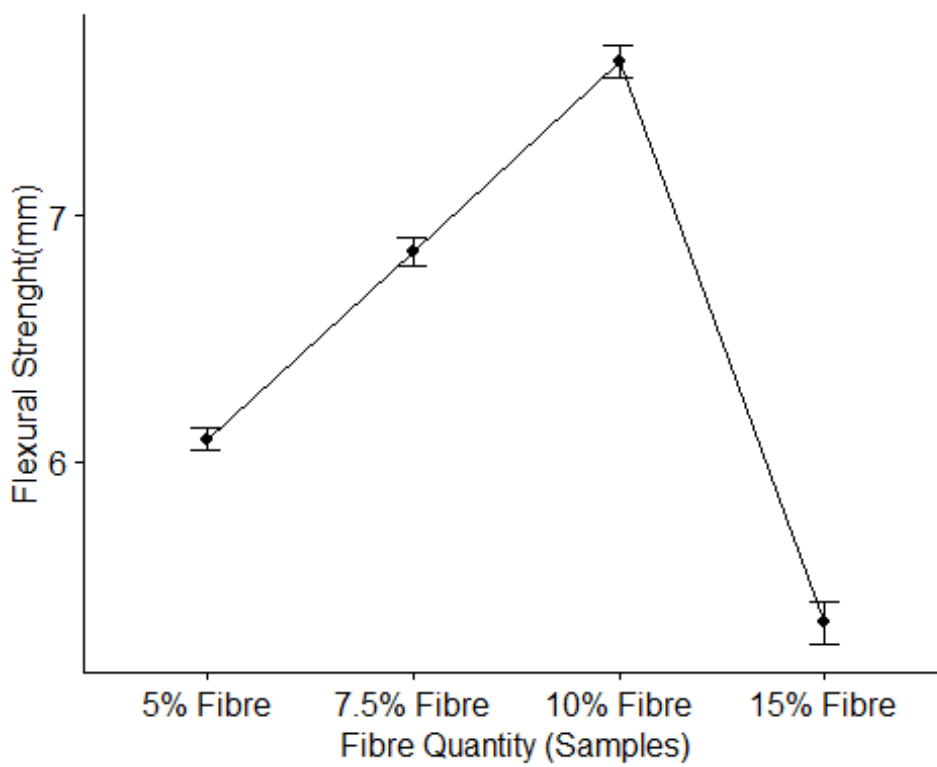
Figure 4.12: Generated quantity of coir fibre on flexural strength

Figure 4.13 shows the relationship between Flexural Strength and coir fibre which is express by Polynomial expression model

$$FS = -0.7575q^2 + 3.6405q + 3.0575 \qquad \dots\dots\dots\dots\dots\dots\dots\dots\dots\dots\dots\dots\dots 4.5$$

This implies that Flexural Strength initially increases significantly to a certain point and started decreasing as the quantity of fibre increases.
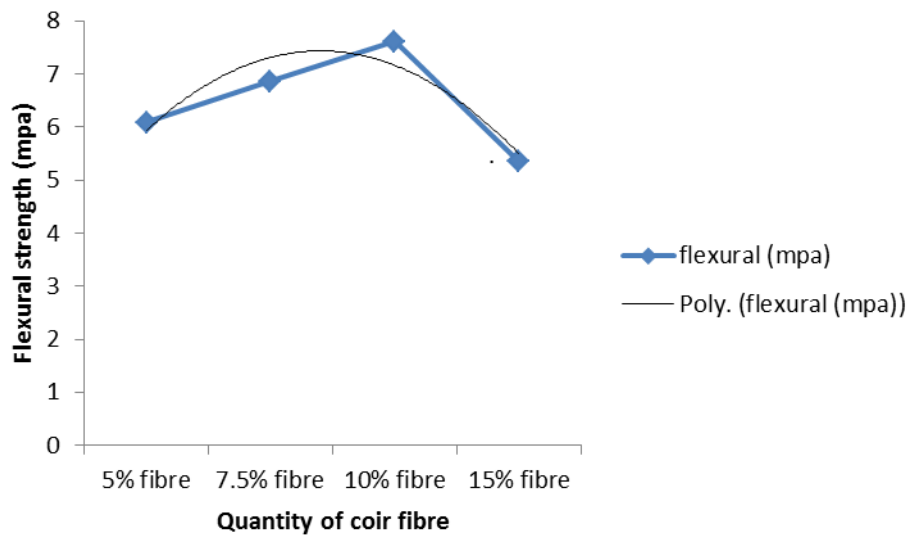
Figure 4.13: Relationships between flexural strength and quantity of coir fibre

$$FS = -0.7575q^2 + 3.6405q + 3.0575$$
$$R^2 = 0.8432$$

4.2.1.5 Effect of coir fibre quantity on compressive strength

It was observed form the test results as shown in Table 4.1 that the compressive strength decreased gradually due to the increase of coir fibre volume percentage in composite. It is important to point out from Figure 4.14 that 5% of coir fibre quantity has the highest compressive strength and continue to decrease as the coir fibre quantity increasing.

The lowest value of compressive strength (5.72mpa) from Figure 4.14 is given by the composite with 15% of coir fibre while the highest value of compressive strength which is 11.43mpa obtained from composite contains 5% of coir fibre quantity. The compressive strength result from this study is consistent with some earlier findings that showed that compressive strength decreased as fibre concentration increased (Asasutjarit, Charoenvai, Hirunlabh, and Khedari, 2009; Khedari Suttisonk, Pratinthong and Hirunlabh 2001).

Generally, when the density is of low value, the strength is also of low value Table 4.1. So when there is increase in volume percentage of coir fibre, the density will be lower and therefore resulting in less compressive strength. The decrease in compressive strength as the quantity of coir fibre is increased is due to the lack of water for composite with both mixing ratio (10% and 15%) causes the mixing not workable and difficult to mix homogenously. In reality, if the coir fibre is stiff from the lack of water and cement paste in the mixture, packing the fibre becomes challenging at high coir fibre quantities, and voids are introduced into the result (Abdullah et al, 2011).

Figure 4.15 shows the relationship between Compressive Strength and coir fibre which is express by Polynomial expression model

$CS = 0.0025q^2 - 1.7515q + 12.932$ …………………………………… 4.6

This implies that as compressive strength decreases significantly, the quantity of fibre increases.
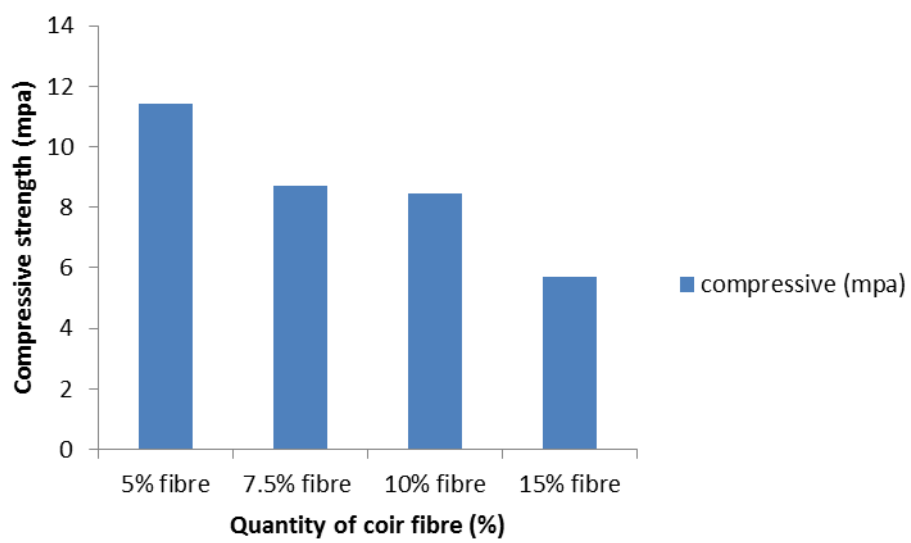
Figure 4.14: Influence of quantity of coir fibre on compressive strength
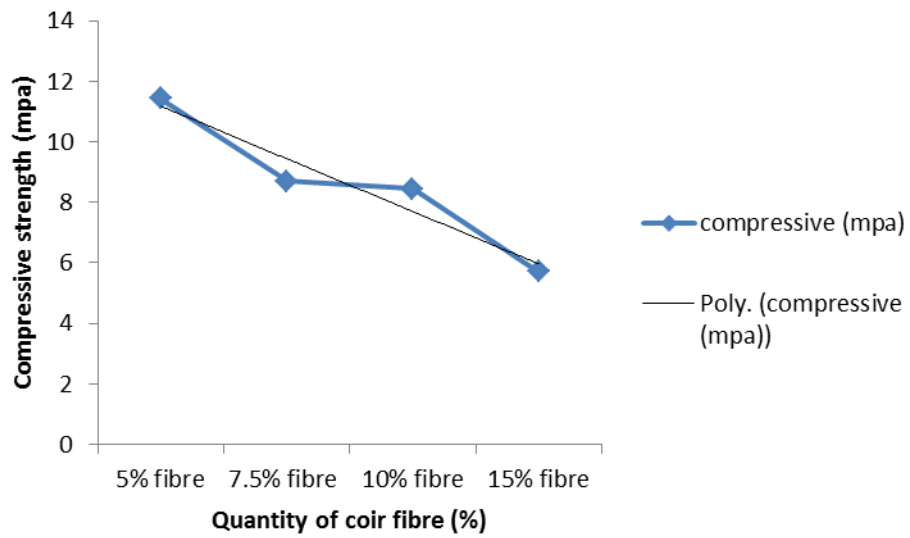
Figure 4.15: Relationships between compressive strength and quantity of coir fibre

$$CS = 0.0025q^2 - 1.7515q + 12.932$$
$$R^2 = 0.9256$$

4.2.1.6 Effect of coir fibre quantity on modulus of elasticity

The effect of coir fibre quantity in the modulus of elasticity of composite as presented in Table 4.1 shows that the variation in the modulus of elasticity value from 5% of coir fibre composite increase with the amount of coir fibre up to a certain threshold (10%). Then from (10%), modulus of elasticity begins to reduce with further increase in the amount of coir fibre (15%) Figure 4.16

The lowest value of modulus of elasticity as shown in Figure 4.16 (813.24mpa) is given by the composite with 5% of coir fibre and the composite that contains 10% of coir fibre has the highest value of modulus of elasticity which is 1428.85mpa. It was observed that the maximum reinforcement in polyester matrix composites was found to be achieved at a coir fibre content of 10%.

The same finding was also noted in earlier studies evaluating the impact of the volume fraction of coir fibres on the mechanical characteristics of a polymer matrix composite according to Aramide, Oladele and Folorunso, (2009) which reported that modulus of elasticity will increased as the bagasse fibre quantity increased up to 10% of bagasse fibre quantity and then begins to reduce with further increase in the amount of bagasse fibre.

These are due to lower interaction between the fibre/matrix reducing the reinforcement effect on the polymer. The findings also demonstrate that the polyester becomes more brittle and less ductile when bagasse fibre is added. Without significant deformation and through rapid crack propagation, brittle fracture occurs (Aramide et al, 2009).

A one-way between subjects ANOVA was conducted and the results presented according to Table 4.1.4 to examine the effect of fibre quantity on MOE. The different fibre quantity sizes considered are: 5% fibre, 7.5% fibre, 10% fibre and 15% fibre. The findings show that coir fibre composite has a significant influence of fibre quantity on MOE $p < .05$ level for at least two of the fibre quantity sizes under consideration $[F(3,12) = 32.98$, $p < .001$. From the mean plot computed from Figure 4.17 when examining the effect of fibre quantity on MOE, it can be observed that 10% fibre quantity computed the highest mean while 15% fibre computed the lowest mean.
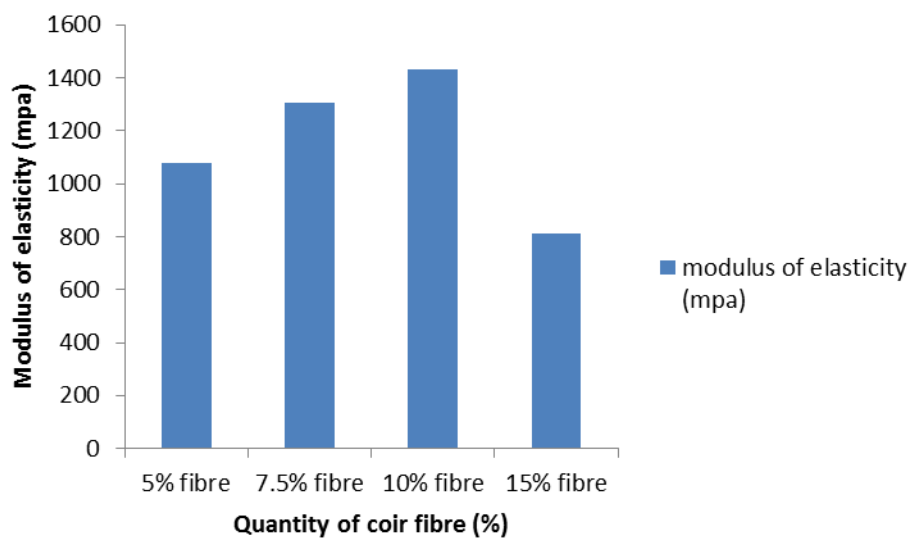
Figure 4.16: **Influence of quantity of coir fibre on modulus of elasticity**

Table 4.1.4 Statistical result of MOE test for coir fibre

Parameters	df	Sum sq	Mean sq	F-value	Pr (>F)
Sample	3	894301	298100	32.98	4.48e-06
Residuals	12	108478	9040		
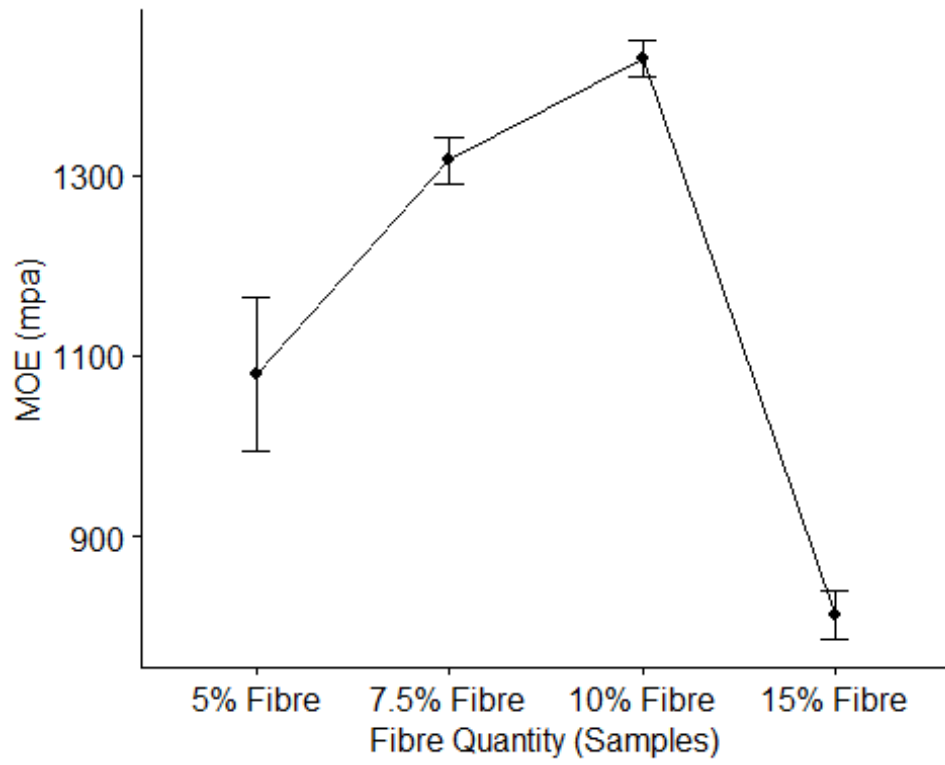
Figure 4.17: **Generated quantity of coir fibre on modulus of elasticity**

Figure 4.18 shows the relationship between Modulus of Elasticity and coir fibre which is express by Polynomial expression model

M.O.E = -210.84q^2 + 986.9q + 270.78 ……………………………….. 4.7

This implies that modulus of elasticity increases significantly to a certain level and then started decreasing as the quantity of fibre increases.
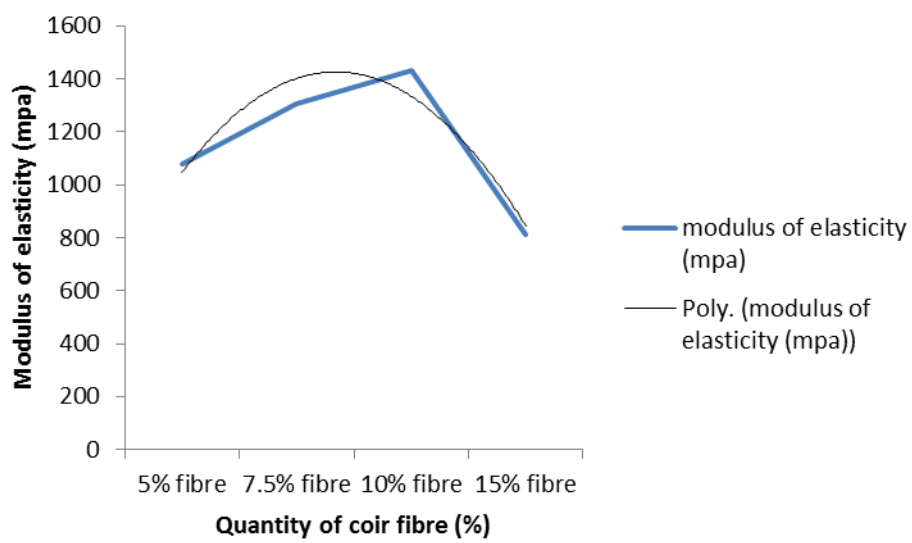
Figure 4.18: Relationship between modulus of elasticity (mpa) and quantity of coir   fibre (%)

$$M.E = -210.84q^2 + 986.9q + 270.78$$
$$R^2 = 0.9091$$

4.2.1.7 Effect of coir fibre quantity on modulus of rupture

Modulus of rupture of coir fibre composites as presented in Table 4.1 and Figure 4.19 indicated the trend of increasing in MOR with the addition of coir fibre from 5% of coir fibre quantity to 10% of fibre quantity, and there is sharp decrease in modulus of rapture when the coir fibre quantity in the composite is at 15% fibre quantity.

The lowest value of modulus of rapture (4.37mpa) from Figure 4.19 is given by the composite with 5% of coir fibre quantity and the composite contains 10% of coir fibre quantity has the highest value of MOR which is 5.34mpa. It was observed that coir fibre increase the strength of cement matrix unit to its optimum percentage of coir fibre. From Figure 4.19, the optimum quantity of coir fibre is 10% of coir fibre quantity.

The modulus of rapture results obtained in this work is similar to the previous works of Abdullah et al (2011) in his research on coir fibre-reinforced composite cement. Physical and mechanical characteristics as well as fracture behaviour demonstrate that the modulus of rapture increased as coir fibre quantity increased to the optimal level and subsequently reduced as coir fibre quantity increased further. (Abdullah et al, 2011).

The composites with high coir fibre quantity did not have good workability and lack of adequate water since the water per cement ratio was fixed for the entire composition. The only internal cement bond in the cement mixture contributed as an adhesion bond to control the strength, resulting in the lowest strength (Asasutjarit, Hirunlabh, Khedari, Daguenet and Quenard, 2005).

A one-way between subjects ANOVA was conducted and the results presented according to Table 4.1.5 to examine the effect of fibre quantity on MOR. The different fibre quantity sizes considered are: 5% fibre, 7.5% fibre, 10% fibre and 15% fibre. The findings show that coir fibre composite has a significant influence of fibre quantity on MOR $p<.05$ level for at least two of the fibre quantity sizes under consideration $[F(3,12) = 8.02$, $p < .01$. From the mean plot computed from Figure 4.20 when examining the effect of fibre quantity on MOR, it can be observed that 10% fibre quantity computed the highest mean while 5% fibre computed the lowest mean.
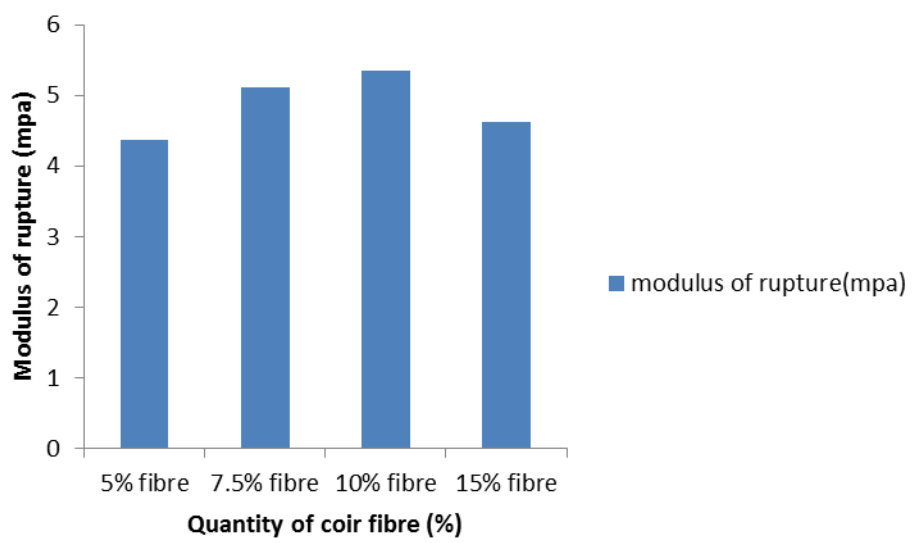
Figure 4.19: Influence of quantity of coir fibre on modulus of rupture

Table 4.1.5 Statistical result of MOR test for coir fibre

Parameters	df	Sum sq	Mean sq	F-value	Pr (>F)
Sample	3	2.338	0.7793	8.02	0.00337
Residuals	12	1.166	00.972		
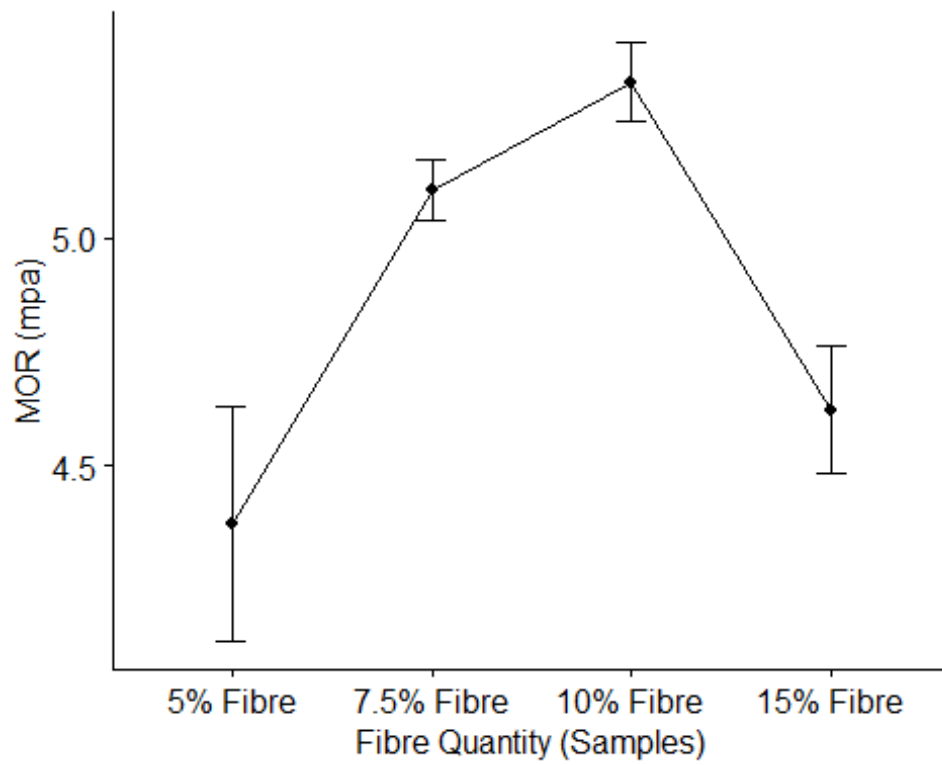
Figure 4.20: Generated quantity of coir fibre on modulus of rupture

Figure 4.21 shows the relationship between Modulus of Rupture and coir fibre which is express by Polynomial expression model

$$M.O.R = -0.365q^2 + 1.923q + 2.79 \qquad \text{…… …..…... 4.8}$$

This implies that modulus of rupture increases slightly to a certain level and then started decreasing as the quantity of fibre increases.
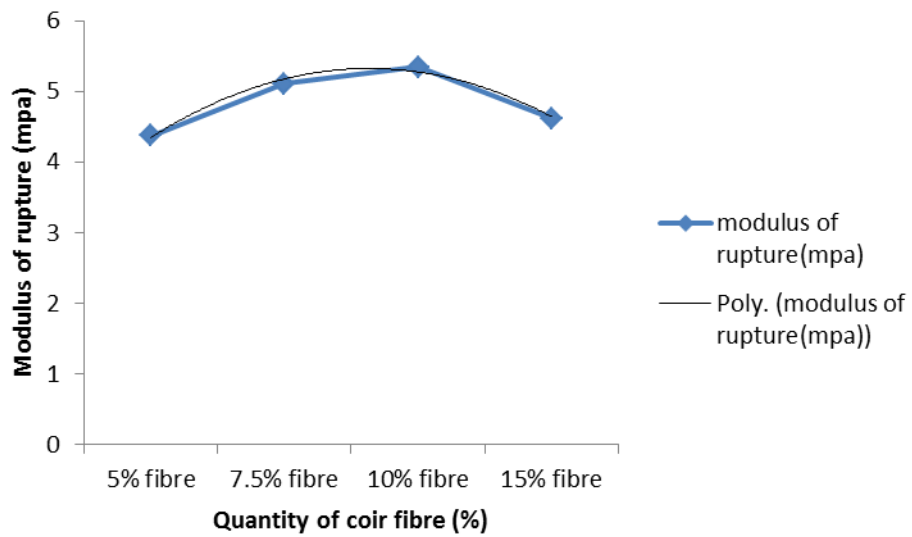
Figure 4.21: Relationships between modulus of rupture and quantity of coir fibre
$$M.R = -0.365q^2 + 1.923q + 2.79$$
$$R^2 = 0.9836$$

4.2.1.8 Effect of coir fibre quantity on impact strength

The effect of coir fibres quantity on the impact strength as observed from Table 4.1 shows that the addition of coir fibre in the composite leads to improved impact strength of the composite from 5% of coir fibre quantity to 10% of coir fibre quantity and then slightly decreased at 15% coir fibre quantity. The result shows that increase in coir fibre quantity leads to increase in impact strength of composite because coir fibres provide strength to the composite, but at 15% coir fibre quantity the impact strength decreased. Figure 4.22 shows the highest impact strength of $4.35N/mm^2$ is obtained from composite at 10% coir fibre quantity while the lowest impact strength was recorded at 5% coir fibre quantity ($1.19N/mm^2$).

The same observation was also reported in previous study about mechanical properties of coir fibre reinforced with epoxy polymer composites that as the coir fibre quantity increased in the composites impact strength increases. Further increase of coir fibre of the composite causes the impact strength to decrease (Satender, Kakali, and Suresh 2016). The impact strength decreased due to the poor interface bonding between fibre and resin. As the coir fibre quantity increases more than 10%, interface bonding between matrix and fibre goes on decrease.

A one-way between subjects ANOVA was conducted and the results presented according to Table 4.1.6 to examine the effect of fibre quantity on Impact strength. The different fibre quantity sizes considered are: 5% fibre, 7.5% fibre, 10% fibre and 15% fibre. The findings show that coir fibre composite has a significant influence of fibre quantity on Impact strength $p<.05$ level for at least two of the fibre quantity sizes under consideration [$F(3,20) = 78475$, p $<.001$

From the mean plot computed from Figure 4.23 when examining the effect of fibre quantity on impact, it can be observed that 10% fibre quantity computed the highest mean while 5% fibre computed the lowest mean.

Figure 4.24 shows the relationship between Impact strength and coir fibre which is express by Exponential expression model

$I.S = 0.729e^{0.4604q}$ ……………………………………………………………… 4.9

This implies that Impact strength increases slightly as the quantity of fibre increases to certain level and started decreasing as the quantity of coir fibre increases.
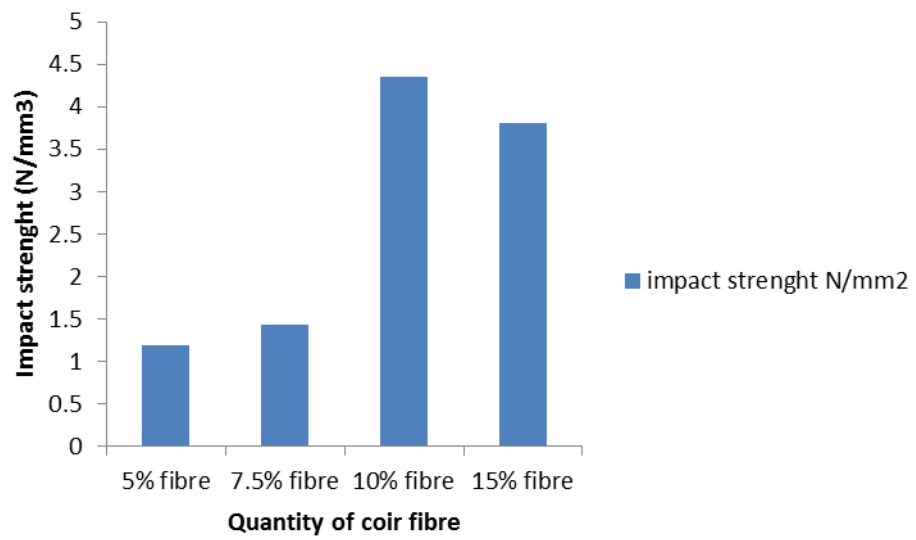
Figure 4.22: Influence of quantity of coir fibre on impact strength

Table 4.1.6   Statistical result of impact strength test for coir fibre

Parameters	df	Sum sq	Mean sq	F-value	Pr (>F)
Sample	3	23.542	7.847	78475	<2e - 16
Residuals	8	0.001	0.000		
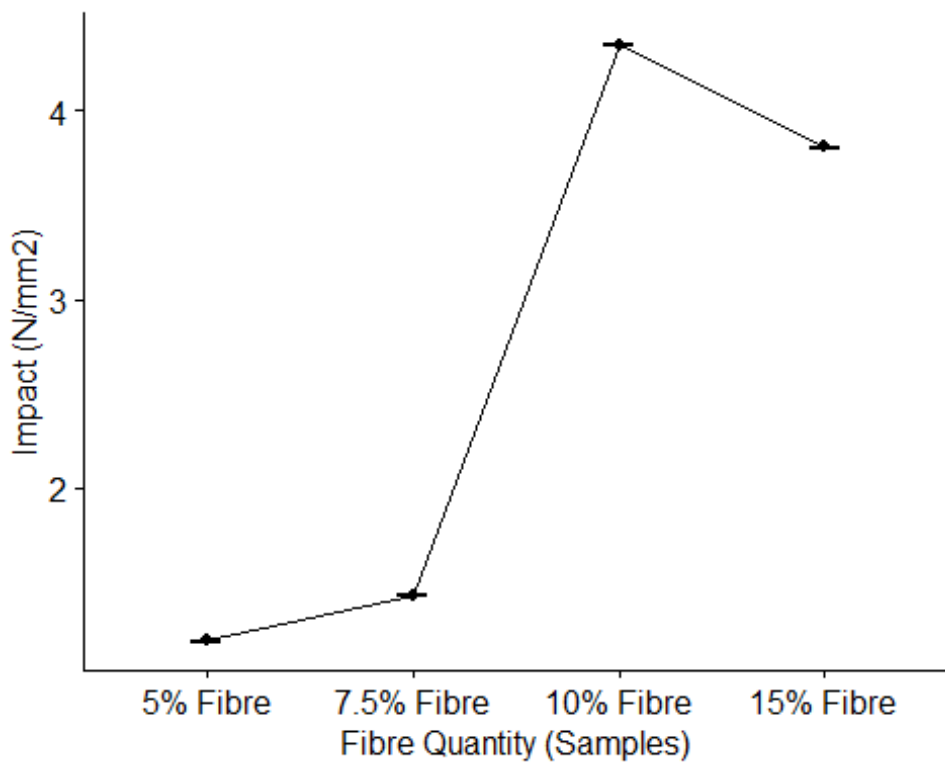
Figure 4.23: Generated quantity of coir fibre on impact strength
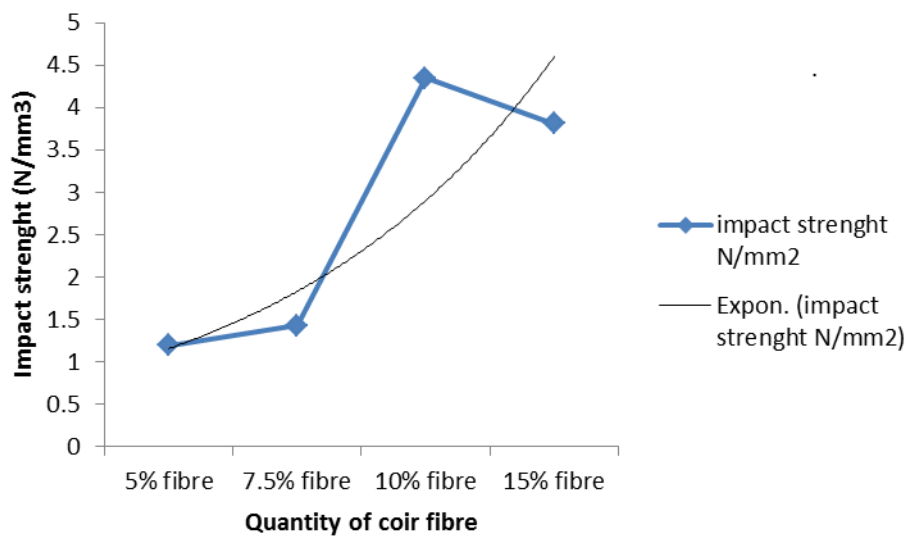
Figure 4.24: Relationship between impact strength (N/mm³) and quantity of coir fibre (%)

$$I.S = 0.729e^{0.4604q}$$

$$R^2 = 0.8022$$

4.2.2 Results and discussion on coir dust quantity

4.2.2.1 Effect of coir dust quantity on water absorption

The water absorption increases as the coir dust increase in the composites. It was observed from Table 4.2 and Figure 4.25 that water absorption at 5% coir dust quantity increases from 5% coir dust quantity into 15% of coir dust. It was noted from Figure 4.25 that 5% coir dust quantity absorbs lowest water content (27.5%) while 15% coir dust quantity showed highest water absorption (69.06%).

The results here are similar to the previous works, Rahman, Islam, Rahman, Hannan, Dungan and Abdul (2013) in his study about flat-pressed wood plastic composites from saw dust and recycled polyethylene terephthalate (PET), that water absorption of the composites increased with the increase of saw dust content. The hydrophilic nature of fibre and wood is primarily responsible for these results. Fibre/wood is a hydrophilic porous composite composed of cellulose, lignin, and hemicellulose polymers rich in functional groups such as hydroxyls, which easily interact with water molecules via hydrogen bonding (Clemons, 2002).

A one-way between subjects ANOVA was conducted and the results presented according to Table 4.2.1 to examine the effect of dust quantity on water absorption. The different dust quantity sizes considered are: 5% Dust, 7.5% Dust, 10% Dust and 15% Dust. The findings show that coir dust composite has a significant influence of dust quantity on water absorption $p<.05$ level for at least two of the dust quantity sizes under consideration $[F(3,20) = 1093.4$, p $<.001$.

From the mean plot computed from Figure 4.26 when examining the effect of dust quantity on water absorption, it can be observed that 5% dust quantity computed the lowest mean while 15% dust computed the highest mean. The mean plot of density portrays a positive trend across the 4 categories of dust quantity samples under consideration. This shows that when the percentage of dust quantity increases, the water absorption increases.

Figure 4.27 shows the relationship between Water Absorption and coir dust which is express by Polynomial expression model

$$W.A = - 1.915q^2 + 24.111q + 4.315 \qquad\qquad ……..\ 4.10$$

Table 4.2: Summary of the result carried out using coir dust quantity

Sample (Dust)	5%	7.5%	10%	15%
Water Absorption (%)	27.57	41.70	62.59	69.06
Thickness Swelling (%) 2HRS	1.37	2.07	2.60	3.68
24HRS	1.90	3.00	4.00	5.11
Density (g/mm^3)	.00148	0.00143	0.00122	0.00103
Flexural Strength (mpa)	14.02	9.13	5.84	2.10
Compressive Strength (mpa)	11.16	9.66	5.35	0.95
MOE (mpa)	1916.31	1509.00	1074.81	330.64
MOR (mpa)	3.79	3.42	2.96	1.61
Impact Strength (N/mm^2)	2.18	1.63	1.09	0.86
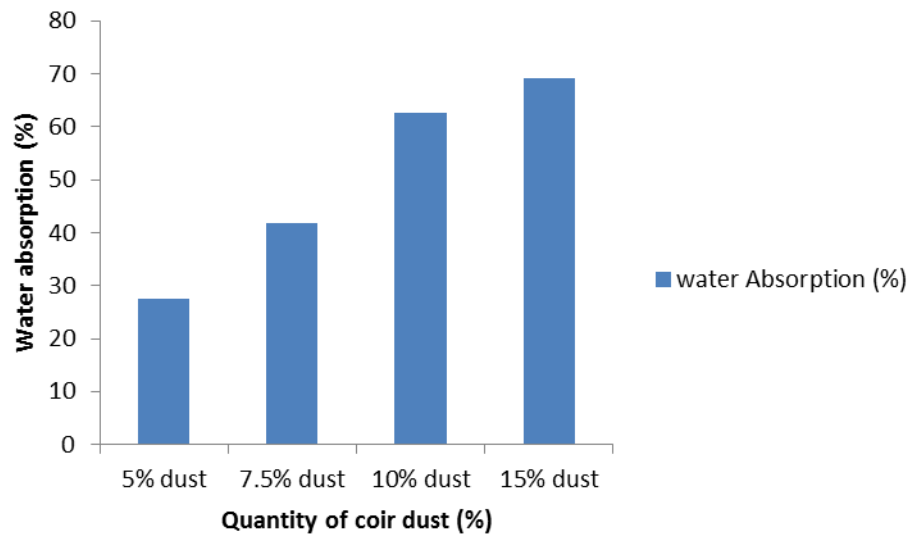
Figure 4.25:   Influence of quantity of coir dust on water absorption

Table 4.2.1 Statistical result of water absorption test for coir dust

Parameters	Df	Sum sq	Mean sq	F-value	Pr (>F)
Sample	3	3280	1093.4	10674	9.57e – 15
Residuals	8	1	0.1		
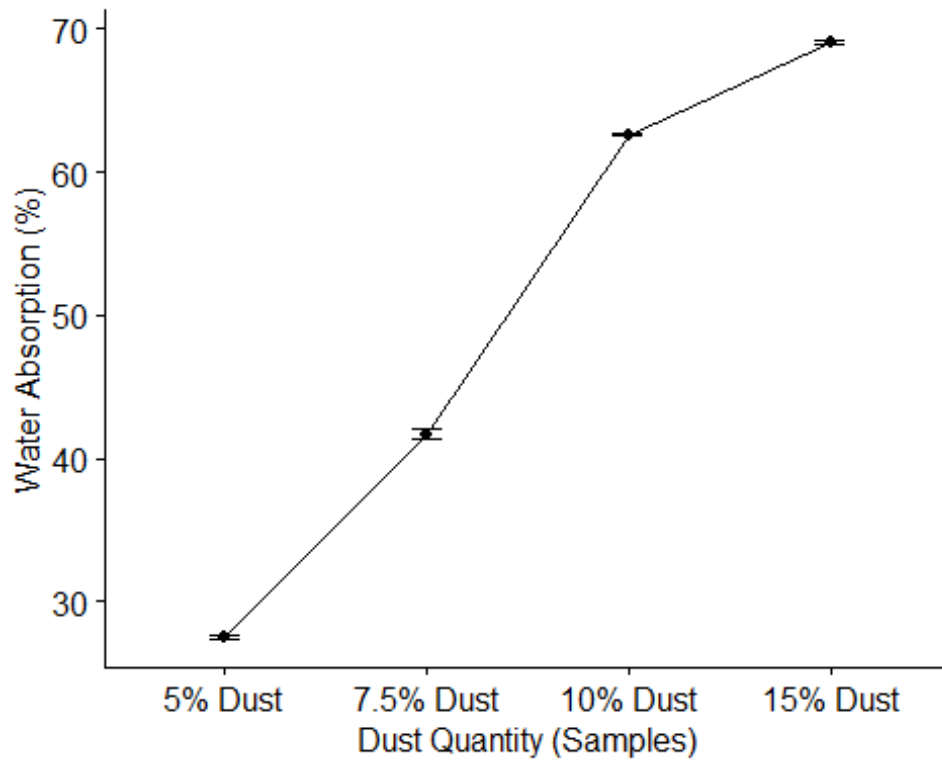
Figure 4.26:   Generated quantity of coir dust on water absorption
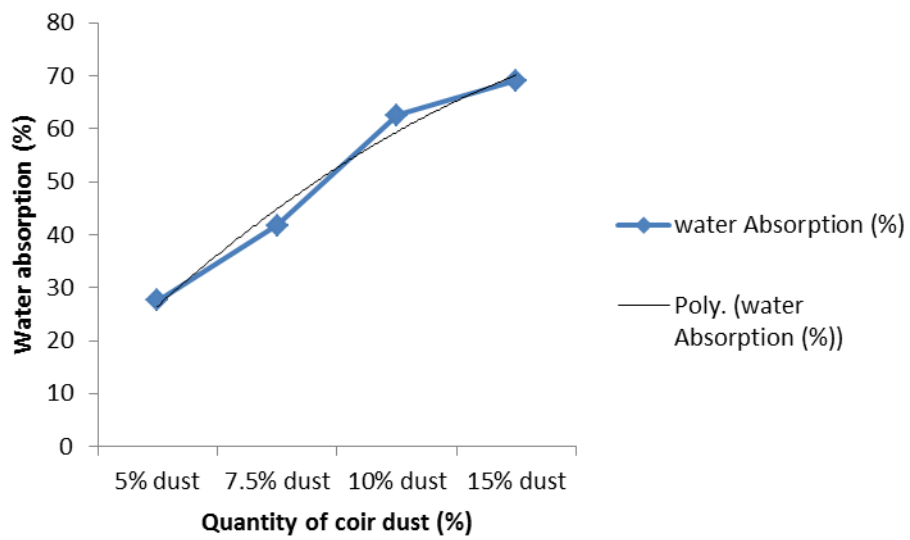
Figure 4.27: **Relationship between water absorption (%) and quantity of coir dust (%)**

$$W.A = -1.915q^2 + 24.111q + 4.315$$

$$R^2 = 0.9795$$

This implies that as water absorption increases significantly, the quantity of coir dust also increases.

4.2.2.2 Effect of coir dust quantity on thickness swelling

The effect of coir dust quantity in thickness swelling as presented in Table 4.2 shows the thickness swelling increased as the quantity of coir dust increases in the composites. Thickness swelling started increasing from 5% of coir dust quantity and then continues to increase to 15% of coir dust quantity. The highest thickness swelling values in 2hours and 24hours were 3.68% and 5.11% respectively, and these values are given by the composite with 15% coir dust quantity and the composite contains 5% coir dust quantity has lowest values of 1.37% and 1.90% Figure 4.28. Thus, the higher the coir dust quantity, the higher the thickness swelling.

The total thickness swelling results obtained in this work corresponds to the previous work of Rahman et al (2013) In his research on recycled polyethylene terephthalate (PET) and flat-pressed wood plastic composites made from sawdust: that as the saw dust content increased in the composites, thus, increasing the total thickness swelling values. The tendency of thickness swelling was similar to the water absorption as it was illustrated from water absorption.

A one-way between subjects ANOVA was conducted and the results presented according to Table 4.2.2 to examine the effect of dust quantity on thickness swelling. The different dust quantity sizes considered are: 5% Dust, 7.5% Dust, 10% Dust and 15% Dust. The findings show that coir dust composite has a significant influence of dust quantity on thickness swelling $p<.05$ level for at least two of the dust quantity sizes under consideration [$F(3,20) =18.69$, $p <.001$.

From the mean plot computed from Figure 4.29 when examining the effect of dust quantity on thickness swelling, it can be observed that 5% dust quantity computed the lowest mean while 15% dust computed the highest mean. The mean plot of density portrays a positive trend across the 4 categories of dust quantity samples under consideration. This is an indication that the thickness swelling increases as the percentage of dust quantity increases.
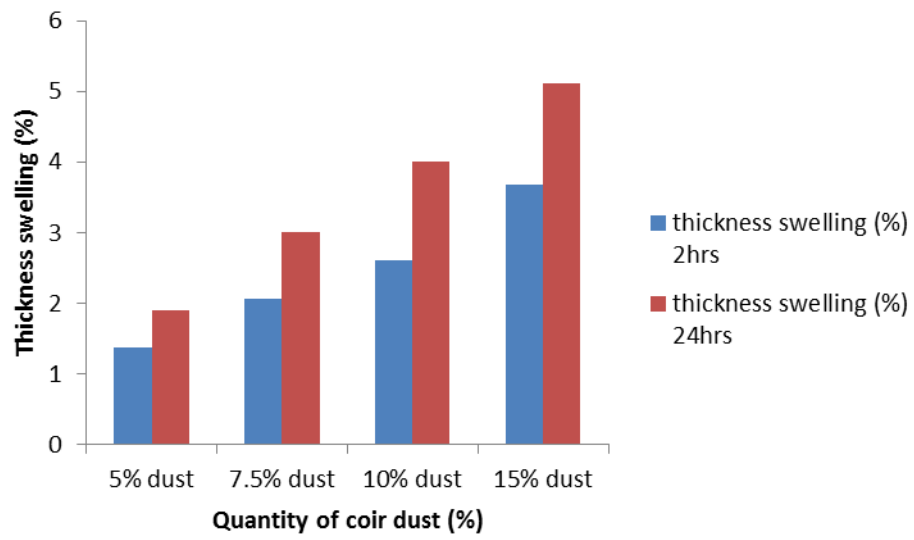
Figure 4.28:   Influence of quantity of coir dust on thickness swelling

Table 4.2.2 Statistical result of thickness swelling test for coir dust

Parameters	Df	Sum sq	Mean sq	F-value	Pr (>F)
Sample	3	24.605	8.202	18.69	5.09e – 06
Residuals	20	8.774	0.439		
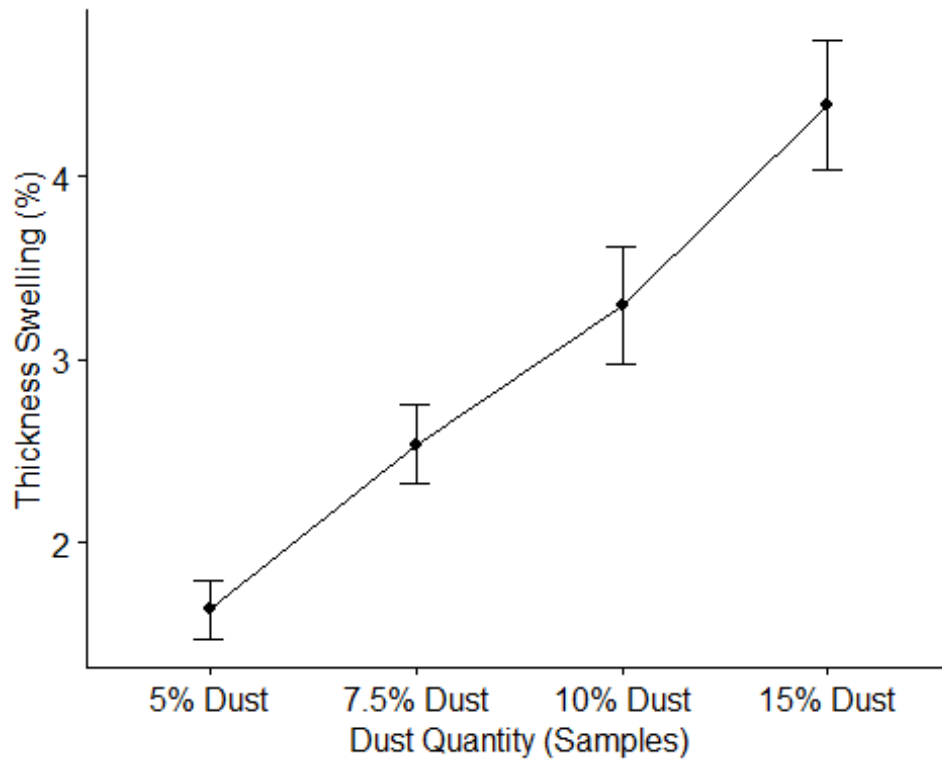
Figure 4.29: Generated quantity of coir dust on thickness swelling

Figure 4.30 shows the relationship between Thickness Swelling and coir dust which is express by Polynomial expression model for 2hrs and 24hrs is given respectively as

$$T.S_2 = 0.095q^2 + 0.271q + 1.04 \qquad\qquad .... \quad 4.11$$

$$T.S_{24} = 0.0025q^2 + 1.0505q + 0.8575 \qquad\qquad ...... \quad 4.12$$

This implies that as thickness swelling increases, the quantity of coir dust also increases. There is slightly increase in the value of thickness swelling.
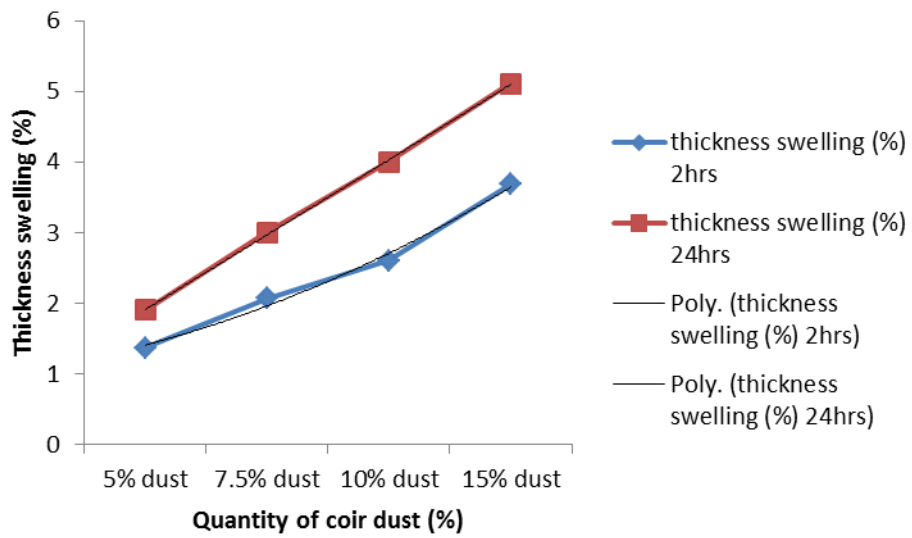
Figure 4.30: Relationships between thickness swelling (%) and quantity of coir dust (%)

$$\text{T.S}_2 = 0.095q^2 + 0.271q + 1.04$$
$$R^2 = 0.9909$$
$$\text{T.S}_{24} = 0.0025q^2 + 1.0505q + 0.8575$$
$$R^2 = 0.9996$$

4.2.2.3 Effect of coir dust quantity on density

The variation of density for varying percentage of coir dust according to Table 4.2 shows that the density of composites decreased with increase in coir dust quantity. Figure 4.31 shows that density started decreasing from 5% of coir dust quantity and then continues to decrease to the 15% coir dust quantity.

The highest value of density from Figure 4.31 was obtained from 5% of coir dust quantity ($0.00148g/mm^3$) while the lowest value of density ($0.00103g/mm$) is given by the composite with 15% of coir dust quantity. This happened because as the quantity of coir dust increases in composite, so the density and strength decreased.

 The density results obtained in this work are similar to the previous works by Boob (2014) in his study on the effectiveness of saw dust in inexpensive sandcrete blocks found that as the percentage of saw dust increase in the composite, the density decreases.

Figure 4.32 show the relationship between Density and coir dust which is express by Polynomial expression model

$$D = -3E\text{-}05q^2 + 2E\text{-}05x + 0.0015 \qquad \text{……………..} \quad 4.13$$

This implies that as Density decreases slightly, the quantity of coir dust increases.
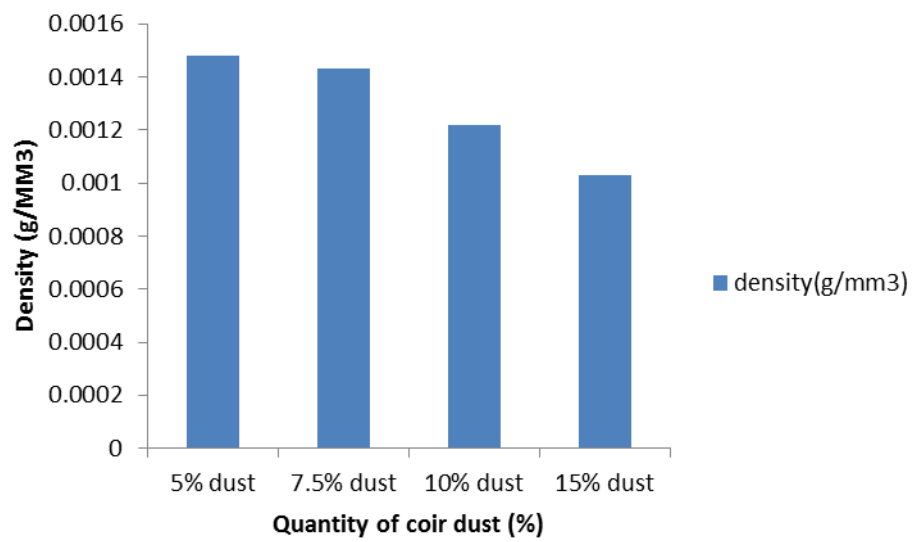
Figure 4.31: Influence of quantity of coir dust on density
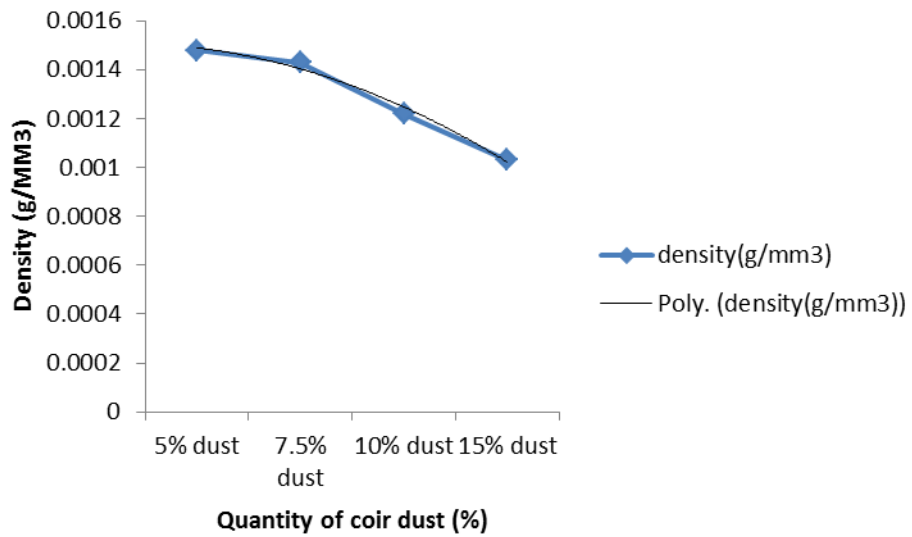
Figure 4.32: Relationship between density and quantity of coir dust

$$D = -3\text{E-}05q^2 + 2\text{E-}05q + 0.0015$$
$$R^2 = 0.9874$$

4.2.2.4 Effect of coir dust quantity on flexural strength

The effect of coir dust on the flexural strength as shown from Table 4.2 and Figure 4.33 indicate that the addition of coir dust in the composite leads to decreased flexural strength values from 5% coir dust quantity and then continue to decrease in values by adding coir dust up to 15% coir dust quantity. It was noted from Figure 4.33 that the lowest value of flexural strength was obtained in 15% coir dust quantity (2.10mpa) while the highest value of flexural strength was given by the quantity with lowest amount (5%) of coir dust (14.02mpa).

According to Ku, Donald, Cardona and Trada (2012) in their previous works about flexural properties of saw dust-reinforced epoxy composites postcured in microwaves reported that flexural strength value decreased as the saw dust content increasing. Moslewicki, Borrajo and Aranguren (2005) reported that increasing the weight fraction of composite fibre would lead to more voids in the composites, which would alter the physical and mechanical characteristics of the composite.

Thus, the greater the amount and size of saw dust in the samples, the larger the voids in the composites and hence the lower the physical and mechanical properties of the composites (Moslewicki et al, 2005). Moreover, increase in the quantity of coir dust in the composites will change material from the hard to brittle state and this increased flexibility and then reduces flexural properties

A one-way between subjects ANOVA was conducted and the results presented according to Table 4.2.3 to examine the effect of dust quantity on Flexural Strength. The different dust quantity sizes considered are: 5% Dust, 7.5% Dust, 10% Dust and 15% Dust. The findings show that coir dust composite has a significant influence of dust quantity on Flexural Strength $p<.05$ level for at least two of the dust quantity sizes under consideration [$F(3,8) = 926.1$, $p <.001$.

From the mean plot computed from Figure 4.34 when examining the effect of dust quantity on Flexural Strength, it can be observed that 5% dust quantity computed the highest mean while 15% dust computed the lowest mean. The mean plot of density portrays a negative trend across the 4 categories of dust quantity samples under
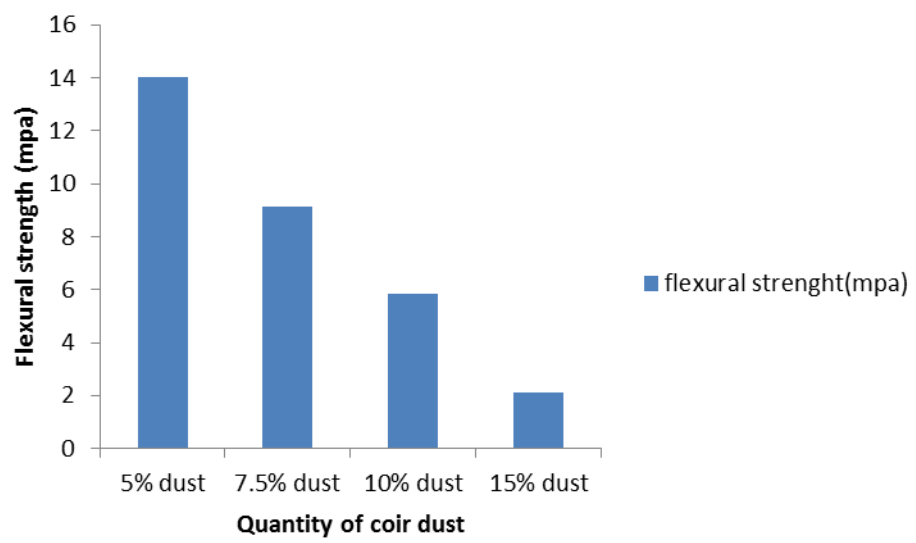
Figure 4.33: **Influence of quantity of coir dust on flexural strength**

4.2.3: Statistical result of flexural strength test for coir dust

Parameters	Df	Sum sq	Mean sq	F-value	Pr (>F)
Sample	3	230.37	76.79	926.1	1.67e-10
Residuals	8	0.66	0.08		
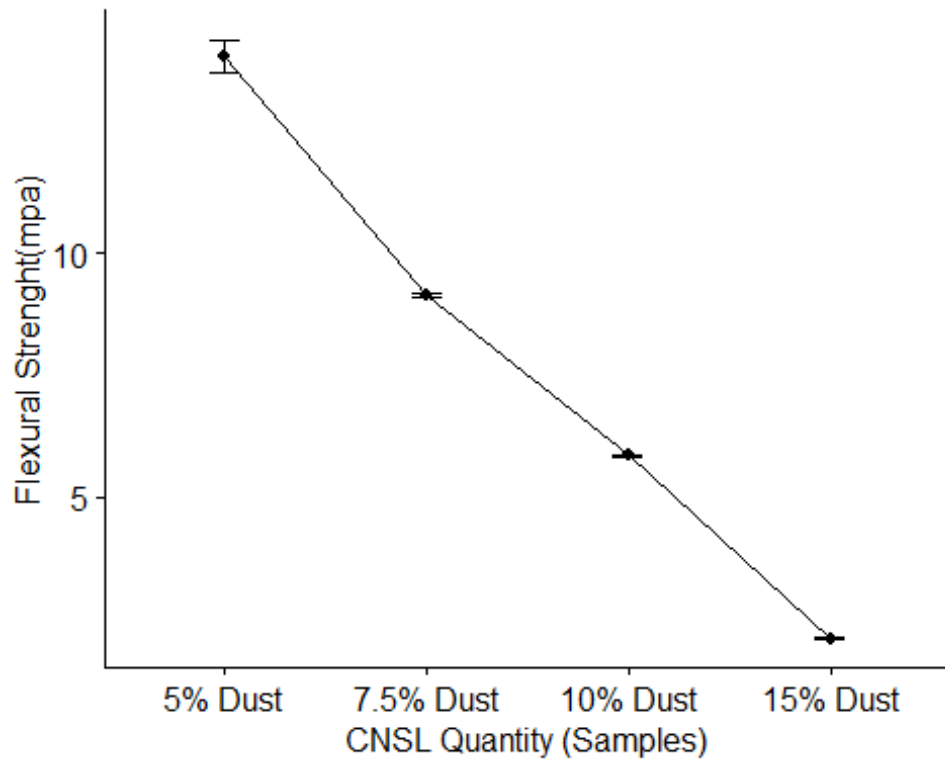
Figure 4.34: Generated quantity of coir dust on flexural strength

consideration. This is an indication that the Flexural Strength decreases as the percentage of dust quantity increases.

Figure 4.35 shows the relationship between Flexural Strength and coir dust which is express by Polynomial expression model.

$$F.S = 0.2875q^2 - 5.3425q + 18.973 \qquad\qquad ……..\ 4.14$$

This implies that Flexural strength decreases slightly as coir dust increases.
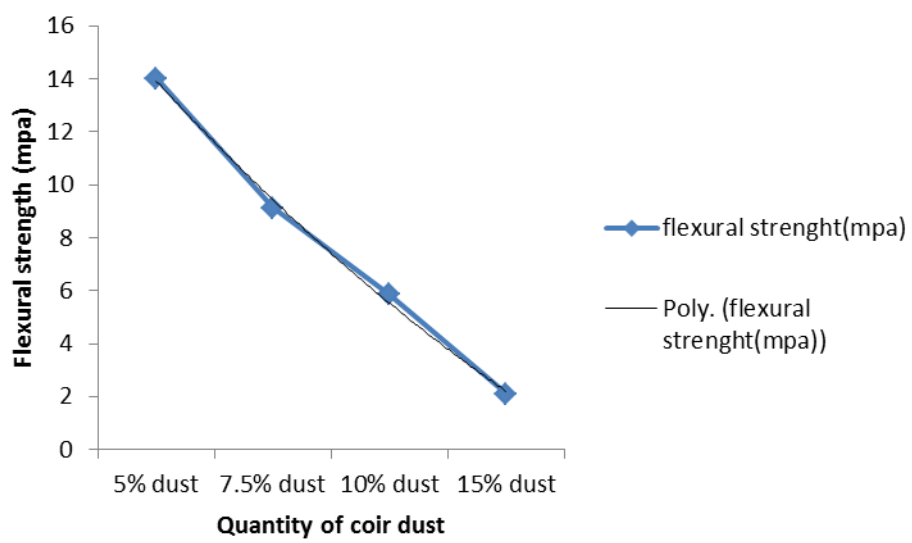
Figure 4.35: Relationship between flexural strength (mpa) and quantity of coir dust

$$F.S = 0.2875q^2 - 5.3425q + 18.973$$

$$R^2 = 0.9973$$

4.2.2.5 Effect of coir dust quantity on compressive strength

The effect of coir dust quantity in the compressive strength of composites as presented in Table 4.2 shows the variations in the compressive strength value at 5% of coir dust quantity continue to decrease as the coir dust quantity increasing in the composite. 5% of coir dust quantity from Figure 4.36 has the highest value of compressive strength (11.16mpa) while the lowest value of compressive strength (0.95mpa) is given by the composite with 15% coir dust quantity. It was observed that as the percentage coir dust quantity increased in the mix, the compressive strength decreased.

The compressive strength results obtained in this work are similar to the previous works by Chitra, Thendral, Arunya and Mohan (2019) in there study about experimental study on strength of concrete by partial replacement of fine aggregate with saw dust. Also note that, compressive strength values decreases as the coir dust quantity was increasing in the composite.

However, a number of factors may have contributed to the general decrease in strength in all the composite classes as the coconut dust percentage rose. One of these was the large void content in the concrete mixtures brought on by the decreased workability as the coconut dust content increased. The low workability made it difficult to achieve proper compact of the concrete during moulding. Moreover, coconut dust is hygroscopic. Therefore, when it absorbed water, it exhibited volumetric changes that caused internal tensions in the concrete mix (Thomas, 2015).

Figure 4.37 shows the relationship between Compressive Strength and coir dust which is express by Polynomial expression model

$$C.S = -0.725q^2 + 0.131q + 11.89 \qquad\qquad \text{........ } 4.15$$

This implies that as compressive strength decreases significantly, the quantity of coir dust increases.
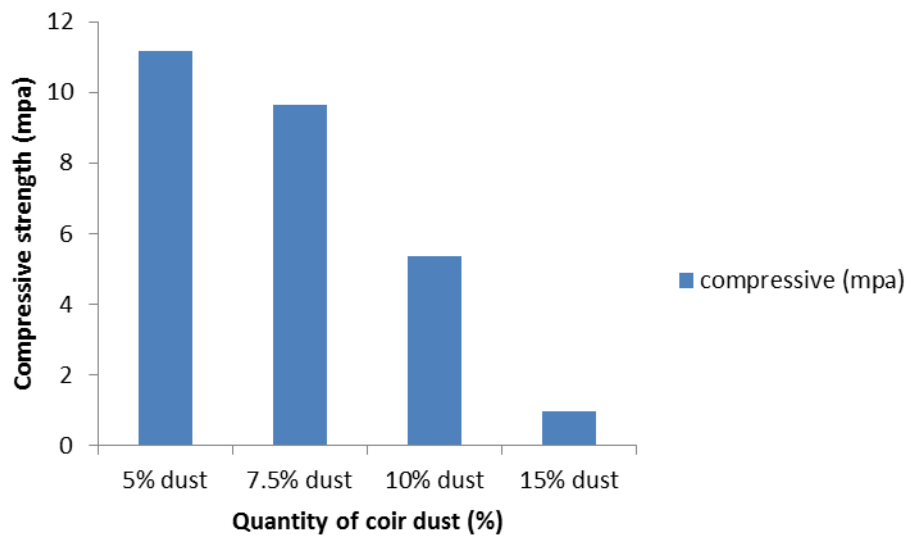
Figure 4.36: Influence of quantity of coir dust on compressive strength
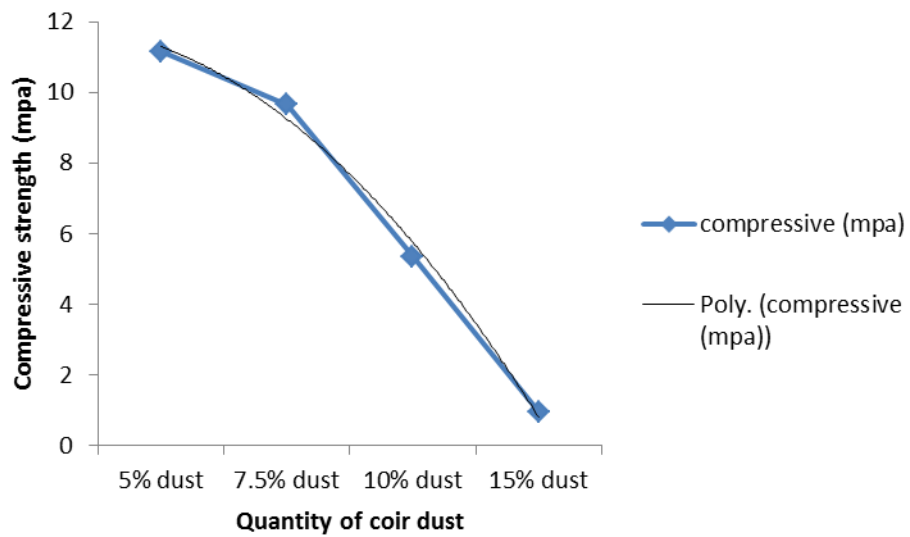
Figure 4.37: Relationship between compressive strength and quantity of coir dust

$$C.S = -0.725q^2 + 0.131q + 11.89$$
$$R^2 = 0.9942$$

4.2.2.6 Effect of coir dust quantity on modulus of elasticity

Modulus of elasticity of coir dust composites from Table 4.2 indicated the trend of decreasing MOE with the addition of coir dust from 5% of coir dust quantity to 15% of coir dust quantity. It was observed that modulus of elasticity decreased as the coir dust quantity increasing in the composites.

The highest value of MOE obtained from Figure 4.38 was given by the composite of 5% coir dust quantity (1916.31 mpa) while the lowest value was given by the composite of 15% coir dust quantity (330.64 mpa). At 15% of coir dust quantity composite, due to large quantities of coir dust in the composite lead to poor interaction between coir dust and cement and then causes long setting of the composite due to slow hydration of the cement and poisoning effect of particle on cement hydration. Also greater quantities of dust particles in the composite will change material from hard to brittle state.

The modulus of elasticity results obtained in this work is similar to the plastic composites from saw dust and recycled polyethylene terephthalate (PET), that the MOE values of composites decreased along with higher sawdust loading (Rahman et al, 2013). Poor interfacial interaction between the sawdust and PET may be responsible for the variation. The lower MOE value may be primarily accounted for by the inadequate interfacial interaction between the polymeric matrix and sawdust (Shibata, Takachiyo, Ozawa, Yosomiya and Takeishi, 2002).

A one-way between subjects ANOVA was conducted and the results presented according to Table 4.2.4 to examine the effect of dust quantity on MOE. The different dust quantity sizes considered are: 5% Dust, 7.5% Dust, 10% Dust and 15% Dust. The findings show that coir dust composite has a significant influence of dust quantity on MOE $p<.05$ level for at least two of the dust quantity sizes under consideration $[F(3,12) = \mathbf{\mathit{42.47}}, p <.001.$

From the mean plot computed from Figure 4.39 when examining the effect of dust quantity on MOE, it can be observed that 5% dust quantity computed the highest mean while 15% dust computed the lowest mean. The mean plot of density portrays a negative trend across the 4 categories of dust quantity samples under consideration.
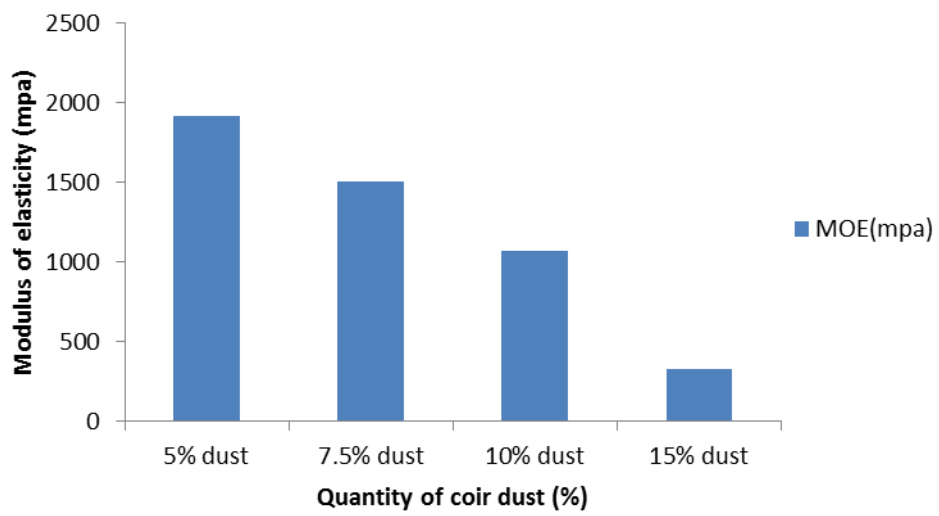
Figure 4.38: **Influence of quantity of coir dust on modulus of elasticity**

Table 4.2.4 Statistical result of MOE test for coir dust

Parameters	df	Sum sq	Mean sq	F-value	Pr (>F)
Sample	3	5519192	1839731	42.47	1.15e-06
Residuals	12	519815	43318		
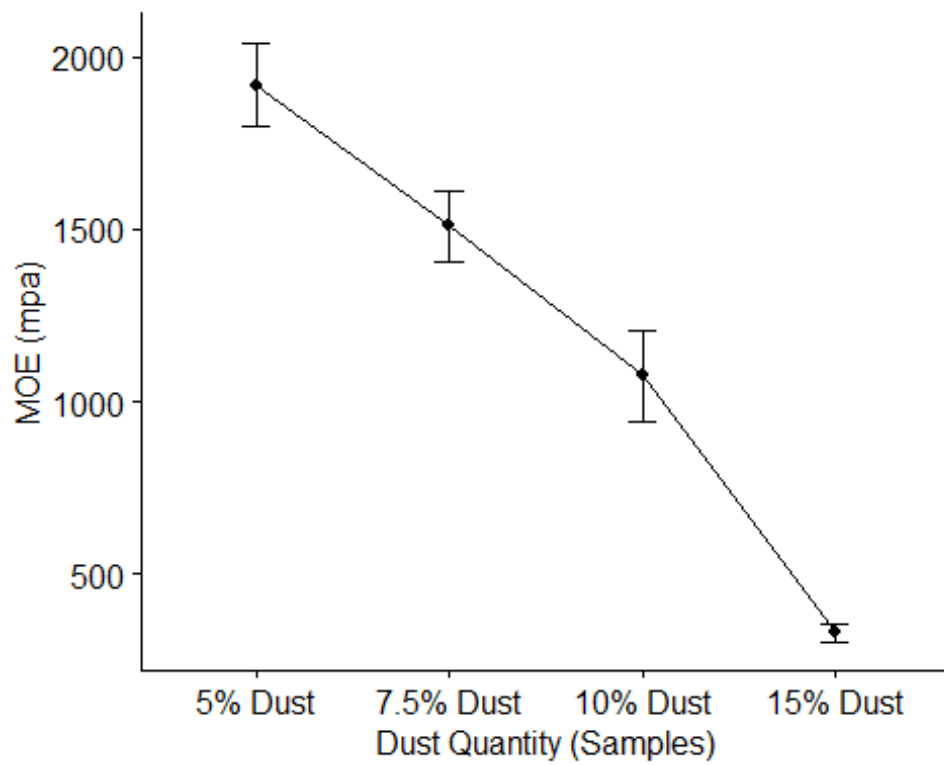
Figure 4.39: Generated quantity of coir dust on modulus of elasticity

This is an indication that the MOE decreases as the percentage of dust quantity increases.

Figure 4.40 shows the relationship between Modulus of Elasticity and coir dust which is given by Polynomial expression model

$$M.O.E = -84.215q^2 - 98.045q + 2084.4 \qquad \ldots \ldots 4.16$$

This implies that as the modulus of elasticity decreases significantly, the quantity of coir dust increases.
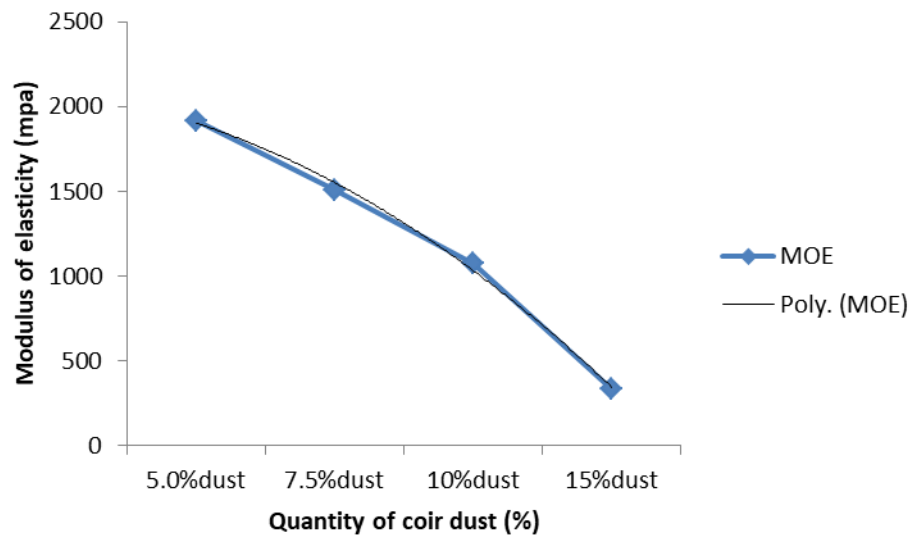
Figure 4.40: Relationship between modulus of elasticity (mpa) and quantity of coir dust (%)

$$M.O.E = -84.215q^2 -98.045q + 2084.4$$
$$R^2 = 0.9971$$

4.2.2.7 Effect of coir dust quantity on modulus of rupture

Modulus of rupture of coir dust composites as indicated from Table 4.2 and Figure 4.41 illustrates the effects of coir dust quantity on the dust cement composites modulus of rapture decreasing slightly with addition of coir dust quantity from 5% of coir dust quantity to 15% coir dust quantity. The lowest value of modulus of rupture (1.61 mpa) according to Figure 4.41 is given by the composite with 15% of coir dust quantity and this happened due to greater quantities of coir dust quantity in the composite that leads to poor mixing and poor interaction between dust and cement composite, which also cause slow hydration on the cement. And the composite with 5% of coir dust quantity has highest value of MOR which is 3.79 Mpa.

It was observed that MOR decreased as the coir dust quantity was increasing in the composites. The modulus of rupture results obtained in this works are similar to the previous work, Rahman et al (2013), in his study about flat pressed wood plastic composites from saw dust and recycled polyethylene terephthalate (PET), that the modulus of rapture of the saw dust composites decreased with the increase of saw dust content in the composites. The tendency of the modulus of rupture was similar to the modulus of elasticity.

A one-way between subjects ANOVA was conducted and the results presented according to Table 4.2.5 to examine the effect of dust quantity on MOR. The different dust quantity sizes considered are: 5% Dust, 7.5% Dust, 10% Dust and 15% Dust. The findings show that coir dust composite has a significant influence of dust quantity on MOR $p<.05$ level for at least two of the dust quantity sizes under consideration $[F(3,12) = \mathit{116.1}, p < .001.$

From the mean plot computed from Figure 4.42 when examining the effect of dust quantity on MOR, it can be observed that 5% dust quantity computed the highest mean while 15% dust computed the lowest mean. The mean plot of density portrays a negative trend across the 4 categories of dust quantity samples under consideration. This is an indication that the MOR decreases as the percentage of dust quantity increases.

Figure 4.43 shows the relationship between Modulus of Rupture and coir dust which is express by Polynomial expression model

$$\text{M.O.R} = -0.245q^2 + 0.525q + 3.47 \qquad\qquad\qquad …..…. 4.17$$

This implies that as modulus of rupture decreases slightly, the quantity of coir dust increases.
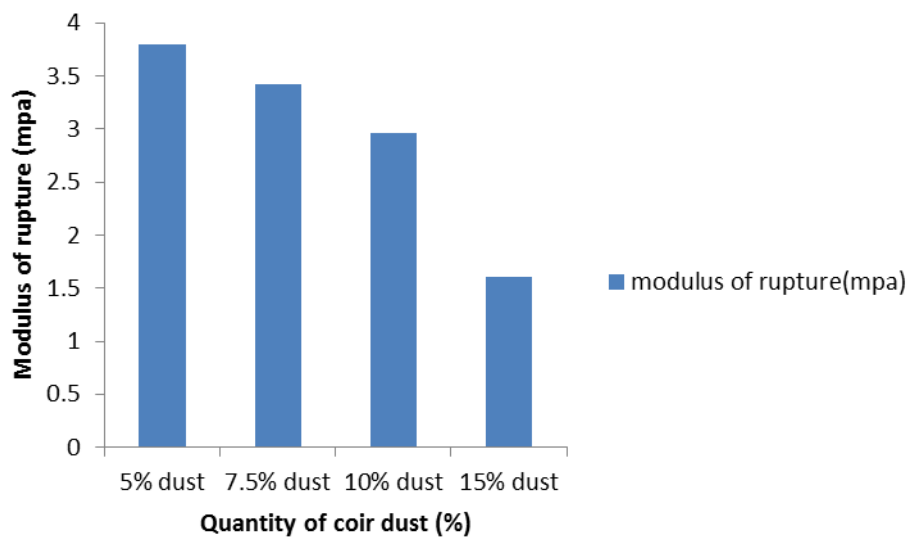
Figure 4.41: Influence of quantity of coir dust on modulus of rupture

Table 4.2.5 Statistical result of MOR test for coir dust

Parameters	Df	Sum sq	Mean sq	F-value	Pr (>F)
Sample	3	10.924	116.1	116.1	3.94e-09
Residuals	12	0.376	0.031		
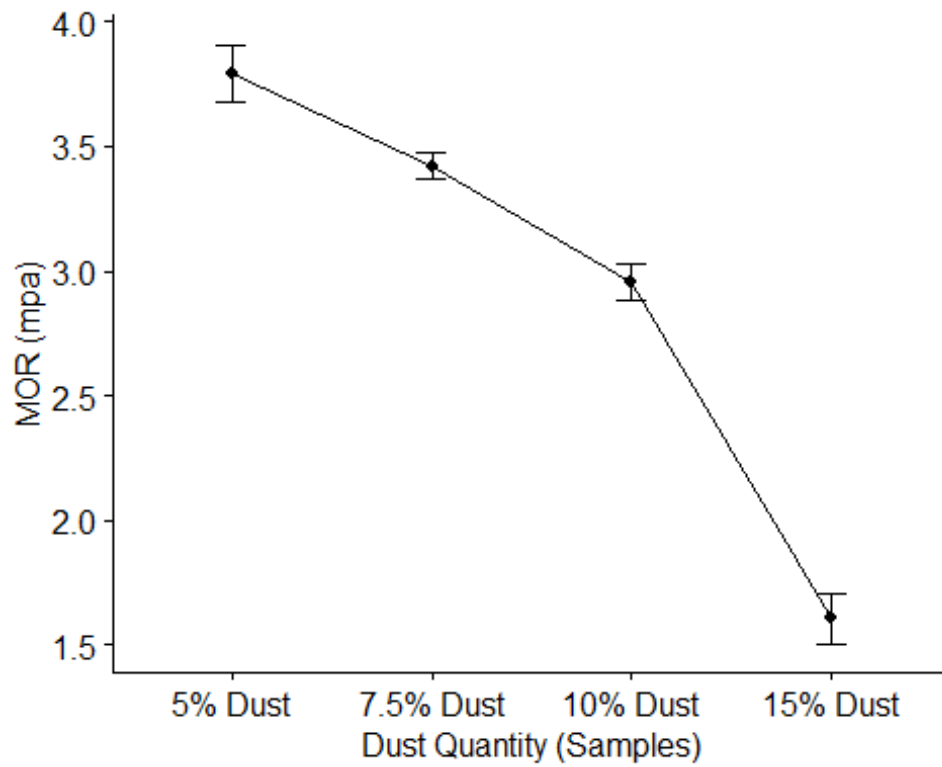
Figure 4.42: Generated quantity of coir dust on modulus of rupture
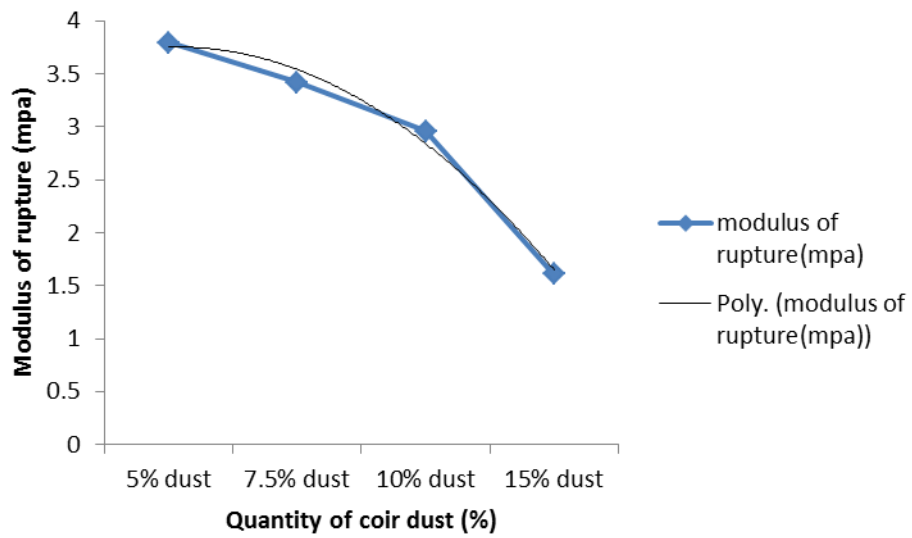
Figure 4.43: Relationship between modulus of rupture (MPa) and quantity of coir dust (%)

$$M.O.R = -0.245q^2 + 0.525q + 3.47$$
$$R^2 = 0.9882$$

4.2.2.8 Effect of coir dust quantity on impact strength

The impact strength of coir dust reinforced composite as shown from Table 4.2 indicate gradual decreased in the impact strength with an increase in percentage weight of coir dust quantity at 5% to 15% of coir dust quantity. From Figure 4.44, a maximum of 2.18 N/mm^2 was obtained at 5% of coir dust quantity and it was observed that impact strength decreased as the coir dust quantity increasing in the composite. At 15% of coir dust quantity the minimum value of impact strength (0.86 N/mm^2) obtained and this was due to high dust content that leads to poor interaction between dust and cement in the composite.

According to Heckadka, Nayok, Gouthaman, Talwar, Ravishankar, Thomas and Mathur (2018), In there earlier research on the effects of sawdust bio-filler on the tensile, flexural, and impact properties of Mangifera indica leaf stalk fibre-reinforced polyster composites, he also noted that increasing the dust content further decreased the composite capacity to absorb impact load. Reduction in mechanical of composites is due to high quantity of dust which results in ineffective stress transfer between the various phases in composites materials (Heckadka et al, 2018).

A one-way between subjects ANOVA was conducted and the results presented according to Table 4.2.6 to examine the effect of dust quantity on impact. The different dust quantity sizes considered are: 5% Dust, 7.5% Dust, 10% Dust and 15% Dust. The findings show that coir dust composite has a significant influence of dust quantity on impact $p < .05$ level for at least two of the dust quantity sizes under consideration $[F(3,8) = \textit{10426}, p < .001$

From the mean plot computed from Figure 4.45 when examining the effect of dust quantity on impact, it can be observed that 5% dust quantity computed the highest mean while 15% dust computed the lowest mean. The mean plot of density portrays a negative trend across the 4 categories of dust quantity samples under consideration. This is an indication that the impact decreases as the percentage of dust quantity increases.

Figure 4.46 shows the relationship between Impact Strength and coir dust which is express by Polynomial expression model
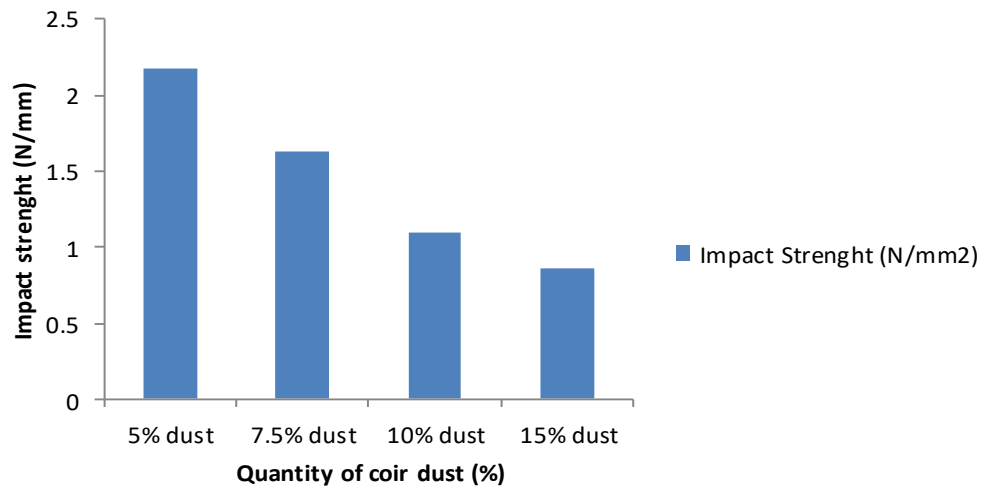
Figure 4.44: Influence of quantity of coir dust on impact strength

Table 4.2.6: Statistical result of impact test for coir dust

Parameters	Df	Sum sq	Mean sq	F-value	Pr (>F)
Sample	3	3.1278	1.0426	10426	1.05e - 14
Residuals	8	0.0008	0.0001		
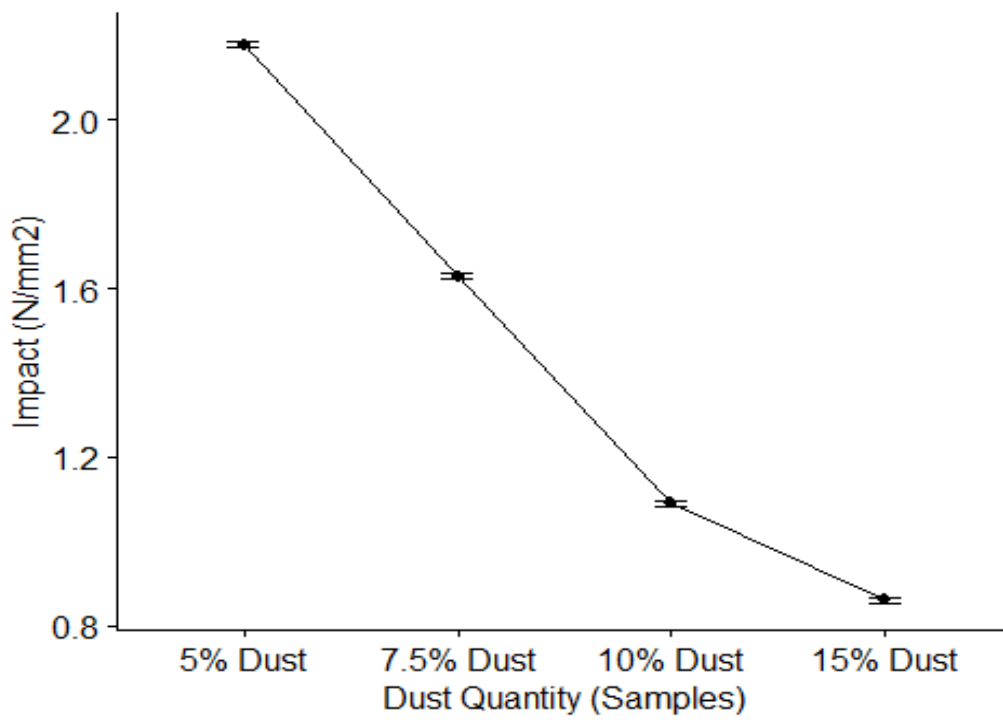
Figure 4.45: Generated quantity of coir dust on impact strength
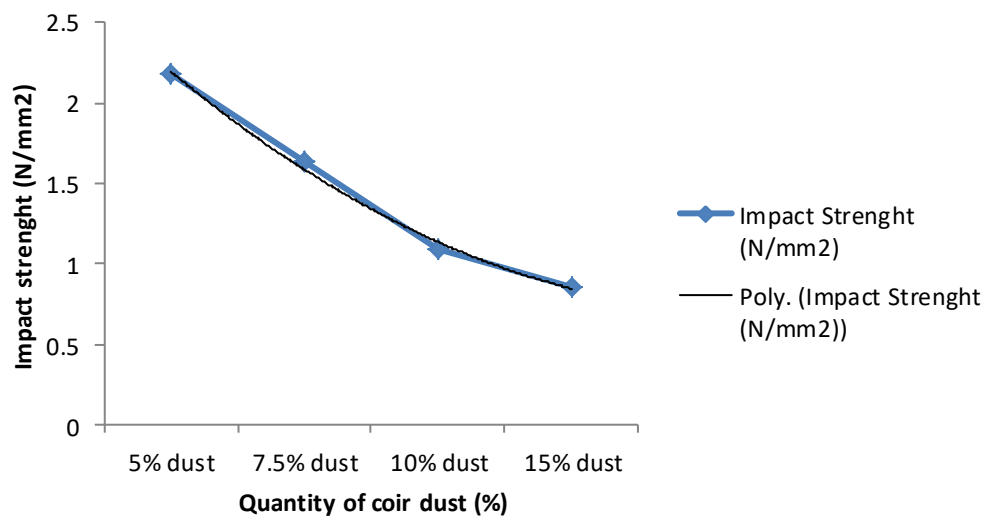
Figure 4.46: Relationship between impact strength (N/mm^2) and quantity of coir dust (%)

$$I.S = 0.08q^2 - 0.85q + 2.965$$
$$R^2 = 0.9957$$

I.S = $0.08q^2 - 0.85q + 2.965$ ………………………………………… 4.18

This implies that as Impact Strength decreases gradually, there is increase in the quantity of the coir dust.

4.2.3 Results and discussion on CNSL quantity

4.2.3.1 Effect of CNSL quantity on water absorption

The effect of Cashew Nut Shell Liquid (CNSL) in water absorption from Table 4.3 and Figure 4.47 shows that, there was a slightly decrease in water absorption when the CNSL content increased from 2.5% to 10% of CNSL. Water absorption further decreased with increase in CNSL content as shown in Figure 4.47. Among all the composites, 2.5% composite absorb highest water content (17.77%) while 10% of CNSL content composite showed lowest water absorption, Figure 4.47. The lower the CNSL content, the higher is the water absorption.

The water absorption results obtained in this work are similar to the previous works, Maraghi, Tabei and Madanipoor (2018), in his study about the effect of board density, resin percentage (urea-formaldehyde), and pressing temperature on particleboard properties made from mixing of poplar wood slab, citrus branch and twings of beech which also reported that by increasing the amount of resin (urea-formaldehyde) from 9 to 11% decreased water absorption.

By increasing resin content the connections between dust particle and resin, there was better coating between dust resins. This provides fewer pathways for water molecule to penetrate the composite material, which enhances the stability of boards produced. Lubi and Thachil (2007), Dahmordeh, Nazerian and Bayatkashkoli (2013) and Lin, Hiziroglu, Kan and Lai (2008) have reported that by increasing the resin, the stability of particleboard improves.

A one-way between subjects ANOVA was conducted and the results presented according to Table 4.3.1 to examine the effect of CNSL composite on water absorption. The different CNSL samples considered are: 2.5% CNSL, 5% CNSL, 7.5% CNSL and 10% CNSL. According to the findings, the CNSL composite has a
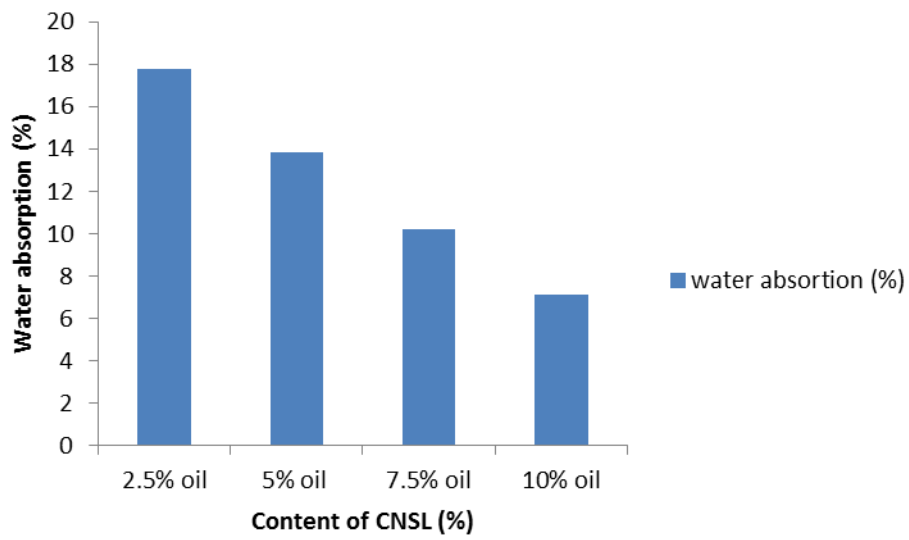
Figure 4.47: Influence of quantity of CNSL on water absorption

Table 4.3: Summary of the results carried out using CNSL content

Sample (CNSL)		2.5%	5%	7.5%	10%
Water Absorption (%)		17.77	13.85	10.23	7.14
Thickness Swelling	2HRS	1.69	1.35	1.04	0.70
(%)	24 HRS	2.71	2.14	1.61	0.93
Density (g/mm^3)		0.00151	0.00147	0.00137	0.00131
Flexural Strength (mpa)		5.10	5.96	4.78	3.59
Compressive Strength (mpa)		7.25	5.19	2.61	2.18
MOE (mpa)		1054.09	784.53	519.93	306.01
MOR (mpa)		2.36	2.09	1.93	1.71
Impact Strength (N/mm^2)		1.09	1.63	1.72	2.57

significant influence on the water absorption p<.05 level for at least two of the CNSL samples under consideration [F(3,12) = 241, p <.001.

From the mean plot computed from Figure 4.48 when examining the effect of CNSL composite on water absorption, it can be observed that 2.5% CNSL sample computed the highest mean while 10% CNSL sample computed the lowest mean. The mean plot of density portrays a negative trend across the 4 categories of CNSL samples under consideration. This is an indication that the water absorption decreases as the percentage of CNSL increases.

Figure 4.49 shows the relationship between Water Absorption and CNSL which is express by Polynomial expression model

$$W.A = 0.2075q^2 - 4.5885q + 22.163 \qquad\qquad ……..\ 4.19$$

This implies that as water absorption decreases significantly, CNSL content increases.

Table 4.3.1: Statistical result of water absorption test for CNSL

Parameters	df	Sum sq	Mean sq	F-value	Pr (>F)
Sample	3	189.6	6319	241	3.51e - 08
Residuals	8	2.1	0.26		

Figure 4.48: Generated quantity of CNSL on water absorption
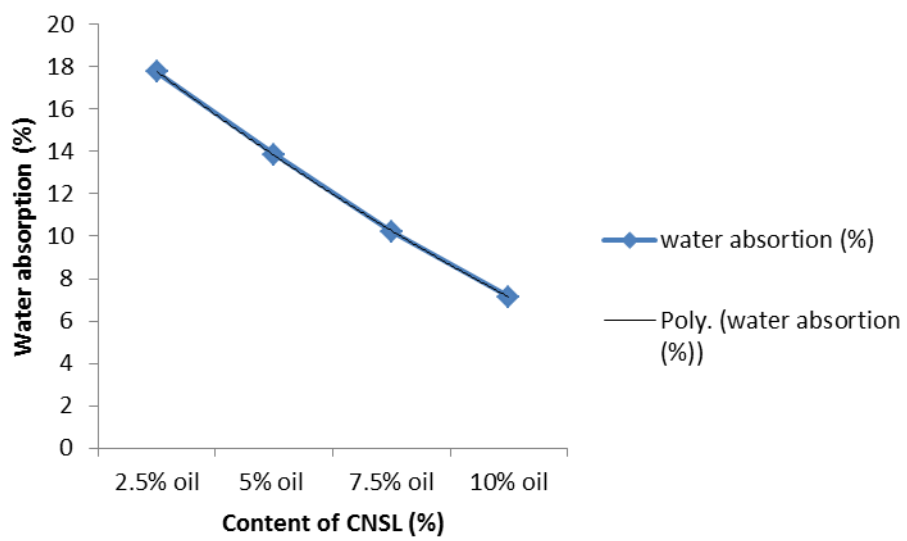
Figure 4.49: Relationship between water absorption (%) and quantity of CNSL (%)

$$W.A = 0.2075q^2 - 4.5885q + 22.163$$
$$R^2 = 1$$

4.2.3.2 Effect of CNSL quantity on thickness swelling

The results from Table 4.3 showed thickness swelling of the CNSL composite board after 2hours and 24hours immersion in water. The thickness swelling from Figure 4.50 decreased as the volume of CNSL content increase in the composites. Thickness swellings from Figure 4.50 started decreasing from 2.5% of CNSL content and then continue to decrease to 10% of CNSL content.

The thickness swelling values for highest CNSL particle board from Figure 4.50 were only 0.70% and 0.93% after 2hours and 24hours water immersion respectively, while the thickness swelling values for lowest CNSL particleboard were only 1.69% and 2.71% after 2hours and 24hours water immersion respectively. The thickness swelling results obtained in this work are similar to the previous works, Abdulkareem, Raji, and Adeniyi, (2017), in there study about manufacture of particleboard from waste Styrofoam and sawdust, reveals that the thickness swelling values of resin particle board decreased with increasing in resin content.

This has a tendency to prevent more water from penetrating the composite material, comparable to the reaction of CNSL content in water absorption. The findings about the thickness swelling of the particleboards demonstrated that the composition affects how dimensionally stable a particleboard is in a moist environment (Abdulkareem et al, 2017).

A one-way between subjects ANOVA was conducted and the results presented according to Table 4.3.2 to examine the effect of CNSL composite on thickness swelling. The different CNSL samples considered are: 2.5% CNSL, 5% CNSL, 7.5% CNSL and 10% CNSL. According to the findings, the CNSL composite has a significant influence on the thickness swelling $p<.05$ level for at least two of the CNSL samples under consideration [$F(3,20) = 10.98$, $p <.001$.

From the mean plot computed from Figure 4.51 when examining the effect of CNSL composite on thickness swelling, it can be observed that 2.5% CNSL sample computed the highest mean while 10% CNSL sample computed the lowest mean. The mean plot of thickness swelling portrays a negative trend across the 4 categories of CNSL
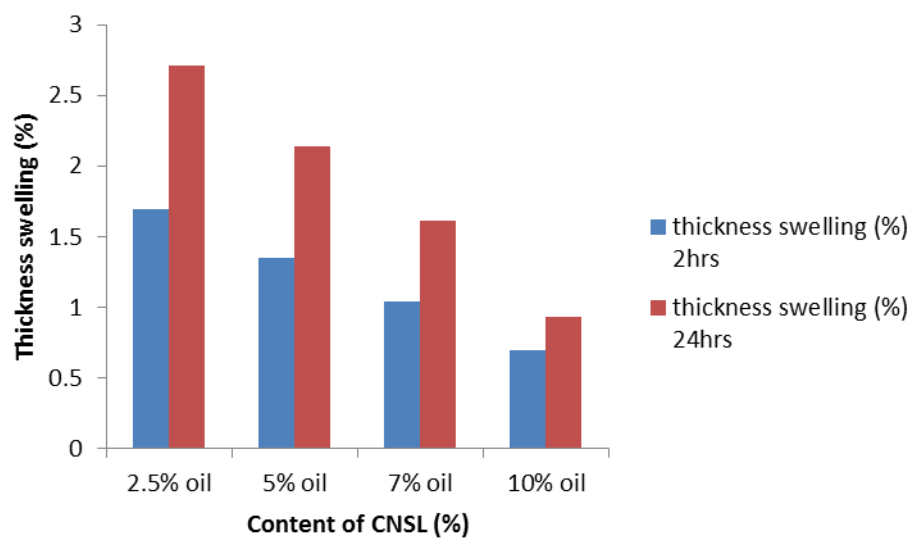
Figure 4.50: Influence of quantity of CNSL on thickness swelling

Table 4.3.2: Statistical result of thickness swelling test for CNSL

Parameters	df	Sum sq	Mean sq	F-value	Pr (>F)
Sample	3	6.352	2.1175	10.98	0.000177
Residuals	20	3.857	0.1928		
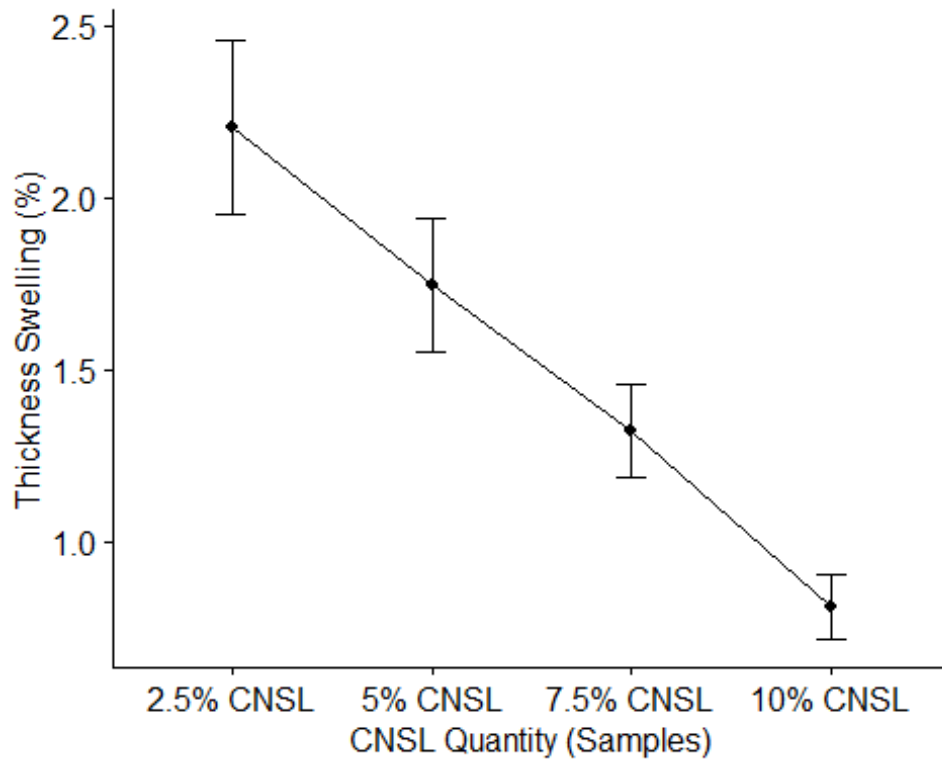
Figure 4.51: Generated of quantity of CNSL on thickness swelling

samples under consideration. This is an indication that the thickness swelling decreases as the percentage of CNSL increases.

Figure 4.52 show the relationship between Thickness Swelling and CNSL which is express by Polynomial expression model for 2hrs and 24hrs is given respectively

$$T.S_2 = -0.328q + 2.015 \qquad \qquad \text{.... } 4.20$$

$$T.S_{24} = -0.0275q^2 - 0.4495q + 3.1775 \qquad \qquad \text{.... } 4.21$$

This implies that as thickness swelling decreases slightly, the CNSL increases.
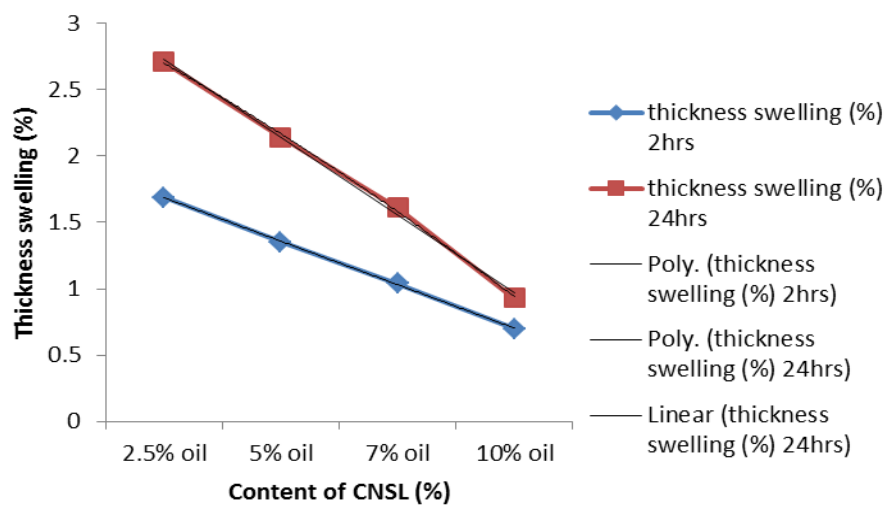
Figure 4.52: Relationship between thickness swelling and quantity of CNSL

$$T.S_2 = -0.328q + 2.015$$
$$R^2 = 0.9997$$
$$T.S_{24} = -0.0275q^2 - 0.4495q + 3.1775$$
$$R^2 = 0.999$$

4.2.3.3 Effect of CNSL quantity on density

There is variation of density with CNSL content, Table 4.3. Density from Figure 4.53 decreases gradually as the CNSL content increases from 2.5% of CNSL content to 10%. The density value for highest CNSL particle board according to Figure 4.53 was only $0.00131g/mm^3$ while the composite board with lowest CNSL content was only $0.00151g/mm^3$.

As the CNSL content rises, there is only a very slight change in density. Cardanol or other phenolic side chains in CNSL can cause the chain to pack loosely. In this situation, the adhesive qualities typically aren't as good. Consequently, a decrease in density is possible (Lubi and Thachil, 2007).

Figure 4.54 shows the relationship between Density and CNSL which is express by Polynomial expression model

$$D = -5E\text{-}06q^2 - 4E\text{-}05q + 0.0016 \qquad\qquad ……..\ 4.22$$

This implies that as Density decreases slightly, the CNSL content increases.
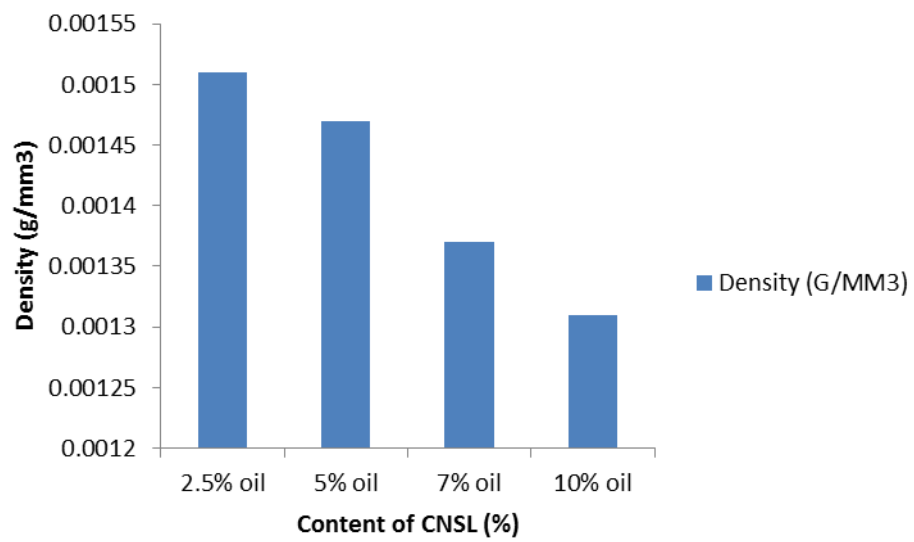
Figure 4.53: Influence of quantity of CNSL on density
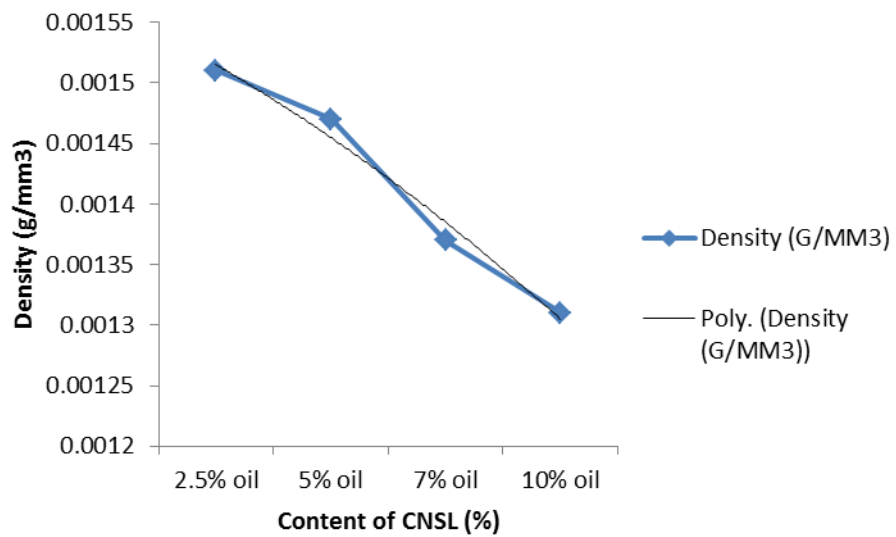
Figure 4.54: Relationship between density (g/mm³) and quantity of CNSL (%)

$$D = -5E\text{-}06q^2 - 4E\text{-}05q + 0.0016$$
$$R^2 = 0.9801$$

4.2.3.4 Effect of CNSL quantity on flexural strength

Table 4.3 and Figure 4.55 show the results of the variation of flexural strength with CNSL. The flexural strength of CNSL composite board from Figure 4.55 increased with the CNSL content from 2.5% up to 5% and then started decreased from 7.5% to 10% of CNSL content. The lowest value of flexural strength (3.59Mpa) from Figure 4.53 is given by composite board with 10% of CNSL while the highest value of flexural strength is given by the composite board with 5% of CNSL content (5.96mpa). Beyond 5% loading, there was an excess of CNSL that had decreased the strength and made the composite board brittle.

The reinforcement-matrix bond had been weakened by the aggregation of dust particles at higher matrix loadings. The increment of the CNSL loading from 2.5% to5% enhanced the bonding strength. This occurred as a result of the 5% CNSL content having more particles that were tightly bound to the matrix, which decreased the voids between dust particles. This resulted from the effective interaction between the CNSL matrix and the dust particle.

The flexural strength results obtained from this work are similar to the previous work, Chiang, Hamdan and Osman (2016) in there study about the properties of Sago particleboards resonated with Urea fomaldehyde and Phenol-resorcinol formaldehyde resin also reported that up to 15% of the resin was effective in increasing the flexural strength of particleboard made of urea formaldehyde, but the strength reduced beyond 15%.

A one-way between subjects ANOVA was conducted and the results presented according to Table 4.3.3 to examine the effect of CNSL composite on Flexural Strength. The different CNSL samples considered are: 2.5% CNSL, 5% CNSL, 7.5% CNSL and 10% CNSL. According to the findings, the CNSL composite has a significant influence on the Flexural Strength $p < .05$ level for at least two of the CNSL samples under consideration [$F_{(3,8)} = 154.9$, $p < .001$.

From the mean plot computed from Figure 4.56 when examining the effect of CNSL composite on Flexural Strength, it can be observed that 5% CNSL sample computed
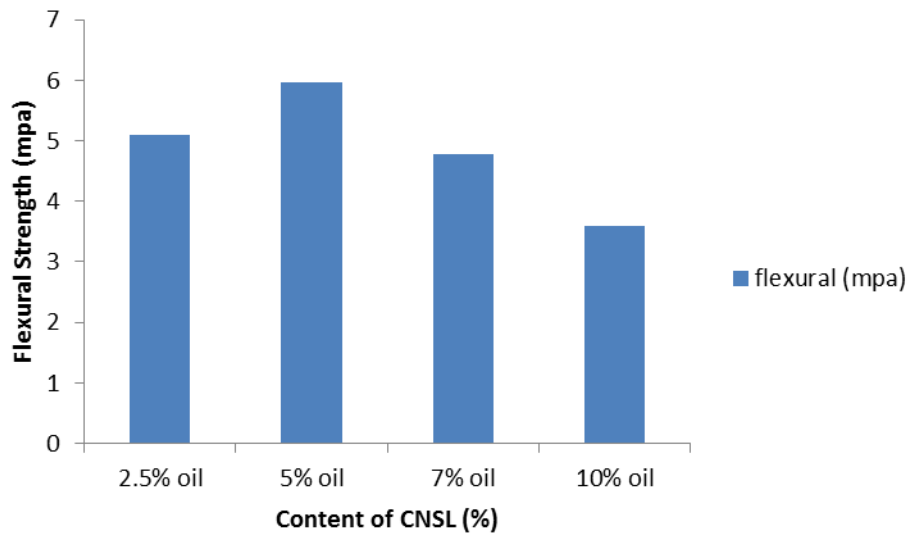
Figure 4.55:   Influence of quantity of CNSL on flexural strength

Table 4.3.3: Statistical result of flexural strength test for CNSL

Parameters	df	Sum sq	Mean sq	F-value	Pr (>F)
Sample	3	866.9	2.8896	154.9	2e - 07
Residuals	8	0.149	0.0186		
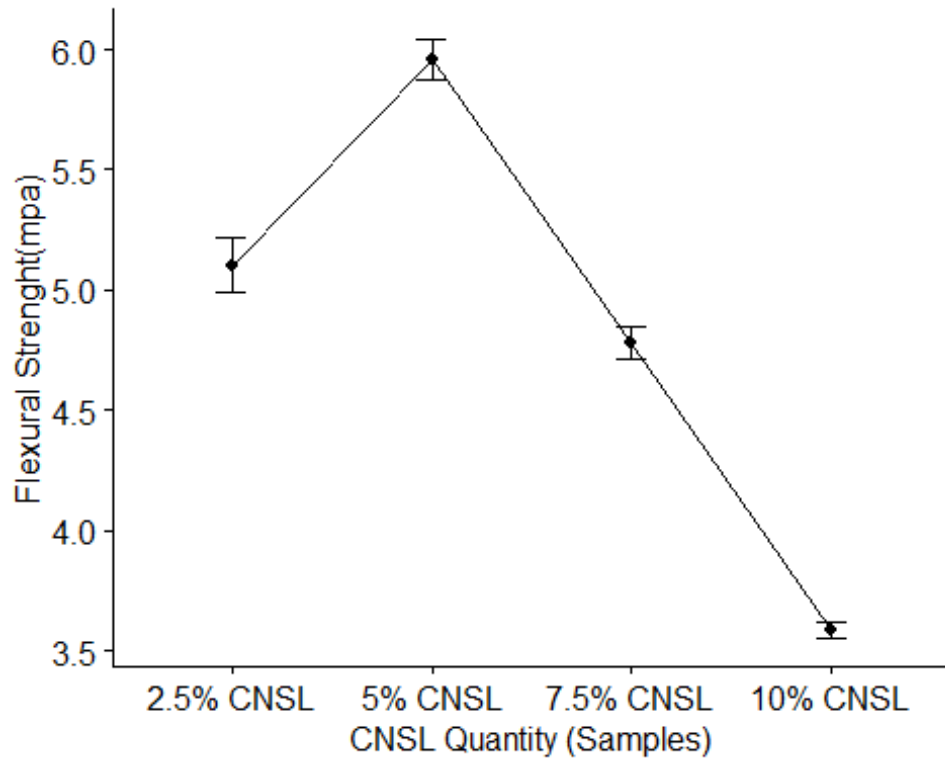
Figure 4.56: Generated quantity of CNL on flexural strength

the highest mean while 10% CNSL sample computed the lowest mean. The mean plot of density portrays a negative trend across the 4 categories of CNSL samples under consideration. This is an indication that the Flexural Strength (curing days) decreases as the percentage of CNSL increases.

Figure 4.57 shows the relationship between Flexural Strength and CNSL which is express by Polynomial expression model

$$\text{F.S} = -0.5125q^2 + 1.9915q + 3.7225 \qquad \qquad \text{…… 4.23}$$

This implies that flexural strength decreases slightly as CNSL content increases.
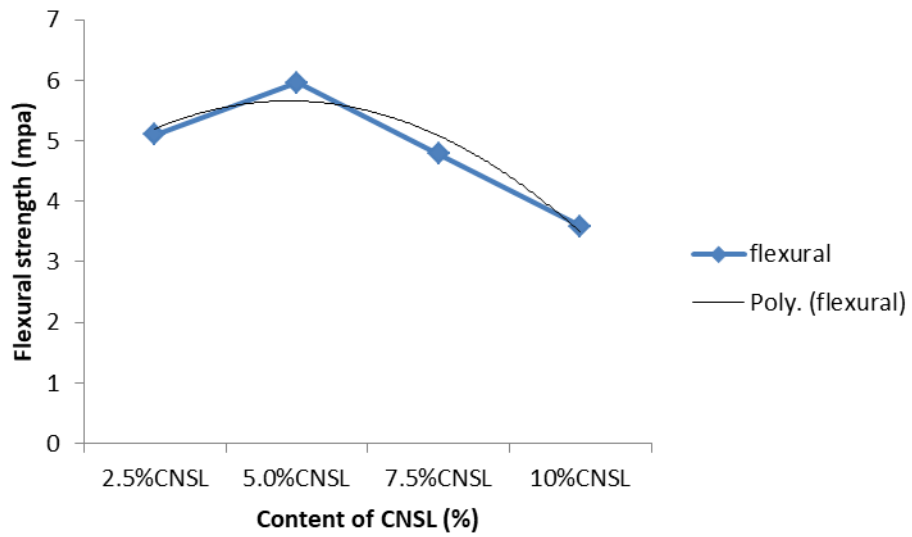
Figure 4.57: Relationship between flexural strength and quantity of CNSL

$$F.S = -0.5125q^2 + 1.9915q + 3.7225$$
$$R^2 = 0.9286$$

4.2.3.5 Effect of CNSL quantity on compressive strength

The effect on CNSL content on the compressive strength as presented from Table 4.3 and Figure 4.58 show that the addition of CNSL in the composite leads to decrease slightly as the CNSL content increased. Compressive strength gradually decreased from 2.5% of CNSL content to 10% of CNSL content, Figure 4.58. It is clearly shown from Figure 4.58 that composite of 10% CNSL content exhibited minimum compressive strength (2.18MPa) while the maximum compressive strength obtained from composite of 2.5% of CNSL content (7.25MPa).

As the CNSL content increased, compressibility was marginally reduced. Compressibility reduces as void space is reduced due to an increase in the bonding between filler particles. The compressive strength results obtained in this work are contradict to the previous works, Zakia, Taha, Mervat, Bahnasawy, Samir, Jutta, and Azra, (2019), In a prior study he conducted on rice straw and flax fibre particle boards made from agricultural waste, an evaluation of technical properties reported that while increasing the content of urea formaldehyde enhanced the compressive strength of the manufactured particleboard, increasing the content of resin from 10% to 14% increased the compressive strength from 1.55 to 4.46 mpa.

Figure 4.59 show the relationship between Compressive Strength and CNSL which is express by Polynomial expression model

$$C.S = 0.4075q^2 - 3.8165q + 10.793 \qquad\qquad …….. \ 4.24$$

This implies that as compressive strength decreases, the CNSL increases. There is significant decrease observed initially but later the decrease is minimal.
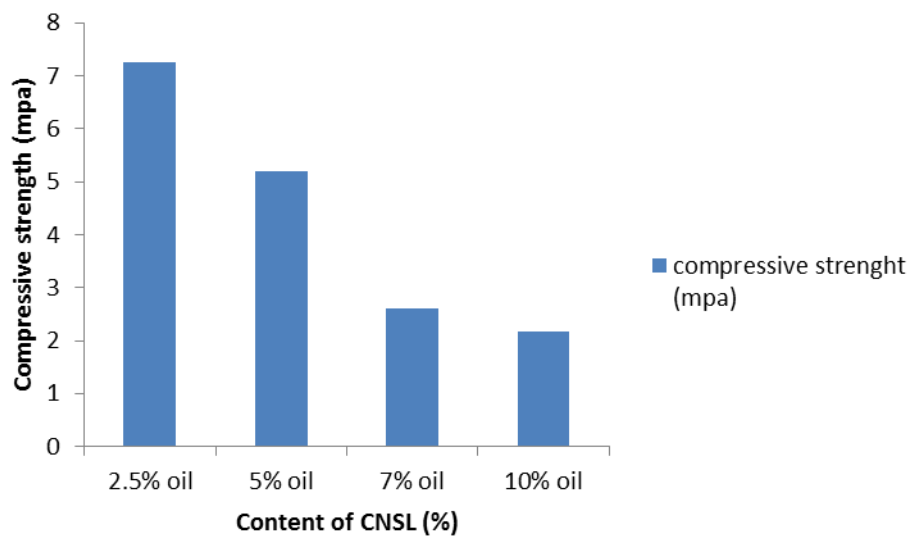
Figure 4.58: Influence of quantity of CNSL on compressive strength
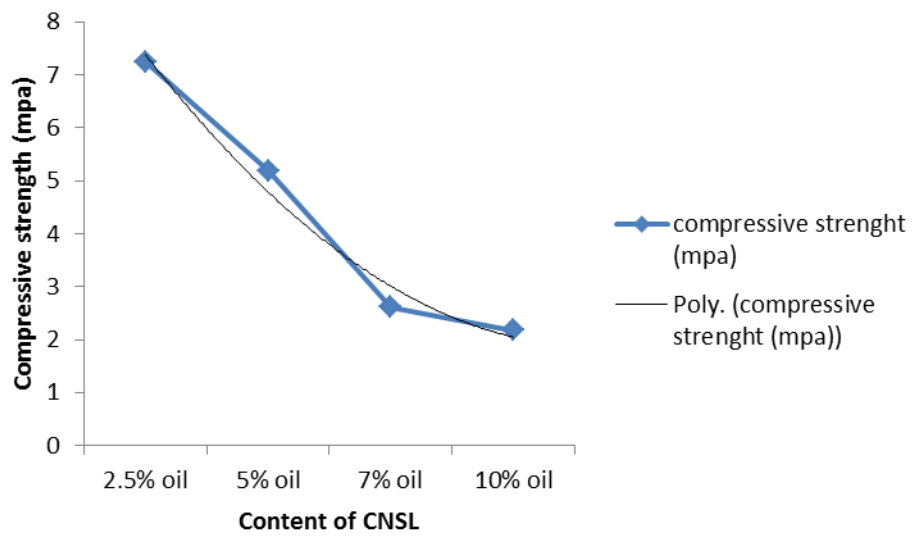
Figure 4.59: Relationship between compressive strength (mpa) and quantity of CNSL (%)

$$C.S = 0.4075q^2 - 3.8165q + 10.793$$
$$R^2 = 0.9788$$

4.2.3.6 Effect of CNSL quantity on modulus of elasticity

The modulus of elasticity results from Table 4.3 and Figure 4.60 illustrate the effect of CNSL with different content on modulus of elasticity. The modulus of elasticity decreases with the increase in the (CNSL) content in the composites. It was revealed that MOE were influenced by the perfect dispersion of individual particles, transverse cohesion, and particle/matrix interface bonding. Composite board with 2.5% of CNSL had the highest MOE value (1054.09 MPa), while composite board with 10% of CNSL content had the lowest value of MOE (306.01 MPa).

The modulus of elasticity reduced by increasing the percentage content of CNSL and the reason for this was the higher matric loading, which increased the stresses that were transferred between the particle and matrix interface. Similar relations were found for MOR. However, the results indicate that the effect of the particles with CNSL on the decrease in MOE was apparent. The results obtained in this work are similar to previous works, Chiang et al (2016), in his study about properties of Sago particleboard resonated with Urea formaldehyde (UF) and Phenol formaldehyde (PF) resin also reported that modulus of elasticity value decreased as the increase of UF and PF in Sago particleboards from 10% loading to 20% of UF and PF resin.

A one-way between subjects ANOVA was conducted and the results presented according to Table 4.3.4 to examine the effect of CNSL composite on MOE. The different CNSL samples considered are: 2.5% CNSL, 5% CNSL, 7.5% CNSL and 10% CNSL. According to the findings, the CNSL composite has a significant influence on the MOE $p<.05$ level for at least two of the CNSL samples under consideration [$F(3,12) = 12.07$, $p <.001$

From the mean plot computed from Figure 4.61 when examining the effect of CNSL composite on MOE, it can be observed that 2.5% CNSL sample computed the highest mean while 10% CNSL sample computed the lowest mean. The mean plot of density portrays a negative trend across the 4 categories of CNSL samples under consideration. This is an indication that the MOE decreases as the percentage of CNSL increases.
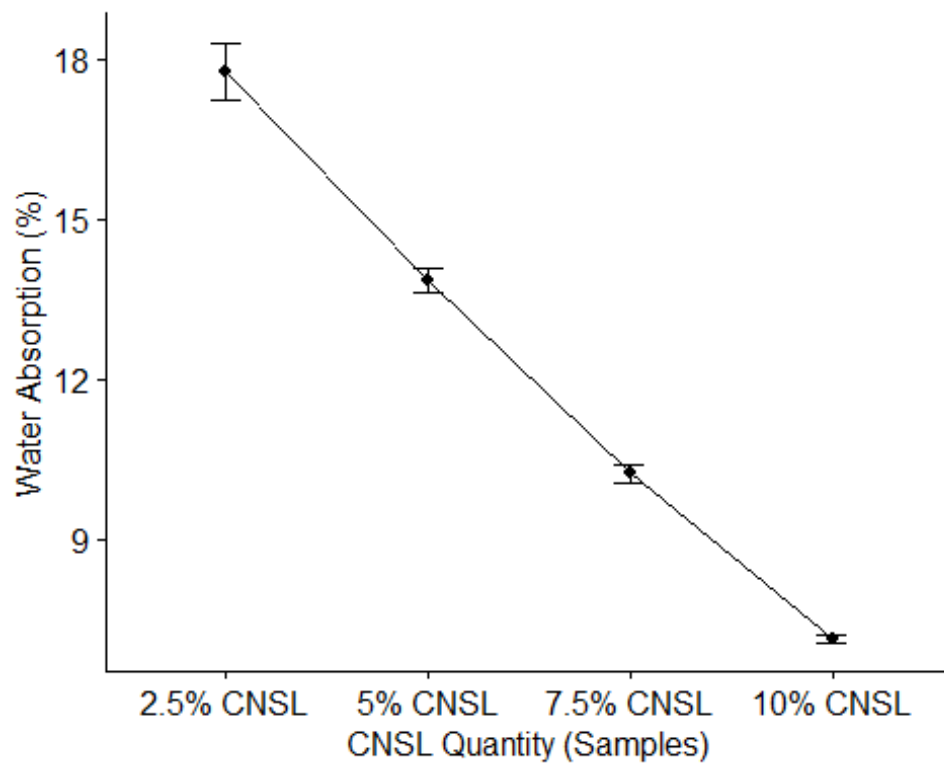
Figure 4.62 shows the relationship between Modulus of Elasticity and CNSL content which is express by Polynomial expression model
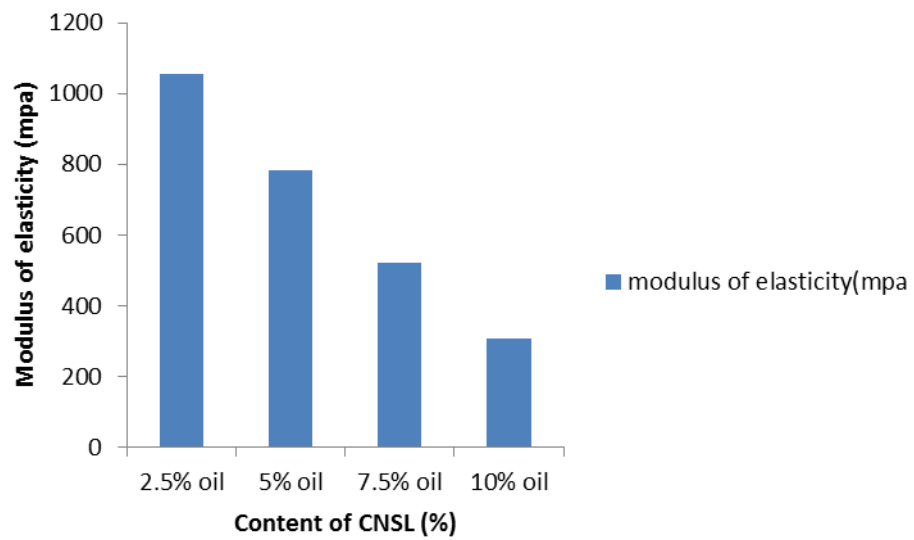
Figure 4.60: Influence of quantity of CNSL on modulus of elasticity

Table 4.3.4: Statistical result of MOE test for CNSL

Parameters	df	Sum sq	Mean sq	F-value	Pr (>F)
Sample	3	1262380	420793	12.07	0.000618
Residuals	12	418206	34851		
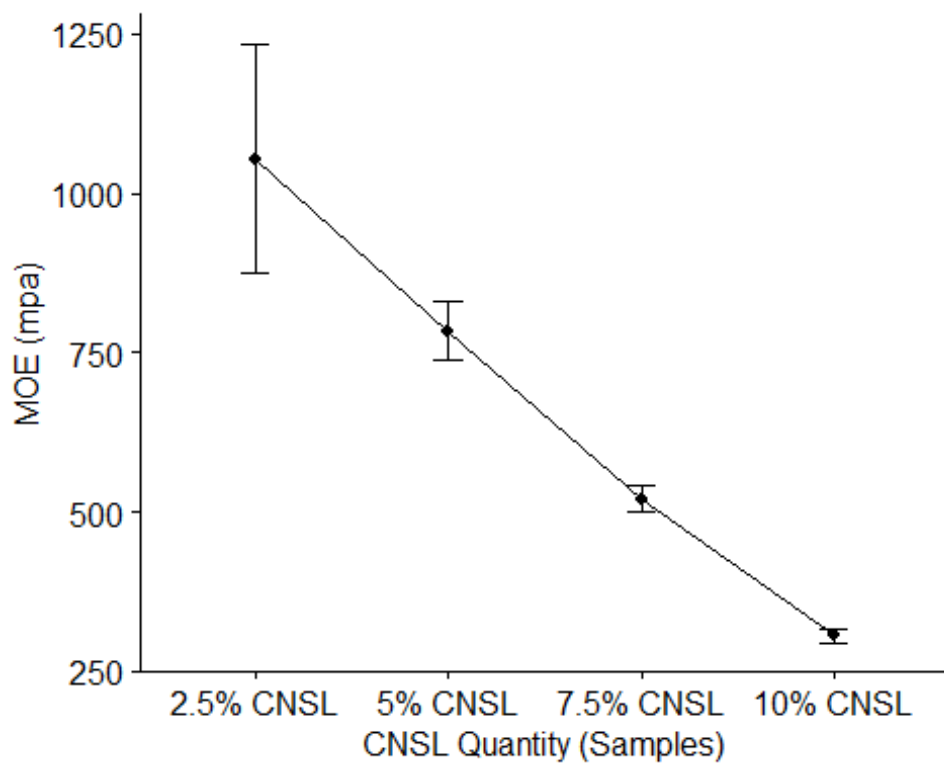
Figure 4.61: Generated quantity of CNSL on modulus of elasticity
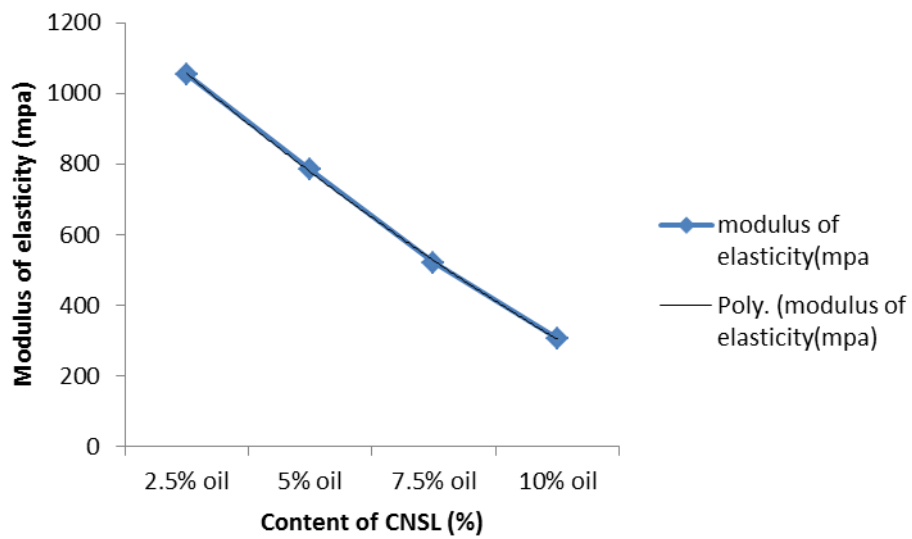
Figure 4.62: Relationship between modulus of elasticity (MPa) and quantity of CNSL (%)

$$M.O.E = 13.91q^2 - 320.43q + 1362.9$$
$$R^2 = 0.9997$$

$$M.O.E = 13.91q^2 - 320.43q + 1362.9 \qquad \text{……………….….. } 4.25$$

This implies that as the modulus of elasticity decreases significantly, the quantity of CNSL increases.

4.2.3.7 Effect of CNSL quantity on modulus of rapture

The effect of CNSL of the modulus of rapture on particleboard as presented form Table 4.3 and Figure 4.63 show the increase of CNSL content in the composite lead to decrease the value of modulus of rapture from 2.5% of CNSL content to 10%. The modulus of rapture in Figure 4.63 decreases with the increase in the CNSL content of the composite.

CNSL showed the decreasing modulus of rapture due to the CNSL loading. At 2.5% loading of CNSL, it revealed the highest value of the modulus of rupture due to the high interfacial interaction between the matrix and the dust at 10% of CNSL; however, a higher loading of CNSL did not promote a better MOR because it would have affected the composite material's brittleness and prevented it from being able to resist the fracture under the applied stress.

The modulus of rapture reduced by increasing the content of CNSL and this resulted from a reduction in the stress transfer across the matrix-particle interface. The findings of this study are comparable to those of previous studies, Chiang et al (2016), in his study about properties of Sago particleboards resonated with urea formaldehyde and phenol formaldehyde resin also reported that modulus of rapture values decreases with increase of urea formaldehyde (UF) and Phenol formaldehyde (PF) in Sago particleboards from 10% to 20% of UF/PF resin (Chiang et al, 2016).

A one-way between subjects ANOVA was conducted and the results presented according to Table 4.3.5 to examine the effect of CNSL composite on MOR. The different CNSL samples considered are: 2.5% CNSL, 5% CNSL, 7.5% CNSL and 10% CNSL. According to the findings, the CNSL composite has a significant influence on the MOR $p<.05$ level for at least two of the CNSL samples under consideration $[F(3,20) = 18.31, p <.001$.

234
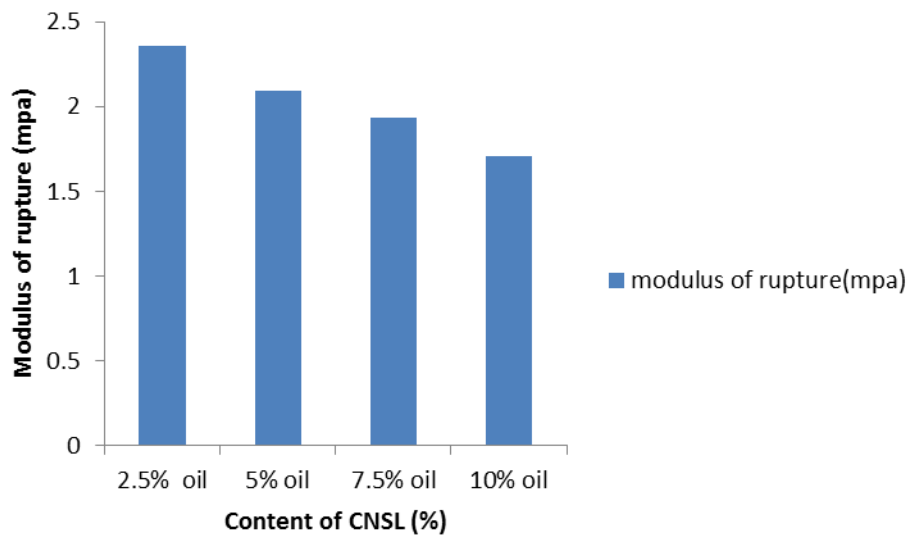
Figure 4.63: Influence of quantity of CNSL on modulus of rupture

Table 4.3.5: Statistical result of MOR test for CNSL

| Parameters	df	Sum sq	Mean sq	F-value	Pr (>F)
Sample	3	0.8773	0.29242	18.31	8.96e - 05
Residuals	12	0.1916	0.01597		

From the mean plot computed from Figure 4.64 when examining the effect of CNSL composite on MOR, it can be observed that 2.5% CNSL sample computed the highest mean while 10% CNSL sample computed the lowest mean. The mean plot of density portrays a negative trend across the 4 categories of CNSL samples under consideration. This is an indication that the MOR decreases as the percentage of CNSL increases. Figure 4.65 shows the relationship between Modulus of Rupture and CNSL which is express by Polynomial expression model

$$M.O.R = 0.0125q^2 - 0.2735q + 2.6125 \qquad \ldots \ldots \ 4.26$$

This implies that as modulus of rupture decreases slightly, the CNSL increases.
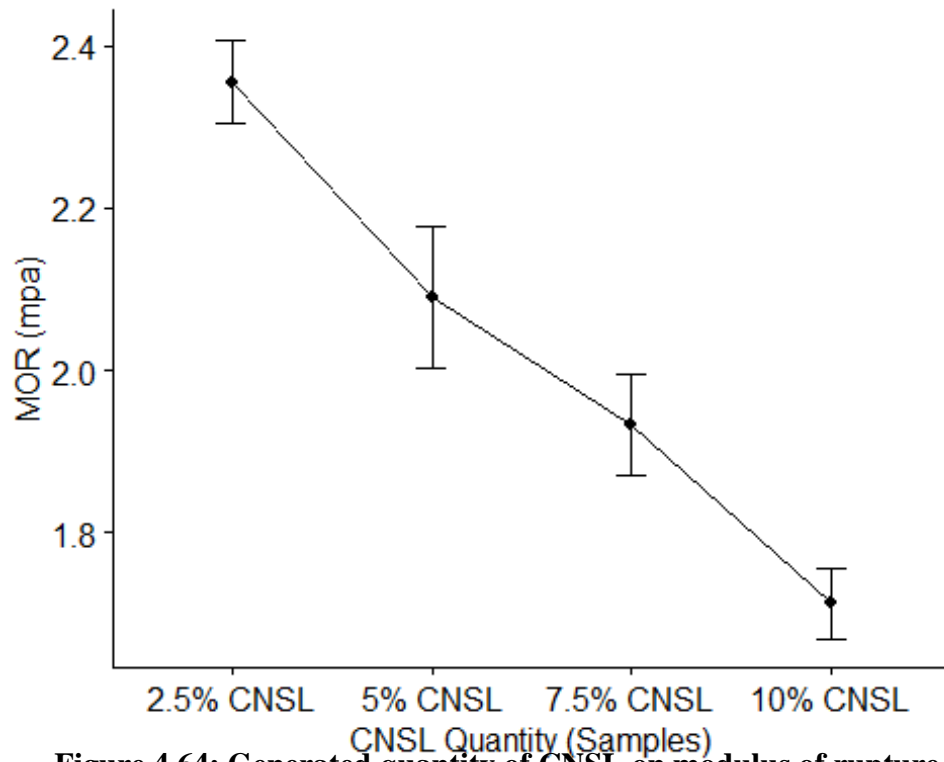
Figure 4.64: Generated quantity of CNSL on modulus of rupture
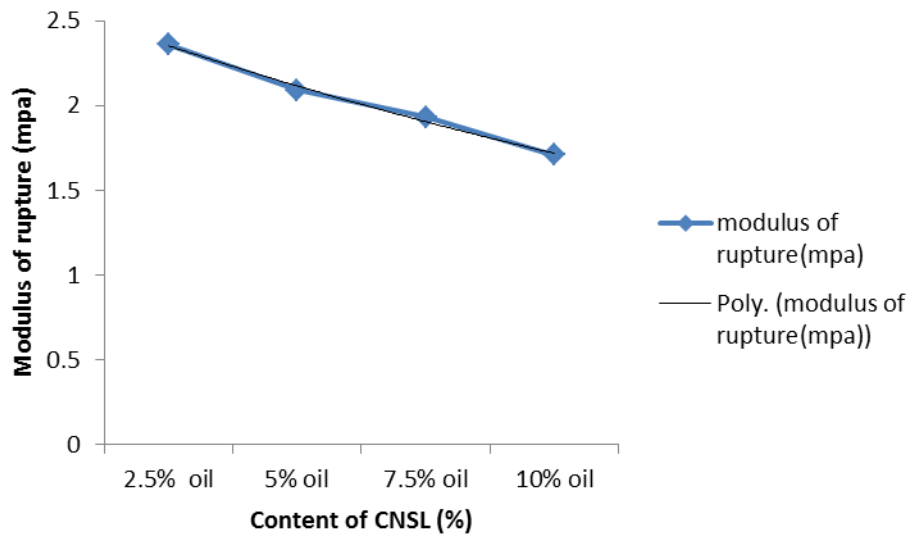
Figure 4.65: Relationship between modulus of rupture (mpa) and quantity of CNSL (%)

$$M.O.R = 0.0125q^2 - 0.2735q + 2.6125$$
$$R^2 = 0.9936$$

4.2.3.8 Effect of CNSL quantity on impact strength

Impact strength of CNSL composites from Table 4.3 and Figure 4.66 indicated the trend of increasing slightly in value of impact strength with the addition of CNSL content in the composites from 2.5% of CNSL content to 10% of CNSL content in the composite. The composite board's strength was increased by the addition of CNSL content. The lowest value of the impact strength as indicated in Figure 4.66 (1.09 N/mm^2) is given by the composite with 2.5% of CNSL content and the composite that contains 10% of CNSL content has the highest value of impact strength which is 2.57N/mm^2.

The results of the impact strengths attained here are equivalent to those of the earlier works accomplished by Chiang et al (2016), in his study about properties of Sago particleboards resonated with Urea formaldehyde and phenol formaldehyde resin reveal that the particleboard was strengthened by the increased of urea formaldehyde loading.

A one-way between subjects ANOVA was conducted and the results presented according to Table 4.3.6 to examine the effect of CNSL composite on impact. The different CNSL samples considered are: 2.5% CNSL, 5% CNSL, 7.5% CNSL and 10% CNSL. According to the findings, the CNSL composite has a significant influence on the impact $p < .05$ level for at least two of the CNSL samples under consideration [$F(3,8) = 10371$, $p < .001$.

From the mean plot computed from Figure 4.67 when examining the effect of CNSL composite on impact strength, it can be observed that 2.5% CNSL sample computed the lowest mean while 10% CNSL sample computed the highest mean. The mean plot of density portrays an upward trend across the 4 categories of CNSL samples under consideration. This is an indication that the impact strength increases as the percentage of CNSL increases.

Figure 4.68 shows the relationship between Impact Strength and CNSL which is express by Polynomial expression model

$$I.S = 0.0775q^2 + 0.0655q + 1.0075$$ …………………………………… 4.27
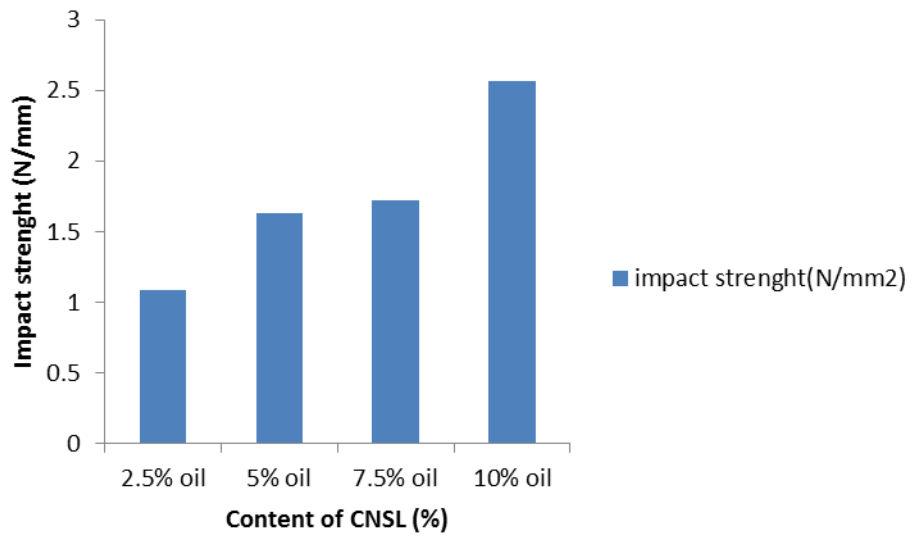
Figure 4.66: Influence of quantity of CNSL on impact strength

Table 4.3.6: Statistical result of impact strength test for CNSL

Parameters	df	Sum sq	Mean sq	F-value	Pr (>F)
Sample	3	3.370	1.1235	10371	1.07e - 14
Residuals	8	0.001	0.0001		
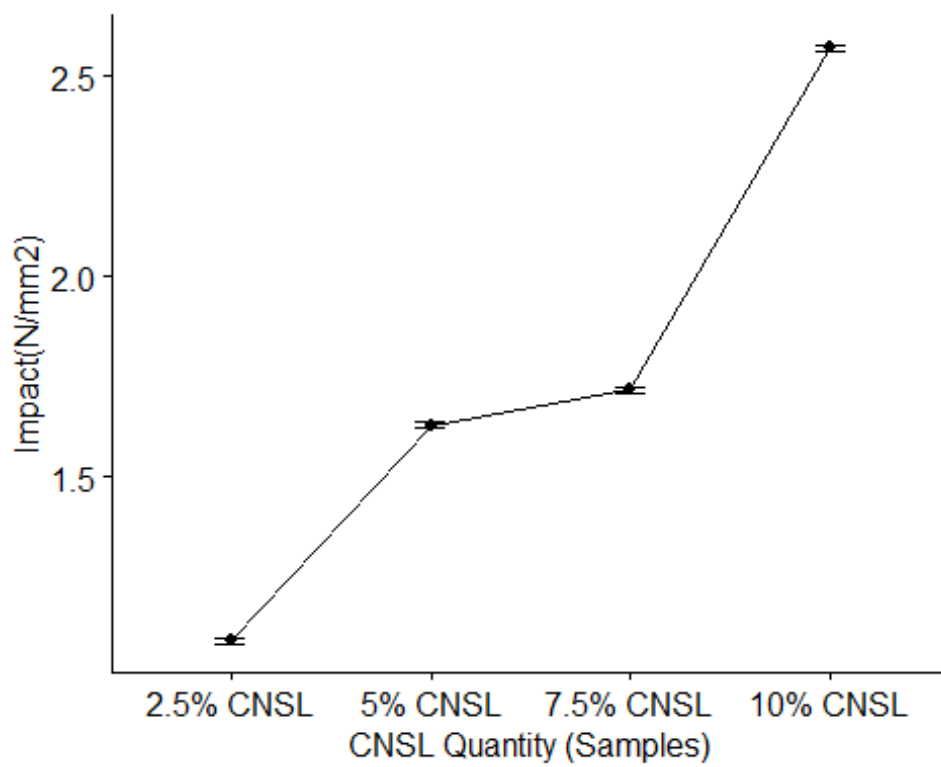
Figure 4.67: Generated quantity of CNSL on impact strength
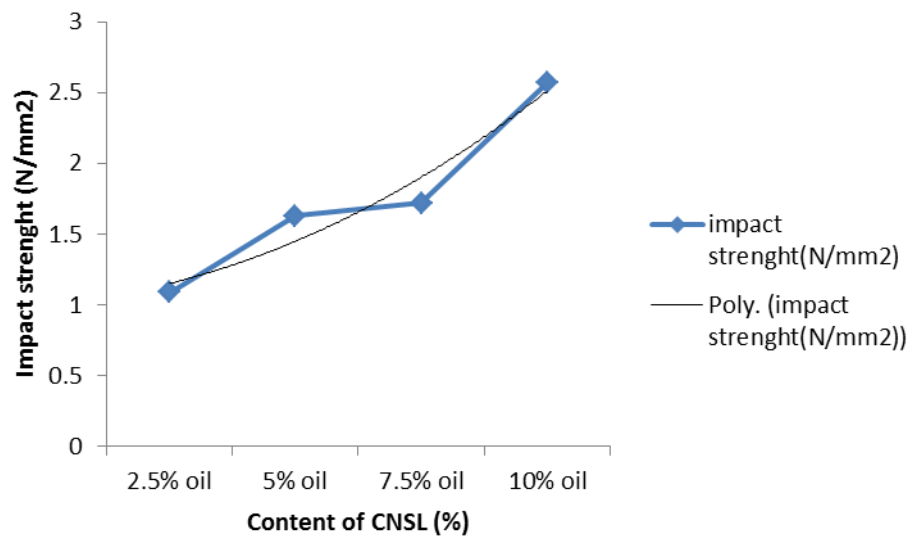
Figure 4.68: Relationship between impact strength (N/mm^2) and quantity of CNSL (%)

$$\text{I.S} = 0.0775q^2 + 0.0655q + 1.0075$$

$$R^2 = 0.9348$$

This implies that as impact strength increases gradually, there is increase also in the CNSL content.

4.2.4   Deduction from results and discussion

Composite board was divided into three categories based on its density: low, medium, and high, and its value vary depending on the national standards of each country. According to the American National Standard Institute for particleboard (ANSI/A208.1, 1999), the density range from <640kg/m^3 (low density), 640-800kg/m^3 (medium density) and >800kg/m^3 (high density). Kenyan requirements standard (DKS 2706-2016) for medium density (MDF) range from 621-780kg/m^3 and Indian standard requirements (Amend No3 to IS 3478:1966) of high density particleboard for both type 1 and type 2 of particleboard range from 900-1200kg/m^3.

In this study, three forms of composite boards were produced: coir fibre composites, coir dust composites and CNSL/coir dust composites.

Coir fibre composite board, the density and thickness swelling of the composite board produced met and also exceeded the minimum standard requirements of ANSI/A208.1 (1999) and EN312 (2010). The thickness swelling of all level of coir fibre composite boards produced met and exceeded minimum standard requirements of Kenyan Standard (KS) on fibre board, KS 2706-2:2017. The mechanical properties of coir fibre composite board, MOE and MOR of 5% and 15% met and exceeded the minimum requirements of grade LD-1 while 7.5% and 10% also met minimum requirements of grade LD-2 of ANSI/A208.1 (1999).

Coir dust composite board, its density ranged from 1480kg/m^3 to 1030kg/m^3 and the thickness swelling ranged from 1.90 to 5.11% met and exceeded minimum requirements of EN 312 (2010) and ANSI/A208.1 (1999). The mechanical properties, MOE in 5% met and exceeded grade M-S, 7.5% and 10% conformed to minimum standard requirements of grade LD-2 of ANSI/A208.1 (1999).

CNSL/coir dust composite board, its density ranged from 1510kg/m^3 to 1310kg/m^3 and thickness swelling ranged from 2.7 to 0.93%, all level of composite boards produced met and exceeded minimum requirements for all grade of particleboards according to

the US standard (ANSI/A208.1, 1999) also met EN 312 (2010) and KS 2706-2 2017 standard requirements. The mechanical property, MOE of 5% met and exceeded the minimum standard requirements of grade LD-1 while 2.5% met the minimum standard requirements of grade LD-2 of the American National Standard Institute (ANSI/A208.1, 1999).

4.2.5 Influence of CNSL on composite boards produced

From the results obtained in this work, the analysis of the physical and mechanical properties results shown in Table 4.2 and 4.3 analysed the effect of the CNSL performance on the composite boards. During the manufacturing and drying process, Urea formaldehyde and Phenol formaldehyde releases toxic gases that are harmful to human health and to the environment, this may prevent the beneficial environmental effect of using coir fibre/dust as raw materials. Therefore, the use of CNSL emerges as an intriguing choice, considering that it poses no threat to human health.

It was noticed from this study that addition of CNSL as little as 2.5% shown the significant effect on the composite boards produced and leads to the decrease in thickness swelling in all cases, meaning a lower water absorption and higher dimensional stability. The CNSL oil-based resin improved the physical properties preparation and little reduction in mechanical properties, which mean the composite boards produced can be used for both interior and exterior purposes also for non-structural purposes.

CHAPTER FIVE
SUMMARY, CONCLUSION AND RECOMMENDATIONS

5.1 Summary

This study investigated the feasibility of using CNSL as a polymer due to its non-toxicity to human health compared to urea formaldehyde and phenol formaldehyde. For composite board production, CNSL was mixed with coir dust and other materials. And various tests like, water absorption, thickness swelling, compressive strength, modulus of rupture, modulus of elasticity, and impact strength were conducted on the boards produced to check for the suitability of the boards for building construction. The use of CNSL significantly improved the physical properties and also had a significant effect on the mechanical properties of the applications composite boards, which made the boards suitable for both indoor and outdoor use.

5.2 Conclusion

It has been shown that, composite boards can be developed from cement and CNSL reinforced with coir inclusions whose properties conform to specifications.

1. Machine was developed which was capable of controlling the critical processes of feeding, mixing, pressing, compacting and heating in the production of the composite boards.

2. The percentage of water absorption and thickness swelling of composite board also increased hence the composite board can only be used for indoor purposes at higher percentage of rea.

3. Addition of coir fibre/dust in the composites decreased the density of composite board hence it can be used as light weight material in the building constructions.

4. The density observed in all levels of composite boards produced in this study conformed to the medium standard requirements of ANSI/A208.1, 1999.

5. Modulus of rupture and modulus of elasticity of coir fibre and coir dust composite boards show their highest values in 10% and 5% respectively.

6. The modulus of elasticity and modulus of rupture in 7.5% and 10% of coir fibre composite boards produced conformed with grade LD-2 composite board

while 5% and 15% conformed to grade LD-1 composite board of standard requirements of American National Standard Institute for composite board (ANSI/A208.1, 1999).

7. The modulus of elasticity at 5% coir dust composite board met and exceeded grade M-S particleboard, 7.5% and 10% conformed to grade LD-2 particleboard while modulus of rupture in 5% and 7.5% exceeded grade LD-1 particleboard of standard requirements of ANSI/A208.1, 1999.

8. The use of CNSL in the production of coir dust composite boards improved the physical properties of the boards hence it can be used in both indoor and outdoor purposes in the building.

9. It was observed that the percentage of CNSL at 2.5% and 5% resulted in higher modulus of elasticity and lower modulus of rupture.

10. The modulus of elasticity in 2.5% of CNSL/coir dust composite board met and exceeded grade LD-2 composite board while 5% and 7.5% exceeded grade LD-1 composite board of standard requirements of ANSI/A208.1, 1999.

11. ANOVA was used to compare the different and determine suitability level of the cement composite produced.

12. Modelling was employed to describes and predict the suitability of the composite boards produced.

13. Light weight composite boards produced from CNSL/coir dust enhanced dimensional stability which are suitable for both indoor and outdoor applications were successfully developed to reduce the problems of depletion of national forests and inadequate of housing materials.

5.3 Recommendations

This project had laid a solid foundation for the development of cement matrix modification with cashew nut shell liquid. The following points are recommended for further research works.

1. Machines should be locally developed for extraction of CNSL and for de-husk of coir fibres.

2. The machine developed can be modified to be automated machine for faster operation.

3. Different curing techniques should be tested/ experimented.

4. Fire resistance, durability and fatigue of the particleboard as ceiling boards may also be determined.

5.4 Contributions to knowledge

This project made more contributions to knowledge in the following areas.

1. The developed machine is capable of controlling the critical processes of feeding, mixing, pressing, compacting and heating the cement composite.
2. Experimental method employed for further processing of the material to ensure optimum strength and excellent performance has been developed.
3. The addition of CNSL significantly improved all the physical properties and also resulted in a more dimensionally stable composite.
4. Identification of optimum condition and product formulations necessary for producing acceptable composite boards from coconut fibre/dust cement composite has been developed.
5. Composite boards from coconut husk in terms of strength, stiffness and dimensional stability were established.
6. A model that can describe and predict the suitability behaviour of the cement composite has been developed.

REFERENCES

Abdulkareem, S.A., Raji, S.A. and Adeniyi, A.G. (2017). Development of particleboard from waste styrofoam and sawdust. *Nigerian Journal of Technology Development.* 14:18-22.

Abdullah, A., Baharin, S.J., Noor, M.M. and Hussin, K. (2011). Composite cement reinforced coconut fibre: physical and mechanical properties and fracture behavior. *Australian Journal of Basic and Applied Sciences,* 5.7:1228- 1240

Aggarwal, L.K (1995). Bagasse-reinforced cement composites. *Cem Concr Compo.* 17.2:107-112

Aigbodion, A.I. and Okieimen, F.E. (1995). Kinetics of the preparation of rubber seed Oil Alkyds. *Eur. Poly. Journal* 32.9: 1105-1108.

Aigbomian, E. P. (2013). *Development of wood-crete building material* (Doctoral dissertation, Brunel University).

Ajayi, B. (2002). Preliminary investigation of cement-bonded particleboard from maize stalk residues. *Nig. J. For*. 32.1: 33-37.

Akaranta, O. and Aluko, A.O. (1999). Bituminous coating: effects of cashew nut shell liquid-tannin resins. *Pigment and Resin Technology,* 28.6:336-340.

Akash, R.K., Gopta, N. and Kuman, D. (2016). Mechanical properties of sisal/coir fibre reinforced hybrid composites fabricated by cold pressing method: *IOP Conference series: materials science and Engineering.*149. 012092.

American National Standard for Particleboard. (1999). A208.1 ANSI/A208.1. and reproductive structures of Juniperus virginiana. 367-377.

Anonymous. (1975). High strength building panels based on crushed peanut shells-bonded with urea formaldehyde adhesive. Assignee: (THEB) J Theaut, Patent, P.N: FR 2235793, I.D: 750307

Anonymous. (2010a). More on product from CNSL .Retrieved on Jul. 30, 2020, from (http:/www.adarshsanoor.com/adarshindustrialchemicals/products/ cashew nut-shell-liquid)

AOAC. (1990). Association of official analytical chemists. Official Methods of Analysis, 15th Edition. Washington D.C. 69-88

Aramide, F., Oladele, I. and Folorunso, D. (2009). Evaluation of the effect of fibre volume fraction on the mechanical properties of a polymer matrix composite. *Leonardo Electronic Journal of Practices and Technologies,* 7:14.

Asasutjarit, C., Charoenvai, S., Hirunlabh, J. and Khedari, J. (2009). Materials and mechanical properties of pretreated coir-based green composites. Composites: Part B, 40:633-637.

Asasutjarit, C., Hirunlabh, J., Khedari, J., Daguenet, D. and Quenard, D. (2005). Coconut coir cement board. *International Conference on Durability of Building Materials and Components. Lyon, France.*

Asselanis and Mehta. (2001). Microstructure of concrete from a crack-free structural Designed to last a thousand years. *Third CANMET/ACI International Symposium on Sustainable Development of Cement and Concrete*, ACI SP 202:349-357

ASTM. 2647-89. (1994). Resistance of dried film of varnishes to water and alkalie. *Ann Book of Am. Soc. For Testing and Material Standards.*

ASTM. D. 1037. (1999). Standard test methods for evaluating properties of wood-base fibre and particle panel materials.

ASTM. 1640-83. (1991). Test for drying, curing or film formation of organic coatings at room temperature. *Ann. Book of Am. Soc.268-269.*

ASTM. D. 1106. (1984). Standard test method for acid-insoluble lignin in wood.

Badejo, S.O.O. (1987). A preliminary investigation of the bonding potential of elephant grass and chromolaena for cement-bonded particle board production. *J. Trop. For. Res.* 3: 42-53.
Bangladesh-*Daffodil. International University Journal of Science and Technology.* 2: 32-37.

Banthia, N., Yan, C. and Mindess, S. (1996). Restrained shrinkage cracking in fibre-reinforced concrete: A Novel Test Technique," *Cement and Concrete Research.* 26. 1: 9-14.

Bisanda E., Ogola, W. and Tesha, J. (2003). Characterisation of tannin resin blends for particle board application. *Cement and Concrete Composites.* 25. 6: 593- 598

Bismarck, A., Mohanty, A.K., Aranberri, A.I., Czapla, S., Misra, M. and Hinrichsen, G. (2001). Surface characterization of natural fibres; surface properties and the water up-take behaviour of modified sisal and coir fibres. *Green Chemistry,* 3:100-107

BMT surveys. Coconut (Coir) fibres. CargoHandbook.com.

Boob, T.N. (2014). Performance of saw-dust in low cost sandcrete blocks. *American Journal of Engineering Research* 3: 197-206.
Book of Am. Soc. for Testing and Material Standards.

Brufau, G., Boatella, J., and Rafecas, M. (2006). Nuts: source of energy and macronutrients. *British Journal of Nutrition*, *96*(S2), S24-S28.

BSI – BS 1881-118. (1983). Testing concrete method for determination of flexural.

BSI - BS 1881-119. (1983). Method for determination of compressive strength using portion of beams broken in flexure..

BSI -BS 5669-1. Methods of sampling, conditioning and test (particleboard part 1)

Butty, J. (1989). Palm oil in the lobby. *West Africa Magazine* 146-147.

Cabrera, J.G. and Nwaubani, S.O. (1990). Experimental methods for the preparation of palm fruit and other natural fibres for use in reinforced cement composites. In : Vegetable plants and their fibres as building materials: *Union of Testing and Research Laboratories for Materials and Structures* 29-36.

Cabrera, R., Hodgson, F., Armas, M. D., Santiago, C. T., Lorenzo, C. D., Prendes, C. and Plata, P. (1990). A fungus disease of canary palm. (Phaenixcanariensischab.) *produced by Graphiolaphaenicis (Mong)Poit. Fisher in the Canary Islands.* Phytoma Espana, 18:21-25.

Chanakan, A., Sarocha, C., Jongjit, H. and Joseph, K. (2009). Material properties of pretreated coir-based green composites. *Composite part B: Engineering* 40.7: 633-637.
characterisation of low cost polymer composites from coconut coir. *American Journal Materials Science* 5.3c:62-68.

Chemocart. Application of CNSL. Retrieved Jul. 31, 2020 from

Chen, T.S., Sinin, H. and Mohd, S.O. B . (2016). Properties of sago particleboards resonated with UF and PF resin. *Advances in Materials Science and Engineering.* Vol. 2016, Article ID 5323890, 12 pages.

Chiang, T.C., Hamdan, S. and Osman, M. (2016). Properties of sago particleboards resonated with urea formaldehyde and phenol formaldehyde resin. *Advances in Materials Science and Engineering,* 11:1-12.

Chitra, R., Thendral, S., Arunya, A. and Mohan, S.J. (2019). Experimental study on strength of concrete by partial replacement of fine aggregate with saw dust. *International Journal of Civil Engineering and Technology* 10.3: 535-538.

Chow, P. (1975). Dry formed composite board from selected agricultural fibre residues. Food and Agriculture Organization of the United Nations (FAO); *World Consultation on Wood Based Panels.* India. 8p.

Clemons, C.M. (2002). Wood-plastic composites in the United States: the interfacing of two industries. *Forest Product Journal* 52: 10-18..
Composite Materials 46:2879-2890.

Dahmardeh, M., Nazerian, M. and Bayatkashkoli, A. (2013). Experimental from bagasse and industrial wood particles. *International Journal of Agriculture and Crop Sciences*,5.15:1626-1631.

Das, A.R., Radhakrishnan, S., Sumy, S., Abesh, R., Geena, M.G., Divya, P., Sinjula, C.S. and Satheeshkumar, R. (2016). Coir pith: wealth from waste. India International Coir Fair (IICF) at CODISSIA 15-18th July 2016, Coir board 4th ed. Coimbatore.

Das, G. and Biswas, S. (2016). Physical, mechanical and water absorption behaviour of coir fibre reinforced epoxy composite filled with Al_2O_3. particulates. *IOP Conference Series: Materials Science and Engineering*, 115:1.012012.

Das, P. and Ganesh, A. (2003). Bio-oil from pyrolysis of cashew nut shell a near fuel. *Biomas and Bioenergy*, 25:113-117

Das, P., Sreelatha, T. and Ganesh, A. (2004). Bio oil from pyrolysis of cashew nut shell characterization and related properties. Biomas and Bioenergy, 27.3:265-275

Debesh, M., Bohuslav, V.K. and John, N. (1992). Performance of surface modified nutshell flour in HDPE composites. *International Journal of Polymeric Materials and polymeric biomaterials* 17.1-2:1-16.

Donald M., Ku, H., Cardona, F. and Trada M. (2012). Flexural properties of sawdust reinforced epoxy composites post cured in microwaves. *Journal of*

Eco-care Education. (2005). Building material: composition of ordinary Portland cement. Retrieved Jul. 29, 2020 from

English, B. (1994). Waste into wood: composites are promising new resources. *National Institute of Environmental Health Sciences,* 102.2:168-170

English, B., Chow, P. and Bajwa, D. (1997). Processing into composites. *In: paper and composites from Agro-Based Resources*, Roger M Rowell et'al, eds. CRC Press, Inc. Lewis Publishers. Chapter 8, 269-300.

English, B., John, A. Y. and Andrej M. K. (1994). Lignocellulosic composites, In: cellulose polymers, blends and composites New York. Eds. Hanse Publishers. Chapter 6:115-130.
environmental credentials and market forces. *Journal of the Science of Food and Agriculture* 86:1781–1789.

EPA. (2002). Environmental Protection Agency. U.S. EPA, Toxicity and exposure assessment for children's health. Formaldehyde: TEACH Summary. http://www.epa.gov/teach/.

European Standard Specification for particleboards. (2010). EN 312:2010

Fan, M., Ndikontar, M.K., Zhou, X. and Ngamveng, J.N., (2012). Cement-bonded composites made from tropical woods: Compatibility of wood and cement. *Construction and Building Materials*, *36*, pp.135-140.

FAO. (1994). Nigerian wood products data bases

FAO. (2001). Azam-Ali, S.H and Judge, E.C. Small scale cashew nut processing. (ITDG), *Schumacher Centre for Technology and Development*, Bourton on Dunsmore, Rugby, Warwickshire, UK. Retrieved on 15/02/2011.

Flaws, L.J. and Palmer, E.R. (1968). Production of particle board from cassava stalk. *Tropical Products Institute (TPI) Report* 34:1-3.

Fowler, P., Hughes, M. and Elias, R.M. (2006). Biocomposites: technology,

George, M.F. (1982). Freezing avoidance by undercooling of tissue water in

Ghalehno, M.O. Nazerian, M. and Bayatkashkoli, A. (2013). Experiment particle board from bagasse and industrial wood particles. *International Journal of Agriculture and Crop Sciences* 5.1: 1626-1631.

Gordon, F.D.S. (2002). Coconut coir fibre as an eco-friendly renewable resource for soil and water conservation. *12th ISCO Conference*, Beijing.

Green Report. (2002). Particleboard and medium –density fibreboard. Retrieved on 25th Feb. 2010 from.

Green Report. (2001). Particleboard and medium-density fibreboard. Retrieved on 23rd Oct. 2015.

Gregor, V. (2003). Glass concrete thin sheets reinforced with prestressed aramid fabrics. PhD. Thesis. Dept. of Arts and Sciences, University of Columbia.

Hall, A.S., Holowenko, A.E. and Laughlin, H.G. (2002). Sachaum's outline series theory and problems of machine design. 4th edition New York; McGraw-Hill companies Inc. pp 223-267.

Heckadka, S., Nayok, S., Gouthaman, P., Talwar, A., Ravishankar, V., Thomas, L. and Mathur, A.(2018). Influence of sawdust bio-filler on the tensile, flexural and impact properties of Mangifera Indica leaf stalk fibre reinforced polyester composites. *Matec Web of Conference,* 144.3:02024.

(http://www.adarshsanoor.com/adarshindustrialchemicals/products/cashew   nut-shell-liquid)

(http://www.cargohandbook.com/index.php/Coconut(coir)fibre)

(http://www.chemocart.com>msds>CNSL)

(http://www.ecocareeducation.com/building-material.html)

(http://www.epa.gov/safewater/pdfs/factsheets/ioc/nitrates)

(http://www.infohouse.p2ric.org/ref/17/16555)

(http://www.isse.utk.edu/ccp/pubs/pdfs/CGR-PB+MDF)

Hofstrand, A. D., Moslemi, A.A. and Garcia, J.F. (2012). Curing characteristics of wood particles from nine northern rocky mountains species mixed with Portland cement. *Agris Journal*, 34:57-61.

ICFRE. (1995). Forestry Statistics, India. Indian Council of Forestry Research and Education, *New Forest*, Pp.200.

Ikhuoria, E.U. and Aigbodion, A.L. (2006). Determination of solution of viscosity characterization of rubber seed oil based alkyd resins. *Journal of Applied. Polymer. Science* 101. 5.

Indian Standard Specification for high density wood particleboards. (1966). IS: 3478.

Indian Standard Specification of cashew nut shell liquid. (1964). IS: 840.
Journal of Applied Polymer Science 85.1:129-138.

Kenyan Standard on fibre board specification. (2017). KS 2706-2.

Kenyan Standard on fibreboards specification part 2. (2016). Requirements for dry process boards (MDF) DKS 2706-2.

Khan, B. (2007). Uses of coir fibre, its products and implementation of geo-coir in

Khedari, J., Suttisonk, B., Pratinthong, N. and Hirunlabh. (2001). New lightweight composite construction materials with low thermal conductivity, cement and concrete composites.23:65-70.

Khurmi, R. S. and Gupta, J. K. (2005). A textbook of machine design. 14th Edition, Eurasia Publishing House (PVT) Ltd, Ram Nagar, New Delhi.

Kjeldahl, J. (1883). Neve methode zur bestimmung des stickstoffs in organischen Körpern [New method for the determination of nitrogen in organic substances.] *Scientific Research Journal,* 22:366-383.

Ku, H., Donald, M., Cardona, F. and Trada, M. (2012). Flexural properties of sawdust reinforced epoxy composites post-cured in microwaves. *Journal of Composite Materials,* 46:2879-2890.

Kyei, S. K., Eke, W. I., Darko, G., and Akaranta, O. (2022). Natural polyhydroxy resins in surface coatings: a review. *Journal of Coatings Technology and Research*, *19*(3), 775-794.

Li, C., Wu, M., Chen, Q., and Jiang, Z. (2018). Chemical and mineralogical alterations of concrete subjected to chemical attacks in complex underground tunnel environments during 20–36 years. *Cement and Concrete Composites*, *86*, 139-159.

Lin, C., Hiziroglu, S., Kan, S.M. and Lai, H.W. (2008). Manufacturing particleboard panels from betel palm (Areca catechu Linn). *Journal of Materials Processing Technology*, 197:445-448.

Lubi, M. C., and Thachil, E. T. (2000). Cashew nut shell liquid (CNSL)-a versatile monomer for polymer synthesis. *Designed Monomers and polymers*, *3*(2), 123-153.

Luci, C.M. and Thachil, E.T. (2007). Particleboard from cashew nut shell liquid. *Polymer Plastics Technology and Engineering* 46.1: 393- 400.

Lucidchart. Retrieved March15, 2023from http:// www.lucidchart.com.

Maloney, T.M. (1993). Modern particleboard and dry-process fibreboard manufacturing. San Francisco, CA: Miller Freeman Publishing, Inc. 681p.

Maraghi, M.M.R., Tabei, A. and Madanipoor, M. (2018). Effect of board density, resin percentage and pressing temperature on particleboard properties made from mixing of poplar wood slab, citrus branches and twigs of beech. *Wood research,* 63.4:669-682.

Maria, A.R.F. (2009). Sintese aplicabilidabe de antioxidantes derivados do cardanol hidrogenado, PhD.Thesis. Dept. of Organic and Inorganic Chemical, Federal University of Ceara, Brazil.

Maria, A.R.F., Selma, E.M., Jose, O.B.C. and Glaucione, G.B. (2007). Evaluation of antioxidant properties of a phosphorated cardanol compound on mineral oil (NH10 and NH20) fuel. 86:2416-21.

Maria, A.S.R., Franscisco, A.M.S. and Selma, E.M. (2009). Study of antioxidant properties of 5-n-pentadecyl-2-tert-amylphenol. Energy Fuel, DOI: 10.1021/ef800994j.In Press.

Maria, L.S. and Gouvan, C.M. (1999). Utilization of cashew nut shell liquid from anacardium occidentale as starting material for organic synthesis: A novel route to lasiodiplodin from cardols. *Journal of Brazilian Chemical Society* 10.1:13-20.

Martin, H.B.S., Edwin, R.P.K., Martien, J.A. and Jan, E.G. (2005). Coir based building and packaging materials. Final report of project CFC/FIGHF/11, CFC. Technical Paper Nr. 43

Matoke, G.M., Owido, S.F. and Nyaanga D.M. (2012). Effect of production methods and material ratios on physical properties of the composites. *American International Journal of contemporary research*, 2:2.1-3.

Mehta,P.K. and Monteiro, P.J.M. (1993). Concrete: structure, properties and materials. 2nd ed. Prentice Hall, New Jersey.

Menon, A.R.R., Aigbodion, A.I., Pilla,i C.K.S., Mathew, N.M. and Bhagawan, S.S. (2002). Process ability characteristics and physico-mechanical properties of natural rubber modified with cashew nut shell liquid and cashew nut shell liquid formaldehyde resin. *European Polymer Journal* 38.1:163-168.

Xing, Y. (2016). Global value chains and China's exports to high-income countries. *International Economic Journal*, 30(2), 191-203.

Millrath, K. (2002). Modifying concrete matrices with beneficiated dredged material or other clayed constituents. PhD. Dissertation at Columbia University, New York. Mindess, Young and Darwin. 2003. Concrete. 2nd ed. Prentice Hall, New Jersey.

Milon, F.G., Michae1, R.B. and Michael, J.B. (1982). Freezing avoidance by deep undercooling of tissue water in winter-hardy plant. *Crobiology* 19.6: 628-639.

Mindess, S., Young, J.F., and Darwin, D. (2003). Concrete. 2nd Edition, Prentice-Hall Inc., Englewood Chiffs, New Jersey.

Mitsuhiro, S., Kei-Ichiro, T., Koichi, O., Ryutoku, Y. and Hiroyuku, T. (2002). Biodegradable polyester composites reinforced with short abaca fibre.

Mohammed, M.R.M., Asghar, T. and Mostafa, D. (2018). Effect of board density, resin percentage and pressing temperature on particleboard properties made from mixing of poplar wood slab, citrus branches and twigs of beeches. *Wood Research* 63. 4: 669-682.

Moslemi, A.A. and Lim, Y.T. (1984). Compatibility of southern hardwoods with Portland cement. *Forest Products Journal* 34.7/8: 22-26.

Moslewicki, M., Borrajo, J. and Aranguren, M.I. (2005). Mechanical properties of woodflour/linseed oil resin composites. *Polymer International* 54. 5: 829-836.

Mwaikambo, L.Y. and Ansell, M.P. (2003). Hemp fibre reinforced cashew nut shell liquid composites. *Composites Science and Technology* 63.9: 1297-1305.

Nagaraja, G. and Basavaiah, C. (2010). Uses of coir fibre, its products and utilization of geo-coir in India. *International Journal of Commerce and Business Management* 3.2: 274-278.

Narayanamurti, D. and Singh, J. (1953). Studies of building boards: utilization of tapioca stems and hoop pine bark. *Composite Wood.*1.1: 10-17.

Narayanan, N. (2004). Development and characterization of acoustically efficient cementitous materials. PhD. Thesis. Dept. of Civil Engineering, Purdue University, India. 224-235.

Nayak, M., and Paled, M. (2018). Trends in area, production, yield and export-import of cashew in India-an economic analysis. *Journal homepage: http://www. ijcmas. com*, 7(12), 2018.

Nemli, G. and Kalaycioglu, H. (2001). Suitability of date palm (Phoenix dactylifera) branches for particleboard production. Holz als Roh-und Werkstoff 59:411-412

Odozi, T.O., Onu, C.O. and Nweke, A. (1986). Corn cob adsorbent for removing crude oil from water surface. *Journal of Nigerian Society of Chemical Engineers* l.5.1:25-28.

Olorunnisola, A., Pitman, A. and Mansfield-William, H. (2005). Strength properties and potential uses of rattan-cement composites. *Journal of bamboo and rattan* 4: 343-352.

Omoniyi, T.E. (2009). Development and evaluation of bagasse-reinforced cement composite roofing sheets. PhD. Thesis. Dept. of Agricultural and Environmental Engineering. University of Ibadan.

Ortiz, J. D., Khedmatgozar Dolati, S. S., Malla, P., Nanni, A., and Mehrabi, A. (2023). FRP-Reinforced/Strengthened Concrete: State-of-the-Art Review on Durability and Mechanical Effects. *Materials*, *16*(5), 1990.

Oyagade, A. O. (1988). Thickness swelling and water absorption of cement – bonded particle-board as influenced by three process variables. *Journal of Forestry* 18.1 and 2: 20 -27.

Oyagade, A. O.(1990). Effect of cement/wood ratio on the relationship between cement-bonded particleboard density and bending properties. *Journal of Tropical Forest Science* 2.2: 211-219.

Pandey, S.N. and Mehta, A.K. (1980). Particle boards from cotton plant stalks. *Research and industry* 25: 67-70.

Pandey, S.N., Mehta, S.A.K. and Tamhankar, S.H.V. (1979). Particle boards from cotton plant stalks. Assignee: *Indoor Council of Agricultural Research,*. Patent, P.N: IN 145866, ID: 790113

Papadopoulos, A. (2007). Natural durability in ground stake test of propionylated particleboards. *Holz Roh- Werkst* 65.2:171-172.

Paturau, J.M. (1988). Alternative uses of sugarcane and its by products in agro industries. *.FAO Animal Production and Health Paper.*

Philqsqphy, D. U. (2007). *Novel Applications of CAS* (Doctoral dissertation, Cochin University).

Pillai, S,M., Sudhakaran, M. and Fernandez, C . (2000). Coir-An effective component for consolidation. *Proceedings Geosynthetics.* Asia 2000-GA 2000 Kuala Lumpur, 20-31st May, 2000, 2:207-212.

Pillai, S.M., Sudhakaran, M. and Vasudev, R. (2001). Applications of coir in agricultural textiles. *Proceeding International Seminar on technical textiles,* Mumbai, India 2-3rd June, 2001.

Pravin, V.D. and Viveka, D.M. (2015). Natural fibre reinforced building materials. *IOSR Journal of Mechanical and Civil Engineering,* 12.3II:104-107.

Radhakrishnan, S., Anita, D.R., Abesh, R., and Geena, M.G. (2018). An apposite medium for cultivation of vegetable/medicinal/ornamental plant. Cord 34.1.

Rahman, K.S., Islam, N., Rahman, M., Hannan, O., Dungan, R. and Abdul, K. H.P.S. (2013). Flat-pressed wood plastic composites and from saw dust and recycle polyethylene terephthalate (PET): physical and mechanical properties. *SpringerPlus* 2: 629.

Rajan, A., Senan, R.C., Pavithran, C. and Abraham, T.E. (2005). Bio softening of coir fibre using selected microorganisms. *Bioprocess and Biosystems Engineering 28.3:*165-173.

Ranganna, S. (1986). Handbook of analysis and quality control for fruit and vegetable products. 2nd ed, Published Tata Mc Grow-Hill,New Delhi, India.

Rao, K.V., Gupta, N.S. and Kumar, D.S. (2016). Mechanical properties of sisal/coir fibre reinforced hybrid composites fabricated by cold pressing method. *IOP Conference Series: Materials Science and Engineering,* 149.1:012092.

Ravikantha, P., Abishek, K.A. and Dhyanchandra. (2015). Development and Retrieved on 20/04/2010.

Rixom, M.R. and Mailvaganam, N.P. (1999). Chemical admixtures for concrete. 3rd. ed. E & SPON 4Brown, R. 1992. Honduran cashew fruit drying: *Report to Fine Dried Foods.*

Rowell, R.M. (1997).Opportunities for composites from agro-based resources. *Paper and Composites from A gro-Based Resources.* R.M. Rowell, R.A. Young, J.K. Rowel ed. Chapter 12: 377-402.

Satender, K., Kakali, D. and Suresh, P. (2016). Mechanical properties of coconut fibre reinforced epoxy polymer composites. .*International Research Journal of Engineering and Technology* 03.7

Sharma, P., Gaur, V. K., Sirohi, R., Larroche, C., Kim, S. H., and Pandey, A. (2020). Valorization of cashew nut processing residues for industrial applications. *Industrial Crops and Products*, *152*, 112550.

Shibata, M., Takachiyo, K., Ozawa, K., Yosomiya, R. and Takeishi, H. (2002). Biodegradable polyester composites reinforced with short abaca fibre. *Journal of Applied Polymer Sciences,* 85:129-138.

Shukla, K.S. and Prasad, J. (1985). Building boards from bagasse: Part I. PF bonded particleboards. *Journal of the Timber Development Association of India.* 3.4:: 20-27.

Siakeng, R., Jawaid, M., Ariffin, H. and Sapuan, S. (2018). Physical properties of coir and pineapple leaf fibre reinforced polylactic acid hybrid composites. 10P conference series : Materials Science and Engineering, volume 290.

Simatupang, M.H. (1979). The water requirement of manufacture cement-bonded wood particleboard. Holz Roh- Werkstoff 37:379-382.

Smith, W. B., Vissage, J. S., Darr, D. R. and Sheffield, R. M. (2002). Forest Resources of the United States, 1997, General Technical Report NC-219.St. Paul, MN, U.S. Forest Service North Central Research Station.

Soukatchoff, P. (2000). Major improvements in long-term strength and toughness of glass-fibre reinforced concrete. *High-Performance fibre-Reinforced concrete Thin Sheet Products,* ACI SP-190:165-182.

Srinivas, S.H., Suhas, Y.N., Gouthainan, P.V., Abhishek, T., Ravishankar, V.A., Linto, G.T. and Ankur, M. (2018). Influence of sawdust bio-filler on the tensile, flexural and impact properties of mangifera indica leaf stalk fibre reinforced polyester composites. Matec web conferences, volume, 144.

Sudhakaran, P.M. and Vasudev, R. (2001). Applications of coir in agricultural textiles *International seminar on technical textiles.Mumbai, India, 2-3 June 2001*.

Taylor, H.F.W. (1997). Cement chemistry. 2nd ed. Thomas Telford.

Thomas, J.O. (2015). Study on the feasibility of using saw dust as partial replacement for sand in concrete. Journal of University of Nairobi.

Thomas, M. M. (1993). Modern particleboard and dry-process fibreboard manufacturing. *APA* 6th ed. San Francisco Miller Freeman Publications.

Tola, J., and Mazengia, Y. (2019). Cashew production benefits and opportunities in Ethiopia: a review. *Journal of Agricultural and Crop Research*, *7*(2), 18-25.

Tropical Products Institute, 7p.

Tropical Products Institute. (1963). Examination of a sample of bagasse from the West Indies for particle board production. Rep. 14/63.London, England

U.S. Environmental Protection Agency. (2009). Consumer factsheet on nitrates/nitrites. Retrieved on 25th Nov. 2010 from

Voirin, C., Caillol, S., Sadavarte, N. V., Tawade, B. V., Boutevin, B., and Wadgaonkar, P. P. (2014). Functionalization of cardanol: towards biobased polymers and additives. *Polymer Chemistry*, *5*(9), 3142-3162.

Waldie, J.M. (1983). Oil and Colour Chemists' Association of Australia. Surface Coatings, Vol.1: Raw Materials and Their Uses, Chapman and Hall, London, UK, 1: 1.

Wilson, E., and Philip, N. (2015). The Influence of Fibres in Concrete: A Review. *International Journal of Civil Engineering (IJCE)*, *4*(6), 1-10.

Wimalsiri, P., Sinnatamby, A., Samaranayake, S. and Samarasinghe, C.R. (1971). Cashew apple wine. *Industry Prospect Report*, 44, 15-19.

Woodroof, J.G. (1970). Coconut production and processing products .The AVI publishsing company, Inc. 1970: 241.

Yi, Z., Zhongli, P., Ruihong, Z., Bryan, M.J. and Sherry, B. (2006). Properties of medium density particleboard from saline athel wood. *Industrial Crops and Products*, 23.3: 318-326.

Zakia, H., Taha, A., Mervat, K., Bahnasawy, A.H., Samir, A.A., Jutta, H. and Azra, K. (2019). Rice straw and flax fibre particleboards as a product of agricultural waste: An evaluation of technical properties. *Journal of Applied Science* 9:3878.1-20.

Zheng, Y., Pan, Z., Zhang, R., Jenkins, B.J. and Blunk, S. (2006). Properties of medium density particleboard from saline athel wood. *Industrial Crops and Products* 23:318-326.

CALCULATION FOR RESULT OF COIR FIBRE CEMENT COMPOSITE BOARD
ON WATER ABSORPTION TEST PRESENTED IN TABLE 4.1

Coir fibre water absorption test results

Sample	Size (mm)	Constant Mass (g)m1	Mass (g) (24hrs)m2	Water Absorption (%)	Average Water Absorption (%)
5% Fibre	100*100*8	118.8	157.8	32.83	
5% Fibre	100*100*8	118	157.3	33.31	33.14
5% Fibre	100*100*8	118.1	157.4	33.28	
7.5%Fibre	100*100*8	104.3	149	42.86	
7.5%Fibre	100*100*8	103.9	148.8	43.21	43.08
7.5%Fibre	100*100*8	103.8	148.6	43.16	
10% Fibre	100*100*8	91.1	139.5	53.13	
10% Fibre	100*100*8	91.4	139.3	52.41	52.79
10% Fibre	100*100*8	91.4	139.7	52.84	
15% Fibre	100*100*8	75.9	128.9	69.83	
15% Fibre	100*100*8	76.2	129.1	69.42	69.46
15% Fibre	100*100*8	76.8	129.9	69.14	

CALCULATION FOR RESULT OF COIR FIBRE CEMENT COMPOSITE BOARD ON THICKNESS SWELLING TEST PRESENTED IN TABLE 4.1

Coir fibre thickness swelling test results for 2 hours

Sample	Size (mm)	Constant Thickness (mm)	Thickness (mm 2hrs)	Thickness Swelling (%)	Average Thickness Swelling (%)
5% Fibre	100*100*8	8.9	8.95	0.56	
5% Fibre	100*100*8	8.92	8.99	0.78	0.67
5% Fibre	100*100*8	8.94	9	0.67	
7.5%Fibre	100*100*8	9	9.1	1.11	
7.5%Fibre	100*100*8	8.96	9.07	1.23	1.11
7.5%Fibre	100*100*8	9.07	9.16	0.99	
10% Fibre	100*100*8	9.06	9.2	1.55	
10% Fibre	100*100*8	8.99	9.16	1.89	1.44
10% Fibre	100*100*8	9.1	9.18	0.88	
15% Fibre	100*100*8	9.28	9.43	1.62	
15% Fibre	100*100*8	9.33	9.48	1.61	1.61
15% Fibre	100*100*8	9.29	9.44	1.61	

CALCULATION FOR RESULT OF COIR FIBRE CEMENT COMPOSITE BOARD
ON THICKNESS SWELLING TEST PRESENTED IN TABLE 4.1.

Coir fibre thickness swelling test results for 24 hours

Sample	Size (mm)	Constant Thickness (mm)	Thickness (mm)(24hrs)	Thickness Swelling (%)	Ave. Thickness Swelling (%)
5% Fibre	100*100*8	8.9	8.98	0.9	
5% Fibre	100*100*8	8.92	9.03	1.23	1.12
5% Fibre	100*100*8	8.94	9.05	1.23	
7.5%Fibre	100*100*8	9	9.19	2.11	
7.5%Fibre	100*100*8	8.96	9.15	2.12	1.89
7.5%Fibre	100*100*8	9.07	9.2	1.43	
10% Fibre	100*100*8	9.06	9.27	2.32	
10% Fibre	100*100*8	8.99	9.25	2.89	2.54
10% Fibre	100*100*8	9.1	9.32	2.42	
15% Fibre	100*100*8	9.28	9.56	3.02	
15% Fibre	100*100*8	9.33	9.66	3.54	3.23
15% Fibre	100*100*8	9.29	9.58	3.12	

CALCULATION FOR RESULT OF COIR FIBRE CEMENT COMPOSITE BOARD ON DENSITY TEST PRESENTED IN TABLE 4.1.

Coir fibre density test results

Sample	Size (mm)	Mass (g)	Thickness (mm)	Length (mm)	Width (mm)	Volu (mm3)	Density (g/mm3)	Ave. Density (g/mm3)
5% Fibre	100*100*8	157.8	8.98	101.83	101.5	92814.99	0.0017	0.00169
5% Fibre	100*100*8	157.3	9.03	101.86	101.53	93386.87	0.00168	0.00169
5% Fibre	100*100*8	157.4	9.05	101.85	101.49	93.547.65	0.00168	0.00168
7.5%Fibre	100*100*8	149	9.19	101.04	101.33	94090.74	0.00158	0.00158
7.5%Fibre	100*100*8	148.8	9.15	101.07	101.35	93727.52	0.00159	0.00158
7.5%Fibre	100*100*8	148.6	9.2	101.06	101.36	94239.66	0.00158	0.00158
10% Fibre	100*100*8	139.5	9.27	102.87	102.25	97506.1	0.00143	0.00143
10% Fibre	100*100*8	139.3	9.25	102.9	102.27	97343.14	0.00143	0.00143
10% Fibre	100*100*8	139.7	9.32	102.89	102.25	98051.08	0.00142	0.00142
15% Fibre	100*100*8	128.9	9.56	100.55	99.5	95855	0.00135	0.00135
15% Fibre	100*100*8	129.1	9.66	100.58	99.53	96703.63	0.00134	0.00135
15% Fibre	100*100*8	129.9	9.58	100.54	99.52	95855	0.00136	0.00136

CALCULATION FOR RESULT OF COIR FIBRE CEMENT COMPOSITE BOARD
ON FLEXURAL STRENGTH TEST PRESENTED IN TABLE 4.1

Coir fibre flexural strength test results

Sample	Size (mm)	Force(KN)	Peak (mm)	Displacement (mm)	Flexural Strength (mm)	Average Flexural Strength(mm)
5%Fibre	100*100*100	23.43	32.17	13.31	6.04	
5%Fibre	100*100*100	23.31	32.10	13.25	6.06	6.09
5%Fibre	100*100*100	23.64	32.54	13.16	6.18	
7.5%Fibre	100*100*100	18.28	26.75	9.91	6.75	
s7.5%Fibre	100*100*100	18.33	26.78	9.75	6.87	6.86
7.5%Fibre	100*100*100	18.41	26.90	9.68	6.95	
10% Fibre	100*100*100	13.79	18.47	6.07	7.67	
10% Fibre	100*100*100	13.71	18.40	6.13	7.50	7.61
10% Fibre	100*100*100	13.88	18.54	6.01	7.71	
15% Fibre	100*100*100	14.71	20.80	10.00	5.20	
15% Fibre	100*100*100	14.82	20.93	9.78	5.35	5.35
15% Fibre	100*100*100	14.97	21.24	9.65	5.50	

CALCULATION FOR RESULT OF COIR FIBRE CEMENT COMPOSITE BOARD
ON COMPRESSIVE STRENGTH TEST PRESENTED IN TABLE 4.1

Coir fibre compressive strength test results

Sample	size(mm)	Force (kN)	Peak(KN)	Compressive Strength(mpa)	average compressive strength(mpa)
5%Fibre	100*100*100	85.42	114.01	11.4	
5%Fibre	100*100*100	85.71	114.32	11.43	11.43
5%Fibre	100*100*100	85.99	114.63	11.46	
7.5%Fibre	100*100*100	64.58	86.7	8.67	
7.5%Fibre	100*100*100	65.02	87.35	8.74	8.7
7.5%Fibre	100*100*100	64.69	86.86	8.69	
10% Fibre	100*100*100	62.67	84.19	8.42	
10% Fibre	100*100*100	62.71	84.25	8.43	8.44
10% Fibre	100*100*100	63.01	84.73	8.47	
15% Fibre	100*100*100	41.86	57.08	5.71	
15% Fibre	100*100*100	4236	57.47	5.75	5.72
15% Fibre	100*100*100	41.8	56.99	5.7	

CALCULATION FOR RESULT OF COIR FIBRE CEMENT COMPOSITE BOARD
ON MODULUS OF ELASTICITY TEST PRESENTED IN TABLE 4.1

Coir fibre modulus of elasticity test results

Sample	Size (mm)	Displacement (mm)Δ	P (N)	PL3	4BD3Δ	MOE (mpa)	Average MOE (mpa)
5% Fibre	195*50*10	2.48	84	622849500	496000	1255.74	
5% Fibre	195*50*10	2.5	80	593190000	500000	1186.38	1078.49
5% Fibre	195*50*10	2.65	70	519041250	530000	979.32	
5% Fibre	195*50*10	2.7	65	481966875	540000	892.53	
7.5%Fibre	195*50*10	2.47	88	652509000	494000	1320.87	
7.5%Fibre	195*50*10	2.49	86	637679250	498000	1320.48	1306.25
7.5%Fibre	195*50*10	2.43	90	667338750	486000	1373.13	
7.5%Fibre	195*50*10	2.52	85	630264375	504000	1250.52	
10% Fibre	195*50*10	2.37	92	682168500	474000	1439.17	
10% Fibre	195*50*10	2.34	90	667338750	468000	1425.94	1428.85
10% Fibre	195*50*10	2.39	95	704413125	478000	1473.67	
10% Fibre	195*50*10	2.37	88	652509000	474000	1376.6	
15% Fibre	195*50*10	3.58	82	608019750	716000	849.19	
15% Fibre	195*50*10	3.63	72	533871000	726000	735.36	813.24
15% Fibre	195*50*10	3.61	80	593190000	722000	821.59	
15% Fibre	195*50*10	3.59	82	608019750	718000	846.82	

CALCULATION FOR RESULT OF COIR FIBRE CEMENT COMPOSITE BOARD ON MODULUS OF RUPTURE TEST PRESENTED IN TABLE 4.1

Coir fibre modulus of rupture test results

Sample	Size (mm)	P (N)	3PL	2BD2	MOR (mpa)	Average MOR (mpa)
5% Fibre	195*50*10	84	49140	10000	4.91	
5% Fibre	195*50*10	80	46800	10000	4.68	4.37
5% Fibre	195*50*10	70	40750	10000	4.1	
5% Fibre	195*50*10	65	38025	10000	3.8	
7.5%Fibre	195*50*10	88	51480	10000	5.15	
7.5 Fibre	195*50*10	86	50310	10000	5.03	5.11
7.5 Fibre	195*50*10	90	52650	10000	5.27	
7.5 Fibre	195*50*10	85	49725	10000	4.97	
10% Fibre	195*50*10	92	53820	10000	5.38	
10% Fibre	195*50*10	90	52650	10000	5.27	5.34
10% Fibre	195*50*10	95	55575	10000	5.56	
10% Fibre	195*50*10	88	51480	10000	5.15	
15% Fibre	195*50*10	82	47970	10000	4.8	
15% Fibre	195*50*10	72	42120	10000	4.21	4.62
15% Fibre	195*50*10	80	46800	10000	4.68	
15% Fibre	195*50*10	82	47970	10000	4.8	

CALCULATION FOR RESULT OF COIR FIBRE CEMENT COMPOSITE BOARD
ON MODULUS OF RUPTURE TEST PRESENTED IN TABLE 4.1

Coir fibre impact strength test results

Sample	D (inch)	D (mm)	WD (f*d)	Surface Area (mm)	Impact (N/mm2)	Average Impact (N/mm2)
5% Fibre	0.663	16.85	589.75	500	1.18	
5% Fibre	0.669	17	595	500	1.19	1.19
5% Fibre	0.675	17.15	600.25	500	1.2	
7.5%Fibre	0.808	20.53	718.55	500	1.44	
7.5%Fibre	0.8	20.33	711.55	500	1.42	1.43
7.5%Fibre	0.804	20.43	715.05	500	1.43	
10% Fibre	2.452	62.28	2179.8	500	4.36	
10% Fibre	2.445	62.1	2173.5	500	4.35	4.35
10% Fibre	2.441	62	2170	500	4.34	
15% Fibre	2.138	54.3	1900.5	500	3.8	
15% Fibre	2.142	54.4	1904.5	500	3.81	3.81
15% Fibre	2.149	54.59	1910.65	500	3.82	

APPENDIX A 2

CALCULATION FOR RESULT OF COIR DUST CEMENT COMPOSITE BOARD
ON WATER ABSORPTION TEST PRESENTED IN TABLE 4.2

Coir Dust water absorption test results

Sample	Size (mm)	Constant Mass (g) m1	Mass (g) (24hrs)m2	Water Absorption (%)	Average Water Absorption (%)
5% Dust	100*100*8	114.3	146	27.73	
5% Dust	100*100*8	115	146.4	27.3	27.57
5% Dust	100*100*8	114.5	146.2	27.69	
7.5%Dust	100*100*8	102.2	145.1	41.98	
7.5%Dust	100*100*8	102	144.9	42.06	41.7
7.5%Dust	100*100*8	103	145.3	41.07	
10% Dust	100*100*8	80.1	130.3	62.67	
10% Dust	100*100*8	80.3	130.6	62.64	6259
10% Dust	100*100*8	80.8	131.26	62.45	
15% Dust	100*100*8	63.8	107.9	69.12	
15% Dust	100*100*8	64.2	108.4	68.85	69.06
15% Dust	100*100*8	64	108.3	69.22	

CALCULATION FOR RESULT OF COIR DUST CEMENT COMPOSITE BOARD
ON THICKNESS SWELLING TEST PRESENTED IN TABLE 4.2

Coir dust thickness swelling test results for 2 hours

Sample	Size (mm)	Constant Thickness (mm)	Thickness (mm)(2hrs)	Thickness Swelling (%)	Average Thickness Swelling (%)
5% Dust	100*100*8	9.43	9.58	1.59	
5% Dust	100*100*8	9.5	9.6	1.05	1.37
5% Dust	100*100*8	9.51	9.65	1.47	
7.5%Dust	100*100*8	9.66	9.85	1.97	
7.5%Dust	100*100*8	9.62	9.81	1.98	2.07
7.5%Dust	100*100*8	9.7	9.92	2.27	
10% Dust	100*100*8	10.03	10.28	2.49	
10% Dust	100*100*8	9.99	10.26	2.7	2.6
10% Dust	100*100*8	10.01	10.27	2.6	
15% Dust	100*100*8	9.84	10.22	3.86	
15% Dust	100*100*8	9.74	10.1	3.7	3.68
15% Dust	100*100*8	9.79	10.13	3.47	

CALCULATION FOR RESULT OF COIR DUST CEMENT COMPOSITE BOARD
ON THICKNESS SWELLING TEST PRESENTED IN TABLE 4.2

Coir dust thickness swelling test results for 24 hours

Sample	Size (mm)	Constant Thickness (mm)	Thickness (mm)(24hrs)	Thickness Swelling (%)	Average Thickness Swelling(%)
5% Dust	100*100*8	9.43	9.62	2.01	
5% Dust	100*100*8	9.5	9.65	1.58	1.9
5% Dust	100*100*8	9.51	9.71	2.1	
7.5%Dust	100*100*8	9.66	9.94	2.9	
7.5%Dust	100*100*8	9.62	9.92	3.12	3
7.5%Dust	100*100*8	9.7	9.99	2.99	
10% Dust	100*100*8	10.03	10.43	3.99	
10% Dust	100*100*8	9.99	10.4	4.1	4
10% Dust	100*100*8	10.01	10.4	3.9	
15% Dust	100*100*8	9.84	10.4	5.69	
15% Dust	100*100*8	9.74	10.22	4.93	5.11
15% Dust	100*100*8	9.79	10.25	4.7	

CALCULATION FOR RESULT OF COIR DUST CEMENT COMPOSITE BOARD
ON DENSITY TEST PRESENTED IN TABLE 4.2

Coir dust density test results

Sample	Size (mm)	Mass (g)	Thickness (mm)	Length (mm)	Width (mm)	Volume (L*B*H)	Density Mass/Volume)	Ave. Density (g/mm³)
5% Dust	100*100*8	146	9.62	100.13	101.88	98135.97	0.00149	
5% Dust	100*100*8	146.4	9.65	100.15	101.92	98500.33	0.00149	0.00149
5% Dust	100*100*8	146.2	9.71	100.16	101.89	99093.49	0.00148	
7.5%Dust	100*100*8	145.1	9.94	101.6	100	100990.4	0.00144	
7.5%Dust	0*8	144.9	9.92	101.65	99.98	100816.63	0.00144	0.00144
7.5%Dust	100*100*8	145.3	9.99	101.63	100.04	101568.98	0.00143	
10% Dust	100*100*8	130.3	10.43	101.84	100.99	107270.69	0.00121	
10% Dust	100*100*8	130.6	10.4	101.83	101.04	107004.59	0.00122	0.00122
10% Dust	100*100*8	131.26	10.4	101.87	101.02	107025.44	0.00123	
15% Dust	100*100*8	107.9	10.4	101.47	100.12	105655.43	0.00102	
15% Dust	100*100*8	108.4	10.22	101.5	100.15	103888.6	0.00104	0.00103
15% Dust	100*100*8	108.3	10.25	101.49	100.11	104141.68	0.00104	

CALCULATION FOR RESULT OF COIR DUST CEMENT COMPOSITE BOARD
ON FLEXURAL STRENGTH TEST PRESENTED IN TABLE 4.2

Coir dust flexural strength test results

Sample	Size (mm)	Force (KN)	Peak (KN)	Displacement (mm)	Flexural Strength (mpa)	Average Flexural Strength (mpa)
5% Dust	100*100*100	28.06	39.33	7.01	14.03	
5% Dust	100*100*100	27.11	37.4	6.95	13.45	14.02
5% Dust	100*100*100	8.32	41.26	7.07	14.59	
7.5 Dust	100*100*100	21.22	29.4	8.08	9.1	
7.5%Dust	100*100*100	21.3	29.53	8.01	9.22	9.13
7.5%Dust	100*100*100	21.54	29.9	8.24	9.07	
10% Dust	100*100*100	18.28	25.9	11.09	5.84	
10% Dust	100*100*100	18.19	25.65	10.95	5.86	5.84
10% Dust	100*100*100	18.45	26.15	11.23	5.82	
15% Dust	100*100*100	3.55	8.72	10.37	2.1	
15% Dust	100*100*100	3.43	8.59	10.18	2.11	2.1
15% Dust	100*100*100	3.62	8.85	10.56	2.1	

CALCULATION FOR RESULT OF COIR DUST CEMENT COMPOSITE BOARD
ON COMPRESSIVE STRENGTH TEST PRESENTED IN TABLE 4.2

Coir dust compressive strength test results

Sample	Size(mm)	Force (KN)	Peak (KN)	Compressive Strength(mpa)	Average Compressive Strength(mpa)
5% Dust	100*100*100	83.01	112.08	11.21	
5% Dust	100*100*100	82.27	111.2	11.12	11.16
5% Dust	100*100*100	82.48	111.4	11.14	
7.5%Dust	100*100*100	72.17	96.3	9.63	
7.5%Dust	100*100*100	72.38	96.62	9.66	9.66
7.5%Dust	100*100*100	72.58	96.94	9.69	
10% Dust	100*100*100	40.21	53.85	5.39	
10% Dust	100*100*100	39.92	53.2	5.32	5.35
10% Dust	100*100*100	40.12	53.5	5.35	
15% Dust	100*100*100	4.4	9.51	0.95	
15% Dust	100*100*100	4.33	9.35	0.94	0.95
15% Dust	100*100*100	4.58	9.67	0.97	

CALCULATION FOR RESULT OF COIR DUST CEMENT COMPOSITE BOARD
ON MODULUS OF ELASTICITY TEST PRESENTED IN TABLE 4.2

Coir dust modulus of elasticity test results

Sample	Size (mm)	Displacement (mm)Δ	P (N)	PL3	4BD3Δ	MOE (mpa)	Average MOE (mpa)
5% Dust	195*50*10	1.27	65	481966875	254000	1897.51	
5% Dust	195*50*10	1.29	63	467137125	258000	1810.61	1916.31
5% Dust	195*50*10	1.15	70	519041250	230000	2256.7	
5% Dust	195*50*10	1.33	61	452307375	266000	1700.4	
7.5% Dust	195*50*10	1.21	58	430062750	242000	1777.12	
7.5% Dust	195*50*10	1.55	60	444892500	310000	1435.14	1509
7.5% Dust	195*50*10	1.73	60	444892500	346000	1285.82	
7.5% Dust	195*50*10	1.35	56	415233000	270000	1537.9	
10% Dust	195*50*10	1.51	50	370743750	302000	1227.63	
10% Dust	195*50*10	2.92	54	400403250	584000	685.62	1074.81
10% Dust	195*50*10	1.48	50	370743750	296000	1252.51	
10% Dust	195*50*10	1.57	48	355914000	314000	1133.48	
15% Dust	195*50*10	4.2	32	237276000	840000	282.47	
15% Dust	195*50*10	3.12	26	192786750	624000	308.95	330.64
15% Dust	195*50*10	2.21	24	177957000	442000	402.62	
15% Dust	195*50*10	3.16	28	207616500	632000	328.51	

CALCULATION FOR RESULT OF COIR DUST CEMENT COMPOSITE BOARD
ON MODULUS OF RUPTURE TEST PRESENTED IN TABLE 4.2

Coir dust modulus of rupture test results

Sample	Size (mm)	P (N)	3PL	2BD2	MOR (mpa)	Average MOR (mpa)
5% Dust	195*50*10	65	38025	10000	3.8	
5% Dust	195*50*10	63	36855	10000	3.69	3.79
5% Dust	195*50*10	70	40950	10000	4.1	
5% Dust	195*50*10	61	35685	10000	3.57	
7.5 Dust	195*50*10	58	33930	10000	3.39	
7.5 Dust	195*50*10	60	35100	10000	3.51	3.42
7.5 Dust	195*50*10	60	35100	10000	3.51	
7.5 Dust	195*50*10	56	32760	10000	3.28	
10% Dust	195*50*10	50	29250	10000	2.93	
10% Dust	195*50*10	54	31590	10000	3.16	2.96
10% Dust	195*50*10	50	29250	10000	2.93	
10% Dust	195*50*10	48	28080	10000	2.81	
15% Dust	195*50*10	32	18720	10000	1.87	
15% Dust	195*50*10	26	15210	10000	1.52	1.61
15% Dust	195*50*10	24	14040	10000	1.4	
15% Dust	195*50*10	28	16380	10000	1.64	

CALCULATION FOR RESULT OF COIR DUST CEMENT COMPOSITE BOARD
ON IMPACT STRENGTH TEST PRESENTED IN TABLE 4.2

Coir dust impact strength test results

Sample	D (inch)	D (mm)	WD (f*d)	Surface Area (mm)	Impact (N/mm²)	Average Impact (N/mm²)
5% Dust	1.22	31	1085	500	2.17	
5% Dust	1.226	31.14	1089.9	500	2.18	2.18
5% Dust	1.231	31.28	1094.84	500	2.19	
7.5%Dust	0.917	23.29	815.15	500	1.63	
7.5%Dust	0.924	23.48	821.8	500	1.64	1.63
7.5%Dust	0.909	23.1	808.5	500	1.62	
10% Dust	0.621	15.77	551.95	500	1.1	
10% Dust	0.605	15.36	537.6	500	1.08	1.09
10% Dust	0.613	15.57	544.95	500	1.09	
15% Dust	0.48	12.2	427	500	0.85	
15% Dust	0.482	12.25	428.75	500	0.86	0.86
15% Dust	0.489	12.42	434.7	500	0.87	

APPENDIX A 3

CALCULATION FOR RESULT OF CNSL CEMENT COMPOSITE BOARD ON WATER ABSORPTION TEST PRESENTED IN TABLE 4.3

CNSL water absorption test results

Sample	Size (mm)	Constant Mass (g) m1	Mass (g) (24hrs) m2	Water Absorption (%)	Average Water Absorption (%)
2.5%CNSL	100*100*8	118.9	139.2	17.07	
2.5%CNSL	100*100*8	119.2	140	17.45	17.77
2.5%CNSL	100*100*8	119.8	142.3	18.78	
5% CNSL	100*100*8	117.9	134.1	13.74	
5% CNSL	100*100*8	116.7	133.35	14.27	13.85
5% CNSL	100*100*8	118.5	134.55	13.54	
7.5%CNSL	100*100*8	110.1	121.7	10.54	
7.5%CNSL	100*100*8	109.6	120.5	9.95	10.23
7.5%CNSL	100*100*8	108.8	119.9	10.2	
10% CNSL	100*100*8	106.6	114.1	7.04	
10% CNSL	100*100*8	106.1	113.8	7.26	7.14
10% CNSL	100*100*8	106.8	114.4	7.12	

CALCULATION FOR RESULT OF CNSL CEMENT COMPOSITE BOARD ON
WATER ABSORPTION TEST PRESENTED IN TABLE 4.3

CNSL thickness swelling test results for 2 hours

Sample	Size (mm)	Constant Thickness (mm)	Thickness (mm)(2hrs)	Thickness Swelling (%)	Average Thickness Swelling (%)
2.5%CNSL	100*100*8	8.83	8.99	1.81	
2.5%CNSL	100*100*8	8.87	9.02	1.69	1.69
2.5%CNSL	100*100*8	8.85	8.99	1.58	
5% CNSL	100*100*8	8.86	8.97	1.24	
5% CNSL	100*100*8	8.9	9.05	1.69	1.35
5% CNSL	100*100*8	8.85	8.95	1.13	
7.5%CNSL	100*100*8	8.69	8.77	0.92	
7.5%CNSL	100*100*8	8.66	8.75	1.04	1.04
7.5%CNSL	100*100*8	8.72	8.82	1.15	
10% CNSL	100*100*8	8.6	8.67	0.81	
10% CNSL	100*100*8	8.57	8.64	0.82	0.7
10% CNSL	100*100*8	8.66	8.7	0.46	

CALCULATION FOR RESULT OF CNSL CEMENT COMPOSITE BOARD ON
THICKNESS SWELLING TEST PRESENTED IN TABLE 4.3

CNSL thickness swelling test results for 24 hours

Sample	Size (mm)	Constant Thickness (mm)	Thickness (mm)(24hrs)	Thickness Swelling (%)	Average Thickness Swelling (%)
2.5%CNSL	100*100*8	8.83	9.04	2.38	
2.5%CNSL	100*100*8	8.87	9.15	3.16	2.71
2.5%CNSL	100*100*8	8.85	9.08	2.6	
5% CNSL	100*100*8	8.86	9.05	2.14	
5% CNSL	100*100*8	8.9	9.08	2.02	2.14
5% CNSL	100*100*8	8.85	9.05	2.26	
7.5%CNSL	100*100*8	8.69	8.83	1.61	
7.5%CNSL	100*100*8	8.66	8.81	1.73	1.61
7.5%CNSL	100*100*8	8.72	8.85	1.49	
10% CNSL	100*100*8	8.6	8.68	0.93	
10% CNSL	100*100*8	8.57	8.63	0.7	0.93
10% CNSL	100*100*8	8.66	8.76	1.15	

CALCULATION FOR RESULT OF CNSL CEMENT COMPOSITE BOARD ON
DENSITY TEST PRESENTED IN TABLE 4.3

CNSL density test results

Sample	Size (mm)	Mass (g)	Thickness (mm)	Length (mm)	Width (mm)	Volume L*B*H(mm³)	Density(g/mm³) Mass/Volume	Ave. Density (g/mm³)
2.5%CNSL	100*100*8	139.2	9.04	100.55	101.64	92387.91	0.00151	
2.5%CNSL	100*100*8	140	9.15	100.58	101.67	93567.61	0.0015	0.00151
2.5%CNSL	100*100*8	142.3	9.08	100.57	101.66	92833.43	0.00153	
5% CNSL	100*100*8	134.1	9.05	99.72	100.54	90733.93	0.00148	
5% CNSL	100*100*8	133.35	9.08	99.75	100.57	91089.27	0.00146	0.00147
5% CNSL	100*100*8	134.55	9.05	99.71	100.56	90742.88	0.00148	
7.5%CNSL	100*100*8	121.7	8.83	100.7	98.97	88002.24	0.00138	
7.5%CNSL	100*100*8	120.5	8.81	100.73	99	87855.7	0.00137	0.00137
7.5%CNSL	100*100*8	119.9	8.85	100.69	98.96	88183.9	0.00136	
10% CNSL	100*100*8	114.1	8.68	99.5	100.99	87221.02	0.00131	
10% CNSL	100*100*8	113.8	8.63	99.54	101.19	86925.27	0.00131	0.00131
10% CNSL	100*100*8	114.4	8.76	99.51	100.81	87876.84	0.0013	

CALCULATION FOR RESULT OF CNSL CEMENT COMPOSITE BOARD ON
FLEXURAL STRENGTH TEST PRESENTED IN TABLE 4.3

CNSL flexural strength test results

Sample	Size (mm)	Force (KN)	Peak (KN)	Displacement (mm)	Flexural Strength(mpa)	Average Flexural Strength (mpa)
2.5%CNSL	100*100*100	17.88	19.23	9.78	4.92	
2.5%CNSL	100*100*100	18	19.45	9.58	5.08	5.1
2.5%CNSL	100*100*100	18.2	20.13	9.48	5.31	
5% CNSL	100*100*100	17.87	25	10.49	5.96	
5% CNSL	100*100*100	17.63	24.95	10.74	5.81	5.96
5% CNSL	100*100*100	18.01	25.38	10.4	6.1	
7.5%CNSL	100*100*100	12.67	17.03	8.9	4.78	
7.5%CNSL	100*100*100	12.49	16.88	9.04	4.67	4.78
7.5%CNSL	100*100*100	12.81	17.18	8.78	4.89	
10% CNSL	100*100*100	10.12	15.18	10.58	3.59	
10%C NSL	100*100*100	10.03	15.09	10.68	3.53	3.59
10% CNSL	100*100*100	10.17	15.27	10.48	3.64	

CALCULATION FOR RESULT OF CNSL CEMENT COMPOSITE BOARD ON
COMPRESSIVE STRENGTH TEST PRESENTED IN TABLE 4.3

CNSL compressive strength test results

Sample	size(mm)	Force(KN)	Peak(KN)	Compressive strength(mpa)	Average compressive strength(mpa)
2.5%CNSL	100*100*100	54.33	72.47	7.25	
2.5%CNSL	100*100*100	54.3	72.4	7.24	7.25
2.5%CNSL	100*100*100	54.4	72.54	7.25	
5% CNSL	100*100*100	38.8	51.8	5.18	
5% CNSL	100*100*100	37.92	51.72	5.17	5.19
5% CNSL	100*100*100	38.86	52.06	5.21	
7.5%CNSL	100*100*100	17.17	26.1	2.61	
7.5%CNSL	100*100*100	17.05	25.8	2.58	2.61
7.5%CNSL	100*100*100	17.3	46.4	2.64	
10% CNSL	100*100*100	15.1	21.72	2.17	
10% CNSL	100*100*100	15.01	21.65	2.17	2.18
10% CNSL	100*100*100	16.02	22.09	2.21	

CALCULATION FOR RESULT OF CNSL CEMENT COMPOSITE BOARD ON
MODULUS OF ELASTICITY TEST PRESENTED IN TABLE 4.3

CNSL modulus of elasticity test results

Sample	Size (mm)	Displacement (mm)Δ	P (N)	PL3	4BD3Δ	MOE	Average MOE (mpa)
2.5%CNSL	195*50*10	1.69	40	296595000	338000	877.5	
2.5%CNSL	195*50*10	0.98	42	311424750	196000	1588.9	1054.09
2.5%CNSL	195*50*10	1.7	38	281765250	340000	828.72	
2.5%CNSL	195*50*10	1.65	41	304009875	330000	921.24	
5% CNSL	195*50*10	1.63	39	289180125	326000	887.06	
5% CNSL	195*50*10	1.72	35	259520625	344000	754.42	784.53
5% CNSL	195*50*10	1.66	37	274350375	332000	826.36	
5% CNSL	195*50*10	1.77	32	237276000	354000	670.27	
7.5%CNSL	195*50*10	2.34	35	259520625	468000	554.53	
7.5%CNSL	195*50*10	2.4	30	222446250	480000	463.43	519.93
7.5%CNSL	195*50*10	2.36	33	244690875	472000	518.41	
7.5%CNSL	195*50*10	2.32	34	252105750	464000	543.33	
10% CNSL	195*50*10	3.47	30	222446250	694000	320.53	
10% CNSL	195*50*10	3.63	28	207616500	726000	285.97	306.01
10% CNSL	195*50*10	3.5	31	229861125	700000	328.37	
10% CNSL	195*50*10	3.59	28	207616500	718000	289.16	

CALCULATION FOR RESULT OF CNSL CEMENT COMPOSITE BOARD ON MODULUS OF RUPTURE TEST PRESENTED IN TABLE 4.3

CNSL modulus of rupture test results

Sample	Size (mm)	P (N)	3PL	2BD2	MOR (mpa)	Average MOR (mpa)
2.5%CNSL	195*50*10	40	23400	10000	2.34	
2.5%CNSL	195*50*10	42	24570	10000	2.46	2.36
2.5%CNSL	195*50*10	38	22230	10000	2.22	
2.5%CNSL	195*50*10	41	23985	10000	2.4	
5% CNSL	195*50*10	39	22815	10000	2.28	
5% CNSL	195*50*10	35	20475	10000	2.05	2.09
5% CNSL	195*50*10	37	21645	10000	2.16	
5% CNSL	195*50*10	32	18720	10000	1.87	
7.5%CNSL	195*50*10	35	20475	10000	2.05	
7.5%CNSL	195*50*10	30	17550	10000	1.76	1.93
7.5%CNSL	195*50*10	33	19305	10000	1.93	
7.5%CNSL	195*50*10	34	19890	10000	1.99	
10% CNSL	195*50*10	30	17550	10000	1.76	
10% CNSL	195*50*10	28	16380	10000	1.64	1.71
10% CNSL	195*50*10	31	18135	10000	1.81	
10% CNSL	195*50*10	28	16380	10000	1.64	

CALCULATION FOR RESULT OF CNSL CEMENT COMPOSITE BOARD ON
IMPACT STRENGTH TEST PRESENTED IN TABLE 4.3

CNSL impact strength test results

Sample	D (inch)	D (mm)	WD (f*d)	Surface Area	Impact (N/mm)	Average Impact (N/mm²)
2.5%CNSL	0.613	15.57	544.95	500	1.09	
2.5%CNSL	0.616	15.65	547.75	500	1.1	1.09
2.5%CNSL	0.61	15.49	542.15	500	1.08	
5% CNSL	0.923	23.44	820.4	500	1.64	
5% CNSL	0.917	23.29	815.15	500	1.63	1.63
5% CNSL	0.911	23.14	809.9	500	1.62	
7.5%CNSL	0.963	24.46	856.1	500	1.71	
7.5%CNSL	0.96	24.38	853.3	500	1.71	1.72
7.5%CNSL	0.972	24.69	864.14	500	1.73	
10% CNSL	1.439	36.55	1279.25	500	2.56	
10% CNSL	1.447	36.75	1286.25	500	2.57	2.57
10% CNSL	1.453	36.9	1291.5	500	2.58	

Water absorption test for fibre

```
oke <- read_excel("C:/Users/SCILAB/Desktop/oke.xlsx", sheet =
"Sheet16")
oke$Sample=as.factor(oke$Sample)
fit16=aov(Water_Absorption~Sample, data=oke)
result=summary(fit16)
meantables=model.tables(fit16,type="means",se.contrast=T)
result

## Signif. codes:  0 '***' 0.001 '**' 0.01 '*' 0.05 '.' 0.1 ' '
1

meantables

## Tables of means
## Grand mean
##
## 49.61833
##
##   Sample
## Sample
##   10% Fibre  15% Fibre   5% Fibre 7.5% Fibre
##       52.79      69.46      33.14      43.08

ggline(oke, x = "Sample", y = "Water_Absorption",
       add = c("mean_se"),
       order = c("5% Fibre", "7.5% Fibre", "10% Fibre", "15%
Fibre"),
       ylab = "Water Absorption (%)", xlab = "Fibre Quantity
(Samples)")
```

APPENDIX D2: ANOVA CALCULATION FOR RESULT OF COIR FIBRE CEMENT COMPOSITE BOARD ON THICKNESS SWELLING TEST PRESENTED IN TABLE 4.1.2

Thickness swelling test for fibre

```
oke <- read_excel("C:/Users/SCILAB/Desktop/oke.xlsx", sheet =
"Sheet19")
oke$Sample=as.factor(oke$Sample)
fit19=aov(Thickness_Swelling~Sample, data=oke)
result=summary(fit19)
meantables=model.tables(fit19,type="means",se.contrast=T)
result
```

```
## Signif. codes:  0 '***' 0.001 '**' 0.01 '*' 0.05 '.' 0.1 ' '
1
```

```
meantables
```

```
## Tables of means
## Grand mean
##
## 1.70125
##
##   Sample
## Sample
##   10% Fibre  15% Fibre   5% Fibre 7.5% Fibre
```

```
##      1.9917     2.4200     0.8950     1.4983
```

```
ggline(oke, x = "Sample", y = "Thickness_Swelling",
       add = c("mean_se"),
       order = c("5% Fibre", "7.5% Fibre", "10% Fibre", "15%
Fibre"),
       ylab = "Thickness Swelling (%)", xlab = "Fibre Quantity
(Samples)")
```

APPENDIX D3: ANOVA CALCULATION FOR RESULT OF COIR FIBRE CEMENT COMPOSITE BOARD ON FLUXURAL STRENGTH TEST PRESENTED IN TABLE 4.1.3

Flexural strength test for fibre

```
oke <- read_excel("C:/Users/SCILAB/Desktop/oke.xlsx", sheet =
"Sheet4")
oke$Sample=as.factor(oke$Sample)
fit4=aov(Flexural_Strenght~Sample, data=oke)
result=summary(fit4)
meantables=model.tables(fit4,type="means",se.contrast=T)
result


## Signif. codes:  0 '***' 0.001 '**' 0.01 '*' 0.05 '.' 0.1 ' '
1

meantables

## Tables of means
## Grand mean
##
## 6.481667
##
##   Sample
## Sample
##   10% Fibre  15% Fibre    5% Fibre 7.5% Fibre
##      7.627      5.350       6.093      6.857

ggline(oke, x = "Sample", y = "Flexural_Strenght",
       add = c("mean_se"),
       order = c("5% Fibre", "7.5% Fibre", "10% Fibre", "15%
Fibre"),
       ylab = "Flexural Strenght(mm)", xlab = "Fibre Quantity
(Samples)")
```

APPENDIX D4: ANOVA CALCULATION FOR RESULT OF COIR FIBRE CEMENT COMPOSITE BOARD ON MODULUS OF RUPTURE TEST PRESENTED IN TABLE 4.1.4

MOE test for fibre

```
oke <- read_excel("C:/Users/SCILAB/Desktop/oke.xlsx", sheet =
"Sheet10")
oke$Sample=as.factor(oke$Sample)
fit10=aov(MOE~Sample, data=oke)
result=summary(fit10)
meantables=model.tables(fit10,type="means",se.contrast=T)
result


## Signif. codes:  0 '***' 0.001 '**' 0.01 '*' 0.05 '.' 0.1 ' '
1

meantables

## Tables of means
## Grand mean
##
## 1159.207
##
##   Sample
## Sample
##  10% Fibre  15% Fibre   5% Fibre 7.5% Fibre
##     1428.8      813.2     1078.5     1316.2

ggline(oke, x = "Sample", y = "MOE",
       add = c("mean_se"),
       order = c("5% Fibre", "7.5% Fibre", "10% Fibre", "15%
Fibre"),
       ylab = "MOE (mpa)", xlab = "Fibre Quantity (Samples)")
```

APPENDIX D5: ANOVA CALCULATION FOR RESULT OF COIR FIBRE CEMENT COMPOSITE BOARD ON MODULUS OF RUPTURE TEST PRESENTED IN TABLE 4.1.5

MOR test for fibre

```
oke <- read_excel("C:/Users/SCILAB/Desktop/oke.xlsx", sheet = "Sheet13")
oke$Sample=as.factor(oke$Sample)
fit13=aov(MOR~Sample, data=oke)
result=summary(fit13)
meantables=model.tables(fit13,type="means",se.contrast=T)
result

## Signif. codes:  0 '***' 0.001 '**' 0.01 '*' 0.05 '.' 0.1 ' '
1

meantables

## Tables of means
## Grand mean
##
## 4.86
##
##   Sample
## Sample
##   10% Fibre  15% Fibre   5% Fibre 7.5% Fibre
##      5.340      4.622      4.372      5.105

ggline(oke, x = "Sample", y = "MOR",
       add = c("mean_se"),
       order = c("5% Fibre", "7.5% Fibre", "10% Fibre", "15%
Fibre"),
       ylab = "MOR (mpa)", xlab = "Fibre Quantity (Samples)")
```

APPENDIX D6: ANOVA CALCULATION FOR RESULT OF COIR FIBRE CEMENT COMPOSITE BOARD ON IMPACT STRENGTH TEST PRESENTED IN TABLE 4.1.6

Impact strength test for fibre

```
oke <- read_excel("C:/Users/SCILAB/Desktop/oke.xlsx", sheet =
"Sheet7")
oke$Sample=as.factor(oke$Sample)
fit7=aov(Impact~Sample, data=oke)
result=summary(fit7)
meantables=model.tables(fit7,type="means",se.contrast=T)
result


## Signif. codes:  0 '***' 0.001 '**' 0.01 '*' 0.05 '.' 0.1 ' '
1

meantables

## Tables of means
## Grand mean
##
## 2.695
##
##   Sample
## Sample
##   10% Fibre  15% Fibre    5% Fibre 7.5% Fibre
##        4.35        3.81        1.19        1.43

ggline(oke, x = "Sample", y = "Impact",
       add = c("mean_se"),
       order = c("5% Fibre", "7.5% Fibre", "10% Fibre", "15%
Fibre"),
       ylab = "Impact (N/mm2)", xlab = "Fibre Quantity
(Samples)")
```

Water absorption test for dust

```
oke <- read_excel("C:/Users/SCILAB/Desktop/oke.xlsx", sheet = "Sheet17")
oke$Sample=as.factor(oke$Sample)
fit17=aov(Water_Absorption~Sample, data=oke)
result=summary(fit17)
meantables=model.tables(fit17,type="means",se.contrast=T)
result

## Signif. codes:  0 '***' 0.001 '**' 0.01 '*' 0.05 '.' 0.1 ' '
1

meantables

## Tables of means
## Grand mean
##
## 50.23167
##
##   Sample
## Sample
##   10% Dust   15% Dust    5% Dust 7.5% Dust
##      62.59      69.06      27.57      41.70

ggline(oke, x = "Sample", y = "Water_Absorption",
       add = c("mean_se"),
       order = c("5% Dust", "7.5% Dust", "10% Dust", "15% Dust"),
       ylab = "Water Absorption (%)", xlab = "Dust Quantity (Samples)")
```

Thickness swelling test for dust

```
oke <- read_excel("C:/Users/SCILAB/Desktop/oke.xlsx", sheet =
"Sheet20")
oke$Sample=as.factor(oke$Sample)
fit20=aov(Thickness_Swelling~Sample, data=oke)
result=summary(fit20)
meantables=model.tables(fit20,type="means",se.contrast=T)
result

## Signif. codes:  0 '***' 0.001 '**' 0.01 '*' 0.05 '.' 0.1 ' '
1

meantables

## Tables of means
## Grand mean
##
## 2.965
##
##   Sample
## Sample
##   10% Dust  15% Dust    5% Dust 7.5% Dust
##      3.297     4.392      1.633     2.538

 ggline(oke, x = "Sample", y = "Thickness_Swelling",
       add = c("mean_se"),
       order = c("5% Dust", "7.5% Dust", "10% Dust", "15%
Dust"),
       ylab = "Thickness Swelling (%)", xlab = "Dust Quantity
(Samples)")
```

APPENDIX E3: ANOVA CALCULATION FOR RESULT OF COIR DUST
CEMENT COMPOSITE BOARD ON FLEXURAL STRENGTH TEST

Flexural strength test for dust

```
oke <- read_excel("C:/Users/SCILAB/Desktop/oke.xlsx", sheet =
"Sheet5")
oke$Sample=as.factor(oke$Sample)
fit5=aov(Flexural_Strenght~Sample, data=oke)
result=summary(fit5)
meantables=model.tables(fit5,type="means",se.contrast=T)
result
```

```
## Signif. codes:  0 '***' 0.001 '**' 0.01 '*' 0.05 '.' 0.1 ' '
1

meantables

## Tables of means
## Grand mean
##
## 7.774167
##
##   Sample
## Sample
##  10% Dust  15% Dust   5% Dust 7.5% Dust
##     5.840     2.103    14.023     9.130
```

```
ggline(oke, x = "Sample", y = "Flexural_Strenght",
       add = c("mean_se"),
       order = c("5% Dust", "7.5% Dust", "10% Dust", "15%
Dust"),
       ylab = "Flexural Strenght(mpa)", xlab = "CNSL Quantity
(Samples)")
```

APPENDIX E4: ANOVA CALCULATION FOR RESULT OF COIR DUST CEMENT COMPOSITE BOARD ON MODULUS OF ELASTICITY TEST

MOE test for dust

```
oke <- read_excel("C:/Users/SCILAB/Desktop/oke.xlsx", sheet =
"Sheet11")
oke$Sample=as.factor(oke$Sample)
fit11=aov(MOE~Sample, data=oke)
result=summary(fit11)
meantables=model.tables(fit11,type="means",se.contrast=T)
result


## Signif. codes:  0 '***' 0.001 '**' 0.01 '*' 0.05 '.' 0.1 ' '
1

meantables

## Tables of means
## Grand mean
##
## 1207.687
##
##   Sample
## Sample
##   10% Dust  15% Dust   5% Dust 7.5% Dust
##     1074.8     330.6    1916.3    1509.0

ggline(oke, x = "Sample", y = "MOE",
       add = c("mean_se"),
       order = c("5% Dust", "7.5% Dust", "10% Dust", "15%
Dust"),
       ylab = "MOE (mpa)", xlab = "Dust Quantity (Samples)")
```

APPENDIX E5: ANOVA CALCULATION FOR RESULT OF COIR DUST CEMENT COMPOSITE BOARD ON MODULUS OF RUPTURE TEST PRESENTED IN TABLE 4.2.5

MOR test for dust

```
oke <- read_excel("C:/Users/SCILAB/Desktop/oke.xlsx", sheet = "Sheet14")
oke$Sample=as.factor(oke$Sample)
fit14=aov(MOR~Sample, data=oke)
result=summary(fit14)
meantables=model.tables(fit14,type="means",se.contrast=T)
result


## Signif. codes:  0 '***' 0.001 '**' 0.01 '*' 0.05 '.' 0.1 ' ' 1

meantables

## Tables of means
## Grand mean
##
## 2.944375
##
##   Sample
## Sample
##  10% Dust  15% Dust   5% Dust 7.5% Dust
##     2.958     1.608     3.790     3.422

ggline(oke, x = "Sample", y = "MOR",
       add = c("mean_se"),
       order = c("5% Dust", "7.5% Dust", "10% Dust", "15% Dust"),
       ylab = "MOR (mpa)", xlab = "Dust Quantity (Samples)")
```

APPENDIX E6: ANOVA CALCULATION FOR RESULT OF COIR DUST CEMENT COMPOSITE BOARD ON IMPACT STRENGTH TEST PRESENTED IN TABLE 4.2.6

Impact strength test for dust

```
oke <- read_excel("C:/Users/SCILAB/Desktop/oke.xlsx", sheet =
"Sheet8")
oke$Sample=as.factor(oke$Sample)
fit8=aov(Impact~Sample, data=oke)
result=summary(fit8)
meantables=model.tables(fit8,type="means",se.contrast=T)
result


## Signif. codes:  0 '***' 0.001 '**' 0.01 '*' 0.05 '.' 0.1 ' '
1

meantables

## Tables of means
## Grand mean
##
## 1.44
##
##   Sample
## Sample
##  10% Dust  15% Dust   5% Dust 7.5% Dust
##      1.09      0.86      2.18      1.63

ggline(oke, x = "Sample", y = "Impact",
       add = c("mean_se"),
       order = c("5% Dust", "7.5% Dust", "10% Dust", "15%
Dust"),
       ylab = "Impact (N/mm2)", xlab = "Dust Quantity
(Samples)")
```

APPENDIX F1: ANOVA CALCULATION FOR RESULT OF CNSL CEMENT COMPOSITE BOARD ON WATER ABSORPTION TEST

Water absorption test for CNSL

```
oke <- read_excel("C:/Users/SCILAB/Desktop/oke.xlsx", sheet =
"Sheet18")
oke$Sample=as.factor(oke$Sample)
fit18=aov(Water_Absorption~Sample, data=oke)
result=summary(fit18)
meantables=model.tables(fit18,type="means",se.contrast=T)
result

## Signif. codes:  0 '***' 0.001 '**' 0.01 '*' 0.05 '.' 0.1 ' '
1

meantables

## Tables of means
## Grand mean
##
## 12.24667
##
##   Sample
## Sample
##   10% CNSL 2.5% CNSL    5% CNSL 7.5% CNSL
##      7.140    17.767     13.850    10.230

ggline(oke, x = "Sample", y = "Water_Absorption",
       add = c("mean_se"),
       order = c("2.5% CNSL", "5% CNSL", "7.5% CNSL", "10%
CNSL"),
       ylab = "Water Absorption (%)", xlab = "CNSL Quantity
(Samples)")
```

APPENDIX F2: ANOVA CALCULATION FOR RESULT OF CNSL CEMENT COMPOSITE BOARD ON THICKNESS SWELLING TEST PRESENTED IN TABLE 4.3.2

Thickness swelling test for CNSL

```
oke <- read_excel("C:/Users/SCILAB/Desktop/oke.xlsx", sheet =
"Sheet21")
oke$Sample=as.factor(oke$Sample)
fit21=aov(Thickness_Swelling~Sample, data=oke)
result=summary(fit21)
meantables=model.tables(fit21,type="means",se.contrast=T)
result

## Signif. codes:  0 '***' 0.001 '**' 0.01 '*' 0.05 '.' 0.1 ' '
1

meantables

## Tables of means
## Grand mean
##
## 1.52125
##
##   Sample
## Sample
##   10% CNSL 2.5% CNSL    5% CNSL 7.5% CNSL
##     0.8117    2.2033     1.7467    1.3233

ggline(oke, x = "Sample", y = "Thickness_Swelling",
       add = c("mean_se"),
       order = c("2.5% CNSL", "5% CNSL", "7.5% CNSL", "10%
CNSL"),
       ylab = "Thickness Swelling (%)", xlab = "CNSL Quantity
(Samples)")
```

APPENDIX F3: ANOVA CALCULATION FOR RESULT OF CNSL CEMENT COMPOSITE BOARD ON FLEXURAL STRENGTH TEST PRESENTED IN TABLE 4.3.3

Flexural strength test for CNSL

```
oke <- read_excel("C:/Users/SCILAB/Desktop/oke.xlsx", sheet =
"Sheet6")
oke$Sample=as.factor(oke$Sample)
fit6=aov(Flexural_Strength ~Sample, data=oke)
result=summary(fit6)
meantables=model.tables(fit6,type="means",se.contrast=T)
result


## Signif. codes:  0 '***' 0.001 '**' 0.01 '*' 0.05 '.' 0.1 ' '
1

meantables

## Tables of means
## Grand mean
##
## 4.856667
##
##   Sample
## Sample
##   10% CNSL 2.5% CNSL   5% CNSL 7.5% CNSL
##      3.587     5.103     5.957     4.780

ggline(oke, x = "Sample", y = "Flexural_Strenght",
       add = c("mean_se"),
       order = c("2.5% CNSL", "5% CNSL", "7.5% CNSL", "10%
CNSL"),
       ylab = "Flexural Strenght(mpa)", xlab = "CNSL Quantity
(Samples)")
```

APPENDIX F4: ANOVA CALCULATION FOR RESULT OF CNSL CEMENT COMPOSITE BOARD ON MODULUS OF ELASTICITY TEST PRESENTED IN TABLE 4.3.4

MOE test for CNSL

```
oke <- read_excel("C:/Users/SCILAB/Desktop/oke.xlsx", sheet =
"Sheet12")
oke$Sample=as.factor(oke$Sample)
fit12=aov(MOE~Sample, data=oke)
result=summary(fit12)
meantables=model.tables(fit12,type="means",se.contrast=T)
result


## Signif. codes:  0 '***' 0.001 '**' 0.01 '*' 0.05 '.' 0.1 ' '
1

meantables

## Tables of means
## Grand mean
##
## 666.1375
##
##   Sample
## Sample
##  10% CNSL 2.5% CNSL   5% CNSL 7.5% CNSL
##     306.0    1054.1     784.5     519.9

ggline(oke, x = "Sample", y = "MOE",
       add = c("mean_se"),
       order = c("2.5% CNSL", "5% CNSL", "7.5% CNSL", "10%
CNSL"),
       ylab = "MOE (mpa)", xlab = "CNSL Quantity (Samples)")
```

APPENDIX F5: ANOVA CALCULATION FOR RESULT OF CNSL CEMENT COMPOSITE BOARD ON MODULUS OF RUPTURE TEST PRESENTED IN TABLE 4.3.5

MOR test for CNSL

```
oke <- read_excel("C:/Users/SCILAB/Desktop/oke.xlsx", sheet =
"Sheet15")
oke$Sample=as.factor(oke$Sample)
fit15=aov(MOR~Sample, data=oke)
result=summary(fit15)
meantables=model.tables(fit15,type="means",se.contrast=T)
result


## Signif. codes:  0 '***' 0.001 '**' 0.01 '*' 0.05 '.' 0.1 ' '
1

meantables

## Tables of means
## Grand mean
##
## 2.0225
##
##   Sample
## Sample
##  10% CNSL 2.5% CNSL    5% CNSL 7.5% CNSL
##    1.7125    2.3550    2.0900    1.9325

ggline(oke, x = "Sample", y = "MOR",
       add = c("mean_se"),
       order = c("2.5% CNSL", "5% CNSL", "7.5% CNSL", "10%
CNSL"),
       ylab = "MOR (mpa)", xlab = "CNSL Quantity (Samples)")
```

APPENDIX F6: ANOVA CALCULATION FOR RESULT OF CNSL CEMENT COMPOSITE BOARD ON IMPACT STRENGTH TEST PRESENTED IN TABLE 4.3.6

Impact strength test for CNSL

```
oke <- read_excel("C:/Users/SCILAB/Desktop/oke.xlsx", sheet =
"Sheet9")
oke$Sample=as.factor(oke$Sample)
fit9=aov(Impact~Sample, data=oke)
result=summary(fit9)
meantables=model.tables(fit9,type="means",se.contrast=T)
result


## Signif. codes:  0 '***' 0.001 '**' 0.01 '*' 0.05 '.' 0.1 ' '
1

meantables

## Tables of means
## Grand mean
##
## 1.751667
##
##   Sample
## Sample
##   10% CNSL 2.5% CNSL   5% CNSL 7.5% CNSL
##     2.5700    1.0900    1.6300    1.7167

ggline(oke, x = "Sample", y = "Impact",
       add = c("mean_se"),
       order = c("2.5% CNSL", "5% CNSL", "7.5% CNSL", "10%
CNSL"),
       ylab = "Impact(N/mm2)", xlab = "CNSL Quantity
(Samples)")
```

Coir fibre modeling

Water absorption (%) test of coir fibre content

WA Equation = $1.6825q^2 + 3.4545q +$

28.362

R^2 value = 0.9964

Quantity	WA
1	33.499
2	42.001
3	53.868
4	69.1
5	87.697

APPENDIX G2: MODELLING RESULTS FROM THE COIR FIBER THICKNESS SWELLING IN EQUATION 4.2

Thickness swelling (%) test of coir fibre content

TS 2hrs Equation = $-0.0675q^2 +$

$0.6525q + 0.0825$

R^2 value = 0.9998

Quantity

1	0.6675
2	1.1175
3	1.4325
4	1.6125
5	1.6575

APPENDIX G3: MODELLING RESULTS FROM THE COIR FIBRE THICKNESS
SWELLING IN
EQUATION 4.3

Thickness swelling (%) test of coir fibre content

TS 24 Equation = $0.02q^2 +$

$0.798q + 0.35$

R^2 value = 0.9995

Quantity	TS24
1	1.128
	1.866
3	2.564
4	3.222
5	3.84

APPENDIX G4: MODELLING RESULTS FROM THE COIR FIBRE DENSITY IN EQUATION 4.4

Density (g/mm^3) test of coir fibre content

D equation = 8E-06q^2 -

0.0002q + 0.0018

R^2 value= 0.9913

Quatity	Density
1	8E-5.998
2	8E-23.999
3	8E-53.999
4	8E-95.999
5	8E-149.999

APPENDIX G5: MODELLING RESULTS FROM THE COIR FIBRE FLEXURAL
STRENGTH IN
EQUATION 4.5

Flexural (Mpa) test of coir fibre content

FS equation = $-3.95q^2 + 19.378q -$

8.08

R^2 value = 0.8022

Quantity	Flex.
1	7.348
2	14.876
3	14.504
4	6.232
5	-9.94

APPENDIX G6: MODELLING RESULTS FROM THE COIR FIBRE COMPRESSIVE

STRENGTH IN

EQUATION 4.6

Compressive (Mpa) test of coir fibre content

CS equation = $-0.6925q^2 + 0.1435q +$

11.278

R^2 value = 0.9942

Quantity	C
1	10.729
2	8.795
3	5.476
4	0.772
5	-5.317

APPENDIX G7: MODELLING RESULTS FROM THE COIR FIBRE MODULUS OF
ELASTICITY IN
EQUATION 4.7

MOE (Mpa) test of coir fibre content

MOE equation = $-210.84q^2 + 986.9q + 270.78$

R^2value = 0.9091

Quantity	MOE
1	1046.84
2	1401.22
3	1333.92
4	844.94
5	-65.72

APPENDIX G8: MODELLING RESULTS FROM THE COIR FIBRE MODULUS OF

RUPTURE IN

EQUATION 4.8

MOR (Mpa) test of coir fibre content

MOR equation = $-0.365q^2 + 1.923q$

$+2.79$

R^2 value = 0.9836

Quantity	MOR
1	4.348
2	5.176
3	5.274
4	4.642
5	3.28

APPENDIX G9: MODELLING RESULTS FROM THE COIR FIBRE IMPACT STRENG

IN

EQUATION 4.9

Impact strength N/mm^3) test of coir fibre content

IS equation $=0.729e0.460q$

R^2 value = 0.8022

Quantity	IS
1	0.883
2	2.351
3	3.429
4	4.117
5	4.415

APPENDIX H1: MODELLING RESULTS FROM THE COIR DUST WATER

ABSORPTION IN

EQUATION 4.10

Coir dust modelling

Water absorption (%) test of coir dust content

WA equation = $-1.915q^2 + 24.11q$

$+ 4.315$

R^2value = 0.9795

Quantity	WA
1	26.511
2	44.877
3	59.413
4	70.119
5	76.995

APPENDIX H2: MODELLING RESULTS FROM THE COIR DUST THICKNESS

SWELLING IN

EQUATION 4.11

Thickness swelling (%) test of coir dust content

TS2 equation = $0.095q^2 + 0.271q$

+ 1.04

R^2 value = 0.9909

Quantity	TS2
1	1.406
2	1.962
3	2.708
4	3.644
5	4.77

APPENDIX H3: MODELLING RESULTS FROM THE COIR DUST THICKNESS SWELLING IN

EQUATION 4.12

Thickness swelling (%) test of coir dust content

TS24 equation $= 0.0025q^2 + 1.0505q + 0.8575$

R^2value $= 0.9996$

Quantity	TS24
1	1.9111
2	2.969
3	4.032
4	5.1
5	6.173

APPENDIX H4: MODELLING RESULTS FROM THE COIR DUST DENSITY IN EQUATION 4.13

Density (g/mm^3) test of coir dust content

D equation = -3E-05q^2 + 2E -05q

+ 0.0015

R^2 value = 0.9874

Quantity	Density
1	8.672
2	6.293
3	5.853
4	2.412
5	-1.45

APPENDIX H5: MODELLING RESULTS FROM THE COIR DUST FLEXURAL STRENGTH IN EQUATION 4.14

Flexural strength (Mpa) test of coir dust content

FS equation = $-0.475q^2 - 0.063q +$

10.32

R^2 value = 0.9614

Quantity	Flex.
1	9.782
2	8.294
3	5.856
4	2.468
5	-1.87

APPENDIX H6: MODELLING RESULTS FROM THE COIR DUST COMPRESSIVE STRENGTH IN EQUATION 4.15

Compressive (Mpa) test of coir dust content

CS equation = $-0.6925q^2 + 0.1435q + 11.278$

R^2 value = 0.9942

Quantity	CS
1	10.729
2	8.795
3	5.476
4	0.772
5	-5.317

APPENDIX H7: MODELLING RESULTS FROM THE COIR DUST MODULUS OF ELASTICITY IN EQUATION 4.16

MOE (Mpa) test of coir dust content

MOE equation= $-84.215q^2 - 98.045q + 2084.4$

R^2 value = 0.9971

Quantity	MOE
1	1902.14
2	1551.45
3	1032.33
4	344.78
5	-511.2

APPENDIX H8: MODELLING RESULTS FROM THE COIR DUST MODULUS OF RUPTURE IN EQUATION 4.17

MOR (Mpa) test of coir dust content
MOR equation = $-0.245q^2 +$
$0.525q + 3.47$
R^2 value = 0.9882

Quantity	MOR
1	3.75
2	3.54
3	2.84
4	1.65
5	-0.03

APPENDIX H9: MODELLING RESULTS FROM THE COIR DUST IMPACT STRENGTH IN EQUATION 4.18

Impact strength (N/mm^3) test of coir dust content

IS equation = $0.08q^2 - 0.85q + 2.965$

R^2 value = 0.9957

Quantity	IS
1	2.195
2	1.585
3	1.135
4	0.845
5	0.715

CNSL/dust modelling

Water absorption test (%) of CNSL

WA equation $= 0.2075q^2 - 4.588q + 22.163$

R^2 value $=1$

Quantity	WA
1	17.78
2	13.82
3	10.27
4	7.13
5	4.41

APPENDIX I2: MODELLING RESULTS FROM THE CNSL/DUST THICKNESS SWELLING IN EQUATION 4.20

Thickness swelling (%) of CNSL

TS2 equation = -0.328q + 2.015

R^2 value = 0.9997

Quantity	TS2
1	1.687
2	1.359
3	1.031
4	0.703
5	0.378

APPENDIX I3: MODELLING RESULTS FROM THE CNSL/DUST THICKNESS SWELLING IN EQUATION 4.21

Thickness swelling (%) of CNSL

TS24 equation = $-0.0275q^2 - 0.4495q + 3.1775$

R^2 value = 0.999

Quantity	TS24
1	2.701
2	2.169
3	1.582
4	0.94
5	0.243

APPENDIX I4: MODELLING RESULTS FROM THE CNSL/DUST THI SWELLING IN EQUATION 4.22

Density (g/mm^3) of CNSL

D = -5E - 06x2 - 4E - 05x + 0.0016

R2 = 0.9801

Quantity	D
1	6.453
2	4.786
3	4.243
4	2.674
5	1.867

APPENDIX I5: MODELLING RESULTS FROM THE CNSL/DUST FLEXURAL STRENGTH IN EQUATION 4.23

Flexural (Mpa) test of CNSL

FS equation $= -0.176q^2 - 0.0156q + 6.555$

R^2 value $= 0.8468$

Quantity	FS
1	6.363
2	5.82
3	4.924
4	3.677
5	2.077

APPENDIX I6: MODELLING RESULTS FROM THE CNSL/DUST COMPRESSIVE STRENGTH IN EQUATION 4.24

Compressive (Mpa) test of CNSL

CS equation= $0.3875q^2 - 3.6265q + 10.248$

R^2 value = 0.9783

Q	CS
1	7.009
2	4.545
3	2.856
4	1.942
5	1.803

APPENDIX I7: MODELLING RESULTS FROM THE CNSL/DUST MODULUS OF ELASTICITY IN EQUATION 4.25

MOE (Mpa) test of CNSL

MOE equation = $13.91q^2$-2 320.43q + 1362.9

R^2 value = 0.9997

Quantity	MOE
1	1056.38
2	777.68
3	526.8
4	303.74
5	108.5

APPENDIX I8: MODELLING RESULTS FROM THE CNSL/DUST MODULUS OF RUPTURE IN EQUATION 4.26

MOR (Mpa) test of CNSL

MOR equation = $0.0125q^2 - 0.2735q + 2.6125$

R^2 value = 0.9936

Quantity	MOR
1	2.352
2	2.116
3	1.905
4	1.719
5	1.558

APPENDIX I9: MODELLING RESULTS FROM THE CNSL/DUST IMPACT STRENGTH IN EQUATION 4.27

Impact strength (N/mm^3) of CNSL

IS equation $= 0.0775q^2 + 0.0655q + 1.0075$

R^2 value $= 0.9348$

| Quantity	IS
1	1.151
2	1.449
3	1.902
4	2.51
5	3.273

APPENDIX J: THE PROPERTY REQUIREMENTS, AS SPECIFIED BY THE AMERICAN NATIONAL STANDARD FOR PARTICLEBOARD A208.1 (ANSI/A208.1, 1999) VARIOUS GRADES OF PARTICLEBOARD PRODUCTS WERE USED TO COMPARED CEMENT COMPOSITE BOARDS PRODUCED IN CHAPTER 4.2.4

Grade [a]	MOR (MPa)	MOE (Mpa)	Density (Kg/m^3)	Density (g/mm^3)
H-1	16.5	2400	> 800	> 0.0008
H-2	20.5	2400	> 800	> 0.0008
H-3	23.5	2750	> 800	> 0.0008
M-1	11.0	1725	640 – 800	0.00064 – 0.0008
M-S	12.5	1900	640 – 800	0.00064 – 0.0008
M-2	14.5	2225	640 – 800	0.00064 – 0.0008
M-3	16.5	2750	640 – 800	0.00064 – 0.0008
LD-1	3.0	550	< 640	< 0.00064
LD-2	5.0	1025	< 640	< 0.00064
Grade [b]				
PBU	11.0	1725	-	-
D-2	16.5	2750	-	-
D-3	19.5	3100	-	-

Grade M-S refers medium density; special grade added to standard after grades M-1, M-2, and M-3. Grade M-S fails between M-1 and M-2 physical properties.

PBU   = underlayment: D   = manufactured home decking.

APPENDIX K: ETHER WAS USED DURING THE EXTRACTION OF CNSL IN

CHAPTER 3.1 - 3.2
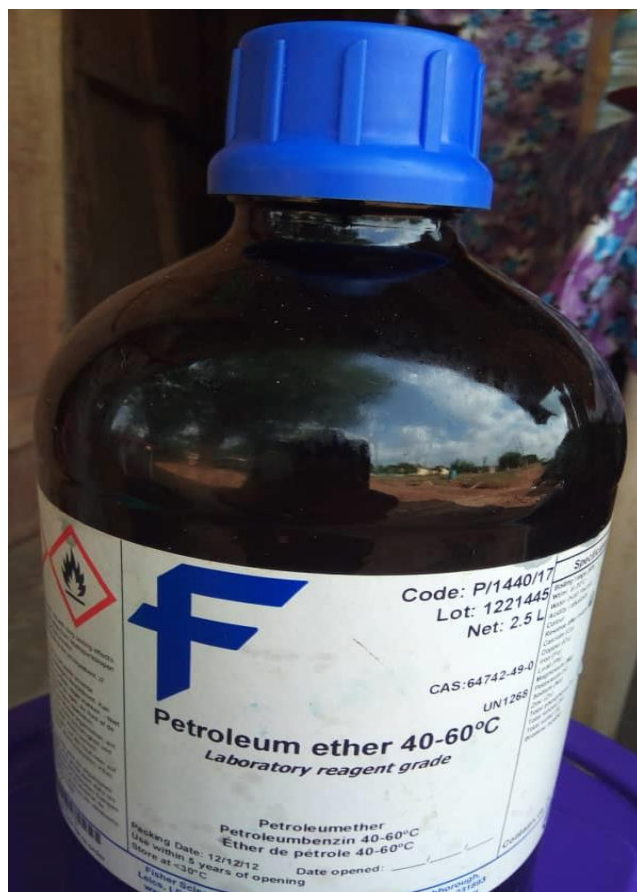
Ether

Development of electrically operated board machine